LEVERAGING MACROCYCLIC ARCHITECTURES IN THE DEVELOPMENT OF

POLYMERIC CARBON NANOMATERIALS

by

RUTH L. MAUST

A DISSERTATION

Presented to the Department of Chemistry and Biochemistry
and the Division of Graduate Studies of the University of Oregon
in partial fulfillment of the requirements
for the degree of
Doctor of Philosophy

June 2021

DISSERTATION APPROVAL PAGE

Student: Ruth L. Maust

Title: Leveraging Macrocyclic Architectures in the Development of Polymeric Carbon Nanomaterials

This dissertation has been accepted and approved in partial fulfillment of the requirements for the Doctor of Philosophy degree in the Department of Chemistry and Biochemistry by:

| | |
|---|---|
| Darren W. Johnson | Chairperson |
| Ramesh Jasti | Advisor |
| Michael M. Haley | Core Member |
| Deb Morrison | Institutional Representative |

and

Andrew Karduna          Interim Vice Provost for Graduate Studies

Original approval signatures are on file with the University of Oregon Division of Graduate Studies.

Degree awarded June 2021

DISSERTATION ABSTRACT

Ruth L. Maust

Doctor of Philosophy

Department of Chemistry and Biochemistry

June 2021

Title: Leveraging Macrocyclic Architectures in the Development of Polymeric Carbon
  Nanomaterials

Carbon-based materials—such as graphene nanoribbons, fullerenes, and carbon

nanotubes—are promising candidates for many applications due to their wide-ranging

properties. However, a lack of methods for precise synthesis, functionalization, and

assembly of complex carbon materials has hindered efforts to define structure-property

relationships and develop new carbon materials with unique properties. To overcome this

challenge, we employed cycloparaphenylenes (CPPs) and similar macrocycles which can

be accessed with atomic precision in combination with polymer chemistry methods to

construct new polymeric carbon materials. This approach allowed us to carefully examine

the effects of structural modifications to the monomers on the final polymer properties.

We successfully prepared a range of new types of $sp^2$-carbon-dense polymers, marking

an important advance toward bridging the gap between small molecules and functional

carbon-based materials.

Chapter I provides an overview of the design parameters available for tuning

polymer properties, the role of macrocycles in polymers, and the intersection of polymer

chemistry with organic synthesis. Chapter II describes the controlled polymerization of

norbornene cycloparaphenylenes. Through ring-opening metathesis polymerization, we

accessed homopolymers as well as block and statistical copolymers constructed from "carbon nanohoops" with a high degree of structural control. These polymers exhibit tunable fluorescence emission and supramolecular responses based on composition and sequence. Chapter III relays our research into conjugated polymers with hybrid linear-radial pi systems. Unique electronic properties arise from orbital mixing in these CPP-based polymers. Finally, Chapter IV covers two strategies to use ring-opening of strained macrocycles to access new polymeric materials.

This dissertation includes previously published and unpublished coauthored material.

CURRICULUM VITAE

NAME OF AUTHOR:  Ruth L. Maust

GRADUATE AND UNDERGRADUATE SCHOOLS ATTENDED:

University of Oregon, Eugene
Eastern Mennonite University, Harrisonburg

DEGREES AWARDED:

Doctor of Philosophy, Chemistry, 2021, University of Oregon
Bachelor of Arts, Chemistry, 2013, Eastern Mennonite University

AREAS OF SPECIAL INTEREST:

Synthetic Organic Chemistry
Polymer Chemistry
Green Chemistry

PROFESSIONAL EXPERIENCE:

Graduate Teaching Fellow, University of Oregon, 2016-2018

Development Technician, PPG Industries, 2014-2016

Research & Resource Coordinator, Green Building Alliance, 2013-2014

GRANTS, AWARDS, AND HONORS:

First place, Virtual 3-Minute Thesis Competition, University of Oregon, 2020

Graduate Research Fellowship Program, National Science Foundation, 2018

Knight Campus Student Innovation Fellowship, University of Oregon, 2017

First Year Merit Award, University of Oregon, 2016

Segal AmeriCorps Education Award, AmeriCorps, 2014

Outstanding Chemistry Senior Award, Eastern Mennonite University, 2013

Honors Scholarship, Eastern Mennonite University, 2009

PUBLICATIONS:

Maust, R. L.; Li, P.; Shao, B.; Zeitler, S. M.; Sun, P. B.; Reid, H. W.; Zakharov, L. N.; Golder, M. R.; Jasti, R. Controlled Polymerization of Norbornene Cycloparaphenylenes Expands Carbon Nanomaterials Design Space. *ACS Central Science* **2021**, *Accepted.*

Peters, G. M.; Grover, G.; Maust, R. L.; Colwell, C. E.; Bates, H.; Edgell, W. A.; Jasti, R.; Kertesz, M.; Tovar, J. D. Linear and Radial Conjugation in Extended Pi-Electron Systems. *J. Am. Chem. Soc.* **2020**, *142*, 2293-2300.

Lynde, B. E.; Maust, R. L.; Li, P.; Lee, D. C.; Jasti, R.; Boydston, A. J. Ring-Opening Metathesis Polymerization of a Strained Stilbene-Based Macrocyclic Monomer. *Mater. Chem. Front.* **2020**, *4*, 252-256.

PATENT APPLICATIONS:

Jasti, R.; Maust, R.; Li, P. Nanohoop-Functionalized Polymer Embodiments and Methods of Making and Using the Same. Publication number US20210095069A1.

Jasti, R.; Maust, R.; Colwell, C.; Tovar, J. D.; Peters, G.; Bates, H.; Kertesz, M.; Grover, G. Polymer Embodiments Comprising Nanohoop-Containing Polymer Backbones and Methods of Making and Using the Same. Publication number US20210095070A1.

ACKNOWLEDGMENTS

First and foremost, I want to thank my family and friends for their support over the past 5 years, even though I was far away and working on a niche research topic. Thanks to my parents, Martha Yoder and Rodney Maust, for being curious about my work and for reminding me what a great opportunity it is to engage with difficult questions and to learn so much in the process. I want to thank my life partner, Sudhanshu Shekhar, who encouraged me from the beginning of the graduate school application process, gave me an up-close view of what it means to pursue a PhD in the sciences, and moved to Oregon to be with me.

I want to express sincere appreciation to Prof. Ramesh Jasti for his mentorship. Ramesh always made it clear that the highest priority for a student at any level is to learn. The journey toward a PhD has been the most intense challenge I've ever undertaken, and it has truly been an education. I also want to thank Ramesh for being so supportive, amiable, open about the politics of the scientific enterprise, and eager to share his excitement for aesthetically pleasing or simply cool molecules. I want to thank the entire Jasti research group, including all current members and group alumni. Special thanks to Jeff Van Raden, Brittany White, and honorary group member Spencer Mathieu for your incredible friendship.

Many other people had a role to play in my PhD journey. I want to thank my high school chemistry teacher, Dan McNally, and my chemistry professors—Tara Kishbaugh, Matt Siderhurst, and Sheldon Shank—at Eastern Mennonite University, all of whom encouraged me as a chemist and showed me that there's much more to being a scientist than the lab work. Thanks to my committee members Darren Johnson, Mike Haley, and

To my younger self, who was called naïve for thinking an education in sustainable chemistry would give me the best chance to change the world – this one's for you.

TABLE OF CONTENTS

Chapter                                                                          Page

LIST OF FIGURES

xvi

LIST OF TABLES

# LIST OF SCHEMES

# CHAPTER I

## INTRODUCTION

This chapter was written by myself with input from Professor Ramesh Jasti.

Chapter II is adapted from a manuscript published in *ACS Central Science* under the title "Controlled Polymerization of Cycloparaphenylene Norbornenes Expands Carbon Nanomaterials Design Space."[1] Further permissions related to material excerpted from this article should be directed to the ACS. Excerpts from this article were written by myself. Dr. Penghao Li, Brian Sun, and Harrison Reid contributed to monomer synthesis and characterization. Dr. Baihao Shao conducted solid-state optical measurements. Sarah Zeitler and Prof. Matthew Golder carried out multi-angle light scattering (MALS) analysis. Dr. Lev Zakharov conducted X-ray crystallography analysis. Prof. Ramesh Jasti edited the manuscript and provided guidance on the project.

Chapter III includes published and unpublished co-authored material. Section 3.2 is based on a manuscript published in *Journal of the American Chemical Society* under the title "Linear and Radial Conjugation in Extended Pi-Electron Systems."[2] Dr. Garvin Peters and Haley Bates carried out polymer synthesis and optoelectronic characterization of the resultant polymers. Dr. Girishma Grover performed computations. Dr. Curtis Colwell and W. Alex Edgell contributed to monomer synthesis and characterization. Prof. J. D. Tovar wrote the manuscript and Prof. Ramesh Jasti and Prof. Miklos Kertesz edited the manuscript. Section 3.3 is based on unpublished work co-authored with Eric Peterson, Prof. J. D. Tovar, Prof. Miklos Kertesz, and Prof. Ramesh Jasti.

Chapter IV includes published and unpublished co-authored material. Section 4.2 is based on a manuscript published in *Materials Chemistry Frontiers* under the title "Ring-Opening Metathesis Polymerization of a Strained Stilbene-Based Macrocyclic Monomer."[3] Dr. Brock Lynde and Dr. Daniel Lee performed polymerization studies. Dr. Brock Lynde wrote the manuscript. Prof. Ramesh Jasti and Prof. A. J. Boydston edited the manuscript. Section 4.3 is based on unpublished work co-authored with Jinghui Yang, Prof. Yan Xia, and Prof. Ramesh Jasti.

1

## 1.1 Societal Importance of Polymeric Materials

Synthetic polymers' versatility and highly tunable properties make them attractive for a wide range of applications from food packaging to medical devices to furniture and clothing.[4] Since the molecular structure of polymers began to be understood about a century ago,[5,6] there has been a deluge of new types of polymers, each with properties quite distinct from the rest. Today it is hard to imagine life without synthetic polymers. Although society now faces growing concerns over end-of-life management of polymers and polymer composites,[7] these materials continue to be widely used because they serve so many purposes in so many sectors. For some applications, such as paints, coatings, and adhesives, there are no alternatives to polymers that can provide the needed properties. In other cases, such as with single-use plastic items, alternatives exist, but the overall environmental impacts of plastics versus alternative materials like paper are sometimes unclear and/or counterintuitive.[8] Despite the problems that have arisen from the sheer volume of polymers in use in the modern economy, it is evident that the range of properties attainable from polymers remains unmatched in any other class of materials.

## 1.2 Progress in Polymer Synthesis

Major breakthroughs in polymer chemistry in recent decades have enabled the preparation of polymers with complex architectures, controlled dispersities, and high degrees of functionality.[9–11] The number of polymer synthesis methods has increased,[11] with perhaps the most important development being the introduction of controlled or "living" polymerization methods.[12–17] In addition to the most prevalent commodity polymers, many types of highly specialized polymers now exist, including polymers for chemical and biological sensing,[18] supramolecular or "reversible" polymers,[19–22] two-dimensional polymers,[23,24] pollutant-adsorbing polymers,[25,26] topology-switching polymers,[27] and polymers which mimic the functions of skin.[28] Controlled polymerization methods have also enabled the synthesis of gradient[29] and block copolymers which can assemble into even larger structures (Fig. 1.1).[30,31] Amphiphilic block copolymers can be exceptional surfactants,[32] while gradient polymers can compatibilize otherwise immiscible polymer blends.[33] Taking inspiration from nature, efforts have been dedicated to the synthesis of sequence-controlled polymers, and significant advances have been

made in this challenging area.[34,35] Polymer chemists currently have unprecedented ability to construct polymers containing wide-ranging functionalities with a high level of control.
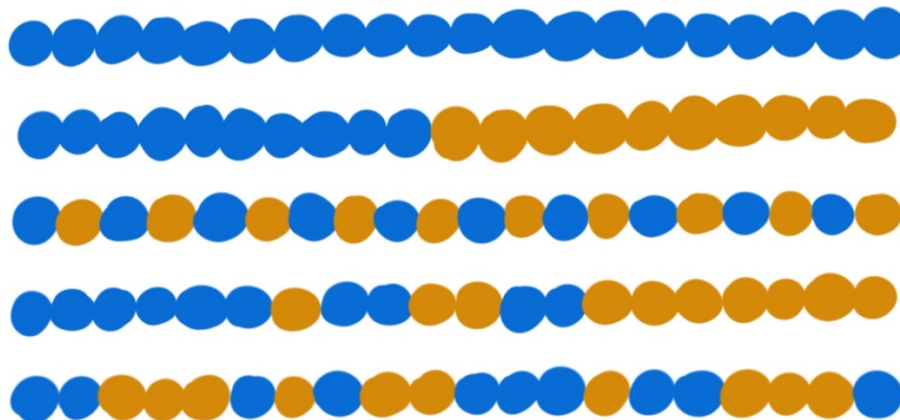


**Figure 1.1.** Polymers can vary not only by composition but also by sequence of repeat units. Shown here are cartoon depictions of (top to bottom) a homopolymer, block copolymer, alternating copolymer, gradient/tapered copolymer, and a random/statistical copolymer.

## 1.3 Polymers Are More Than the Sum of Their Monomers

One of the earliest findings supporting the macromolecular nature of polymers was the discovery that properties of polymers with the same composition varied with molecular weight.[36] The increased level of control in polymer synthesis since then has enabled study of polymers not only with varied compositions and sequences but also with varied topologies, such as branched, bottlebrush, and cyclic polymers (Fig. 1.2). An everyday example is linear high-density polyethylene (HDPE) and branched low-density polyethylene (LDPE), polymers which share the same chemical identity but are used in different applications due to their differing melting temperatures, toughness, and other physical properties.[37] As another example, self-assembled bottlebrush block copolymers form larger domains and different types of nanostructures compared to assemblies of their linear block copolymer counterparts.[38] Polymers with cyclic topologies have recently gained attention. While cyclic polymers have historically been present as low-level impurities in many polymer samples, synthetic methods allowing preparation of cyclic polymers with high purity[39–44] have revealed numerous differences between cyclic

3

and linear polymers. Cyclic and linear polymers with the same chemical identity and molecular weight can differ dramatically in their diffusion, solubility, crystallinity, viscosity, and other properties.[39] Cyclic polymers also have slower degradation profiles compared to their linear counterparts.[45] Exciting work in recent years has led to the production of cyclic analogues of commodity polymers.[46,47] Blending cyclic and linear polymers leads to yet a different set of properties than what is accessible using either topology alone.[48] This means that polymers with cyclic and other topologies can be used as dopants to modify the physical properties of a bulk polymer sample without changing its chemical nature.[32] Many other polymer topologies continue to be explored,[49] offering the promise of still more materials stemming from the same building blocks but exhibiting unique properties.
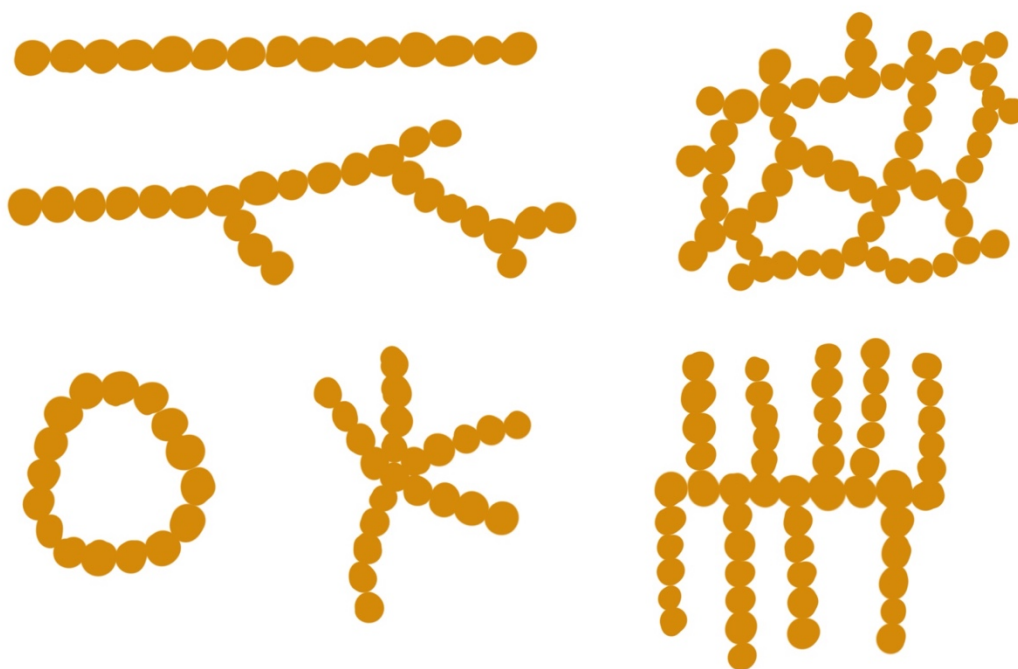


**Figure 1.2.** Polymer topology plays an important role in polymer properties. Shown here are cartoon depictions of (top to bottom, left to right) a linear polymer, branched polymer, cyclic polymer, star polymer, network polymer, and bottlebrush polymer.

Another materials design parameter under investigation is molecular weight distribution. The molecular weight distribution encompasses dispersity as well as the skew in a polymer sample toward high or low molecular weights (Fig. 1.3). Dispersity

and the shape of the molecular weight distribution can be thought of as additional ways to alter polymer properties without changing chemical composition, similar to branching or molecular weight.[50,51] For instance, low and high dispersity samples of the same polymer type have been shown to differ in terms of viscosity, Young's modulus, glass transition temperature ($T_g$), stiffness, thermal stability, flexibility, and interaction with nanoparticles, bacteria, and other substances.[50–58] Dispersity and molecular weight distribution also affect self-assembly of block copolymers in solution and the solid state.[59–65] While low dispersity is often a prized marker of a successful polymer synthesis, dispersity is better thought of as a parameter to tune based on the desired application. It is important to note that even polymer samples with extremely low dispersity values still differ drastically in their properties compared to samples of discrete chain lengths. Studies of discrete polymers are few, because obtaining these materials requires time-consuming separation or in certain cases, clever reaction manipulation,[66] but uniform polymer samples have been reported to have smaller domain sizes, to be more crystalline, and to be less stable than typical, disperse polymer samples.[50,67,68] In addition to these physical properties, electronic properties of discrete species also differ from those of polymer samples with a range of molecular weights. For example, each oligomer in a series of discrete oligo(3-hexylthiophene)s showed a unique emission color, which was not apparent in the oligomer mixture.[69] Thus the distribution of chain lengths in a polymer sample can also be used to tune overall properties.

**1.4 New Carbon Materials at the Intersection of Polymer Chemistry and Organic Synthesis**

The tools and techniques used to study discrete small molecules are insufficient for characterizing polymer samples and vice versa, so polymer chemistry and traditional organic synthesis are often thought of as being quite distinct. With the scope of functionalities that can be incorporated into polymers rapidly expanding and the control over polymer structures approaching the molecular level, however, these two fields are overlapping more and more.[70] Now techniques from both fields are required to characterize ever-more-sophisticated polymeric materials. In addition, concepts can be borrowed from both fields in order to design new materials.

5
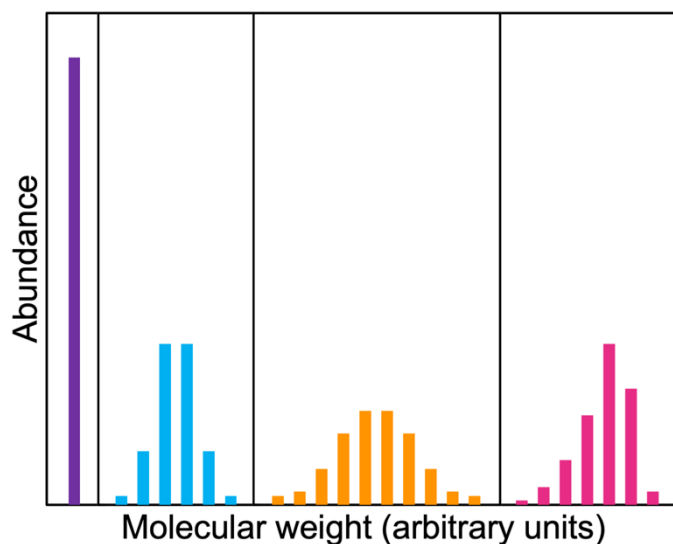
**Figure 1.3.** These cartoon histograms show the relative abundance of polymer chains with certain molecular weights for polymer samples with a discrete chain length (purple), narrow dispersity (blue), broad dispersity (orange), and skewed molecular weight distribution (pink).

One area which can benefit from both polymer chemistry and organic synthesis approaches is design and synthesis of carbon nanomaterials. Apart from molecular nanocarbons such as corannulene and fullerenes, preparing well-defined carbon nanomaterials is an enduring challenge. Carbon nanotubes (CNTs) and graphene can be thought of as unconventional polymers, and perhaps one day they will be accessed as precise structures via a combination of total organic synthesis and controlled polymer synthesis. Fragments of these structures have been prepared with moderate success. The first full carbon nanobelt—fused benzenes mapping onto a (6,6)CNT—was reported in 2017.[71] This molecule marked an important milestone in the field of polyaromatic chemistry, but the low-yielding synthesis suggests it will be quite some time before this route will yield more extended nanotube fragments or enough material to prepare polymers. Carbon nanobelts mapping onto (8,8)CNT, (12,12)CNT, and chiral (18,12)CNT have since been reported.[72,73] Other approaches have led to nanotube fragments with periodic vacancies[74] and conjugated polymer segments of (8,8)CNT.[75] A variety of graphene nanoribbons have been prepared with different levels of precision,[76–79] and research has shown that the electronic properties of these nanoribbons are highly dependent on uniformity and edge structure. Extended diamondoid structures, or carbon

nanothreads, can be prepared by pressure-induced polymerization of benzene, furan, naphthalene, and fluorinated aromatics.[80–83] Multiple (both step-growth and chain-growth) polymerization methods have been used to construct polymers from corannulene units, and these polymers have shown potential for fullerene hosting, gas uptake, and energy storage.[84–86] These examples of materials being developed at the intersection of nanocarbons and polymers hint at the vast possibilities for new carbon materials and their as yet untapped properties.

**1.5 Role of Macrocycles in Polymer Chemistry**

In a similar manner to how cyclic polymers differ from linear ones, cyclic molecules exhibit different properties from linear ones with the same functionality. Building cyclic motifs into polymers can likewise give rise to materials with new properties. Although still relatively uncommon, macrocycle-based polymers demonstrate distinct advantages over polymers made up of acyclic units. Various macrocycles have been shown to improve polymer solubility,[87] decrease crystallinity,[88] and serve as hosts for sensing and separation applications[25,89–92] (Fig. 1.4). Even macrocycles which are embedded in a polymer matrix but not covalently connected to the polymer backbone can change the morphology, stretchability, and electronic performance of the material.[93,94] Macrocycles are useful motifs in supramolecular polymers,[20,95,96] and they are critical components of polymers containing topological bonds, including polycatenanes,[97,98] polyrotaxanes,[99] and slide-ring gels.[100] Polymers with [c2]daisy chain linkages[101] have shown muscle-like actuation capabilities, and polymers with semi-mobile [2]rotaxane cross-links, in which a macrocycle covalently linked to one segment of polymer backbone encircles another polymer chain, exhibit different mechanical properties than totally covalently cross-linked gels.[102,103] While these examples highlight the many desirable features of macrocycle-based polymers, by far the most commonly employed macrocycles are cyclodextrins, leaving other classes of macrocycles underexplored in polymeric materials.
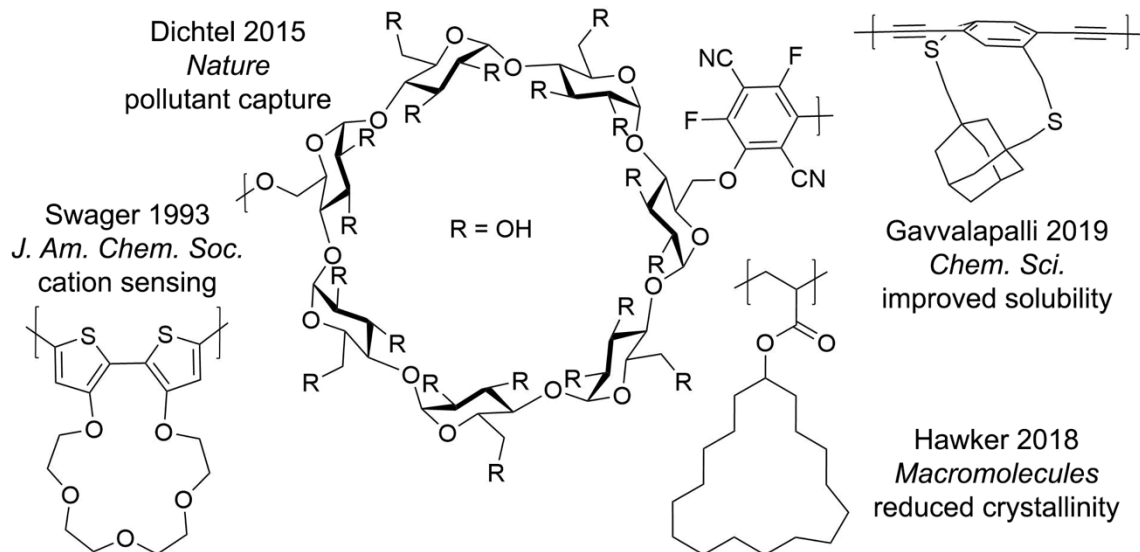
**Figure 1.4.** Macrocycles in polymers can improve solubility, decrease crystallinity, and serve as hosts for sensing and separation applications.

Cyclic structures are also employed to synthesize polymers that do not contain macrocycles in the final material. Ring-opening polymerizations rely on cyclic monomers, and macrocyclic monomers yield alternative polymer backbones compared to those which arise from commonly used small cyclic monomers. Properly designed cyclic monomers can deliver desirable polymer structures with a high degree of control. For example, when subjected to ring-opening metathesis polymerization conditions, [2.2]paracyclophane-1-ene and [2.2]paracyclophane-1,9-diene monomers give access to poly(phenylenevinylene)s[104,105] which previously could not be synthesized in a living manner.[106,107] More recent studies have expanded on this strategy to yield regioregular polymers from asymmetrical [2.2]paracyclophane-1,9-diene derivatives[108] and alternating donor-acceptor polymers with different backbone units.[109] Larger macrocyclic monomers with a predetermined order of functional groups give rise to polymers with longer segments of specific repeating sequences.[34,35] The post-polymerization ring-opening of cyclic structures in polymers can also give rise to a drastic change in properties. Spiropyran and rhodamine derivatives are frequently used in polymers to enable changes in color (visual light absorbance) or fluorescence upon ring-opening of these motifs.[110–112] When incorporated as pendant groups, spiropyrans lead to switchable photochromic polymers,[113] and when placed in the polymer backbone, these motifs are effective for

stress sensing due to their mechanochromic nature.[114,115] Mechanical force has also been used to convert insulating nonconjugated polymers to semiconducting conjugated ones in the process of opening cyclic motifs in the polymer backbone.[116,117] Cyclic structures that can be polymerized are a valuable tool to trigger changes in color, fluorescence, electronics, and other properties using various external stimuli,[118] and new cyclic structures with dramatically different properties from their linear counterparts are highly desirable for this purpose.

**1.6 Cycloparaphenylenes as Polymer Precursors**

We set out to examine the utility of a family of macrocycles known as cycloparaphenylenes (CPPs) for preparing new polymers. The [*n*]CPPs are a family of molecules made of *n* benzene rings curved into size-controlled "nanohoops." These macrocycles, which are structurally equivalent to a cross-section of an armchair carbon nanotube, can be made size-selectively with 5 or more benzene rings (Fig. 1.5). The remarkable architecture of CPPs imparts properties that differ significantly from the properties of acyclic conjugated molecules. For instance, CPPs have smaller HOMO-LUMO gaps than the longest linear paraphenylenes, and red-shifted fluorescence emission as the molecule size decreases, exactly the opposite of what is seen in acyclic conjugated systems.[119] The strain inherent in these nanohoops composed of bent benzene imparts unique modes of reactivity.[120,121] Unlike many other classes of macrocycles, these oligomeric nanohoops can be made in a modular fashion and selectively functionalized at precise positions. This high degree of synthetic control allows a wide range of optoelectronic and physical properties to be accessed with these structures. In recent years, CPP derivatives have become increasingly diverse, as have the uses for these molecules. In addition to the earliest applications of CPPs as blueprints for the bottom-up construction of discrete graphitic materials, predominantly carbon nanotubes,[122–124] now CPP derivatives are also being developed as sensors,[125] fluorescent probes for biological imaging,[126] porous materials for gas uptake,[127,128] and more.

**Cycloparaphenylenes**
Precisely tunable circular pore
Size-dependent bright fluorescence
Enhanced solubility over linear analogues
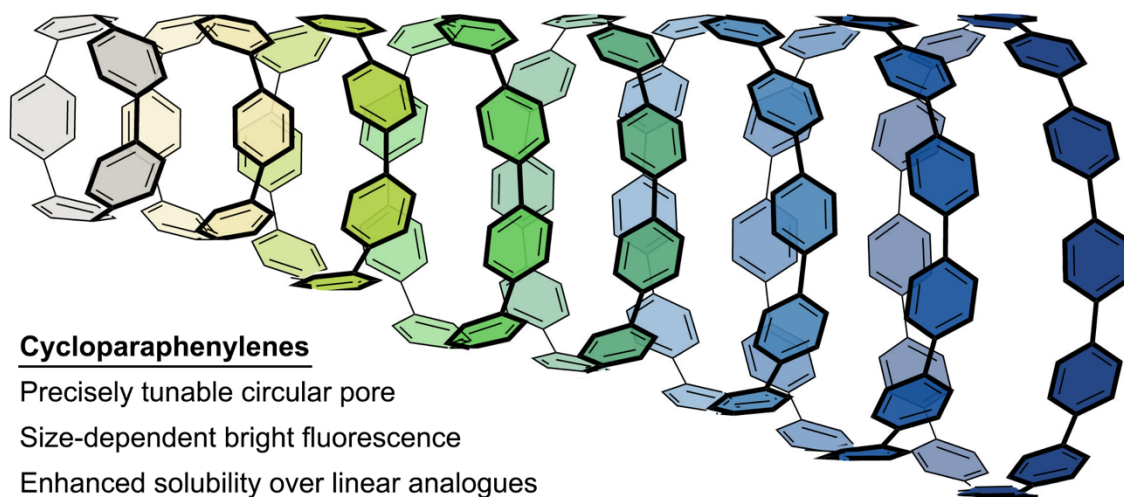
**Figure 1.5.** The cyclic architecture of cycloparaphenylenes impacts their fluorescence emission, solubility, and supramolecular interactions within their pores.

Considering the broad range of properties of and applications for CPPs and their small molecule derivatives, we expected that incorporating CPPs into polymers would provide extensive opportunities to design new polymeric nanomaterials with exciting properties (Fig. 1.6). The bright fluorescence, solubility, host-guest capabilities, and porosity of CPPs are all aspects which could be capitalized on in polymers. Chapters II and III detail two approaches to assembling polymers from CPPs and describe the properties of the resultant materials. These chapters also include discussion of the future prospects for CPP-based polymeric nanomaterials based on what we have learned so far. In addition to polymers containing intact CPP units, we envisioned that polymers could be constructed from CPP-like macrocycles using ring-opening strategies. Chapter IV covers a new macrocyclic monomer scaffold for ring-opening metathesis polymerization as well as an emerging area of study relating to the mechanochemical ring-opening of CPP units in polymers to produce a measurable response. The studies in this dissertation combine the bottom-up synthesis of CPPs (and similar macrocycles) with polymer chemistry approaches to access new carbon materials.
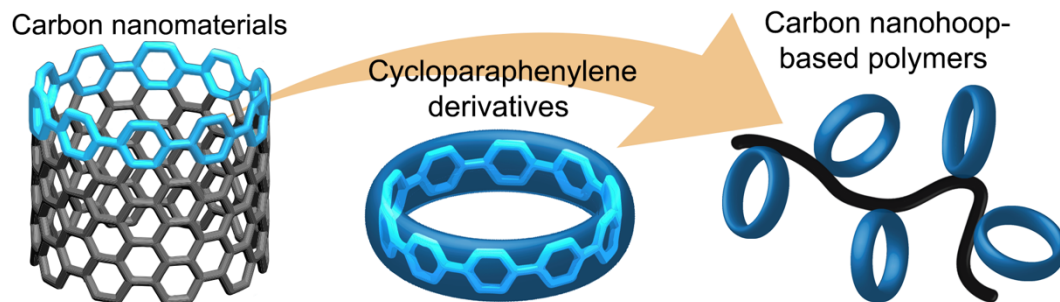
**Figure 1.6.** Cartoon depiction of [10]CPP as a fragment of an armchair carbon nanotube that can be used as a building block for polymers.

CHAPTER II

CONTROLLED POLYMERIZATION OF NORBORNENE

CYCLOPARAPHENYLENES

Chapter II is adapted from a manuscript published in *ACS Central Science* under the title "Controlled Polymerization of Cycloparaphenylene Norbornenes Expands Carbon Nanomaterials Design Space."[1] Further permissions related to material excerpted from this article should be directed to the ACS. Excerpts from this article were written by myself. Dr. Penghao Li, Brian Sun, and Harrison Reid contributed to monomer synthesis and characterization. Dr. Baihao Shao conducted solid-state optical measurements. Sarah Zeitler and Prof. Matthew Golder carried out multi-angle light scattering (MALS) analysis. Dr. Lev Zakharov conducted X-ray crystallography analysis. Prof. Ramesh Jasti edited the manuscript and provided guidance on the project.

## 2.1 Introduction

The versatility of carbon nanomaterials makes them extremely useful. From graphitic structures such as carbon nanotubes and fullerenes, which have become indispensable in electronics,[129,130] to carbon quantum dots with tunable fluorescence,[131] carbon materials have emerged as promising candidates for a wide range of applications. The utility of carbon nanomaterials for various end uses ultimately depends on how well their properties can be fine-tuned. Currently, many carbon materials are prepared through uncontrolled processes, resulting in poorly defined products and hindering the design of new materials based on structure-property relationships. In recent years, significant progress has been made in synthesizing molecular nanocarbons with new geometries, functionalities, and properties,[78,132,133] as well as employing polymer chemistry as a means to access useful carbon-based materials.[18,76,134–136] Major challenges remain, however; the majority of syntheses of extended carbon structures rely on lengthy synthetic sequences—often impeded by substrate insolubility, tedious purification steps, and low yields—or uncontrolled, step-growth polymerization methods. Notwithstanding notable exceptions,[84,105,109,137] the connectivities and functionalities accessible via well-controlled methods remain limited.

To address these challenges, we envisioned that a family of oligomeric nanocarbons—cycloparaphenylenes—could serve as the basis for constructing larger, structurally-defined carbon materials using controlled polymerization (Fig. 2.1). Cycloparaphenylenes (CPPs) are atomically precise cyclic oligomers, and, like discrete linear oligomers,[69] each CPP size exhibits unique properties.[119] In addition to changing the number of phenyl rings, the properties of CPPs can also be influenced by incorporating a *meta* linkage,[138] a donor-acceptor motif,[139] or other structural modifications. The cyclic architecture of CPPs makes them especially exciting building blocks for materials. Other classes of macrocycles have previously been shown to impart improved solubility,[87] enhanced physical properties,[93,140] capabilities for guest uptake,[25,92,141] and opportunities for varied topology[97,100–102] in polymeric materials. CPPs share these desirable traits with other macrocycles[94,142–145] and offer an additional advantage over most other macrocycles in that they can be synthesized and functionalized in a completely modular way.

While CPP-based polymers have previously been prepared via cross-coupling polymerization,[2,75] constructing polymers from CPPs would be especially powerful using controlled or "living" polymerization techniques. Controlled chain-growth polymerization enables synthesis of block copolymers, opening the door to self-assembly and complex hierarchical structures.[31] The ability to control polymer chain length and to prepare block copolymers also provides access to materials which arise from the same monomers but possess different properties. For this study, we selected ring-opening metathesis polymerization (ROMP) as a route that would not present unwanted modes of reactivity with CPPs, which can undergo strain-relieving reactions not seen in linear aromatic molecules.[146,147] ROMP, particularly with Ru-based initiators, is known for being well-controlled and highly tolerant of a variety of functional groups.[148–150] We first sought to demonstrate that ROMP could be used to polymerize all-carbon CPP monomers, with the hopes that this strategy will be applicable to functionalized CPP monomers in the future.
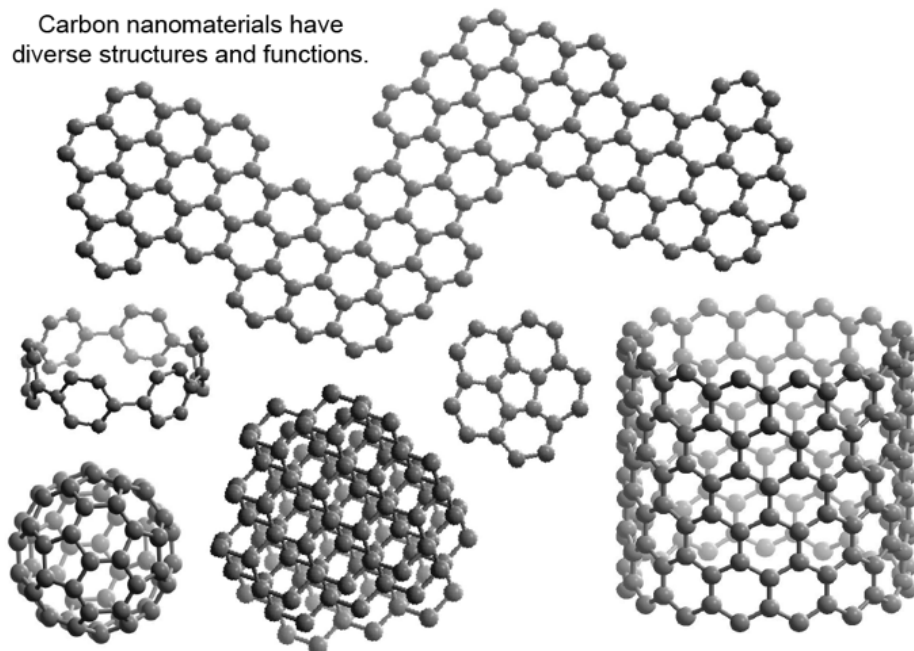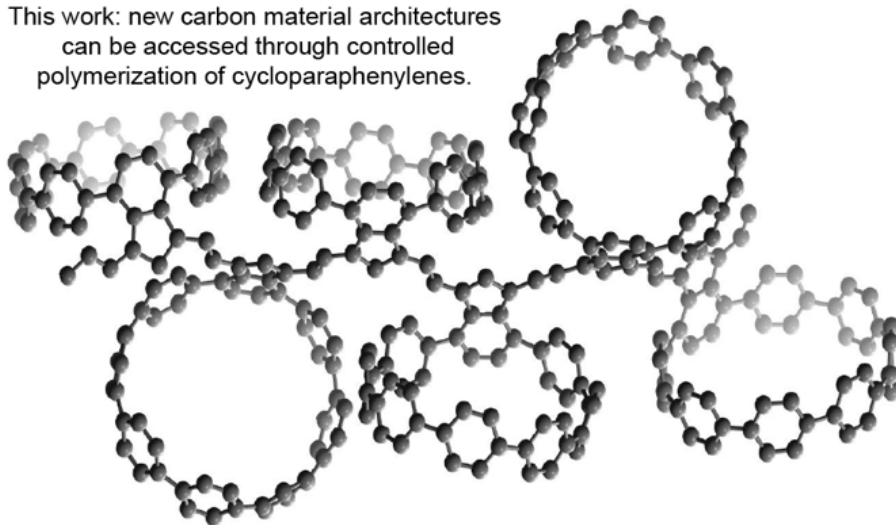
**Figure 2.1.** Combining synthetic organic and polymer chemistry approaches can lead to carbon materials with new properties.

Here we describe the synthesis and characterization of a series of norbornene CPP monomers (**nb[8]CPP**, **nb[9]CPP**, and **nb[10]CPP**) and show their controlled polymerization via ROMP. This approach generated homopolymers with precise cyclic side chains of varying sizes as well as block and statistical copolymers comprising CPP units of two different sizes. The resultant polymers were studied using a variety of methods to gain insight into the degree of control over the polymerization and to begin to

unravel structure-property relationships for this new class of carbon materials. In particular, we found that poly(nbCPP) homopolymers largely retain the fluorescence properties of the constituent monomers, but to our surprise, block and statistical copolymers with the same composition exhibited divergent fluorescence emissions. Likewise, both composition and sequence played a role in the fluorescence response of poly(nbCPP)s to $C_{60}$ addition. To conclude, we offer ideas for further materials development based on these findings.

## 2.2 Results and Discussion

### 2.2.1 Monomer and Polymer Synthesis and Structural Characterization

Our general synthetic strategy toward CPPs hinges on the use of cyclohexadienes as masked phenylenes.[142] These cyclohexadiene units provide the curvature necessary to carry out the macrocyclization step and can be aromatized at the end of the synthetic sequence. Incorporation of a ROMP-reactive benzonorbornadiene unit in the CPP backbone was readily accomplished using this approach (Scheme 2.1). Norbornene-benzoquinone **II.1** was selected as a functionalized cyclohexadiene-containing precursor. Double nucleophilic addition of (4-bromophenyl)lithium to **II.1** followed by *in situ* methylation of the resulting alkoxides yielded dibromide **II.2**. This curved intermediate served as a common coupling partner for forming multiple sizes of norbornene CPPs in a modular manner. Norbornene CPP monomers with 8, 9, and 10 phenyl rings were targeted by varying the length of the unfunctionalized coupling partner. Bisboronate coupling partners **II.3**, **II.4**, and **II.5** were prepared by iterative diastereoselective nucleophilic additions and cross-coupling reactions (see 2.5.5.2). These coupling partners were subjected to dilute Suzuki-Miyaura cross-coupling conditions with **II.2** to obtain macrocycles **II.6**, **II.7**, and **II.8**, respectively. Finally, reductive aromatization of these macrocycles yielded the desired monomers: **nb[8]CPP**, **nb[9]CPP**, and **nb[10]CPP**. ^{1}H NMR spectra of these monomers show distinct signals for the protons on and around the benzonorbornadiene unit, with the remaining protons on the nanohoop backbone appearing as one overlapping peak with the chemical shift dependent on nanohoop size (Fig. 2.8). Monomer structures were confirmed using X-ray crystallography (see 2.5.5.3). The ease of appending a norbornene group onto CPPs in this manner indicates that this

approach could also be effective for synthesizing polymerizable versions of CPPs containing heteroatoms and of other CPP derivatives.
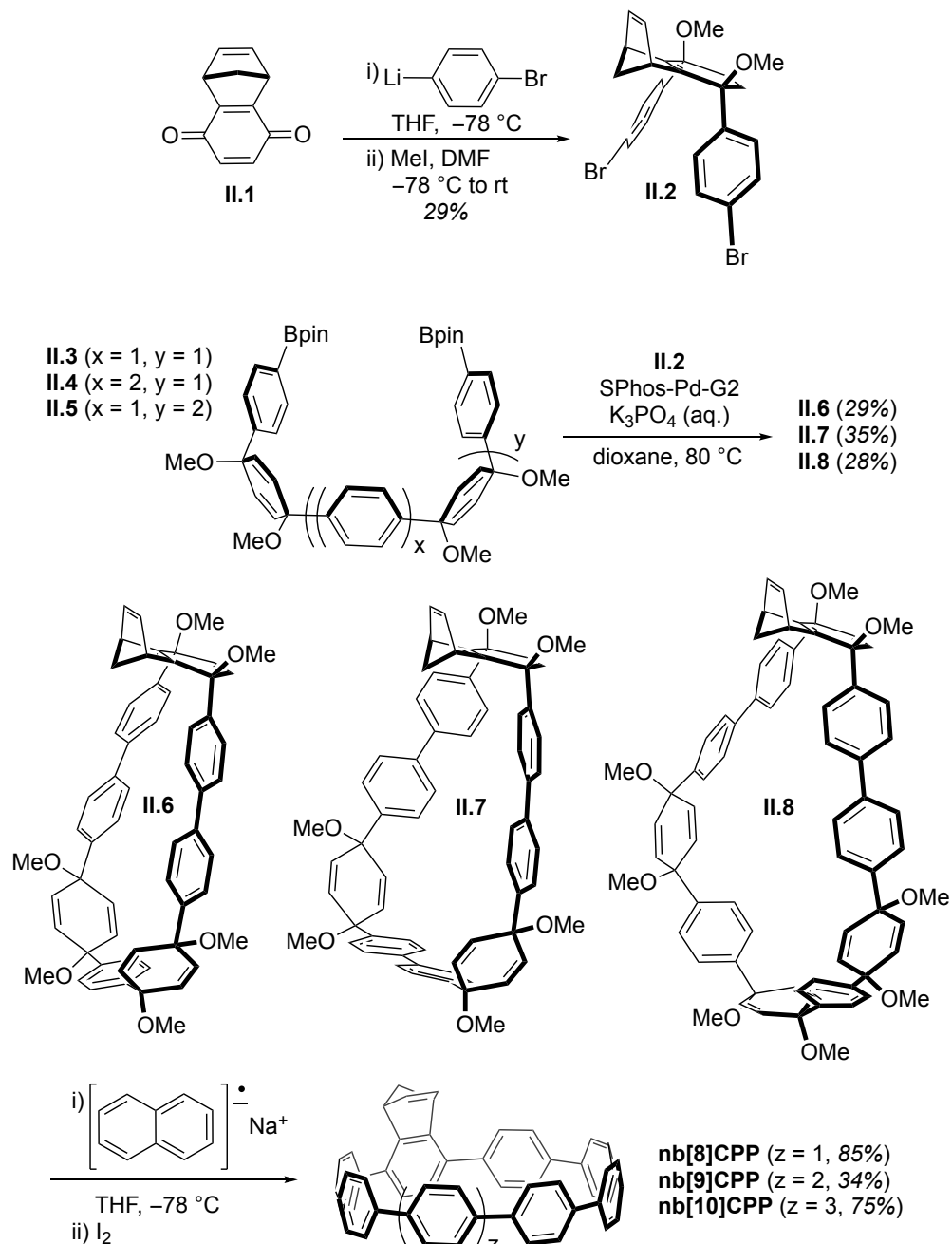


**Scheme 2.1.** Key steps for synthesizing **nb[8]CPP**, **nb[9]CPP**, and **nb[10]CPP** monomers.

With this series of norbornene CPPs in hand, we turned to investigating the polymerization of these compounds. We screened a range of ROMP conditions and evaluated the success of the polymerizations based on conversion of monomer to polymer and resultant polymer dispersity. Conversion was estimated using routine $^1$H NMR spectroscopy to compare the size of polymer peaks to the peaks from residual monomer, if any, and dispersity was determined using gel permeation chromatography (GPC) with a refractive index (RI) detector. We found that we could obtain **poly(nb[8]CPP)**, **poly(nb[9]CPP)**, and **poly(nb[10]CPP)** under a variety of conditions (Fig. 2.2a and Tables 2.3 and 2.4). For instance, polymerizations of **nb[8]CPP** were conducted successfully in tetrahydrofuran (THF), dichloromethane (DCM), and chloroform, with the reactions in chloroform providing the lowest measured dispersity values. Subjecting **nb[10]CPP** to Grubbs G1 did not produce any polymer, but both Grubbs G2 and bromopyridyl Grubbs G3 were effective in initiating polymerization. Except in instances where the polymerization reactions did not go to completion and peaks were still visible from residual monomer, NMR spectra for each polymer type looked identical regardless of reaction conditions, indicating that the resultant polymers had the same backbone structure. In each case, $^1$H NMR spectra of the polymers showed broadening of the overlapping peak from the protons on the nanohoop backbone as well as the appearance of extremely broad peaks centering around 6.66 ppm, 5.65 ppm, and 4.37 ppm (Fig. 2.2b and Fig. 2.8). However, the complex stereochemical environment due to many possible orientations of the CPP side chains around the polymer backbone limited the amount of structural information available from NMR spectroscopy. To further verify formation of the desired polymer products, we obtained matrix-assisted laser desorption ionization (MALDI) mass spectra of samples of **poly(nb[8]CPP)** and **poly(nb[10]CPP)**. Disproportionately high intensity in the lower m/z range prevented determination of the average molecular weights of the samples from the MALDI spectra, but we did observe uniform peak spacing corresponding to the mass of the repeat units (Fig. 2.9), confirming that the CPP structures remained intact during ROMP. Samples referenced hereafter in the main text were prepared in chloroform with Grubbs G3 as the initiator, and comparable results from samples prepared in THF can be found in section 2.5.
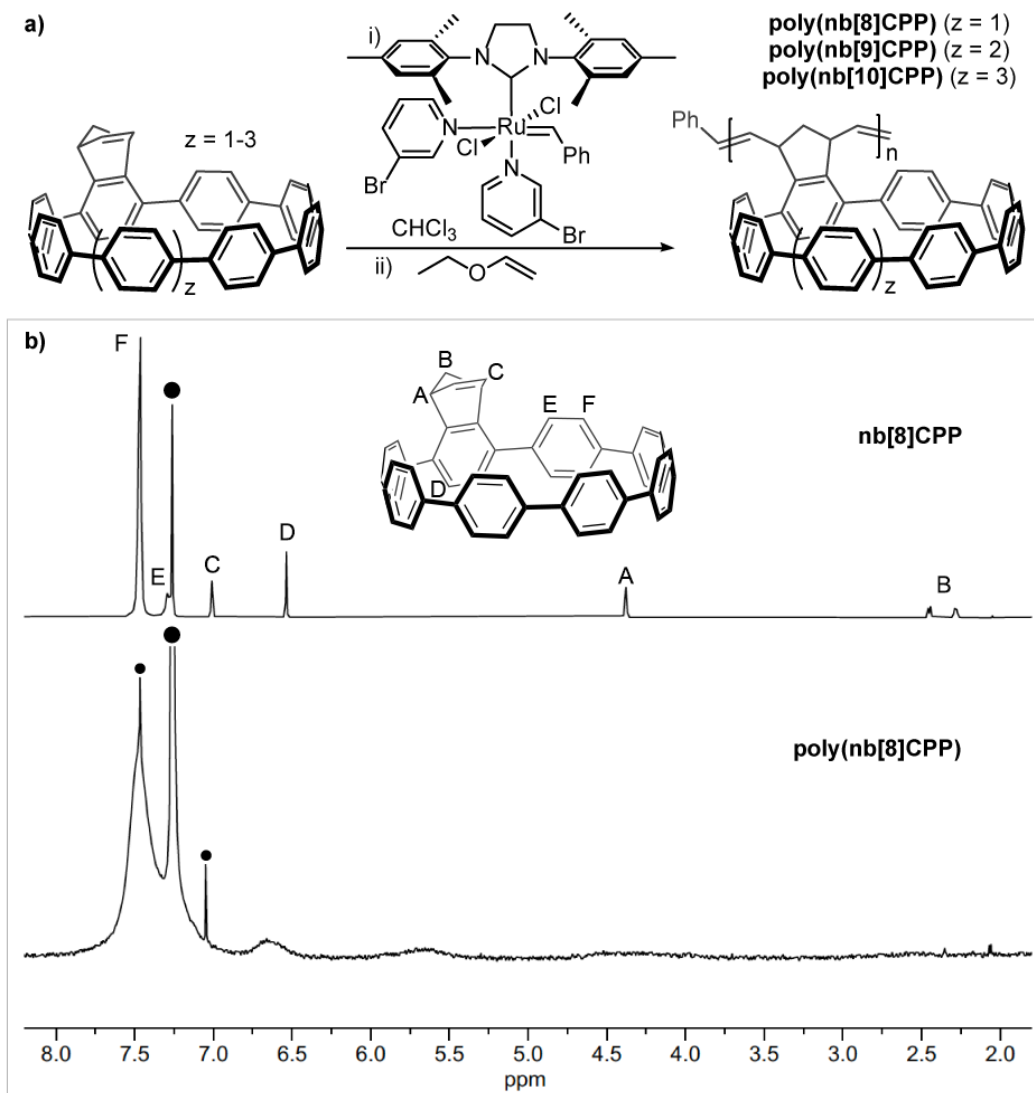
**Figure 2.2.** a) Polymerization of nbCPP monomers under ROMP conditions. b) Stacked ¹H NMR spectra of **nb[8]CPP** and **poly(nb[8]CPP)** (spectrum from sample 4, Table 2.3). CHCl₃ and its satellite peaks are marked with circles. The peak labeled F corresponds to all CPP backbone protons not otherwise assigned.

Once it was clear that **nb[8]CPP**, **nb[9]CPP**, and **nb[10]CPP** undergo ROMP as expected, we next addressed the question of "livingness" of the polymerizations in more detail. Although few polymerizations meet the strictest definition for "living" polymerizations,[151] the key capabilities of practical importance are attaining a range of molecular weights in a predictable manner, achieving dispersity values suitable for the intended application, and synthesizing block copolymers. We were able to demonstrate these attributes in the synthesis of poly(nbCPP)s, showing that the polymerization is

well-controlled, if not entirely "living." By varying the monomer-to-initiator ratio, we targeted several different molecular weights for **poly(nb[8]CPP)**, **poly(nb[9]CPP)**, and **poly(nb[10]CPP)**, focusing mostly on **poly(nb[8]CPP)** and **poly(nb[10]CPP)**. When analyzing GPC$_{RI}$ results from these polymerizations, we noticed dramatic differences between the theoretical molecular weights based on monomer-to-initiator ratios and the measured molecular weight values (versus polystyrene standards, see Fig. 2.10). These discrepancies indicated that although polystyrene is routinely used as a standard for molecular weight measurements of many types of polymers, it exhibits significantly different solution-state conformation and/or interactions with GPC column materials than poly(nbCPP)s, so these molecular weight results should be considered primarily as relative values. Despite this caveat, we were able to establish linear relationships between the monomer-to-initiator ratios and the measured molecular weights for samples of **poly(nb[8]CPP)**, **poly(nb[9]CPP)**, and **poly(nb[10]CPP)** (Fig. 2.3). Dispersity values for these samples ranged from 1.08 to 1.56, with no apparent relationship to degree of polymerization (Table 2.3). Due to the highly unusual nature of poly(nbCPP)s, we conducted control experiments with a low molar mass, acyclic benzonorbornadiene monomer (**diMeObnb**) to validate our polymerization procedure and to contextualize our molecular weight results. We found that while there was still a moderate difference between theoretical and measured molecular weight values for the model polymer, we consistently achieved low (typically ≤ 1.05) dispersity values (Table 2.4). Comparing the model system with the CPP-based polymers, it became apparent that solubility was a critical factor in the polymerization outcomes. Generally for ROMP, high monomer concentrations are ideal for achieving polymer samples with low dispersity.[152] CPP derivatives are well-soluble relative to other polyaromatic hydrocarbons, but are certainly less soluble than a typical low molecular weight monomer, so we had to decrease the concentration of our reactions accordingly. Particularly with **nb[10]CPP**, the least soluble of the monomers, some polymerizations did not go to completion – not due to insufficient reaction time, but rather due to a small amount of monomer being deposited on the sides of the flask rather than being in solution. Solubility also played an important role for analysis of the final polymers. We found that above a certain degree of polymerization (DP), measured molecular weights no longer followed the established

trend because of incomplete solubility of the polymer samples (Table 2.3). Surprisingly, **poly(nb[8]CPP)** had the lowest cutoff for solubility, with samples over DP 100 being noticeably less soluble and DP 200 samples being completely insoluble. Finally, we carried out GPC analysis on select samples using a multi-angle light scattering (MALS) detector to obtain more accurate molecular weight values that could serve as a frame of reference for the remaining poly(nbCPP) samples. The molecular weights obtained from $GPC_{MALS}$ were notably higher than both the previously measured $GPC_{RI}$ values and the theoretical molecular weights (Table 2.1). Interestingly, $GPC_{MALS}$ analysis also indicated lower dispersity values in all cases, and the majority of samples had dispersities less than 1.10. The large divergence between $GPC_{MALS}$ and $GPC_{RI}$ results brings to light the value of acknowledging the limitations of various molecular weight measurement techniques, carefully considering underlying assumptions, and avoiding overinterpretation of ambiguous or imperfect results (for instance, placing undue emphasis on low dispersity when clearly it depends on measurement technique). In addition, $GPC_{MALS}$ was used to assess the solution-state conformation of DP 200 **poly(nb[10]CPP)** (other samples were below the limit of detection). The relationship between radius of gyration and molecular weight for this sample (Fig. 2.14) indicated a dense, sphere-like conformation, a result that could help explain the lower-than-expected molecular weight values obtained from $GPC_{RI}$. Intrinsic viscosity measurements and subsequent Mark-Houwink analysis also indicated hard sphere polymer chain conformations (a < 0.5) for poly(nbCPP)s (Fig. 2.13).[153]

 After determining that ROMP of nbCPPs proceeds in a controlled manner based on the ability to regulate the molecular weight of polymer samples, we were extremely interested in demonstrating that block copolymers composed of CPP units could be prepared this way. One marker of a "living" polymerization is that polymer chain ends remain active until a terminating agent is added, allowing formation of block copolymers by sequential addition of different types of monomers. We focused our attention on the synthesis of block copolymer **poly(nb[10]CPP-*block*-[8]CPP)** and statistical copolymer **poly(nb[8]CPP-*stat*-[10]CPP)** for comparison, both with a 1:1 mole ratio of **nb[8]CPP** and **nb[10]CPP**. **Poly(nb[8]CPP-*stat*-[10]CPP)** samples were prepared by premixing **nb[8]CPP** with **nb[10]CPP**, then treating the mixture with Grubbs G3. In contrast, to
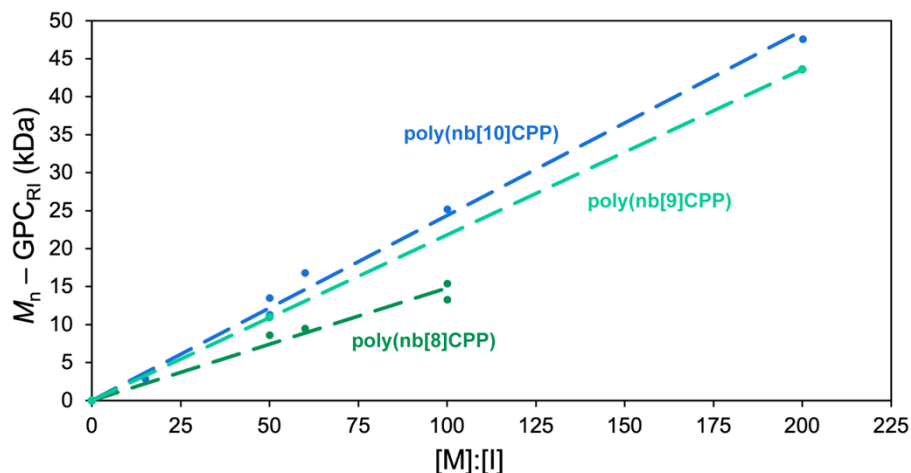
**Figure 2.3.** Plot of measured molecular weights (GPC_{RI}) versus monomer-to-initiator ratio for polymerizations conducted with Grubbs G3 in chloroform (data for plot in Table 2.3).

| Sample[a] | [M]:[I] | Theoretical $M_n$ (g/mol) | $M_n -$ GPC_{RI} (g/mol) | Đ – GPC_{RI} | $M_n -$ GPC_{MALS} (g/mol) | Đ – GPC_{MALS} |
|---|---|---|---|---|---|---|
| p[8] | 50 | 33,700 | 8,500 | 1.18 | 60,500 | 1.07 |
| p[8] | 100 | 67,400 | 13,300 | 1.23 | 98,600 | 1.04 |
| p[9] | 50 | 37,600 | 10,900 | 1.22 | 60,200 | 1.10 |
| p[10] | 50 | 41,400 | 13,600 | 1.19 | 67,200 | 1.06 |
| p[10] | 100 | 82,600 | 25,000 | 1.22 | 118,000 | 1.08 |
| p[10] | 200 | 165,000 | 48,200 | 1.56 | 274,000 | 1.23 |

**Table 2.1.** GPC (RI/MALS) results for selected polymer samples. [a]In Table 2.1 and Table 2.2, **p[8]** = **poly(nb[8]CPP)**; **p[9]** = **poly(nb[9]CPP)**; **p[10]** = **poly(nb[10]CPP)**.

prepare **poly(nb[10]CPP-*block*-[8]CPP)**, **nb[10]CPP** was first added to a flask and polymerized according to the typical procedure, then an aliquot was removed from the reaction for analysis, and a solution of **nb[8]CPP** was transferred into the reaction to form the second block (see 2.5.2 for details). Comparison of ^1H NMR spectra and GPC traces obtained after reaction of the first block and both blocks clearly show that synthesis of the desired block copolymer **poly(nb[10]CPP-*block*-[8]CPP)** was successful (Fig. 2.4). In the NMR spectrum of **poly(nb[10]CPP-*block*-[8]CPP)**, an additional peak appears at 7.47 ppm, corresponding to **nb[8]CPP** units. GPC shows the expected increase in molecular weight with minimal change in dispersity after extension of the polymer chains with the second block. NMR and GPC results for **poly(nb[8]CPP-*stat*-[10]CPP)**

(see section 2.5) were similar to the results for **poly(nb[10]CPP-*block*-[8]CPP)**, indicating that the samples have comparable compositions and molecular weights, as expected, and differ only by sequence of the constituent monomers. MALDI spectra were obtained for some copolymer samples, and while these were again not suitable for determining average molecular weight, they do show differing "fingerprints" for block and statistical copolymers (Fig. 2.9). Successful synthesis of **poly(nb[10]CPP-*block*-[8]CPP)** provides further support for the controlled nature of ROMP of nbCPPs.
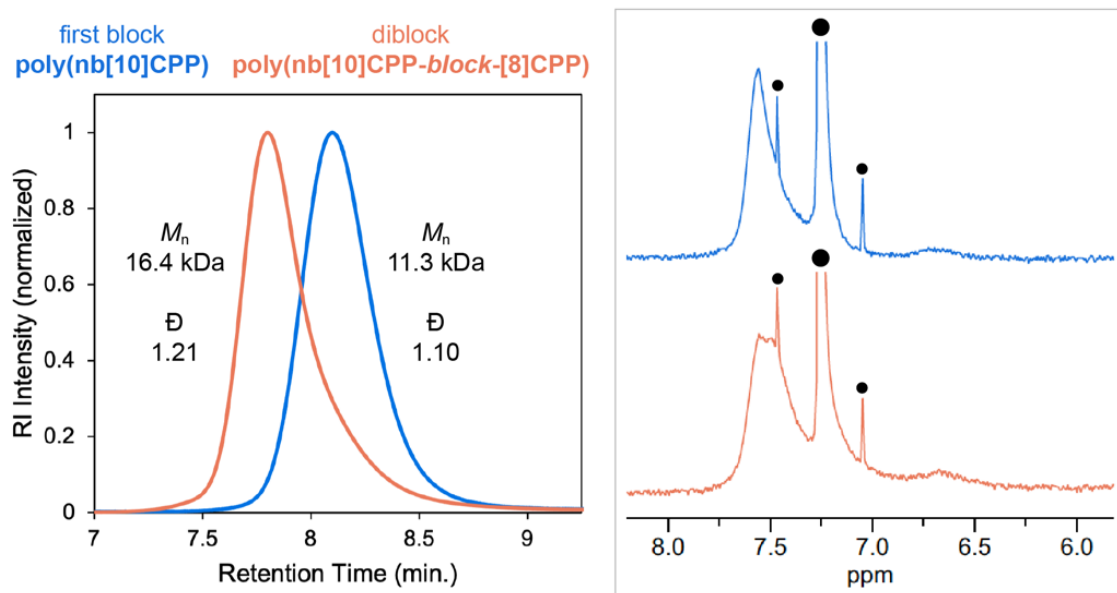


**Figure 2.4.** GPC$_{RI}$ (left) and $^1$H NMR (right) evidence for formation of **poly(nb[10]CPP-*block*-[8]CPP)** (data from sample 1, Table 2.5). CHCl$_3$ and its satellite peaks are marked with circles.

### 2.2.2 Monomer and Polymer Optical Properties

We next used UV-Vis absorption and fluorescence spectroscopies to examine the optical properties of nbCPPs and poly(nbCPP)s. We were interested in 1) determining whether the appended norbornenes would alter the properties of nbCPPs relative to unfunctionalized CPPs, 2) assessing the degree to which the optical properties of nbCPPs are retained in poly(nbCPP)s, and 3) comparing optical properties among poly(nbCPP)s with consideration to the additional materials design parameters of polymer composition and sequence. For context, CPPs have an absorbance maximum near 340 nm regardless

of nanohoop size, but in contrast to linear paraphenylenes, the emission maxima of CPPs red-shift as the number of phenyl units decreases. For instance, the emission maxima for [10]CPP, [9]CPP, and [8]CPP are 466 nm, 494 nm, and 533 nm, respectively.[119] We found that the common absorption band of CPPs was retained in the norbornene CPP monomers, and fluorescence maxima of the norbornene monomers in solution were nearly identical to those of the parent CPPs (Table 2.2). Like with the parent CPPs,[154,155] both the extinction coefficients and quantum yields of nbCPPs increase with nanohoop size, resulting in the larger nanohoops being brighter fluorophores. Although CPPs are bright solids, reports on solid-state fluorescence measurements of these molecules are scarce. The few available examples report much lower quantum yields of CPPs as solids than in solution, except when the CPPs are "diluted" in a polymer matrix.[156–158] We examined the solid-state fluorescence of **nb[8]CPP**, **nb[9]CPP**, and **nb[10]CPP** and found that the trend in quantum yield reverses compared to the solution results, with **nb[8]CPP** having the highest quantum yield as a solid. The difference among the values also narrows, with all of the monomers exhibiting quantum yields between 0.34 and 0.44, quite high for neat solids (Table 2.2). In summary, to the extent we could compare to literature, the optoelectronic properties of **nb[8]CPP**, **nb[9]CPP**, and **nb[10]CPP** are similar to the properties of [8]CPP, [9]CPP, and [10]CPP, respectively.

All of the polymers share an absorbance maximum near 340 nm—essentially no change from what is observed for nbCPP monomers and underivatized CPPs. The emission maxima for **poly(nb[8]CPP)**, **poly(nb[9]CPP)**, and **poly(nb[10]CPP)** are red-shifted a few nm relative to the respective monomers in both solution and the solid state (Table 2.2, Fig. 2.18, and Fig. 2.19). The quantum yields of the homopolymers in solution closely reflect the results for the respective monomers. The monomers themselves are very bright fluorophores, brighter than many common fluorescent dyes,[159] so discovering that poly(nbCPP)s retain a high quantum yield in solution is exciting. These polymers could for instance find use as ultra-bright fluorescent tags. As solids, however, the polymers have much lower quantum yields (Table 2.2), indicating that the polymers pack in a way that allows additional modes of non-radiative relaxation not available to the monomers in the solid state. In the case of copolymers, fluorescence emission varies with polymer sequence. **Poly(nb[10]CPP-*block*-[8]CPP)** exhibits

emission peaks correlating to both types of monomer units, whereas the emission spectrum of **poly(nb[8]CPP-*stat*-[10]CPP)** appears quite similar to that of **poly(nb[8]CPP)** (Fig. 2.5). We attribute this difference to energy transfer occurring between monomer units in **poly(nb[8]CPP-*stat*-[10]CPP)** but not **poly(nb[10]CPP-*block*-[8]CPP)**. Energy transfer between CPPs of different sizes was observed previously in a different system, a heterocatenane composed of [9]CPP and [12]CPP that exhibited a fluorescence emission spectrum closely resembling that of [9]CPP.[160] The occurrence of energy transfer between **nb[10]CPP** and **nb[8]CPP** units in statistical but not in block copolymers can be rationalized by considering the distance between the units in each case. Energy transfer only occurs efficiently at distances shorter than the Förster distance, $R_0$. Based on the overlap integral for the absorbance spectrum of **nb[8]CPP** and the emission spectrum of **nb[10]CPP**, $R_0$ for these molecules is around 2.4 nm (Fig. 2.20). There is a much higher likelihood of **nb[8]CPP** and **nb[10]CPP** units being within 2.4 nm of each other in **poly(nb[8]CPP-*stat*-[10]CPP)** compared to **poly(nb[10]CPP-*block*-[8]CPP)**. The emission spectrum of **poly(nb[10]CPP-*block*-[8]CPP)** can be replicated by blending samples of **poly(nb[8]CPP)** and **poly(nb[10]CPP)**, confirming that by increasing the distance between the two types of CPP units, they each fluoresce independently (Fig. 2.5). Energy transfer still occurs efficiently in statistical copolymers with varied ratios of **nb[8]CPP** and **nb[10]CPP** units, while in block copolymers and polymer blends with different compositions, the relative intensity of the emission peaks changes (Fig. 2.23). Altogether, the optical properties of this set of polymers offer promise for the development of advanced emissive materials. Not only can we obtain CPP-based homopolymers that retain the desirable properties of the constituent fluorophore units, such a high brightness, we can also access copolymers whose fluorescence can be modulated by altering polymer sequence and composition.

### 2.2.3 Fluorescence Response to $C_{60}$

Lastly, we wanted to evaluate poly(nbCPP)s as responsive materials using fullerene $C_{60}$ as an illustrative guest molecule. $C_{60}$ is the best-studied guest for CPPs, and its size-selective binding with [10]CPP (and [10]CPP derivatives) is marked by dramatic

| Sample | Absorbance Maximum, Solution (nm) | Absorbance Maximum, Solid (nm) | Extinction Coefficient $(L \cdot mol^{-1} \cdot cm^{-1})$ | Emission Maximum, Solution (nm) | Quantum Yield, Solution (%) | Emission Maximum, Solid (nm) | Quantum Yield, Solid (%) |
|---|---|---|---|---|---|---|---|
| nb[8]CPP | 334 | 333 | $(1.26 \pm 0.06) \times 10^5$ | 521 | $22.5 \pm 0.6$ | 515 | $43.1 \pm 1.4$ |
| p[8] DP 50 | 332 | 331 | n.d. | 527 | $20.3 \pm 0.8$ | 534 | $2.8 \pm 0.3$ |
| p[8] DP 200 | insoluble | n.d. | insoluble | insoluble | insoluble | 536 | $2.5 \pm 0.2$ |
| nb[9]CPP | 335 | 334 | $(1.29 \pm 0.11) \times 10^5$ | 483 | $53.8 \pm 0.1$ | 492 | $36.4 \pm 1.4$ |
| p[9] DP 50 | 334 | 335 | n.d. | 494 | $52.4 \pm 0.1$ | 496 | $1.0 \pm 0.1$ |
| nb[10]CPP | 336 | 329 | $(1.46 \pm 0.17) \times 10^5$ | 465 | $78.8 \pm 0.3$ | 460 | $34.1 \pm 0.3$ |
| p[10] DP 50 | 334 | 335 | n.d. | 471 | $74.8 \pm 0.5$ | 482 | $0.9 \pm 0.1$ |
| p[10] DP 200 | 334 | 335 | n.d. | 472 | $75.8 \pm 0.6$ | 482 | $2.7 \pm 0.2$ |

**Table 2.2.** Optical properties of **nb[8]CPP**, **nb[9]CPP**, **nb[10]CPP**, and selected polymer samples.
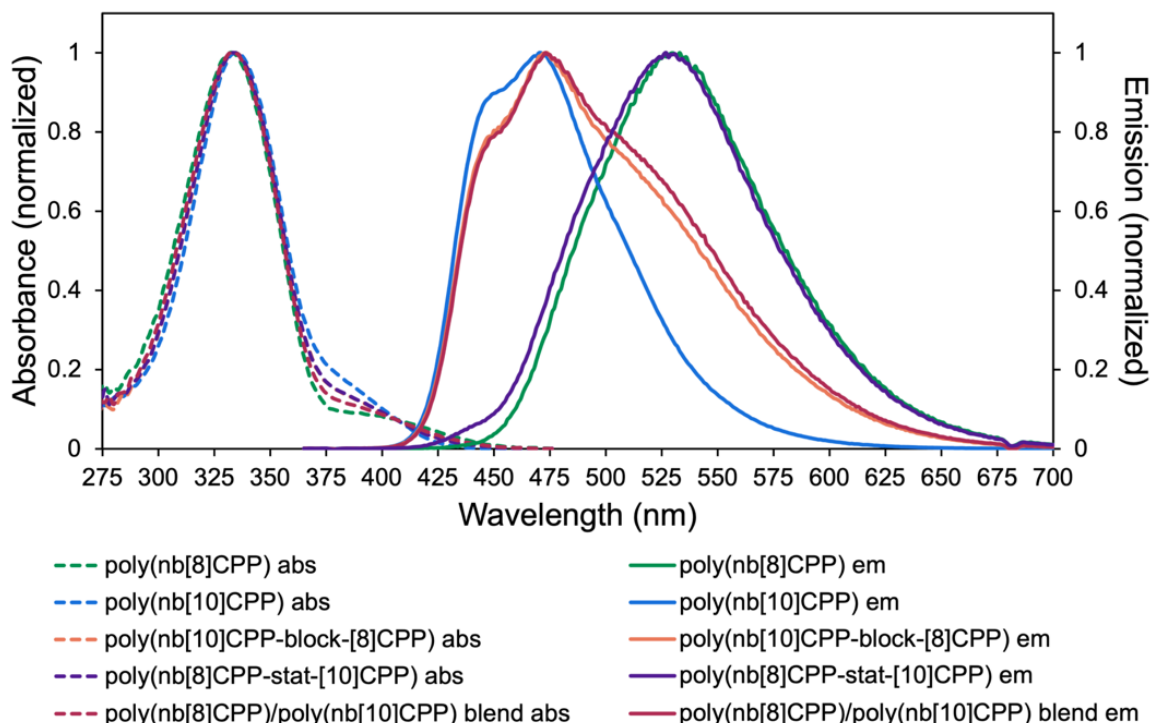
**Figure 2.5.** Absorbance (abs) and fluorescence emission (em) spectra of homopolymer and copolymer samples in THF.

fluorescence quenching.[143] With other sizes of CPPs, $C_{60}$ produces only minor decreases in fluorescence intensity due to dynamic quenching. Before treating polymer samples with $C_{60}$, we verified that addition of $C_{60}$ nearly completely quenches the fluorescence of **nb[10]CPP** but not **nb[8]CPP** (Fig. 2.25). We then compared the magnitude and nature of fluorescence quenching in homopolymer and copolymer samples (all DP 100). As expected, **poly(nb[10]CPP)** exhibits similar quenching behavior to **nb[10]CPP** and [10]CPP, whereas **poly(nb[8]CPP)** exhibits relatively minor quenching (Fig. 2.25). As a rule, lower concentrations of $C_{60}$ were needed to produce the same magnitude of quenching in the polymers relative to the monomers, presumably due to higher local concentrations of CPP units. When **poly(nb[10]CPP)** and **poly(nb[8]CPP)** were blended, $C_{60}$ addition resulted in an intermediate degree of quenching, with the greatest quenching occurring between 420 and 500 nm, the region associated with **poly(nb[10]CPP)** emission (Fig. 2.6). The emission near 530 nm that arises from **poly(nb[8]CPP)** is diminished but persists. Copolymers **poly(nb[8]CPP-*stat*-[10]CPP)** and **poly(nb[10]CPP-*block*-[8]CPP)** also quench to an intermediate degree (Fig. 2.24

26
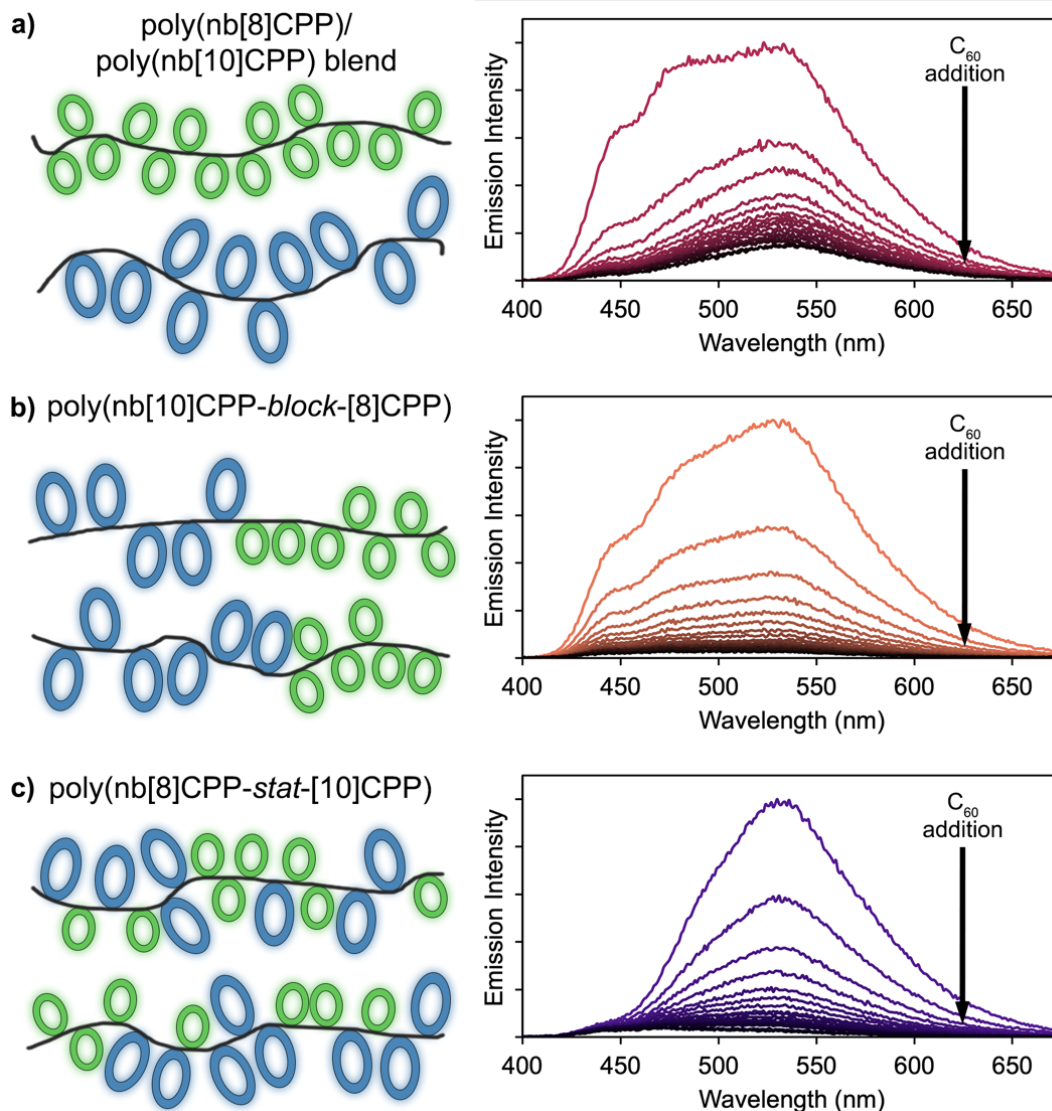
**Figure 2.6.** a) A **poly(nb[8]CPP)/poly(nb[10]CPP)** blend, b) **poly(nb[10]CPP-*block*-[8]CPP)**, and c) **poly(nb[8]CPP-*stat*-[10]CPP)**, represented pictorially on the left, exhibit drastically different emission profiles and fluorescence responses to the addition of $C_{60}$. See 2.5.4 for experimental details.

and Table 2.7). Surprisingly, however, $C_{60}$ addition quenches the fluorescence across the entire emission spectra rather than preferentially at lower wavelengths (Fig. 2.6). Further studies on poly(nbCPP) conformation and cooperative binding effects would be needed to completely explain the underlying reasons for the observed quenching behavior. Nevertheless, the range of accessible fluorescence responses in these polymeric materials from simple combinations of just two monomers is impressive.

**2.3 Conclusions and Outlook**

In this work, we have introduced nbCPPs as a new monomer scaffold and demonstrated a straightforward approach to preparing CPP-based polymers using ROMP. Importantly, this controlled polymerization method gives access to poly(nbCPP)s with varying molecular weights which retain the desirable characteristics of CPPs, such as solubility, size-dependent fluorescence, and host-guest interactions. In contrast to many polymers composed of fluorophores, poly(nbCPP)s fluoresce brightly in solution, making them potential candidates for bright fluorescent tags for imaging applications. Copolymerizing multiple sizes of nbCPPs provides additional avenues to tune the properties of the resultant polymeric materials. The sequence-dependence of the emission and supramolecular chemistry of CPP-based copolymers highlights the importance of accessing these structures through a "living" polymerization method. Looking ahead, access to block copolymers from nbCPPs poses exciting prospects for synthesis of new materials, such as poly(nbCPP)s selectively doped with nitrogen atoms and hybrid materials made with a combination of CPP units and other monomers. Block copolymers with CPP units comprising one or more blocks could serve as organic light-emitters with tunable and perhaps even white light emission. Additionally, one could envision a vast array of interesting self-assembled materials prepared from CPP-containing amphiphilic block copolymers. Self-assembly of poly(nbCPP)s could also be used to prepare materials in which fullerenes or metallofullerenes are hosted in specific regions of a material for organic electronic or magnetic applications. Further progress toward these advanced polymeric materials would benefit from additional tools for modeling complex nonbiological macromolecules. Ultimately, poly(nbCPP)s represent a new form of carbon nanomaterial, uniquely positioned at the intersection of precise organic synthesis and macromolecular chemistry.

**2.4 Preliminary Work Toward Additional nbCPP Monomers**

By nature, the oligomeric CPP scaffold lends itself to synthetic modifications that can be used to alter the properties of CPP monomers and resultant CPP-based polymers. Polymers prepared from **nb[8]CPP**, **nb[9]CPP**, and **nb[10]CPP** still offer countless opportunities for further investigation. For instance, the thermal properties, porosity, and

film-forming ability of poly(nbCPP)s all warrant further study. While the materials possibilities with these monomers are far from exhausted, we have begun to explore the synthesis of additional nbCPP monomers (Fig. 2.7).
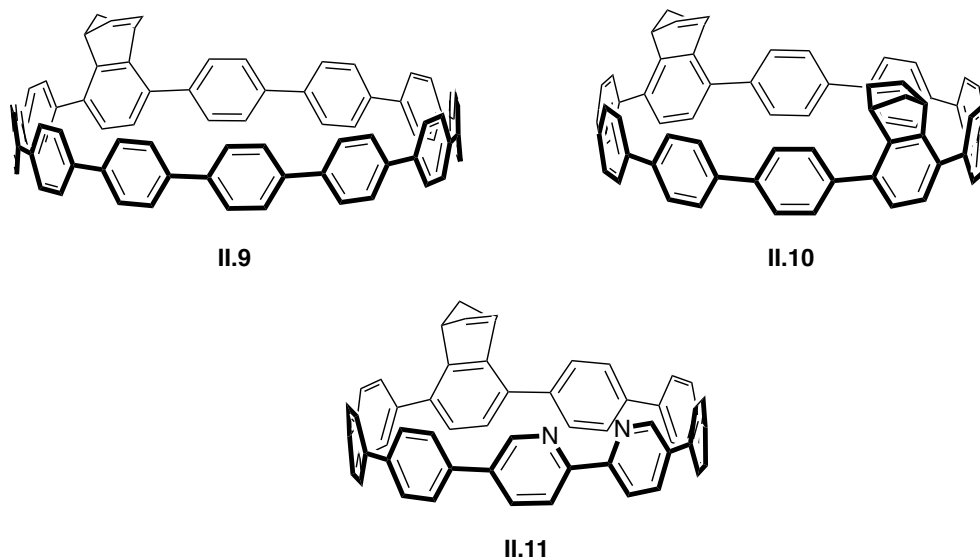


**Figure 2.7.** New norbornene nanohoop architectures include additional sizes, multifunctionalized nanohoops, and nanohoops with heteroatoms.

CPPs are known for their size-dependent properties, and these properties extend to polymers composed of CPPs. Expanding the size range of CPP monomers is one way to add to the available building blocks for polymeric CPP-based materials. In addition to offering different optical properties, different sizes of CPP units will likely have an effect on the porosity of the final materials. Unlike for porous materials made of linear components, where increased linker length tends to lead to increased interpenetration and lower porosity,[161,162] one could expect increased porosity in polyCPPs with increased macrocycle size due to the inability to interpenetrate. Monomer **II.9**, which contains 12 phenylene units, has been synthesized successfully, marking an important step toward expanding the range of CPP monomers.

A second way to alter nbCPP monomers is to introduce multiple functional groups. Monomer **II.10** contains two norbornene handles and could be used as a cross-linker in any polymer made via ROMP. Using this molecule as a cross-linker could be a

29

way to control the density and distribution of host sites for $C_{60}$ in polymers with topologies other than linear.

Lastly, monomer **II.11** is the first foray into nbCPP monomers containing heteroatoms. Heteroatoms can be expected to change the polarity as well as guest affinity of polyCPPs. Nitrogen-doping has previously been used to change the selectivity of porous carbon materials for gases, in particular to increase their affinity for $CO_2$,[163–165] and this strategy could be applied to polyCPPs as well. The bipyridine motif makes CPPs good ligands for metals,[166] and complexation of these units with a metal pre- or post-polymerization[167,168] could rapidly alter the material's properties. This could be especially interesting in a block copolymer or larger self-assembled structure in which only one block or phase contains metals.

These examples of new nbCPP structures hint at the many possible functionalities that could be incorporated into CPP monomers as a part of polymeric materials design. Between the precise functionalization of CPP monomers and the ability to combine nbCPPs with each other and other monomers, whether as blocks or as low mole percent dopants, the possibilities for new materials are endless.

## 2.5 Experimental Section

### 2.5.1 General Experimental

Commercially available materials were used without purification. Moisture- and oxygen-sensitive reactions were carried out in flame-dried glassware and under an inert atmosphere of purified nitrogen using syringe/septa technique. Tetrahydrofuran (THF), 1,4-dioxane, and dimethylformamide (DMF) were dried by filtration through alumina according to the methods described by Grubbs.[169] Thin layer chromatography (TLC) was performed using Sorbent Technologies Silica Gel XHT TLC plates. Developed plates were visualized using UV light at wavelengths of 254 and 365 nm. Silica column chromatography was conducted with Zeochem Zeoprep 60 Eco 40-63 μm silica gel. Automated flash chromatography was performed using a Biotage Isolera One. $^{1}$H and $^{13}$C NMR spectra were recorded on a Bruker Avance III HD 500 MHz ($^{1}$H: 500 MHz, $^{13}$C: 126 MHz) or 600 MHz ($^{1}$H: 600 MHz, $^{13}$C: 151 MHz) NMR spectrometer. All spectra were taken in CDCl$_3$, and the chemical shifts (δ) were reported in parts per million (ppm)

referenced to TMS ($\delta$ 0.00 ppm) for $^{1}$H NMR and residual CHCl$_3$ ($\delta$ 77.16 ppm) for $^{13}$C NMR. Gel permeation chromatography (GPC) for polymer molecular weight determination was performed either on a TOSOH EcoSEC HLC-8320GPC with an Agilent PolyPore column (in THF referenced to polystyrene standards using a refractive index detector) or on an Agilent 1260 HPLC equipped with a Wyatt 8-angle DAWN NEON light-scattering detector, ViscoStar NEON viscometer, and Optilab NEON refractive index detector (flow rate of 1 mL/min in chloroform stabilized with 0.5%-1.0% ethanol through two Agilent PLgel MIXED-C columns at 35 °C). dn/dc values were determined by 100% mass recovery using Astra 7.3. UV-Vis absorption spectra in solution were collected on an Agilent Cary 100 spectrophotometer. Solid-state absorption spectra of drop-casted thin films were collected using Shimadzu UV-1800 UV-Vis spectrophotometer. Fluorescence spectra were collected on a Horiba Jobin Yvon Fluoromax-4 fluorometer (2 nm excitation slit width; 1 nm emission slit width) or a Photon Technology International QuantaMaster 4 spectrofluorometer. All fluorescence measurements were performed with excitation at 340 nm. Quantum yields of THF solutions (~1 × 10$^{-5}$ M.) and solid powders were measured using a Horiba model 914D photomultiplier detector system with a calibrated integrating sphere. The concentration of polymeric samples in THF was estimated by the absorbance of the CPP fragments by comparing the absorption intensities of them with those of the monomers. Quantum yields were calculated based on three consecutive measurements. All absorption and fluorescence measurements were carried out under ambient conditions.

## 2.5.2 Polymer Synthesis and Structural Characterization

*General synthetic procedure for poly(nbCPP)s*

nbCPP monomer was added to a small flame-dried flask with a stir bar, placed under N$_2$, then dissolved in degassed chloroform. A solution of bromopyridyl Grubbs G3 in degassed chloroform was quickly added to the vial via syringe, and the reaction was stirred at room temperature for 20-30 minutes. The reaction was quenched with ethyl vinyl ether, stirred for an additional 5 minutes, and the material was precipitated from cold methanol. The polymer was collected by centrifugation or filtration and dried under vacuum.

|  | Identity | [M]:[I] | Init. | Solvent | Conc. (M) | Time (min) | Conv. | $M_n$ – GPC$_{RI}$ (g/mol) | Đ – GPC$_{RI}$ |
|---|---|---|---|---|---|---|---|---|---|
| 1[†‡] | p[8] | 50 | G3 | CHCl$_3$ | 0.010 | 20 | full | 8,500 | 1.18 |
| 2 | p[8] | 60 | G3 | CHCl$_3$ | 0.010 | 20 | full | 9,500 | 1.08 |
| 3 | p[8] | 100 | G3 | CHCl$_3$ | 0.010 | 20 | full | 15,400 | 1.12 |
| 4[†*] | p[8] | 100 | G3 | CHCl$_3$ | 0.010 | 20 | full | 13,300 | 1.23 |
| 5 | p[8] | 150 | G3 | CHCl$_3$ | 0.010 | 20 | full | 15,900 | 1.30 |
| 6[‡] | p[8] | 200 | G3 | CHCl$_3$ | 0.010 | 20 | full | insoluble | insoluble |
| 7 | p[8] | 200 | G3 | CHCl$_3$ | 0.010 | 20 | full | insoluble | insoluble |
| 8 | p[8] | 200 | G3 | CHCl$_3$ | 0.010 | 20 | full | insoluble | insoluble |
| 9[†‡] | p[9] | 50 | G3 | CHCl$_3$ | 0.010 | 20 | full | 10,900 | 1.22 |
| 10 | p[9] | 200 | G3 | CHCl$_3$ | 0.010 | 20 | >95% | 43,600 | 1.32 |
| 11 | p[10] | 15 | G3 | CHCl$_3$ | 0.010 | 30 | >98% | 2,850 | 1.27 |
| 12[†‡] | p[10] | 50 | G3 | CHCl$_3$ | 0.010 | 30 | full | 13,600 | 1.19 |
| 13 | p[10] | 50 | G3 | CHCl$_3$ | 0.010 | 30 | full | 15,800 | 1.12 |
| 14 | p[10] | 50 | G3 | CHCl$_3$ | 0.010 | 30 | full | 11,300 | 1.10 |
| 15 | p[10] | 60 | G3 | CHCl$_3$ | 0.010 | 20 | >95% | 16,800 | 1.10 |
| 16[†*] | p[10] | 100 | G3 | CHCl$_3$ | 0.010 | 30 | full | 25,000 | 1.22 |
| 17[†‡] | p[10] | 200 | G3 | CHCl$_3$ | 0.010 | 30 | full | 48,200 | 1.56 |
| 18 | p[10] | 250 | G3 | CHCl$_3$ | 0.010 | 30 | >95% | 41,700 | 1.26 |
| 19 | p[10] | 500 | G3 | CHCl$_3$ | 0.010 | 30 | full | 89,600 | 1.45 |

**Table 2.3.** Details for polymerizations carried out according to the general procedure with Grubbs G3 in chloroform. Unshaded rows correspond to data points in Figure 3. Poly(nb[n]CPP) names are abbreviated here as p[n]. [†]Sample used for collection of data in Table 1. [‡]Sample used for collection of data in Table 2.2. [*]Sample used for spectra shown in Figures 2.5 and 2.6.

**Table 2.4.** (next page) Selection of additional polymer samples prepared under different conditions. Poly(nb[n]CPP) names are abbreviated here as p[n]. Poly(diMeObnb) is abbreviated here as pM. [a]Carried out in oven-dried glassware in a glovebox. [b]Solution of monomer was added to initiator.

| | Identity | [M]:[I] | Init. | Solvent | Conc. (M) | Time (min) | Conv. | $M_n$ – GPC$_{RI}$ (g/mol) | Đ – GPC$_{RI}$ |
|---|---|---|---|---|---|---|---|---|---|
| 1 | p[8] | 15 | G3 | THF | 0.035 | 30 | full | 1,060 | 1.24 |
| 2[b] | p[8] | 25 | G3 | THF | 0.027 | 30 | n.d. | 5,980 | 1.30 |
| 3 | p[8] | 35 | G3 | THF | 0.040 | 30 | full | 6,000 | 1.49 |
| 4[b] | p[8] | 40 | G3 | THF | 0.045 | 30 | full | 5,890 | 1.20 |
| 5 | p[8] | 50 | G3 | THF | 0.028 | 30 | n.d. | 11,900 | 1.63 |
| 6[b] | p[8] | 66 | G3 | THF | 0.149 | 30 | full | 8,660 | 1.56 |
| 7[a] | p[8] | 100 | G3 | THF | 0.032 | 15 | n.d. | 17,000 | 1.26 |
| 8[a] | p[8] | 100 | G3 | THF | 0.032 | 15 | n.d. | 15,000 | 1.24 |
| 9[a] | p[8] | 100 | G3 | THF | 0.032 | 15 | n.d. | 15,900 | 1.27 |
| 10 | p[8] | 100 | G3 | DCM | 0.025 | 15 | full | 10,700 | 1.14 |
| 11[b] | p[10] | 40 | G3 | THF | 0.036 | 30 | full | 8,460 | 1.19 |
| 12[b] | p[10] | 64 | G3 | THF | 0.031 | 30 | >98% | 13,300 | 1.27 |
| 13[a] | p[10] | 100 | G3 | THF | 0.024 | 60 | full | 6,870 | 1.86 |
| 14[a] | p[10] | 200 | G3 | THF | 0.035 | 60 | full | 38,300 | 1.39 |
| 15[a] | p[10] | 100 | G1 | THF | 0.024 | 60 | no rxn | 3,100 | 1.40 |
| 16[a] | p[10] | 100 | G2 | THF | 0.024 | 60 | full | 8,150 | 1.99 |
| 17 | pM | 15 | G3 | CHCl$_3$ | 0.010 | 30 | full | 1,540 | 1.11 |
| 18 | pM | 50 | G3 | CHCl$_3$ | 0.010 | 20 | full | 5,630 | 1.05 |
| 19 | pM | 60 | G3 | CHCl$_3$ | 0.010 | 20 | full | 7,020 | 1.04 |
| 20 | pM | 100 | G3 | CHCl$_3$ | 0.010 | 20 | full | 10,700 | 1.03 |
| 21 | pM | 200 | G3 | CHCl$_3$ | 0.010 | 20 | full | 17,000 | 1.05 |
| 22 | pM | 200 | G3 | CHCl$_3$ | 0.010 | 20 | full | 19,000 | 1.04 |
| 23 | pM | 250 | G3 | CHCl$_3$ | 0.010 | 30 | full | 21,100 | 1.04 |
| 24 | pM | 100 | G3 | DCM | 0.025 | 15 | full | 10,000 | 1.04 |
| 25[a] | pM | 100 | G3 | THF | 0.471 | 60 | full | 9,520 | 1.03 |
| 26[a] | pM | 100 | G3 | THF | 0.471 | 20 | full | 8,650 | 1.03 |
| 27 | pM | 100 | G3 | THF | 0.471 | 60 | full | 11,200 | 1.04 |
| 28 | pM | 150 | G3 | THF | 0.989 | 30 | full | 14,000 | 1.10 |
| 29 | pM | 100 | G1 | THF | 0.471 | 60 | ~95% | 7,790 | 1.05 |
| 30 | pM | 100 | G2 | THF | 0.471 | 60 | full | 30,700 | 1.94 |

| | Identity | [M]:[I] | Init. | Solvent | Conc. (M) | Time (min) | Conv. | $M_n$ – GPC$_{RI}$ (g/mol) | Đ – GPC$_{RI}$ |
|---|---|---|---|---|---|---|---|---|---|
| 1* | p[10]b[8] | 50; 50 | G3 | CHCl$_3$ | 0.010 | 50 | full | 16,400 | 1.21 |
| 2$^a$ | p[10]b[8] | 37; 37 | G3 | THF | 0.042 | 30 | full | 10,300 | 1.30 |
| 3$^b$ | p[10]b[8] | 36; 36 | G3 | THF | 0.149 | 60 | full$^b$ | 9,270 | 1.70 |
| 4 | p[10]b[8] | 18; 54 | G3 | THF | 0.067 | 60 | full | 17,600 | 1.50 |
| 5* | p[8]s[10] | 50; 50 | G3 | CHCl$_3$ | 0.010 | 30 | full | 27,300 | 1.24 |
| 6$^b$ | p[8]s[10] | 36; 36 | G3 | THF | 0.149 | 60 | full | 9,650 | 1.12 |
| 7$^b$ | p[8]s[10] | 18; 54 | G3 | THF | 0.067 | 60 | full$^b$ | 20,100 | 1.46 |
| 8 | p[8]s[10] | 30; 30 | G3 | THF | 0.100 | 40 | full | 13,100 | 1.34 |
| 9 | p[8]s[10] | 45; 15 | G3 | THF | 0.199 | 40 | full | 10,300 | 1.32 |
| 10 | p[8]s[10] | 15; 45 | G3 | THF | 0.067 | 40 | full | 13,100 | 1.33 |

**Table 2.5.** Details for polymerization reactions to prepare copolymers. Values for monomer-to-initiator ratio are listed here with equivalents of nb[8]CPP followed by equivalents of nb[10]CPP for each equivalent of initiator. Poly(nb[10]-*block*-[8]CPP) is abbreviated here as p[10]b[8], and poly(nb[8]-*stat*-[10]CPP) is abbreviated as p[8]s[10]. For block copolymer samples, the time listed is total time, half of which was used for polymerizing each block. *Sample used for spectra shown in Figures 2.5 and 2.6. $^a$Carried out in oven-dried glassware in a glovebox. $^b$Solution of monomer was added to initiator.
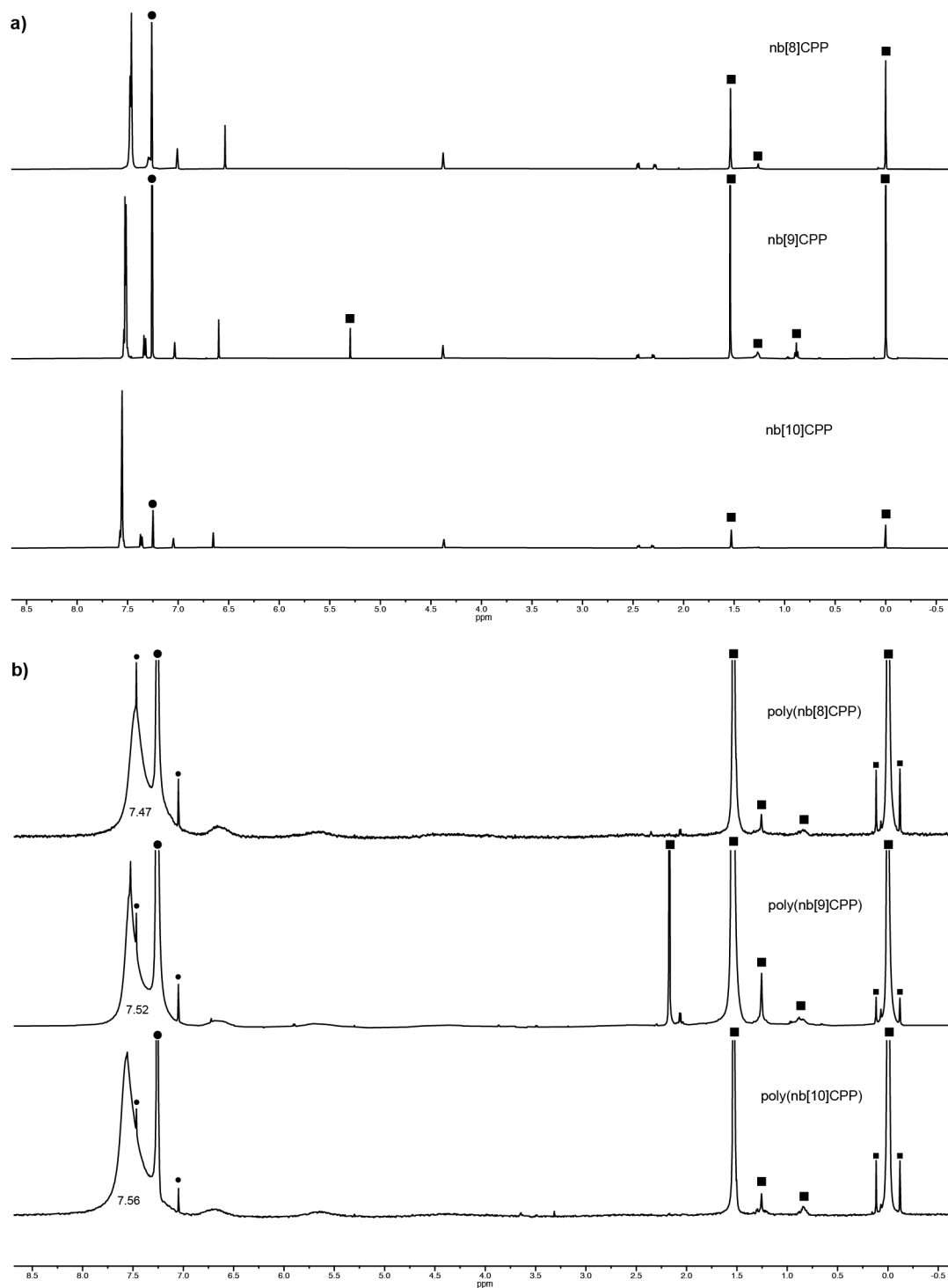
**Figure 2.8.** a) Stacked $^1$H NMR of nb[8]CPP, nb[9]CPP, and nb[10]CPP in CDCl$_3$. b) Stacked $^1$H NMR spectra of poly(nb[8]CPP), poly(nb[9]CPP), and poly(nb[10]CPP) in CDCl$_3$. Polymer NMR spectra from samples 4, 9, and 16, Table 2.3. Chloroform and its satellite peaks are marked with circles, and other residual solvent, alkyl grease, and the reference TMS peak (and satellites) are marked with squares.
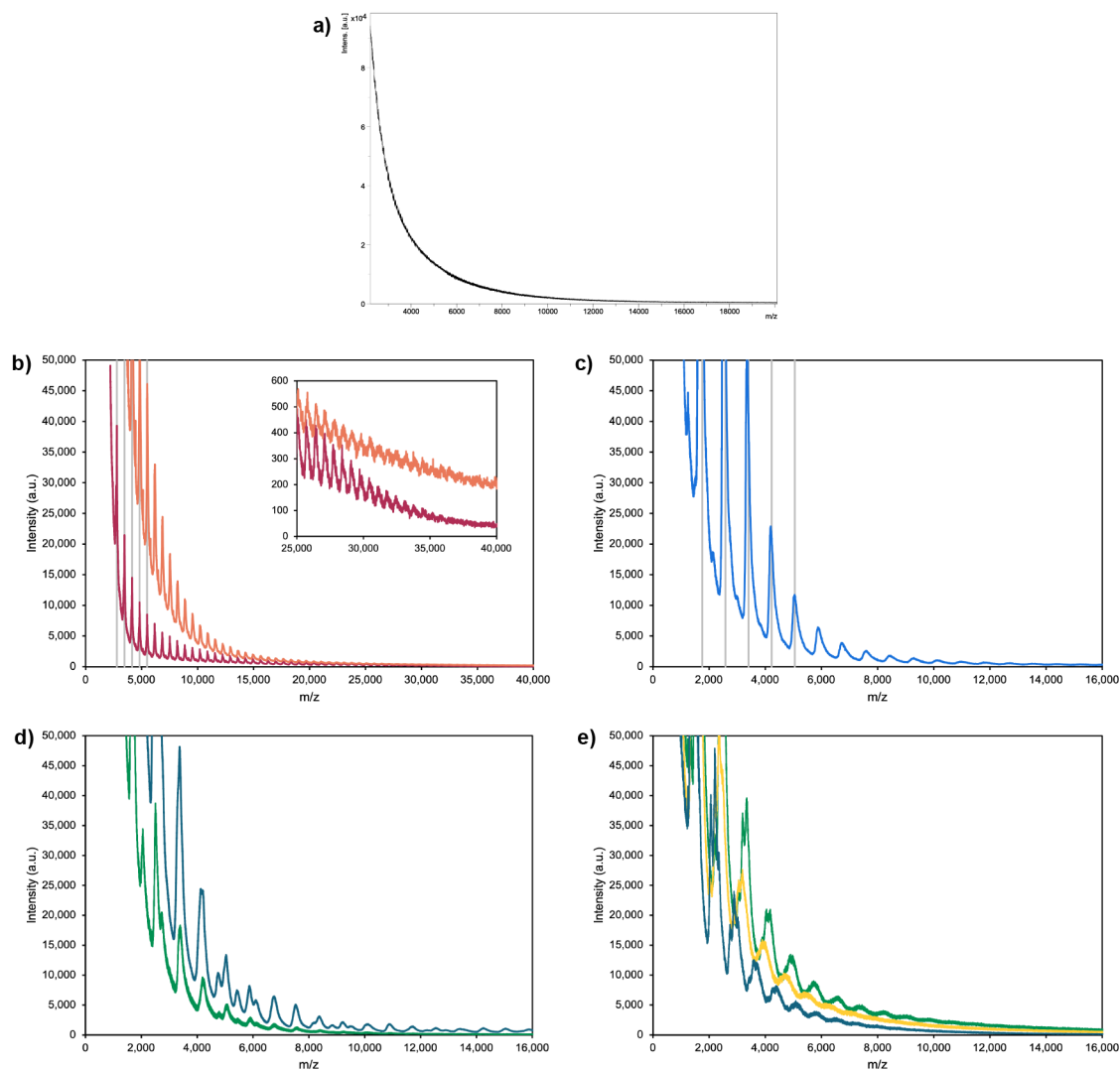
**Figure 2.9.** MALDI spectra of poly(nbCPP) samples. a) Baseline spectrum of the MALDI matrix, *trans*-2-[3-(4-*tert*-butylphenyl)-2-methyl-2-propenylidene]malononitrile (DCTB). b) MALDI spectra of poly(nb[8]CPP) from samples 2 and 4, Table 2.4. Vertical lines at values corresponding to DP 4-8 ($\Delta$m/z = 672.87) have been added to guide the eye. c) MALDI spectrum of poly(nb[10]CPP) from sample 14, Table 2.4. Vertical lines at values corresponding to DP 2-6 ($\Delta$m/z = 825.07) have been added to guide the eye. d) MALDI spectra of poly(nb[10]CPP-*block*-[8]CPP) showing characteristic "fingerprint" for this polymer structure (samples 2-3, Table 2.5). e) MALDI spectra of poly(nb[8]CPP-*stat*-[10]CPP) showing characteristic "fingerprint" for this polymer structure (samples 8-10, Table 2.5).
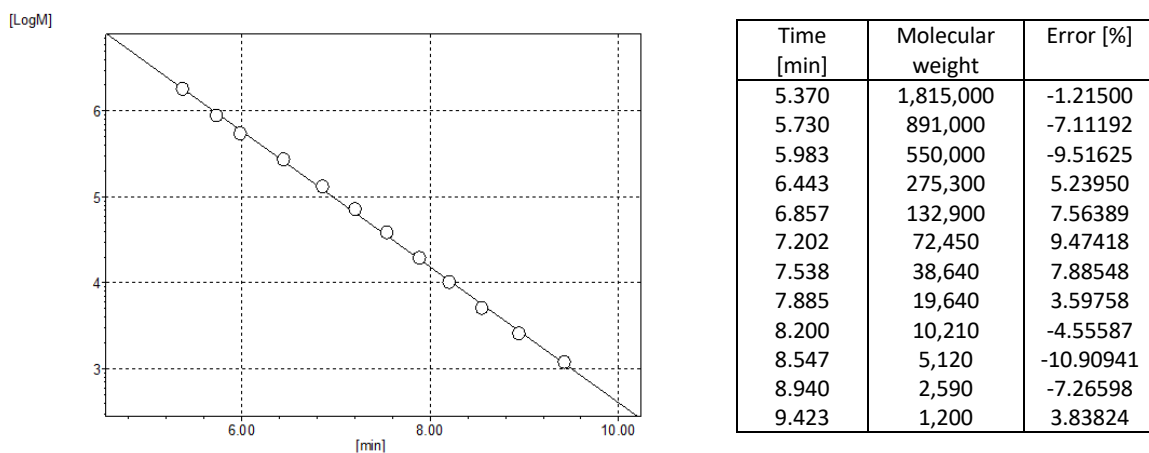
**Figure 2.10.** GPC calibration curve and calibration data based on refractive index measurements with PS.

| Time [min] | Molecular weight | Error [%] |
|---|---|---|
| 5.370 | 1,815,000 | -1.21500 |
| 5.730 | 891,000 | -7.11192 |
| 5.983 | 550,000 | -9.51625 |
| 6.443 | 275,300 | 5.23950 |
| 6.857 | 132,900 | 7.56389 |
| 7.202 | 72,450 | 9.47418 |
| 7.538 | 38,640 | 7.88548 |
| 7.885 | 19,640 | 3.59758 |
| 8.200 | 10,210 | -4.55587 |
| 8.547 | 5,120 | -10.90941 |
| 8.940 | 2,590 | -7.26598 |
| 9.423 | 1,200 | 3.83824 |
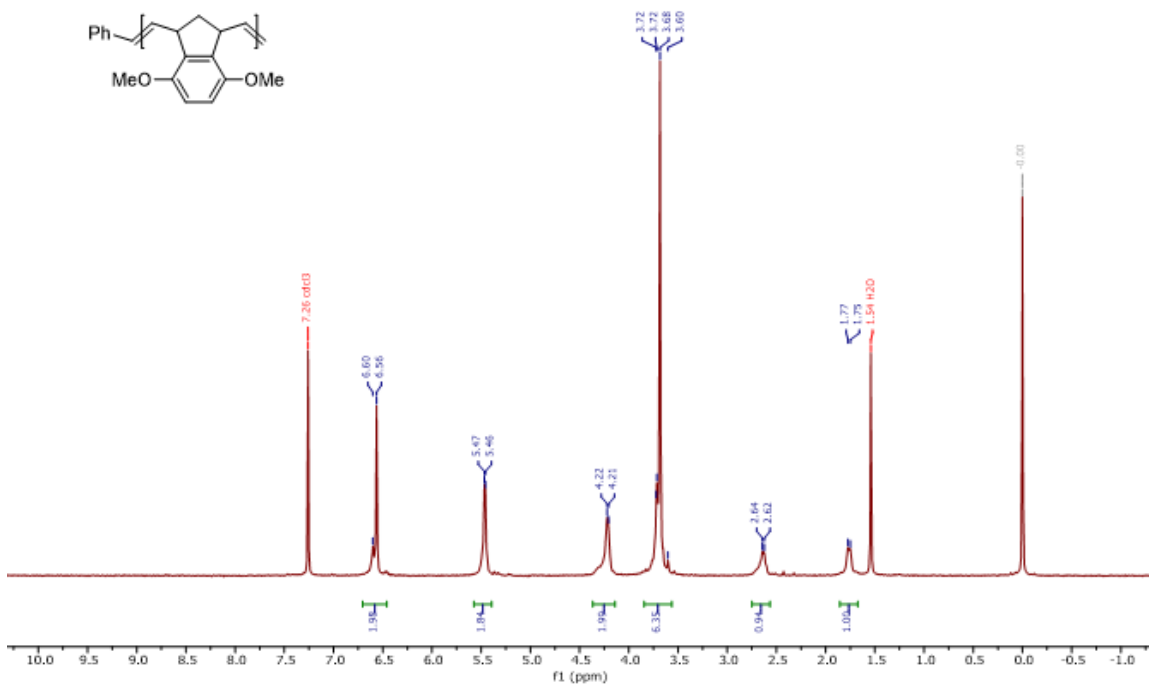


**Figure 2.11.** $^1$H NMR of poly(diMeObnb) in CDCl$_3$. Spectrum from sample 27, Table 2.4.
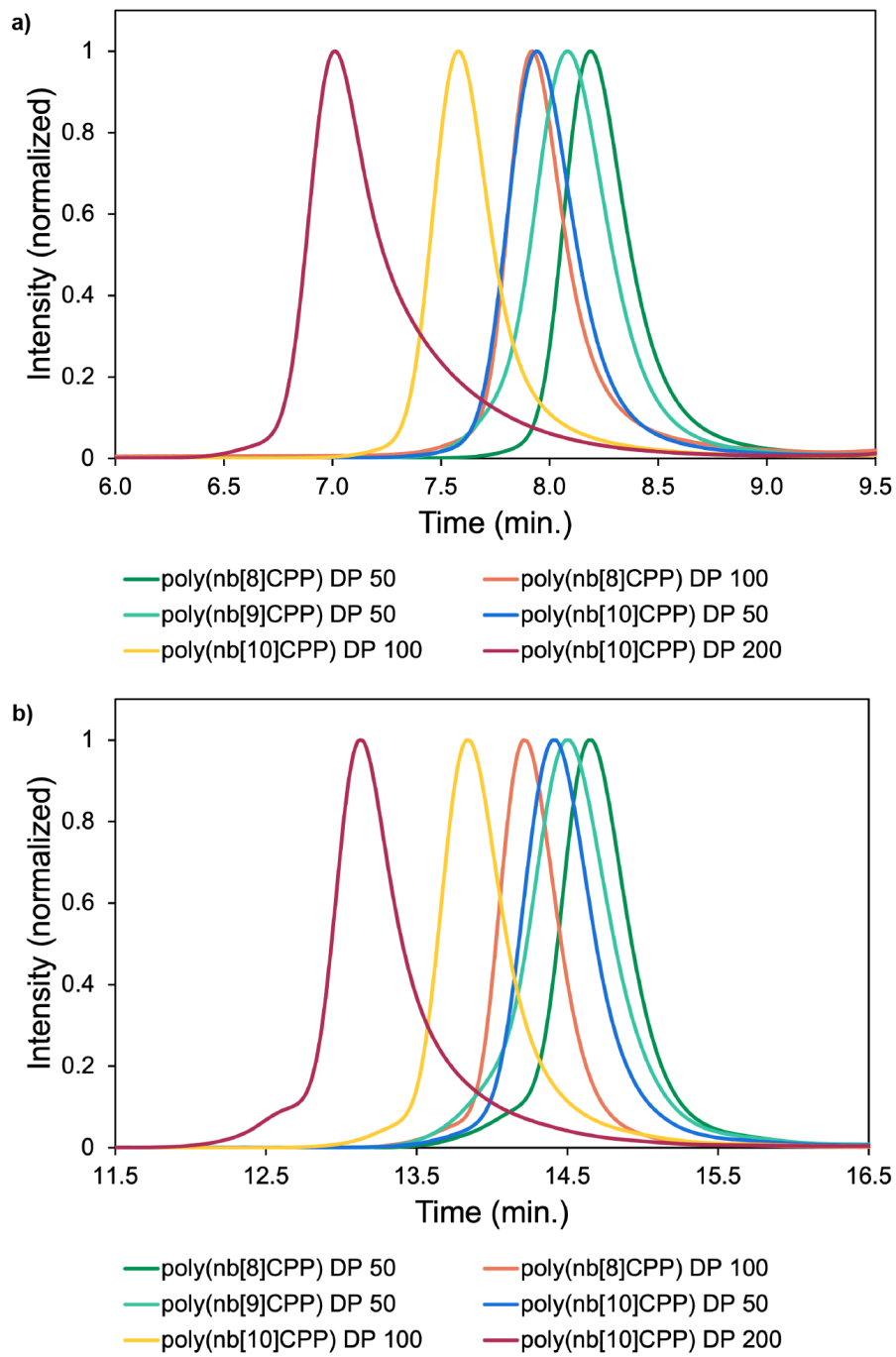
**Figure 2.12.** Comparison between GPC$_{RI}$ (a) and GPC$_{MALS}$ (b) chromatographs for samples in Table 2.1.

| Identity | [M]:[I] | dn/dc (mL/g) |
|---|---|---|
| poly(nb[8]CPP) | 50 | 0.2392 |
| poly(nb[8]CPP) | 100 | 0.2718 |
| poly(nb[9]CPP) | 50 | 0.2967 |
| poly(nb[10]CPP) | 50 | 0.2802 |
| poly(nb[10]CPP) | 100 | 0.3192 |
| poly(nb[10]CPP) | 200 | 0.3121 |

**Table 2.6.** dn/dc values for samples in Table 2.1.



| Identity | K (mL/g) | a |
|---|---|---|
| poly(nb[8]CPP) DP 50 | (1.148 ± 0.064) e-1 | 0.344 ± 0.005 |
| poly(nb[8]CPP) DP 100 | (6.884 ± 0.275) e-1 | 0.202 ± 0.003 |
| poly(nb[9]CPP) DP 50 | (2.975 ± 0.068) e-1 | 0.284 ± 0.002 |
| poly(nb[10]CPP) DP 50 | (7.134 ± 0.302) e-2 | 0.407 ± 0.004 |
| poly(nb[10]CPP) DP 100 | (3.966 ± 0.077) e-1 | 0.279 ± 0.002 |
| poly(nb[10]CPP) DP 200 | (1.782 ± 0.017) e-1 | 0.355 ± 0.001 |
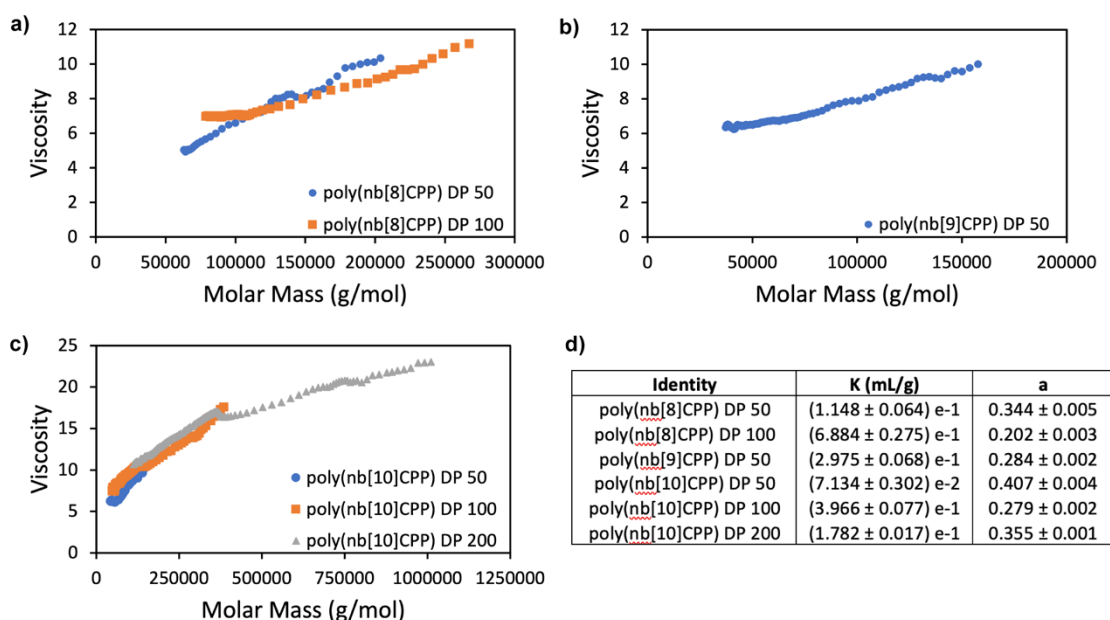
**Figure 2.13.** Mark-Houwink-Sakurada plots for a) poly(nb[8]CPP), b) poly(nb[9]CPP), and c) poly(nb[10]CPP) samples from Table 2.1, and d) K and a parameters from lines of best fit using the equation $\eta = KM^a$.
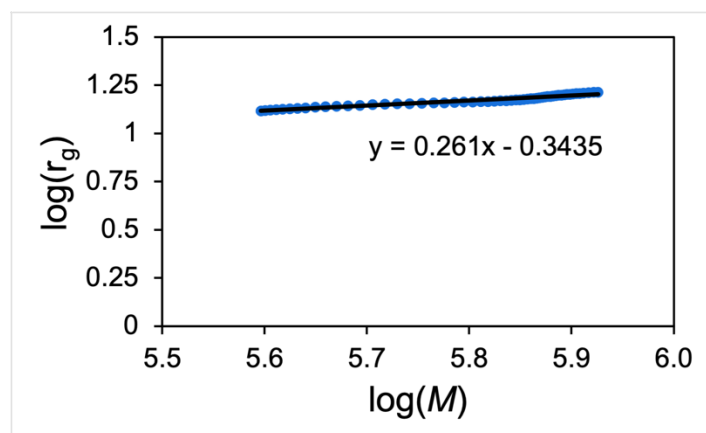
**Figure 2.14.** Log($r_g$) vs. log(*M*) plot for a DP 200 sample of poly(nb[10]CPP) (sample 17 from Table 2.3).
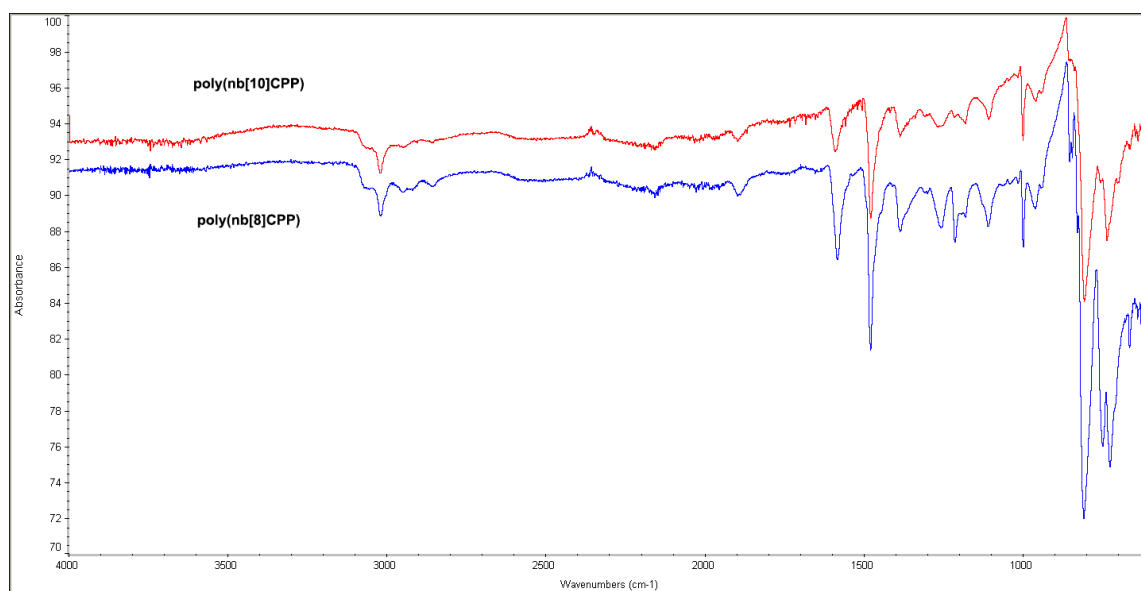


**Figure 2.15.** IR spectra of poly(nb[8]CPP) and poly(nb[10]CPP). Spectra from samples 4 and 16, Table S1.
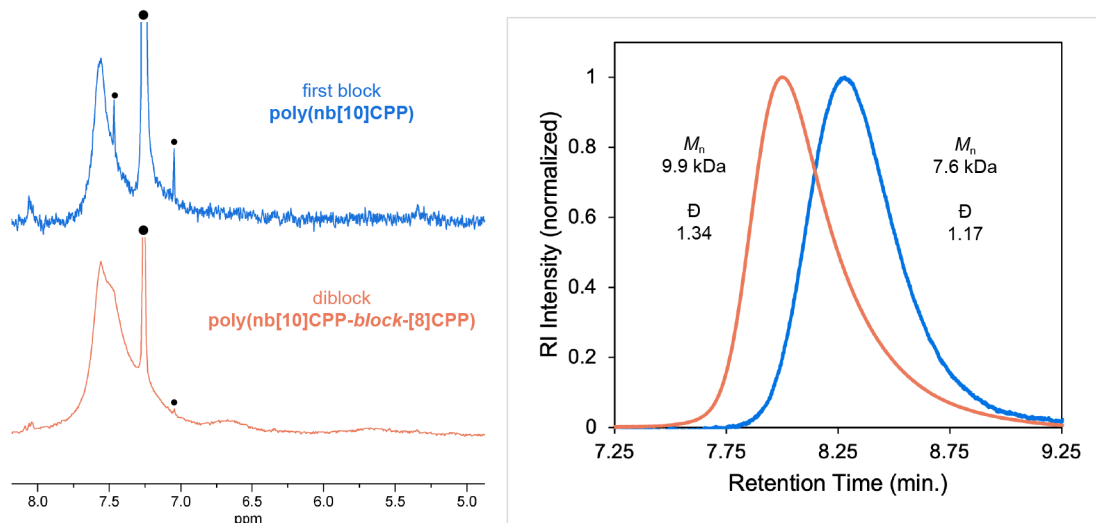
**Figure 2.16.** ^{1}H NMR (left) and GPC (right) evidence for formation of poly(nb[10]CPP-*block*-[8]CPP) (data from sample 2, Table 2.5). Chloroform and its satellite peaks are marked with circles.
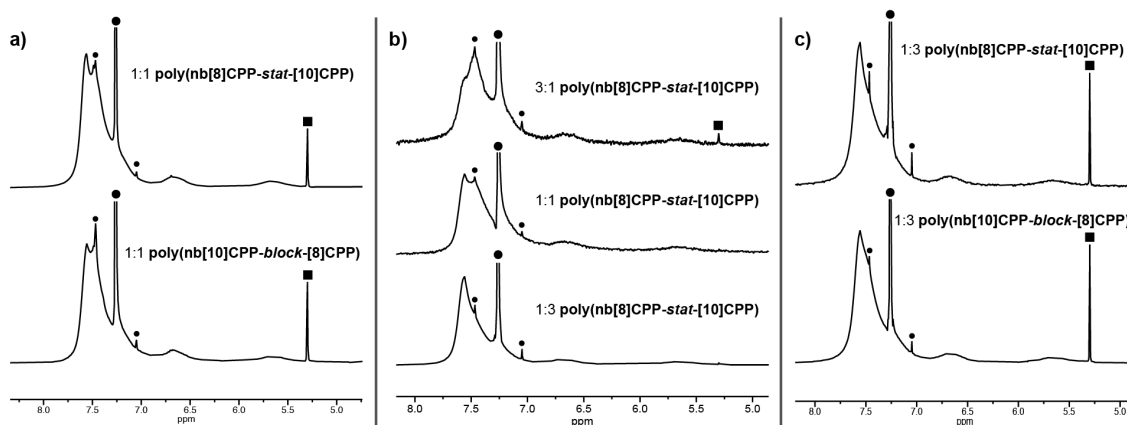


**Figure 2.17.** ^{1}H NMR spectra of block and statistical copolymers with varying ratios of nb[8]CPP and nb[10]CPP units. Ratios are denoted with nb[8]CPP first. a) Spectra from samples 3 and 6, Table 2.5. b) Spectra from samples 8-10, Table 2.5. c) Spectra from samples 4 and 7, Table 2.5. Chloroform and its satellite peaks are marked with circles, and other residual solvent peaks are marked with squares.

## 2.5.3 Photophysical Characterization Data
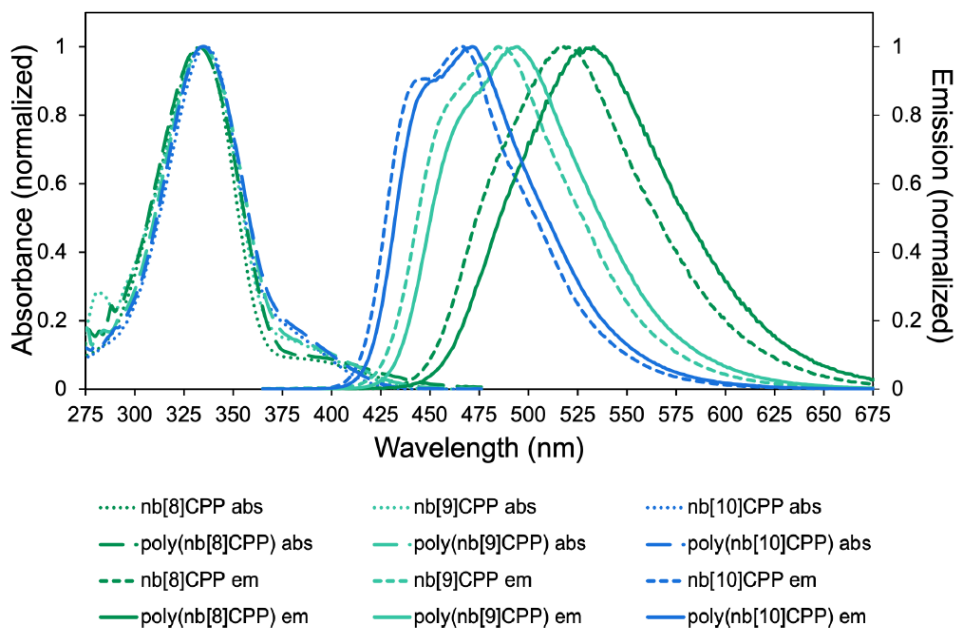


**Figure 2.18.** Absorbance and fluorescence spectra of nbCPPs and poly(nbCPP)s in THF. Polymer data from samples 1, 9, and 12, Table 2.3.
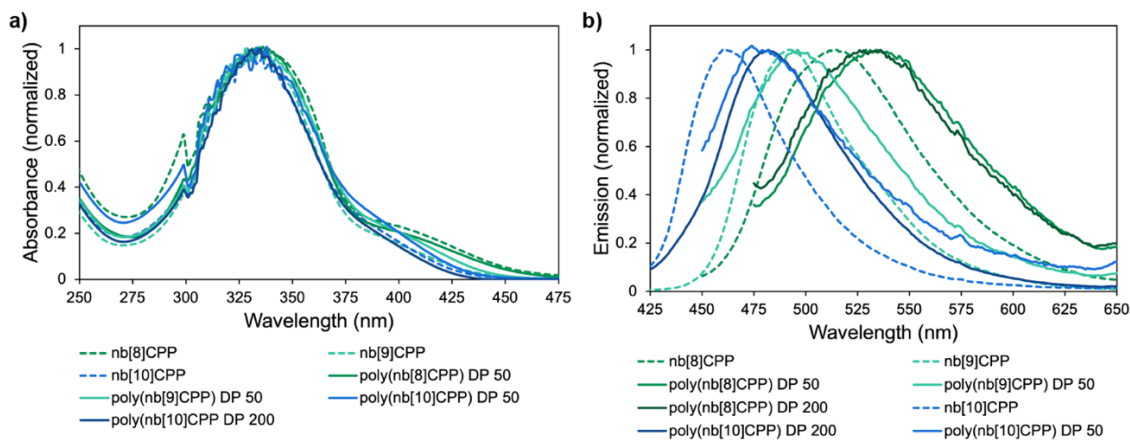


**Figure 2.19.** Solid-state a) absorbance and b) fluorescence emission spectra of nbCPP and poly(nbCPP) powders. Polymer data from samples 1, 6, 9, 12, and 17, Table 2.3.

OBS: Make sure your absorption spectra are in molar absorptivities (units 1/(M cm)).

Overlap integral between 'nb8 abs' and 'nb10 em':
J = 1.764e+13 nm^4/(M*cm)
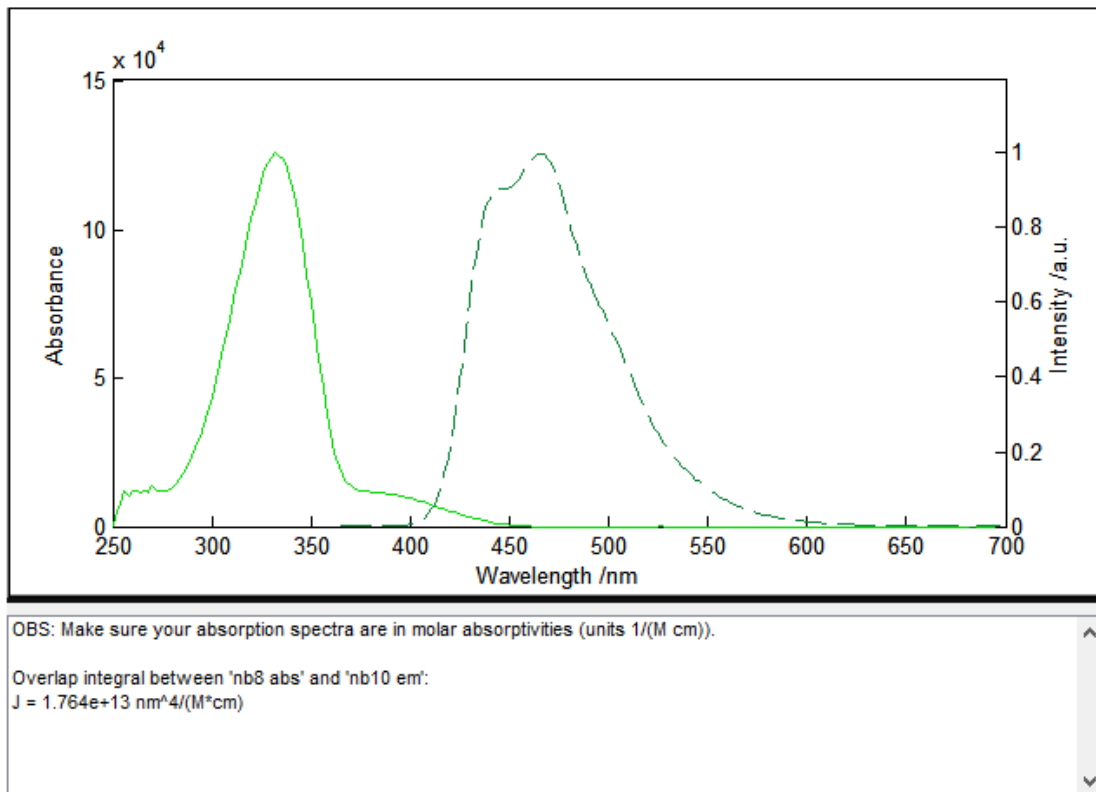
**Figure 2.20.** The Förster distance between nb[10]CPP as a donor and nb[8]CPP as an acceptor was calculated[170] with the equation

$$R_0 = 0.211\left(\kappa^2 n^{-4} Q_D J(\lambda)\right)^{1/6}$$

in which

- $\kappa^2$ was estimated as 2/3,
- $n$, the solvent refractive index, was 1.404 for THF,
- $Q_D$ was 0.788,
- and $J(\lambda)$ was calculated to be $1.764 \times 10^{13}$ using a|e - UV-Vis-IR Spectral Software[171] (see above).
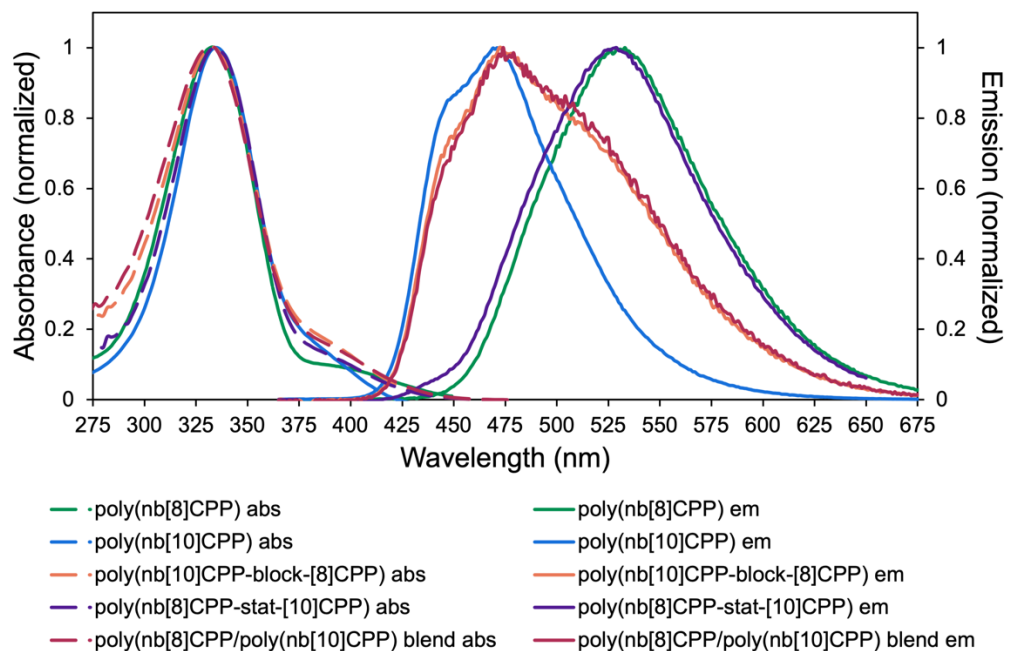
**Figure 2.21.** Absorbance and fluorescence spectra of poly(nbCPP)s synthesized in THF, from samples 6 and 12, Table S2 and samples 2 and 6, Table 2.5.
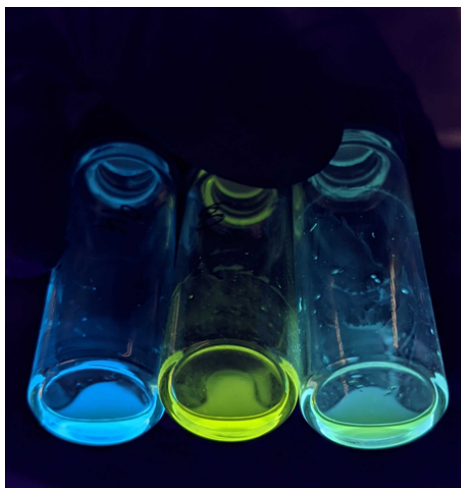


**Figure 2.22.** Image of fluorescence emission under 365 nm UV light of (left to right) poly(nb[10]CPP), poly(nb[8]CPP), and poly(nb[10]CPP-*block*-[8]CPP) from samples 6 and 12, Table 2.4 and sample 3, Table 2.5.
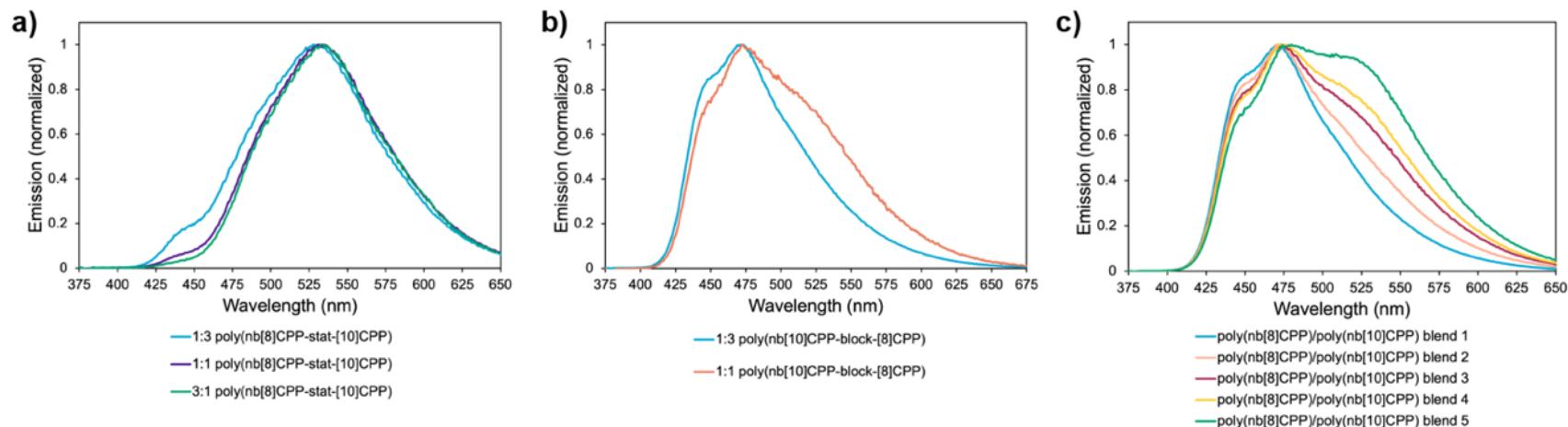
**Figure 2.23.** Fluorescence emission spectra of poly(nbCPP)s with varying composition. a) Fluorescence emission spectra of statistical copolymers with varying ratios of nb[8]CPP and nb[10]CPP units. Spectra from samples 8-10, Table 2.5. b) Fluorescence emission spectra of block copolymers with varying ratios of nb[8]CPP and nb[10]CPP units. Spectra from samples 2 and 4, Table 2.5. Copolymers are shown with nb[8]CPP:nb[10]CPP ratios. c) Fluorescence emission spectra of poly(nb[8]CPP) and poly(nb[10]CPP) blended in different ratios (samples 4 and 16, Table 2.3).

## 2.5.4 Fluorescence Quenching Experiments

*Procedure for fluorescence quenching experiments*

Monomer quenching: A 0.0003 M. stock solution of the monomer and a 0.001 M. stock solution of $C_{60}$ were prepared in toluene. These stock solutions were used to prepare a [H] solution and a [H+G] solution, with monomer at $5.13 \times 10^{-7}$ M. in both and $C_{60}$ at $5.00 \times 10^{-5}$ M. in the latter. Fluorescence measurements were obtained of a toluene blank followed by the [H] solution. [H+G] solution was added to [H] solution in 15 μL increments and the fluorescence was measured. This procedure was performed in triplicate for each monomer (≥15 data points per trial). Fluorescence spectra were integrated (400-625 nm for nb[10]CPP and 425-675 nm for nb[8]CPP), and the fluorescence intensity of each data point was compared to the initial fluorescence intensity.

Polymer quenching: A stock solution of the polymer was prepared using the same polymer mass and solvent volume as was used for the respective monomer stock solution. Due to solubility, polymer stock solutions were prepared in THF. Along with the $C_{60}$ stock solution prepared as described above, the polymer stock solution was used to prepare a [H] solution and a [H+G] solution in toluene. Fluorescence measurements were obtained of a toluene blank followed by the [H] solution. [H+G] solution was added to [H] solution in 2.5 μL increments and the fluorescence was measured. This procedure was performed in triplicate for each monomer (≥15 data points per trial). Fluorescence spectra were integrated from 400 to 675 nm, and the fluorescence intensity of each data point was compared to the initial fluorescence intensity.

Regression: Regression was performed with python using scipy.optimize.least_squares. Although it was outside the scope of this study to assess the equivalence of binding sites in the polymers and the possible contribution of cooperativity,[172] we estimated $K_a$ and $K_{SV}$ values for the monomers and polymers using magnitude of quenching ($F/F_0$ or $F_0/F$) versus total concentration of $C_{60}$. These values are most suitable for comparative purposes.

| Sample | $K_a$ | $K_{SV}$ |
|---|---|---|
| nb[8]CPP | $(5.85 \pm 3.13) \times 10^4$ | $(9.13 \pm 0.27) \times 10^4$ |
| nb[10]CPP | $(2.55 \pm 0.09) \times 10^6$ | $(4.71 \pm 0.15) \times 10^6$ |
| poly(nb[8]CPP) | $(2.22 \pm 0.26) \times 10^7$ | $(4.81 \pm 0.24) \times 10^6$ |
| poly(nb[10]CPP) | $(2.15 \pm 0.49) \times 10^8$ | $(1.65 \pm 0.08) \times 10^8$ |
| poly(nb[10]CPP-*block*-[8]CPP) | $(8.78 \pm 1.34) \times 10^7$ | $(9.95 \pm 1.22) \times 10^7$ |
| poly(nb[8]CPP-*stat*-[10]CPP) | $(8.44 \pm 1.98) \times 10^7$ | $(8.52 \pm 0.41) \times 10^7$ |
| poly(nb[8]CPP)/poly(nb[10]CPP) blend | $(1.13 \pm 0.28) \times 10^8$ | $(3.19 \pm 0.41) \times 10^7$ |

**Table 2.7.** $K_a$ and $K_{SV}$ values for nbCPP monomers and poly(nbCPP)s. Polymer data collected with samples 4 and 16, Table 2.3, and samples 1 and 5, Table 2.5.
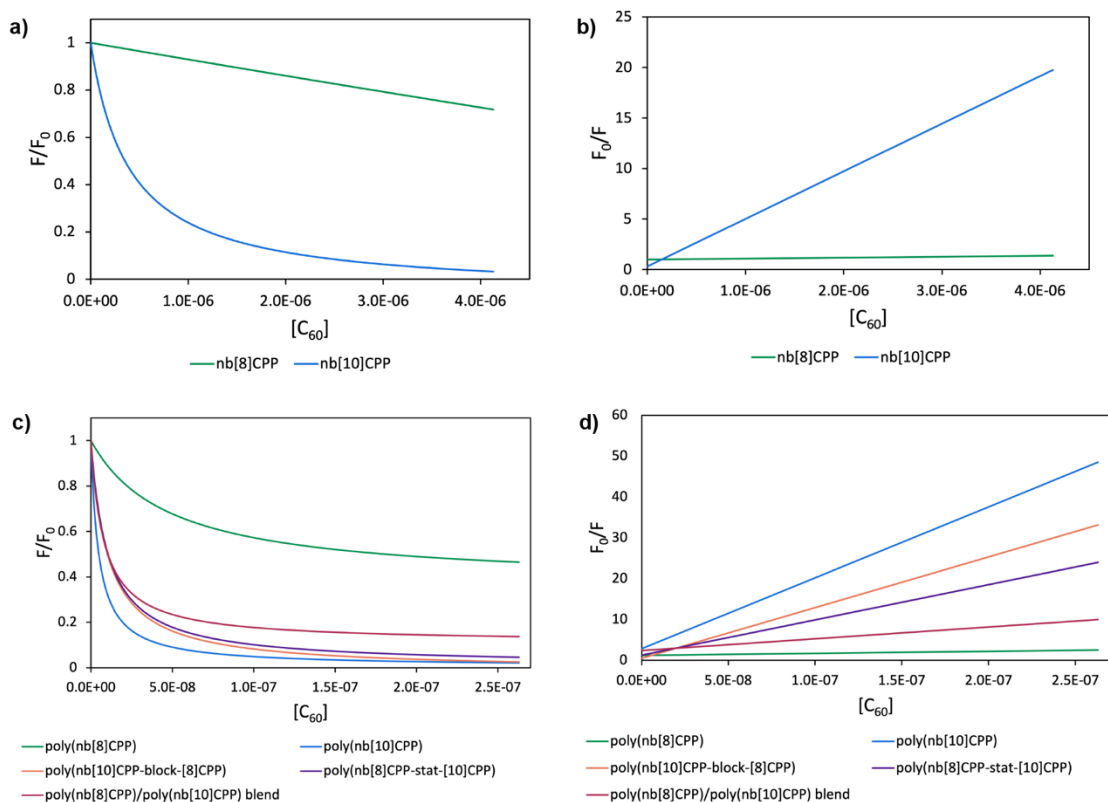


**Figure 2.24.** Plots of $C_{60}$ concentration versus a) $F/F_0$ for nbCPP monomers, b) $F_0/F$ for nbCPP monomers, c) $F/F_0$ for poly(nbCPP)s, and d) $F_0/F$ for poly(nbCPP)s.
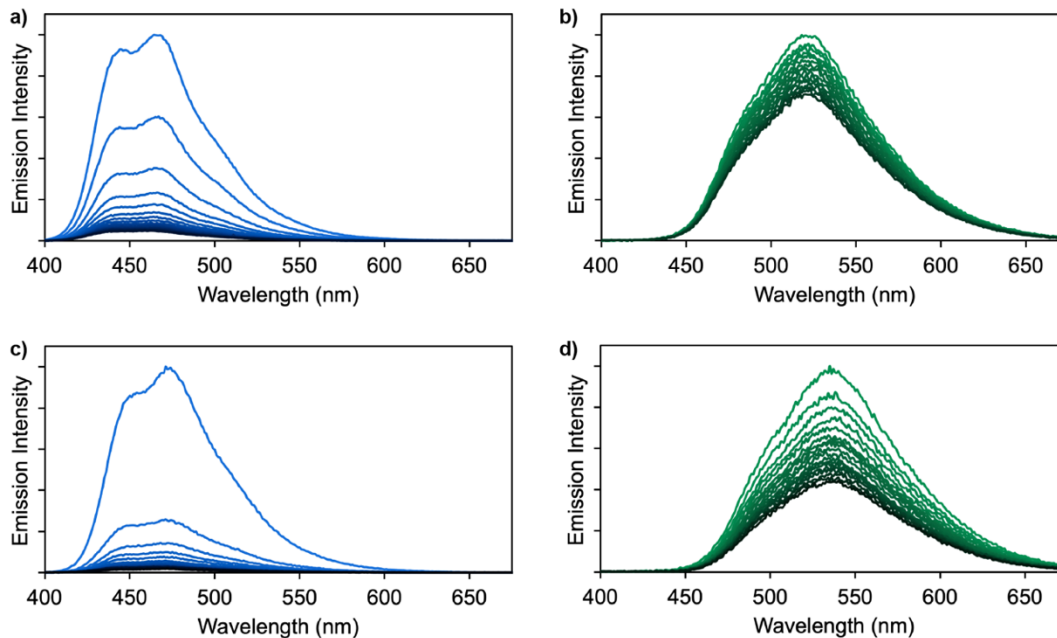
**Figure 2.25.** Fluorescence response of a) nb[10]CPP, b) nb[8]CPP, c) poly(nb[10]CPP), and d) poly(nb[8]CPP) to $C_{60}$ addition. Polymer data from samples 4 and 16, Table 2.3.
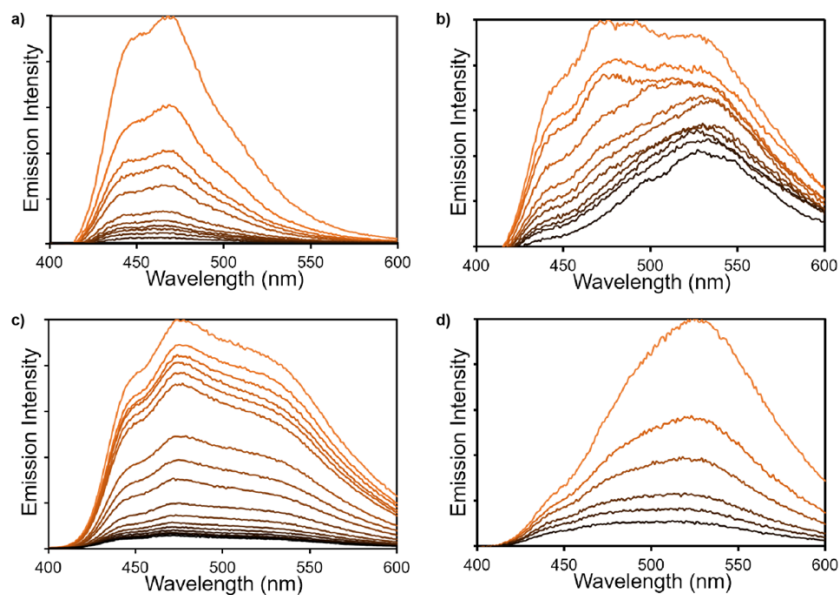


**Figure 2.26.** Fluorescence response of a) poly(nb[10]CPP), b) a poly(nb[8]CPP)/ poly(nb[10]CPP) blend, c) poly(nb[10]CPP-*block*-[8]CPP), and d) poly(nb[8]CPP-*stat*-[10]CPP) to $C_{60}$ addition. Data shown from one trial each with samples 6 and 12, Table 2.4 and samples 2 and 6, Table 2.5. Concentrations of polymer and $C_{60}$ for this set of trials differed from the general procedure above, but the outcomes were the same.

## 2.5.5 Monomer Synthesis and Structural Characterization

## 2.5.5.1 Safety Summary

No unexpected or unusually high safety hazards were encountered.

Care should be taken when using *n*-butyllithium: for example, using a luer lock syringe for *n*-BuLi transfers, using a syringe with double the capacity of the volume to be transferred, and not using *n*-BuLi while working alone.

The following procedure was used for safely handling sodium metal when preparing the sodium naphthalenide reagent: Tweezers, a small beaker, a squirt bottle of hexanes, and a jar containing sodium in oil were gathered. A piece of weigh paper was folded diagonally for later ease of transferring sodium. Using tweezers, a small chunk of sodium was removed from the jar and rinsed with hexanes over the beaker. The piece of sodium was set on a second piece of weigh paper to blot it and/or to turn it to rinse another side. Once the sodium was mostly clean/dry, it was weighed on the folded paper. Additional chunks were cut off the sodium block in the jar using a spatula with a squared end or the broad end of a scoopula, and the rinsing/weighing steps were repeated. Once the desired amount of sodium was obtained, it was folded inside the weigh paper and pounded flat with a mallet. The weigh paper was opened, and the sodium was cut into small pieces with a blade, then carefully poured into a dry reaction flask. Weigh papers, spatulas, tweezers, the blade, and anything else which could have residual sodium on it were placed under running water. (This method should NOT be used to quench larger amounts of sodium!)

## 2.5.5.2 Detailed Synthetic Procedures

Compounds **II.1**,[173,174] **II.3**,[145] **II.4**,[146] **II.12**,[175] **II.13**,[176] **II.15**,[177] SPhos-Pd-G2,[178] and Grubbs G3[179] were prepared according to the literature.

*Three-ring norbornene-fused dibromide **II.2***.
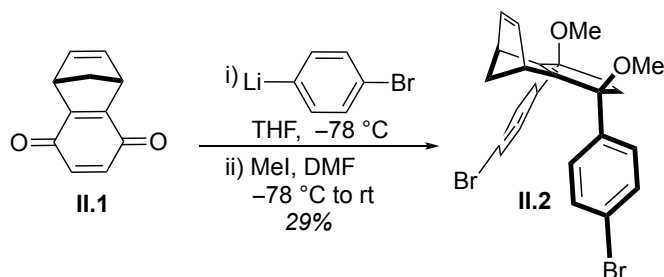


A flame-dried flask was charged with 1,4-dibromobenzene (8.2 g, 34.8 mmol, 3.00 equiv.), which was dissolved in THF (80 mL) and then cooled to -78 °C for 20 minutes. *n*-BuLi (15.8 mL, 24.8 mmol, 3.00 equiv.) was added dropwise. The reaction was stirred at -78 °C for 20 minutes, after which a solution of norbornene-benzoquinone **II.1** (2.00 g, 11.6 mmol, 1.00 equiv.) in THF (8 mL) was added dropwise. The reaction was stirred for 1 hour at -78 °C. Methyl iodide (7.2 mL, 116.2 mmol, 10.00 equiv.) and a few mL of DMF were added to the reaction, which was stirred overnight at room temperature then quenched with water. The THF was removed under reduced pressure, and the resulting solution was extracted with ethyl acetate (3x). The combined organic layers were washed with 5% aqueous LiCl (3x), water (2x), and brine (1x), then dried over sodium sulfate. Concentration under reduced pressure yielded solid product, which was filtered and washed with hexanes. Additional product was obtained by purifying the filtrate via silica gel column chromatography (0 to 8% ethyl acetate in hexanes) followed by a final wash of product-containing fractions with hexanes. Combined yield was 1.69 g (29%). $^1$H NMR (500 MHz, CDCl$_3$): δ 7.49 – 7.44 (m, 4H), 7.34 – 7.30 (m, 4H), 6.87 (t, *J* = 1.9 Hz, 2H), 5.92 (s, 2H), 3.50 (p, *J* = 1.6 Hz, 2H), 3.15 (s, 6H), 1.99 (dt, *J* = 6.3, 1.6 Hz, 1H), 1.89 (dt, *J* = 6.3, 1.7 Hz, 1H). $^{13}$C NMR (126 MHz, CDCl$_3$) δ 153.8, 142.3, 142.2, 134.5, 131.5, 127.8, 121.5, 75.9, 74.1, 52.8, 49.8. IR (neat): 2983.3, 2931.2, 2873.7, 1481.0, 1392.1, 1299.1, 1070.9, 1007.4, 938.4, 823.3, 726.6, 681.9 cm$^{-1}$. HRMS (TOF MS EI+) (m/z): [M]$^+$ calculated for C$_{25}$H$_{22}$Br$_2$O$_2$: 511.9987; found: 511.9997.

*nb[8]CPP macrocycle **II.6**.*
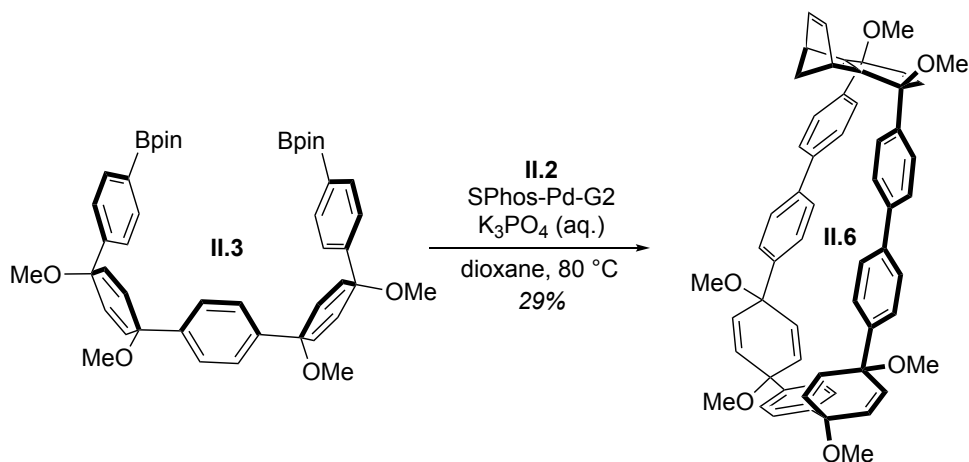


A flame-dried flask was charged with dibromide **II.2** (300 mg, 0.583 mmol, 1.00 equiv.), bisboronate **II.3** (487 mg, 0.642 mmol, 1.10 equiv.), and SPhos-Pd-G2 (42 mg, 0.058 mmol, 0.10 equiv.). The flask was evacuated and backfilled with nitrogen for 5 cycles. Dry dioxane (195 mL) was sparged with nitrogen for 1 hr. A 2.00 M. aqueous solution of $K_3PO_4$ was sparged with nitrogen for 1 hr. Dioxane was added to the reaction flask, which was then heated to 80 °C. 19.5 mL of $K_3PO_4$ solution was added. The reaction was stirred overnight at 80 °C. After the reaction was cooled to room temperature, the dioxane was removed under reduced pressure, then the resulting material was extracted with DCM (3x). The combined organic layers were washed with water (2x) and brine (1x), then dried over sodium sulfate, filtered through celite, and concentrated under reduced pressure. Silica gel column chromatography (6 to 16% ethyl acetate in 50/50 DCM/hexanes) yielded 160 mg (29%). $^1$H NMR (500 MHz, CDCl$_3$): δ 7.55 (d, $J$ = 8.6 Hz, 4H), 7.51 (s, 4H), 7.50 (d, $J$ = 7.9 Hz, 4H), 7.43 (d, $J$ = 8.7 Hz, 4H), 7.21 (d, $J$ = 8.6 Hz, 4H), 6.98 (t, $J$ = 1.8 Hz, 2H), 6.14 – 6.06 (overlapping, 10H), 3.79 (t, $J$ = 1.8 Hz, 2H), 3.48 (s, 6H), 3.40 (s, 6H), 3.23 (s, 6H), 2.05 (dt, $J$ = 6.3, 1.6 Hz, 1H), 1.97 (dt, $J$ = 6.2, 1.6 Hz, 1H). $^{13}$C NMR (126 MHz, CDCl$_3$) δ 154.11, 143.35, 143.19, 142.79, 140.82, 139.61, 139.54, 134.87, 133.60, 133.44, 132.83, 132.70, 127.13, 126.82, 126.38, 126.28, 126.26, 77.61, 74.60, 74.00, 73.79, 53.03, 52.15, 51.78, 49.68. IR (neat): 2934.9, 2897.5, 2821.1, 1712.9, 1491.7, 1448.9, 1397.2, 1175.2, 1073.9, 946.7, 818.3 cm$^{-1}$. HRMS (TOF MS EI+) (m/z): [M]$^+$ calculated for C$_{59}$H$_{54}$O$_6$: 858.3920; found: 858.3954.

*nb[8]CPP.*
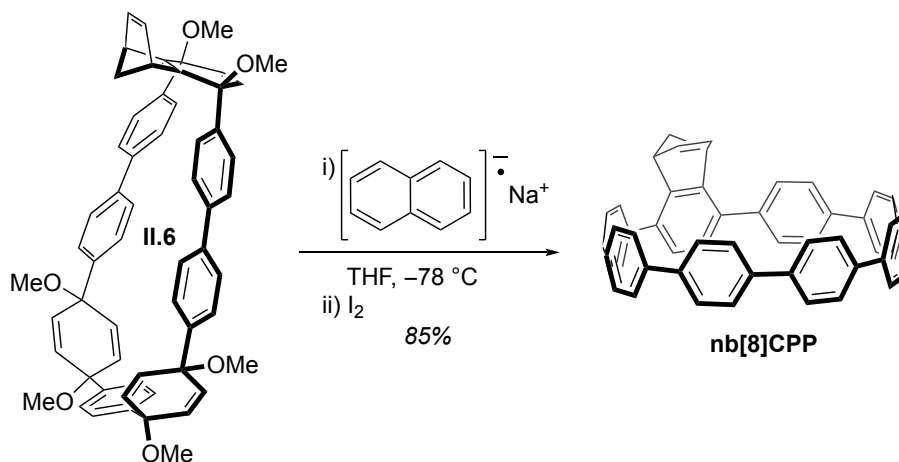


A 0.5 M. sodium naphthalenide solution was prepared by sonicating sodium and naphthalene in THF in a flame-dried flask, then stirring the solution overnight. Macrocycle **II.6** (83 mg, 0.097 mmol, 1.00 equiv.) was dispersed in THF in a flame-dried flask and stirred at -78 °C for 30 min. Sodium naphthalenide (>2.90 mL, 1.45 mmol, 15.00 equiv.) was added dropwise to the reaction flask until the mixture was brown. The reaction was stirred for 30 minutes and then quenched with dropwise addition of 1 M. iodine solution in THF until orange. Sodium thiosulfate was added until the orange color dissipated, and the reaction was warmed to room temperature. THF was removed under reduced pressure, and the resulting solution was extracted with DCM (3x). The combined organic layers were washed with water (2x) and brine (1x), then dried over sodium sulfate and concentrated under reduced pressure. Automated silica gel column chromatography (5 to 40% DCM in hexanes) yielded 55 mg (85%). $^1$H NMR (500 MHz, CDCl$_3$): δ (ppm) 7.47 (overlapping, 24H), 7.28 (d, $J$ = 7.9 Hz, 4H), 7.01 (t, $J$ = 1.9 Hz, 2H), 6.53 (s, 2H), 4.38 (t, $J$ = 1.9 Hz, 2H), 2.45 (dt, $J$ = 7.2, 1.6 Hz, 1H), 2.28 (d, $J$ = 7.4 Hz, 1H). $^{13}$C NMR (126 MHz, CDCl$_3$) δ 148.59, 143.15, 139.08, 138.25, 138.05, 137.91, 137.89, 137.86, 137.80, 132.84, 129.05, 69.44, 49.98. IR (neat): 3021.8, 1889.6, 1582.9, 1480.7, 1388.8, 1256.9, 998.7, 942.1, 809.7, 723.2 cm$^{-1}$. HRMS (TOF MS EI+) (m/z): [M]$^+$ calculated for C$_{53}$H$_{36}$: 672.2817; found: 672.2833.

*nb[9]CPP macrocycle **II.7**.*
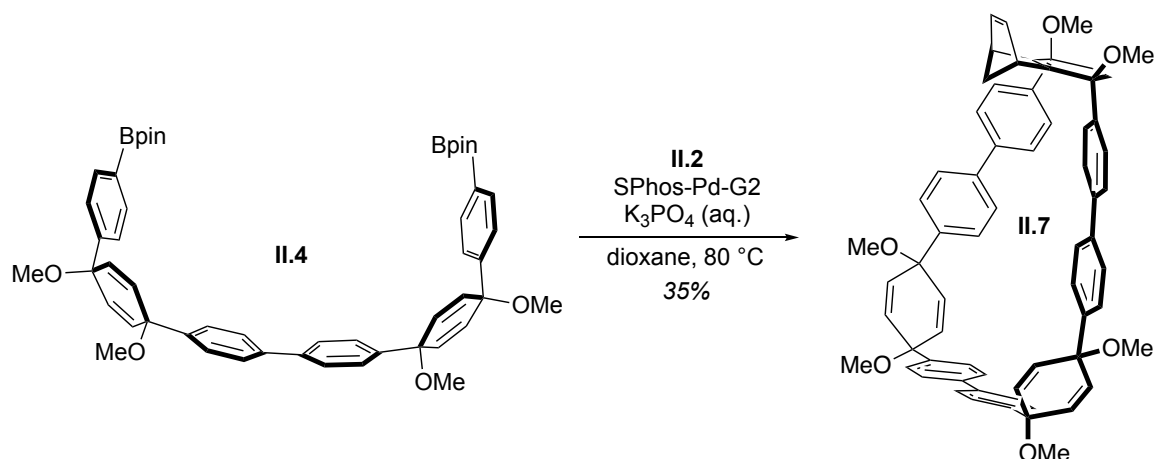


A flame-dried flask was charged with dibromide **II.2** (475 mg, 0.9 mmol, 1.00 equiv.), bisboronate **II.4** (810 mg, 0.1 mmol, 1.05 equiv.), and SPhos-Pd-G2 (67 mg, 0.1 mmol, 0.10 equiv.). The flask was evacuated and backfilled with nitrogen for 5 cycles. A 2.00 M. aqueous solution of $K_3PO_4$ was sparged with nitrogen for 1 hr. Dioxane (308 mL) was added to the reaction flask, sparged for 20 min., then heated to 80 °C for 10 min. 31 mL of $K_3PO_4$ solution was added, and the reaction was stirred for 30 min. at 80 °C. After the reaction was cooled to room temperature, the dioxane was removed under reduced pressure, then the resulting material was filtered through a celite pad with DCM and water. The filtrate was extracted with DCM (3x). The combined organic layers were washed with water (2x) and brine (1x), then dried over sodium sulfate and concentrated under reduced pressure. Silica gel column chromatography (0 to 10% ethyl acetate in DCM) yielded 306 mg (35%). $^1$H NMR (600 MHz, CDCl$_3$): δ (ppm) 7.64 (d, $J$ = 8.3 Hz, 4H), 7.63 (d, $J$ = 8.1 Hz, 4H), 7.59 (d, $J$ = 8.2 Hz, 4H), 7.55 (d, $J$ = 8.2 Hz, 4H), 7.50 (d, $J$ = 8.4 Hz, 4H), 7.48 (d, $J$ = 8.4 Hz, 4H), 6.91 (t, $J$ = 1.9 Hz, 2H), 6.18 (overlapping, 8H), 5.99 (s, 2H), 3.61 (t, $J$ = 2.0 Hz, 2H), 3.48 (s, 6H), 3.47 (s, 6H), 3.20 (s, 6H), 1.98 (d, $J$ = 6.0 Hz, 1H), 1.93 (d, $J$ = 6.0 Hz, 1H). $^{13}$C NMR (151 MHz, CDCl3) δ 153.99, 142.72, 139.74, 134.70, 133.63, 128.52, 75.06, 74.25, 67.21, 52.86, 52.19, 49.94. IR (neat): 2932.6, 2870.8, 1139.2, 1149.2, 1147.9, 1074.4, 1074.4, 1027.6, 950.6, 906.0, 847.7, 753.7 cm$^{-1}$. HRMS (TOF MS EI+) (m/z): [M+H]$^+$ calculated for C$_{65}$H$_{59}$O$_6$: 935.4312; found: 935.5661.

*nb[9]CPP.*
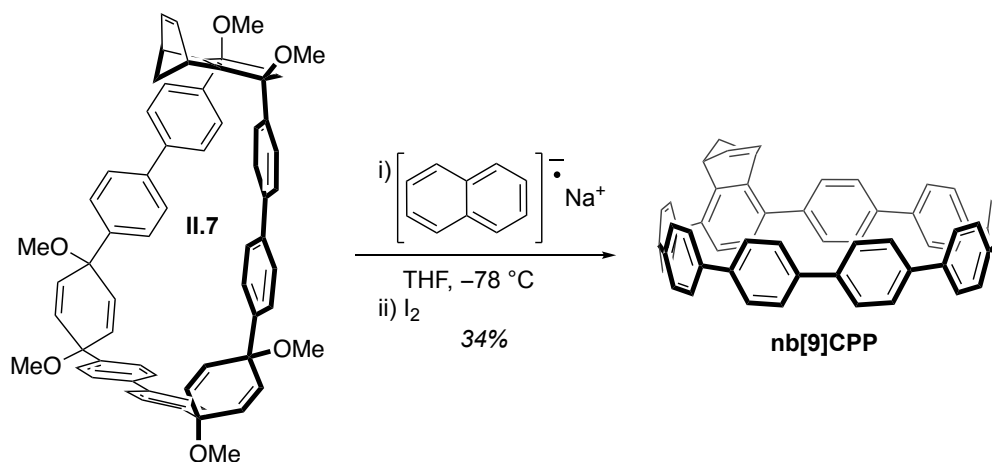


A 0.5 M. sodium naphthalenide solution was prepared by sonicating sodium and naphthalene in THF in a flame-dried flask, then stirring the solution overnight. Macrocycle **II.7** (220 mg, 0.24 mmol, 1.00 equiv.) was dispersed in THF in a flame-dried flask and stirred at -78 °C for 30 min. Sodium naphthalenide (7.1 mL, 3.54 mmol, 15.00 equiv.) was added dropwise to the reaction flask until the mixture was brown. The reaction was stirred for 20 minutes and then quenched with dropwise addition of 1 M. iodine solution in THF until orange. Sodium thiosulfate was added until the orange color dissipated and the reaction was warmed to room temperature. THF was removed under reduced pressure, and the resulting solution was extracted with DCM (3x). The combined organic layers were washed with water (2x) and brine (1x), then dried over sodium sulfate and concentrated under reduced pressure. The material was adsorbed on silica and purified by silica gel column chromatography (19% then 40% DCM in hexanes), yielding 60 mg (34%). $^1$H NMR (600 MHz, CDCl$_3$): δ (ppm) 7.56 (overlapping, 28H), 7.33 (d, $J =$ 8.2 Hz, 4H), 7.04 (t, $J = 1.9$ Hz, 2H), 6.60 (s, 2H), 4.38 (p, $J = 1.7$ Hz, 2H), 2.45 (dt, $J =$ 7.5, 1.6 Hz, 1H), 2.30 (dt, $J = 7.4$, 1.7 Hz, 1H). $^{13}$C NMR (151 MHz, CDCl$_3$) δ 148.80, 143.21, 139.28, 138.18, 133.02, 128.55, 127.52, 69.44, 53.58, 49.95. IR (neat): 3020.4, 1586.4, 1480.2, 1386.7, 1261.0, 999.3, 805.2, 729.5 cm$^{-1}$. HRMS (TOF MS ASAP+) (m/z): [M+H]$^+$ calculated for C$_{59}$H$_{41}$: 749.3208; found: 749.3198.

*Seven-ring dichloride* **II.14.**
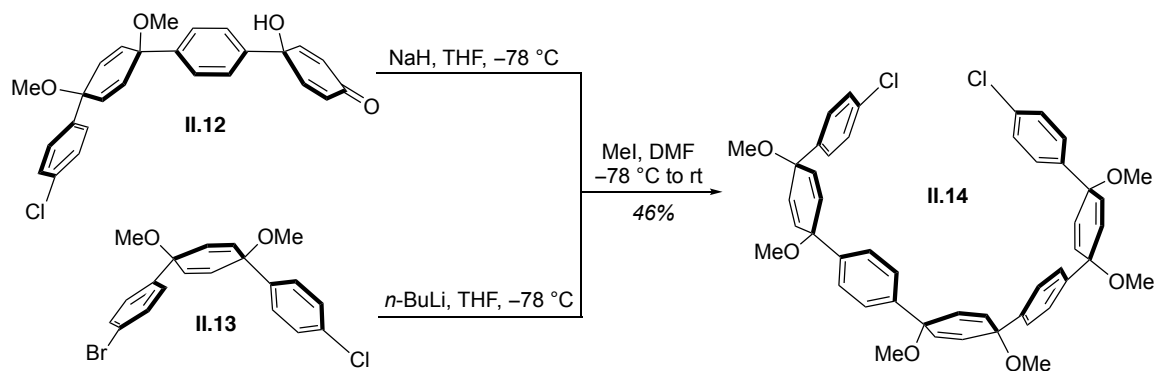


To a slurry of sodium hydride (220 mg, 5.4 mmol, 1.30 equiv.) in 10 mL THF was added a solution of ketone **II.12** (1.80 g, 4.1 mmol, 1.00 equiv.) in 10 mL THF at -78 °C. The reaction mixture was stirred for 2 hrs at -78 °C. In a separate flask, bromochloride **II.13** (2.52 g, 6.2 mmol, 1.50 equiv.) was dissolved in 20 mL THF. This solution was cooled to -78 °C, then *n*-BuLi (2.4 mL, 5.8 mmol, 1.40 equiv.) was added dropwise and the reaction was stirred for 30 min. This mixture was then transferred to the slurry containing the deprotonated ketone. The resulting mixture was stirred for 2 hrs, at which time MeI (2.6 mL, 4.1 mmol, 10.00 equiv.) and dry DMF (5 mL) were added. The reaction was allowed to warm to room temperature overnight. The reaction was quenched with water and extracted with diethyl ether (3x). The combined organic layers were washed with 5% aqueous LiCl (3x), water (2x), and brine (1x), then dried over sodium sulfate and concentrated under reduced pressure. The material was sonicated with hexanes until solid formed, then it was filtered and washed with hexanes. The product was purified further by automated silica gel chromatography in 5 to 12% ethyl acetate in hexanes. 1.50 g were collected (46%). $^1$H NMR (500 MHz, CDCl$_3$): δ 7.37 – 7.24 (overlapping, 16H), 6.11 (d, *J* = 10.2 Hz, 4H), 6.07 (s, 4H), 6.04 (d, *J* = 10.4 Hz, 4H), 3.43 – 3.40 (overlapping, 18H). $^{13}$C NMR (126 MHz, CDCl$_3$) δ 143.09, 142.69, 142.20, 133.84, 133.48, 133.46, 133.12, 128.61, 127.60, 126.21, 126.13, 77.36, 74.70, 74.58, 52.14, 52.13, 52.12. IR (neat): 2939.8, 2819.0, 1489.0, 1452.1, 1403.3, 1228.2, 1179.3, 1070.6, 1013.2, 947.7, 820.3, 729.2, 664.0 cm$^{-1}$. HRMS (TOF MS EI+) (m/z): [M]$^+$ calculated for C$_{48}$H$_{46}$Cl$_2$O$_6$: 788.2671; found: 788.2695.

*Seven-ring bisboronate **II.5**.*
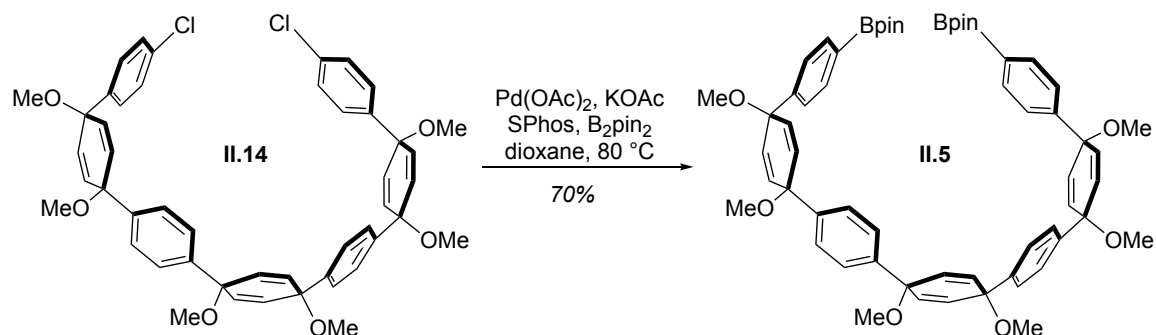


Potassium acetate (373 mg, 3.8 mmol, 6.00 equiv.) was flame-dried in a flask and cooled under nitrogen. Ground $B_2pin_2$ (482 mg, 1.9 mmol, 3.00 equiv.), dichloride **II.14** (500 mg, 0.6 mmol, 1.00 equiv.), $Pd(OAc)_2$ (14 mg, 0.1 mmol, 0.10 equiv.), and SPhos (68 mg, 0.2 mmol, 0.26 equiv.) were added to the flask, which was then evacuated and backfilled with nitrogen for 5 cycles. The flask was sealed with a septum and purged with nitrogen for 1 hr. Dry dioxane (5 mL) was sparged with nitrogen for 1 hr then added to reaction flask. The reaction was heated to 80 °C, then stirred overnight. After the reaction was cooled to room temperature, the mixture was filtered through a plug of celite, and the filtrate was concentrated under reduced pressure. The material was sonicated with methanol and filtered. The product was then run through a very short silica plug using ethyl acetate and concentrated again to yield 430 mg (70%). $^1$H NMR (500 MHz, CDCl$_3$): δ 7.75 (d, $J$ = 8.0 Hz, 4H), 7.40 (d, $J$ = 8.3 Hz, 4H), 7.34 (s, 8H), 6.10-6.06 (m, 12H), 3.42 (m, 18H), 1.33 (s, 24H). $^{13}$C NMR (126 MHz, CDCl$_3$) δ 146.63, 142.94, 142.80, 135.09, 133.54, 133.48, 133.44, 133.27, 126.20, 126.13, 125.45, 83.90, 75.04, 74.79, 74.74, 52.10, 52.08, 25.01, 24.97. IR (neat): 2979.9, 2938.2, 2896.7, 2821.6, 1501.1, 1489.4, 1450.9, 1403.2, 1358.1, 1179.3, 1079.3, 1013.8, 948.7, 826.4, 757.3, 657.2 cm$^{-1}$. HRMS (FTMS ESI) (m/z): [M+Na]$^+$ calculated for $C_{60}H_{70}B_2O_{10}Na$: 995.5047; found: 995.5031.

*nb[10]CPP macrocycle **II.8**.*
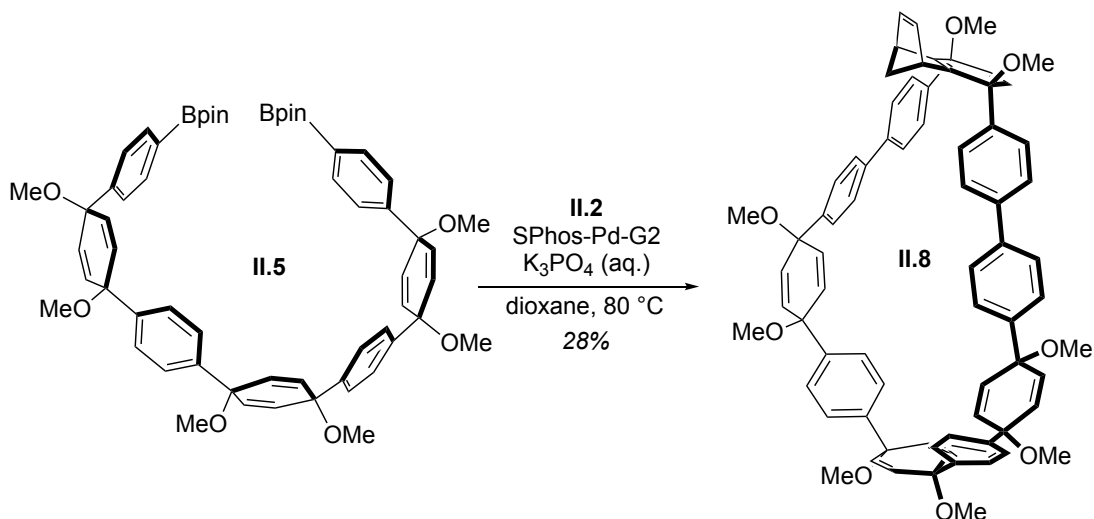


A flame-dried flask was charged with dibromide **II.2** (720 mg, 1.40 mmol, 1.00 equiv.), bisboronate **II.5** (1.43 g, 1.47 mmol, 1.05 equiv.), and SPhos-Pd-G2 (101 mg, 0.14 mmol, 0.10 equiv.). The flask was evacuated and backfilled with nitrogen for 5 cycles. The flask was then purged with nitrogen. A 2.00 M. aqueous solution of $K_3PO_4$ was sparged with nitrogen for 1 hr. Dioxane (470 mL) was added to the reaction flask via cannulation, and the solution was sparged for 20 min. before being heated to 80 °C for 10 min. 47 mL of $K_3PO_4$ solution was added, and the reaction was stirred for 30 min. at 80 °C. After the reaction was cooled to room temperature, the dioxane was removed under reduced pressure, then the resulting material was filtered through a celite pad with DCM and water. The filtrate was extracted with DCM (3x). The combined organic layers were washed with water (2x) and brine (1x), then dried over sodium sulfate and concentrated under reduced pressure. The material was purified by automated silica gel column chromatography (0 to 14% ethyl acetate in DCM), then washed with acetone and filtered, yielding 415 mg (28%). $^1H$ NMR (500 MHz, CDCl$_3$): δ 7.43 – 7.35 (overlapping, 24H), 6.96 (s, 2H), 6.17-6.14 (overlapping, 8H), 6.07 (m, 4H), 6.00 (s, 2H), 3.73 (s, 2H), 3.44 (s, 6H), 3.38 (s, 6H), 3.37 (s, 6H), 3.20 (s, 6H), 2.17 (d, $J$ = 6.0 1H), 2.10 (d, $J$ = 6.2 Hz, 1H). $^{13}C$ NMR (126 MHz, CDCl$_3$) δ 154.21, 143.26, 143.05, 142.97, 142.47, 141.92, 140.42, 140.37, 134.78, 134.01, 133.85, 133.23, 133.02, 132.86, 127.35, 127.25, 126.77, 126.48, 126.29, 126.27, 77.02, 75.00, 74.52, 74.19, 73.96, 52.98, 52.18, 52.06, 50.03. IR (neat): 2978.9, 2936.2, 2896.6, 2821.4, 1608.8, 1490.1, 1450.6, 1403.0, 1358.2, 1173.4,

1072.8, 1013.7, 948.0, 822.2, 656.7 cm$^{-1}$. HRMS (TOF MS EI+) (m/z): [M+Na]$^+$ calculated for $C_{73}H_{68}O_8Na$: 1095.4812; found: 1095.4840.

*nb[10]CPP*.
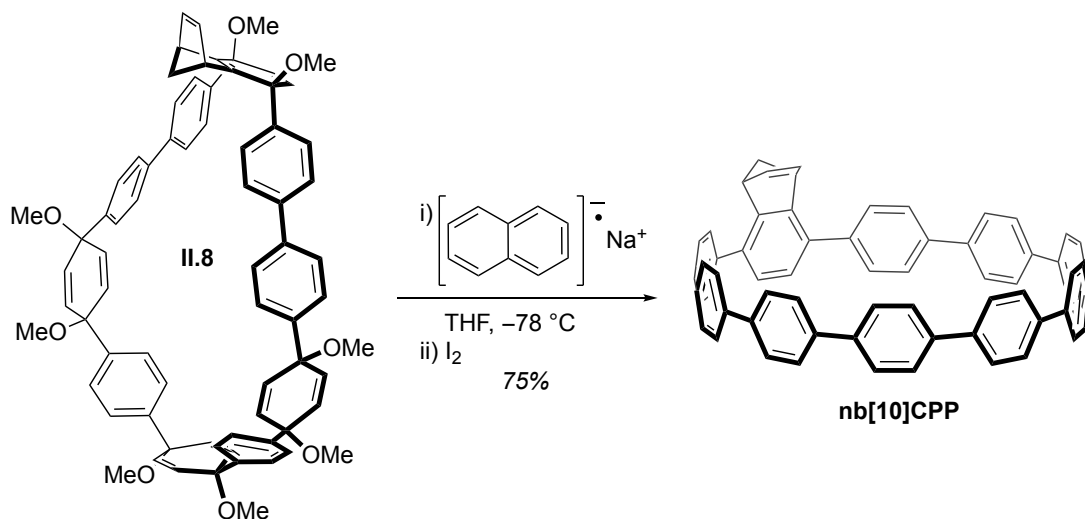


A 0.5 M. sodium naphthalenide solution was prepared by sonicating sodium and naphthalene in THF in a flame-dried flask, then stirring the solution overnight. Macrocycle **II.8** (395 mg, 0.368 mmol, 1.00 equiv.) was dispersed in THF in a flame-dried flask and stirred at -78 °C for 30 min. Sodium naphthalenide (>11.0 mL, 5.52 mmol, 15.00 equiv.) was added dropwise to the reaction flask until the mixture was brown. The reaction was stirred for 20 minutes and then quenched with dropwise addition of 1 M. iodine solution in THF until orange. Sodium thiosulfate was added until the orange color dissipated, and the reaction was warmed to room temperature. The resulting solution was extracted with DCM (3x). The combined organic layers were washed with water (2x) and brine (1x), then dried over sodium sulfate and concentrated under reduced pressure. The material was adsorbed on silica and purified by automated silica gel column chromatography (15-35% DCM in hexanes), yielding 229 mg (75%). $^1$H NMR (500 MHz, CDCl$_3$): δ 7.56 (overlapping, 32H), 7.36 (d, *J* = 8.2 Hz, 4H), 7.05 (t, *J* = 1.7 Hz, 2H), 6.65 (s, 2H), 4.37 (s, 2H), 2.45 (d, *J* = 7.6 Hz, 1H), 2.31 (d, *J* = 7.3 Hz, 1H). $^{13}$C NMR (126 MHz, CDCl$_3$) δ 148.72, 143.11, 139.27, 138.26, 138.19, 138.17, 138.15, 133.07, 128.40, 128.01, 127.40, 127.37, 127.35, 127.24, 127.20, 69.27, 49.76. IR (neat):

3021.3, 1895.4, 1589.7, 1479.3, 1386.6, 1000.2, 905.4, 805.7, 730.6 cm$^{-1}$. HRMS (TOF MS EI+) (m/z): [M]$^+$ calculated for C$_{65}$H$_{44}$: 824.3443; found: 824.3467.

*Dimethoxy benzonorbornadiene **diMeObnb***.
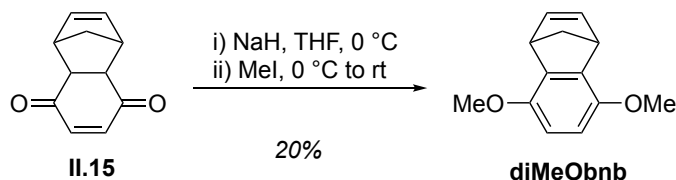


A slurry of sodium hydride (3.44 g, 86.1 mmol, 3.00 equiv.) in 20 mL THF was cooled to 0 °C. A solution of diketone **II.15** (5.00 g, 28.7 mmol, 1.00 equiv.) in 20 mL THF was added in stream. After 10 min., methyl iodide (8.9 mL, 143.5 mmol, 5.00 equiv.) was added, and the reaction was allowed to warm to room temperature. Water was added to quench the reaction, and the resulting mixture was extracted with DCM (3x). The combined organic layers were washed with water (2x) and brine (1x), then dried over sodium sulfate and concentrated under reduced pressure. The crude material was dissolved in 50/50 DCM/hexanes and passed through a plug of silica. Concentration of the filtrate yielded a colorless oil which solidified on standing (1.16 g, 20%). $^1$H NMR (600 MHz, CDCl$_3$): δ 6.83 (t, $J$ = 1.9 Hz, 2H), 6.50 (s, 2H), 4.16 (p, $J$ = 1.7 Hz, 2H), 3.79 (s, 6H), 2.22 (dt, $J$ = 6.9, 1.6 Hz, 1H), 2.18 (dt, $J$ = 6.9, 1.7 Hz, 1H). $^{13}$C NMR (151 MHz, CDCl$_3$) δ 148.86, 143.12, 140.65, 109.67, 70.27, 56.44, 47.13. IR (neat): 2999.2, 2952.8, 2922.5, 2828.5, 1492.7, 1451.1, 1436.6, 1293.9, 1252.8, 1195.6, 1090.0, 1056.0, 1007.1, 965.5, 792.3, 734.2, 709.3, 619.3 cm$^{-1}$. HRMS (TOF MS EI+) (m/z): [M]$^+$ calculated for C$_{13}$H$_{14}$O$_2$: 202.0994; found: 202.0995.

### 2.5.5.3 X-Ray Crystallography Data

Single crystals suitable for crystallographic analysis were grown from slow evaporation of a solution of **II.2** in DCM/hexanes and slow diffusion of pentane into solutions of **nb[8]CPP**, **nb[9]CPP**, and **nb[10]CPP** in THF. Crystal data has been deposited to the Cambridge Crystallographic Database with CCDC numbers 1949617, 1949616, 2051663, and 1949615.

Diffraction intensities were collected at 173 K on a Bruker Apex2 CCD diffractometer using CuK$\alpha$ radiation, $\lambda$= 1.54178 Å. Space groups were determined based on systematic absences. Absorption corrections were applied by SADABS.[180] Structures were solved by direct methods and Fourier techniques and refined on $F^2$ using full matrix least-squares procedures. All non-H atoms were refined with anisotropic thermal parameters. H atoms in all structures were refined in calculated positions in a rigid group model. The structure of **nb[8]CPP** was determined in non-centrosymmetrical space group symmetry $R3c$, but not in possible centro-symmetrical space group $R$-3$c$. The refinement in non-centrosymmetrical space group symmetry $R3c$ shown that the Flack parameter is close to zero, but not to 0.5 as could be expected if the centro-symmetrical space group $R$-3$c$ is correct. Crystals of **nb[8]CPP** are formed as thin strips and give very weak X-ray diffraction at high angles. Even using a strong *Incoatec* I$\mu$S Cu source for **nb[8]CPP** it was possible to collect data only up to $2\theta_{max}$ = 98.44°. However, the collected data provide an appropriate number of measured reflections per a number of refined parameters, 4073/472. In both **nb[8]CPP** and **nb[10]CPP**, solvent pentane molecules fill out empty space in the packing and in the hoops and are highly disordered. These disordered solvent molecules were treated by SQUEEZE.[181] The corrections of the X-ray data by SQUEEZE are 760 and 480 electron/cell; the required values are 756 and 336 electron/cell for eighteen and eight pentane molecules in the full unit cells, respectively in **nb[8]CPP** and **nb[10]CPP**. The five-member ring in **nb[8]CPP** is disordered over two positions with opposite orientations as well. Resolution for **nb[8]CPP** and **nb[10]CPP** structures is relatively low due to a lot of disordered fragments in the structures and weak X-ray diffraction at high angles, but the found X-ray structures clearly shown the structure of the hoops in these compounds. There are two symmetrically independent molecules in the structure of **nb[9]CPP**. Besides the main molecules the crystal structure includes five solvent pentane molecules. They fill out empty space in the packing and in the hoops. These THF molecules were refined with restrictions on its bond lengths: the standard O-C and C-C distances were used in the refinement as the targets for corresponding bonds. Thermal parameters for atoms in these pentane molecules are elongated indicating that they are highly disordered. Some short

H…H contacts in the structure are related to the contacts between these disordered groups. All calculations were performed by the Bruker SHELXL-2014 package.[182]

Crystallographic Data for **II.2**: $C_{25}H_{22}Br_2O_2$, M = 514.24, 0.11 x 0.08 x 0.06 mm, T = 173(2) K, Monoclinic, space group $P2_1/c$, a = 12.3702(5) Å, b = 15.2429(6) Å, c = 12.0344(4) Å, $\beta$ = 112.703(1)°, V = 2093.36(14) Å3, Z = 4, $D_c$ = 1.632 Mg/m3, $\mu$(Cu) = 5.058 mm-1, F(000) = 1032, $2\theta_{max}$ = 133.31°, 16491 reflections, 3694 independent reflections [$R_{int}$ = 0.0496], R1 = 0.0313, wR2 = 0.0848 and GOF = 1.044 for 3694 reflections (262 parameters) with I>2σ(I), R1 = 0.0344, wR2 = 0.0870 and GOF = 1.044 for all reflections, max/min residual electron density +0.573/-0.507 eÅ$^{-3}$.

Crystallographic Data for **nb[8]CPP**: $C_{58}H_{48}$, $C_{53}H_{36}$·$(C_5H_{12})$, M = 744.96, 0.09 x 0.08 x 0.01 mm, T = 173(2) K, Trigonal, space group $R3c$, a = 16.3432(5) Å, b = 16.3432(5) Å, c = 80.413(4) Å, V = 18600.8(14) Å3, Z = 18, $D_c$ = 1.197 Mg/m3, $\mu$(Cu) = 0.508 mm-1, F(000) = 7128, $2\theta_{max}$ = 98.44°, 25725 reflections, 4073 independent reflections [$R_{int}$ = 0.0604], R1 = 0.0534, wR2 = 0.1340 and GOF = 1.085 for 4073 reflections (472 parameters) with I>2σ(I), R1 = 0.0688, wR2 = 0.1424 and GOF = 1.087 for all reflections, max/min residual electron density +0.140/-0.137 eÅ$^{-3}$.

Crystallographic Data for **nb[9]CPP**: $C_{71}H_{64}O_3$, M = 965.22, 0.17 x 0.15 x 0.02 mm, T = 173(2) K, Triclinic, space group $P$-1, a = 9.9507(4) Å, b = 17.1984(7) Å, c = 32.2140(12) Å, $\alpha$ = 82.982(2)°, $\beta$ = 85.750(2)°, $\gamma$ = 89.947(2)°, V = 5456.4(4) Å$^3$, Z = 4, $D_c$ = 1.175 Mg/m$^3$, $\mu$(Cu) = 0.538 mm$^{-1}$, F(000) = 2056, $2\theta_{max}$ = 133.65°, 60692 reflections, 19175 independent reflections [$R_{int}$ = 0.0585], R1 = 0.0978, wR2 = 0.2717 and GOF = 1.058 for 19175 reflections (1333 parameters) with I>2σ(I), R1 = 0.1454, wR2 = 0.3101 and GOF = 1.070 for all reflections, max/min residual electron density +0.565/-0.651 eÅ$^{-3}$.

Crystallographic Data for **nb[10]CPP**: $C_{75}H_{68}$, $C_{65}H_{44}$·2($C_5H_{12}$), M = 969.29, 0.11 x 0.08 x 0.06 mm, T = 173(2) K, Monoclinic, space group $P2_1/c$, a = 6.5747(3) Å, b = 28.3155(16) Å, c = 32.6239(17) Å, $\beta$ = 91.334(4)°, V = 6071.8(5) Å3, Z = 4, $D_c$ = 1.060 Mg/m3, $\mu$(Cu) = 0.447 mm-1, F(000) = 2072, $2\theta_{max}$ = 133.40°, 46166 reflections, 10685 independent reflections [$R_{int}$ = 0.0443], R1 = 0.0507, wR2 = 0.1396 and GOF = 1.051

for 10685 reflections (586 parameters) with I>2σ(I), R1 = 0.0617, wR2 = 0.1461 and GOF = 1.051 for all reflections, max/min residual electron density +0.391/-0.198 eÅ$^{-3}$.
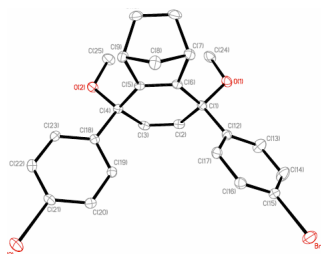


**Figure 2.27.** ORTEP representation of the X-ray crystallographic structure of **II.2** (CCDC Registry # 1949617).
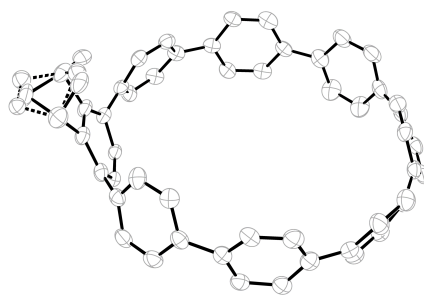


**Figure 2.28.** ORTEP representation of the X-ray crystallographic structure of **nb[8]CPP** (CCDC Registry # 1949616).
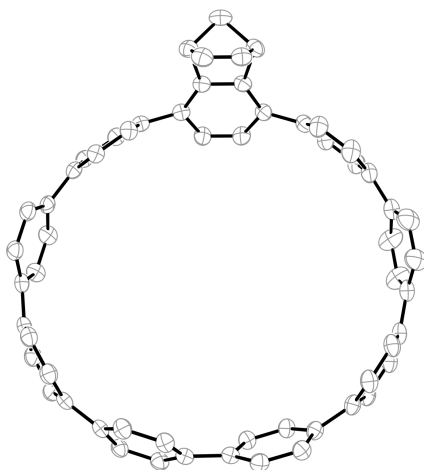


**Figure 2.29.** ORTEP representation of the X-ray crystallographic structure of **nb[9]CPP** (CCDC Registry # 2051663).
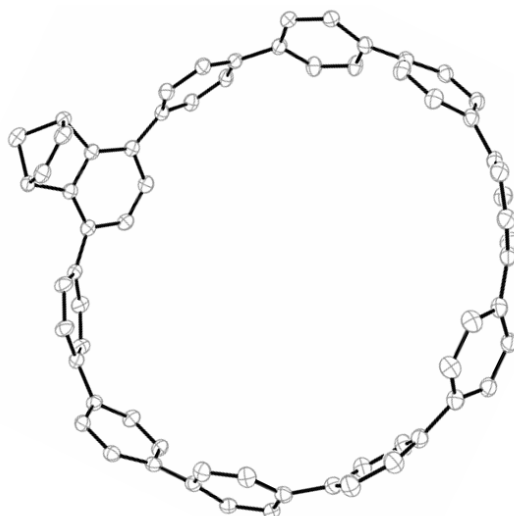
**Figure 2.30.** ORTEP representation of the X-ray crystallographic structure of **nb[10]CPP** (CCDC Registry # 1949615).
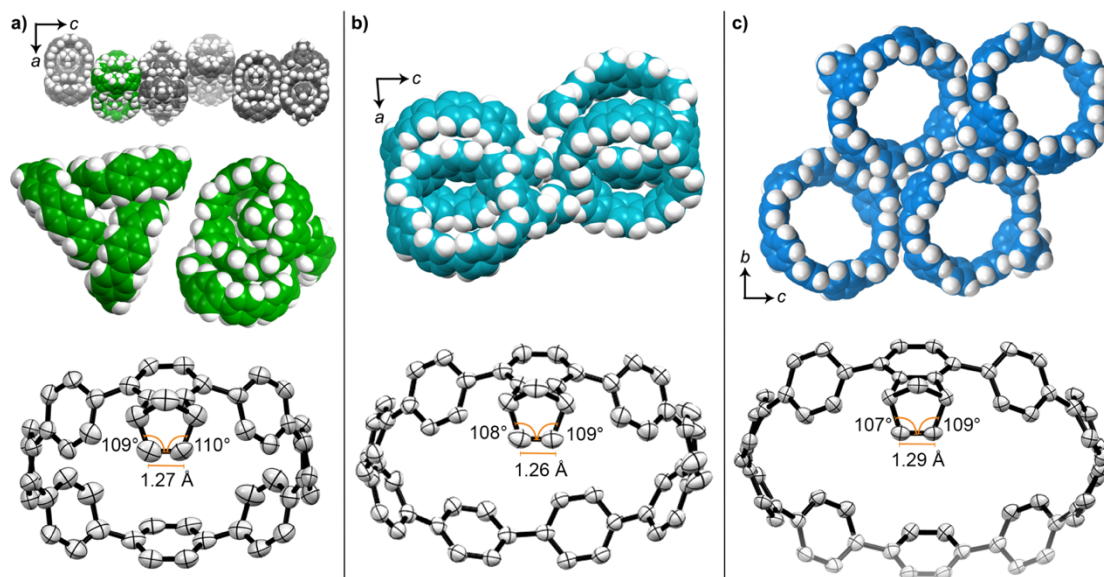


**Figure 2.31.** Analysis of the crystal packing and norbornene bond angles of nb[8]CPP, nb[9]CPP, and nb[10]CPP. The unit cell for nb[8]CPP crystals (a, top) contains 18 nbCPP molecules, comprising six unique trimers. One trimer (green) is shown in two additional views. The unit cell for nb[9]CPP crystals (b, top) contains four nbCPP molecules. The unit cell for nb[10]CPP crystals (c, top) contains four nbCPP molecules. In all cases, solvent molecules have been omitted for clarity. Examination of the norbornene alkene in the crystal structures of nb[8]CPP, nb[9]CPP, and nb[10]CPP (a-c, bottom) shows that the norbornene moiety is largely unaffected by the number of phenyl rings in the hoop.

63

## 2.5.5.4 Synthesis and Preliminary Characterization of Additional nbCPP Monomers

Chloroboronate **II.17**[176], chloroketone **II.21**[183], and pyridine chloroboronate **II.25**[166] were synthesized according to the literature.

*Five-ring norbornene dibromide **II.16***
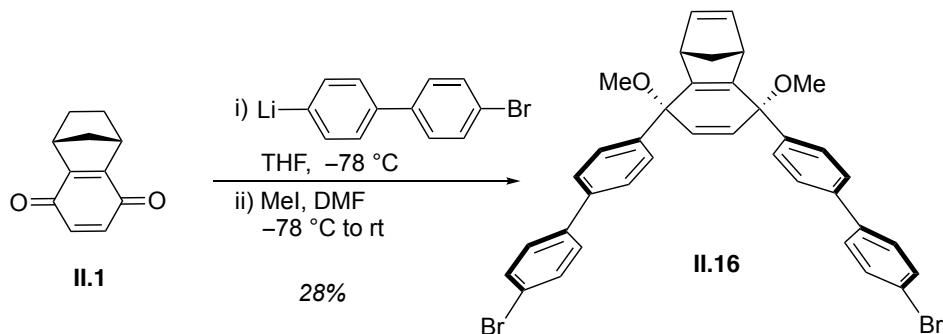


A flame-dried flask was charged with 4,4'-dibromobiphenyl (1.49 g, 4.8 mmol, 3.30 equiv.), which was dissolved in THF (24 mL) and then cooled to -78 °C for 20 minutes. *n*-butyllithium (2.20 mL, 4.1 mmol, 2.80 equiv.) was added dropwise. The reaction was stirred at -78 °C for 20 minutes, after which a solution of norbornene-fused benzoquinone **II.1** (0.25 g, 1.5 mmol, 1.00 equiv.) in THF was added dropwise. The reaction was stirred for 1 hour at -78 °C. Methyl iodide (0.90 mL, 14.5 mmol, 10.00 equiv.) and a few mL of DMF were added to the reaction, which was stirred overnight at room temperature then quenched with water. The THF was removed under reduced pressure, and the resulting solution was extracted with ethyl acetate (3x). The combined organic layers were washed with 5% aqueous LiCl (3x), water (2x), and brine (1x), then dried over sodium sulfate and concentrated under reduced pressure. The product was purified via automated silica gel chromatography (0-3% ethyl acetate in hexanes) to yield 267 mg (28%). $^1$H NMR (500 MHz, CDCl$_3$): δ (ppm) 7.60 – 7.54 (overlapping, 12H), 7.47 (m, 4H), 6.91 (s, 2H), 6.00 (s, 2H), 3.59 (s, 2H), 3.21 (s, 6H), 2.04 (s, 2H).

*Seven-ring dichloride **II.18***



Chloroboronate **II.17** (2.15 g, 4.8 mmol, 2.20 equiv.), 1,4-dibromobenzene (0.51 g, 2.2 mmol, 1.00 equiv.), and Pd(PPh₃)₄ (0.25 g, 0.2 mmol, 0.10 equiv.) were added to a flame-dried flask. The flask was evacuated for 5 minutes and backfilled with nitrogen for 5 cycles. Dry dioxane (30 mL) was sparged with nitrogen for 40 min. then added to reaction flask and sparged 20 additional min. A 2.00 M. aqueous solution of K₃PO₄ was sparged with nitrogen for 1 hr. The reaction mixture was heated to 80 °C, then 3.0 mL of K₃PO₄ solution was added. The reaction was stirred overnight at 80 °C. After the reaction was cooled to room temperature, the dioxane was removed under reduced pressure, then the resulting material was filtered through a celite pad with DCM and water. The filtrate was extracted with DCM (3x). The combined organic layers were washed with water (2x) and brine (1x), then dried over sodium sulfate and concentrated under reduced pressure. Washing with methanol yielded pure product, and automated silica gel column chromatography on the filtrate (0 to 15% ethyl acetate in hexanes) yielded further product, for a total of 0.82 g (52%). ¹H NMR (500 MHz, CDCl₃): δ (ppm) 7.65 (s, 2H), 7.59 (d, J = 7.8 Hz, 2H), 7.46 (d, J=8.5 Hz, 2H), 7.36 (d, J=8.8 Hz, 2H), 7.28 (d, J=8.1 Hz, 2H), 6.18 (d, J=10.3 Hz, 2H), 6.09 (d, J=10.1 Hz, 2H), 3.46 (s, 6H), 3.44 (s, 6H). ¹³C NMR (X MHz, CDCl₃) δ 142.77, 142.47, 140.39, 140.04, 133.86, 133.78, 133.24, 128.71, 127.82, 127.65, 127.24, 126.77, 74.98, 74.86, 52.08. IR (neat): 3029.5, 2977.8, 2936.2, 2820.3, 1488.4, 1401.0, 1082.2, 1066.9, 1013.1, 942.4, 815.7, 666.0 cm⁻¹.

*7-ring bisboronate **II.19***



65

*Seven-ring dichloride **II.18***



Chloroboronate **II.17** (2.15 g, 4.8 mmol, 2.20 equiv.), 1,4-dibromobenzene (0.51 g, 2.2 mmol, 1.00 equiv.), and $Pd(PPh_3)_4$ (0.25 g, 0.2 mmol, 0.10 equiv.) were added to a flame-dried flask. The flask was evacuated for 5 minutes and backfilled with nitrogen for 5 cycles. Dry dioxane (30 mL) was sparged with nitrogen for 40 min. then added to reaction flask and sparged 20 additional min. A 2.00 M. aqueous solution of $K_3PO_4$ was sparged with nitrogen for 1 hr. The reaction mixture was heated to 80 °C, then 3.0 mL of $K_3PO_4$ solution was added. The reaction was stirred overnight at 80 °C. After the reaction was cooled to room temperature, the dioxane was removed under reduced pressure, then the resulting material was filtered through a celite pad with DCM and water. The filtrate was extracted with DCM (3x). The combined organic layers were washed with water (2x) and brine (1x), then dried over sodium sulfate and concentrated under reduced pressure. Washing with methanol yielded pure product, and automated silica gel column chromatography on the filtrate (0 to 15% ethyl acetate in hexanes) yielded further product, for a total of 0.82 g (52%). $^1H$ NMR (500 MHz, $CDCl_3$): δ (ppm) 7.65 (s, 2H), 7.59 (d, J = 7.8 Hz, 2H), 7.46 (d, J=8.5 Hz, 2H), 7.36 (d, J=8.8 Hz, 2H), 7.28 (d, J=8.1 Hz, 2H), 6.18 (d, J=10.3 Hz, 2H), 6.09 (d, J=10.1 Hz, 2H), 3.46 (s, 6H), 3.44 (s, 6H). $^{13}C$ NMR (X MHz, $CDCl_3$) δ 142.77, 142.47, 140.39, 140.04, 133.86, 133.78, 133.24, 128.71, 127.82, 127.65, 127.24, 126.77, 74.98, 74.86, 52.08. IR (neat): 3029.5, 2977.8, 2936.2, 2820.3, 1488.4, 1401.0, 1082.2, 1066.9, 1013.1, 942.4, 815.7, 666.0 cm⁻¹.

*7-ring bisboronate **II.19***

Potassium acetate (0.540 g, 5.5 mmol, 7.00 equiv.) was flame-dried in a flask and cooled under nitrogen. Ground B$_2$pin$_2$ (0.700 g, 2.7 mmol, 3.50 equiv.), dichloride **II.18** (0.570 g, 0.8 mmol, 1.00 equiv.), Pd(OAc)$_2$ (21 mg, 0.1 mmol, 0.12 equiv.), and SPhos (98 mg, 0.2 mmol, 0.31 equiv.) were added to the flask, which was then evacuated for 5 minutes and backfilled with nitrogen for 5 cycles. The flask was sealed with a septum and purged with nitrogen for 1 hr. Dry dioxane (4.6 mL) was sparged with nitrogen for 1 hr. then added to reaction flask. The reaction was heated to 80 °C, then stirred overnight. After the reaction was cooled to room temperature, the mixture was filtered through a plug of celite and activated carbon, and the filtrate was concentrated under reduced pressure. The material was then sonicated with methanol and filtered to yield 0.56 g (79%). $^1$H NMR (500 MHz, CDCl$_3$): δ (ppm) 7.77 (d, $J$ = 7.4 Hz, 4H), 7.65 (s, 4H), 7.59 (d, $J$ = 7.4 Hz, 4H), 7.48 (d, $J$ = 7.4 Hz, 4H), 7.44 (d, $J$ = 7.4 Hz, 4H), 6.14 (overlapping, 8H), 3.46 (overlapping s, 12H), 1.33 (s, 24H). $^{13}$C NMR (X MHz, CDCl$_3$) δ 135.14, 133.47, 127.64, 127.20, 126.81, 125.64, 83.98, 75.21, 74.95, 52.15, 25.08.

*nb[12]CPP macrocycle **II.20***
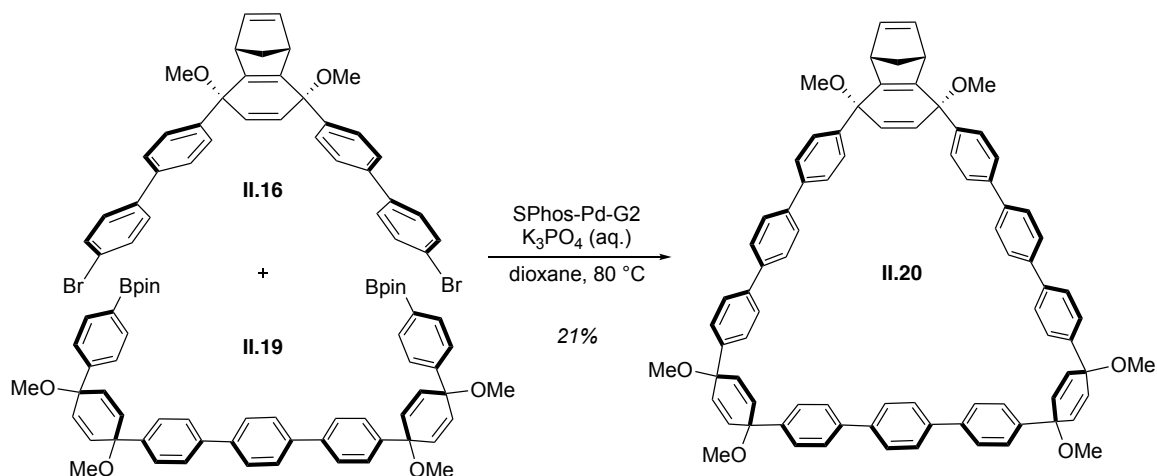


A flame-dried flask was charged with dibromide **II.16** (0.267 g, 0.40 mmol, 1.00 equiv.), bisboronate **II.19** (0.401 g, 0.44 mmol, 1.10 equiv.), and Pd SPhos Gen II (29 mg, 0.04 mmol, 0.10 equiv.). The flask was evacuated for 5 minutes and backfilled with nitrogen for 5 cycles. The flask was then purged with nitrogen for 1 hr. A 2.00 M. aqueous solution of K$_3$PO$_4$ was sparged with nitrogen for 1 hr. Dry dioxane (135 mL) was added to the reaction flask via cannulation, and the solution was sparged for half an hour before

being heated to 80 °C for half an hour. 13 mL of K₃PO₄ solution was added, and the reaction was stirred at 80 °C for 1 hr. After the reaction was cooled to room temperature, the dioxane was removed under reduced pressure, then the resulting material was filtered through a celite pad with DCM and water. The filtrate was extracted with DCM (3x). The combined organic layers were washed with water (2x) and brine (1x), then dried over sodium sulfate and concentrated under reduced pressure. The material was washed with acetone and further purified by automated silica gel column chromatography (5% ethyl acetate in DCM), yielding 100 mg (21%). $^1$H NMR (500 MHz, CDCl₃): δ (ppm) 7.71 – 7.51 (overlapping, 36H), 6.93 (s, 2H), 6.18 (overlapping, 8H), 6.02 (s, 2H), 3.65 (s, 2H), 3.50 (overlapping, 12H), 3.22 (s, 6H), 2.06 (m, 2H).

*nb[12]CPP **II.9***
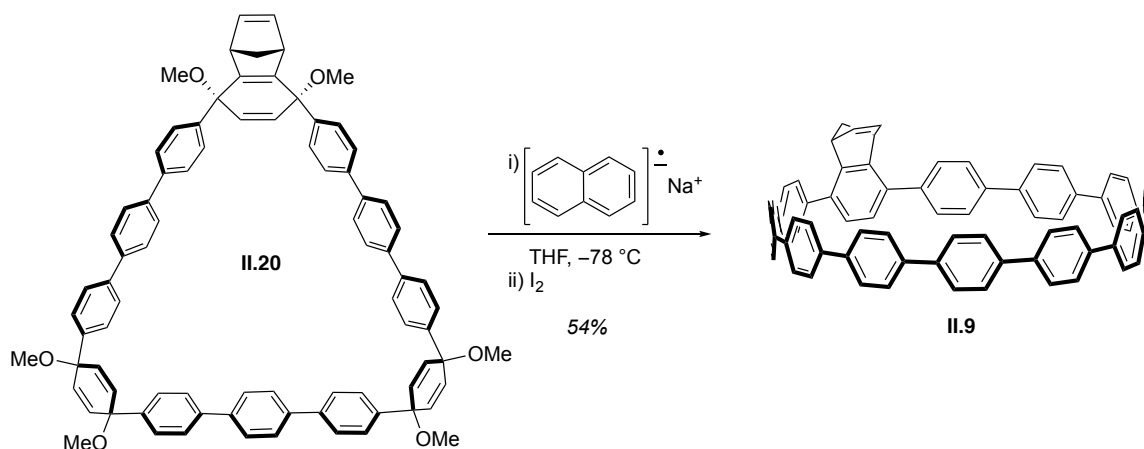


A 0.5 M. sodium naphthalenide solution was prepared by sonicating sodium and naphthalene in THF in a flame-dried flask, then stirring the solution overnight. Macrocycle **II.20** (100 mg, 0.086 mmol, 1.00 equiv.) was dispersed in THF in a flame-dried flask and stirred at -78 °C for 30 min. Sodium naphthalenide (>2.58 mL, 1.29 mmol, 15.00 equiv.) was added dropwise to the reaction flask until the mixture was brown. The reaction was stirred for 30 minutes and then quenched with dropwise addition of 1 M. iodine solution in THF until orange. Sodium thiosulfate was added until the orange color dissipated, and the reaction was warmed to room temperature. THF was removed under reduced pressure, and the resulting solution was extracted with DCM (3x). The combined organic layers were washed with water (2x) and brine (1x), then dried over sodium sulfate and concentrated under reduced pressure. The material was

purified by silica gel column chromatography (19% then 40% DCM in hexanes), yielding 45 mg (54%). $^1$H NMR (500 MHz, CDCl$_3$): δ (ppm) 7.61 (overlapping, 40H), 7.41 (d, $J$ = 7.8 Hz, 4H), 7.08 (s, 2H), 6.74 (s, 2H), 4.36 (s, 2H), 2.43 (d, $J$ = 7.4 Hz, 1H), 2.31 (d, $J$ = 7.5 Hz, 1H). Crystals suitable for X-ray crystallography were grown by the slow evaporation of pentane into a solution of **II.9** in THF. Crystallographic analysis confirmed the identity of the compound although the molecules were disordered over several positions.

*Seven-ring norbornene dichloride II.22*
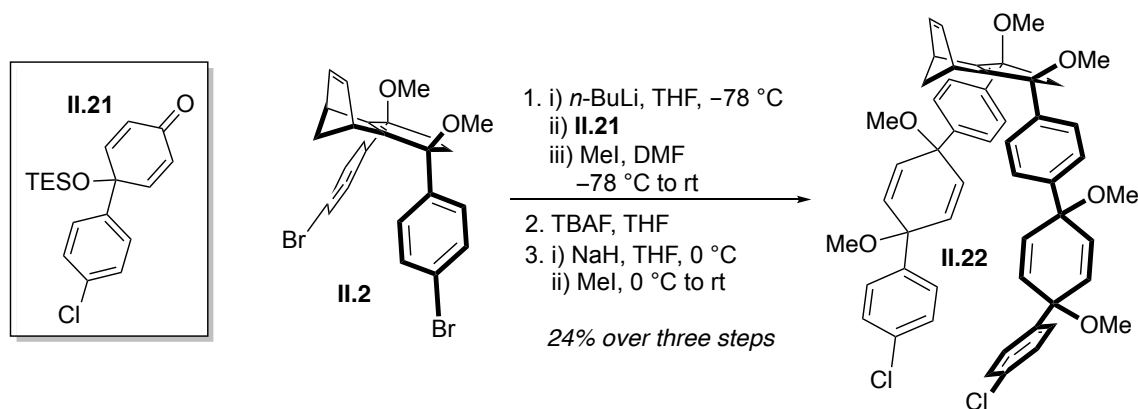


A flame-dried flask was charged with dibromide **II.2** (3.45 g, 6.71 mmol, 1.00 equiv.), which was dissolved in THF (X mL) and then cooled to -78 °C for 20 minutes. *n*-butyllithium (6.7 mL, 14.76 mmol, 2.20 equiv.) was added dropwise. Upon complete *n*-BuLi addition, chloroketone **II.21** (5.17 g, 15.43 mmol, 2.30 equiv.) was immediately added dropwise and rinsed in with a small amount of THF. The reaction was stirred at -78 °C for 1 hour. Methyl iodide (8.4 mL, 134.2 mmol, 20.00 equiv.) and a few mL of DMF were added to the reaction, which was stirred overnight at room temperature then quenched with water. THF was removed under reduced pressure. The resulting material was extracted with DCM (3x), and the combined organic layers were washed with LiCl solution (3x), water (2x), and brine (1x), then dried over sodium sulfate and concentrated. This crude material was added to a flame-dried flask and dissolved in THF (67 mL). TBAF (26.8 mL, 26.80 mmol, 4.00 equiv.) was added, and the reaction was stirred for 1 hour, then quenched with water. THF was removed under reduced pressure, then the material was extracted with EtOAc (3x). The combined organic layers were washed with

68

water (2x) and brine (1x), then dried over sodium sulfate and concentrated under reduced pressure. NaH (2.68 g, 67.10 mmol, 10.00 equiv.) was placed in a flame-dried flask and dispersed in THF at 0 °C. The crude material was added to this flask as a solution in THF, and the reaction was stirred for 2 hours at 0 °C. Methyl iodide (5.0 mL, 80.50 mmol, 12.00 equiv.) and a few mL DMF were added, and the reaction was stirred overnight. The reaction was quenched with water, then concentrated under reduced pressure. The resulting material was extracted with DCM (3x), and the combined organic layers were washed with LiCl solution (3x), water (2x), and brine (1x), then dried over sodium sulfate and concentrated. The material was purified by silica gel column chromatography (0-12% ethyl acetate in DCM), yielding 2.51 g (24% over 3 steps). ^{1}H NMR (600 MHz, CDCl$_3$) δ (ppm) 7.43 (d, $J$ = 8.6 Hz, 4H), 7.36 (d, $J$ = 8.6 Hz, 4H), 7.33 (d, $J$ = 8.6 Hz, 4H), 7.26 (d, $J$ = 7.9 Hz, 4H), 6.86 (t, $J$ = 1.9 Hz, 2H), 6.16 – 6.12 (m, 4H), 6.08 – 6.04 (m, 4H), 5.91 (s, 2H), 3.50 (p, $J$ = 1.7 Hz, 2H), 3.43 (overlapping singlets, 12H), 3.16 (s, 6H), 1.97 (dt, $J$ = 6.1, 1.7 Hz, 1H), 1.93 (dt, $J$ = 6.1, 1.6 Hz, 1H).

*Seven-ring norbornene bisboronate **II.23***
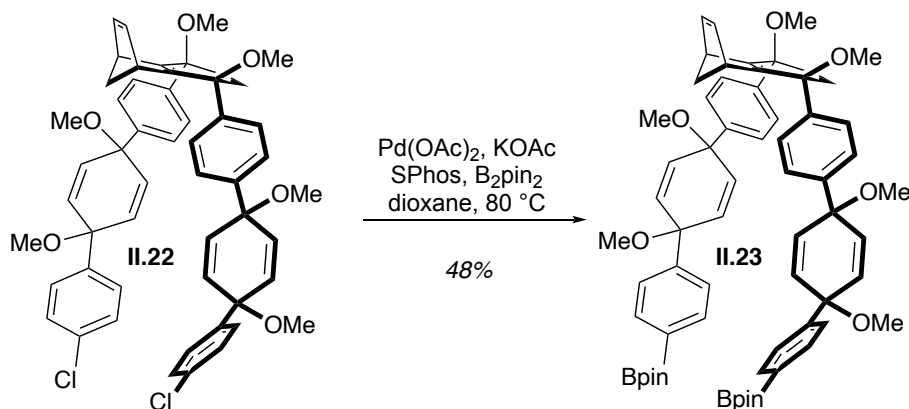


Ground B$_2$pin$_2$ (7.07 g, 27.8 mmol, 8.00 equiv.), dichloride **II.22** (2.97 g, 3.48 mmol, 1.00 equiv.), Pd(OAc)$_2$ (39 mg, 0.17 mmol, 0.05 equiv.), SPhos (185 mg, 0.45 mmol, 0.13 equiv.), and dry potassium phosphate (5.90 g, 27.8 mmol, 8.00 equiv.) were added to a flame-dried flask, which was then evacuated for 5 minutes and backfilled with nitrogen for 5 cycles. The flask was sealed with a septum and purged with nitrogen for 1 hr. Dry dioxane (17.4 mL) was sparged with nitrogen for 1 hr. then added to reaction flask. The reaction was heated to 80 °C, then stirred overnight. After the reaction was

cooled to room temperature, the mixture was filtered through a plug of celite, and the filtrate was concentrated under reduced pressure. The material was then sonicated with methanol and filtered to yield 1.72 g (48%). $^1$H NMR (600 MHz, CDCl$_3$) δ (ppm) 7.75 (d, $J$ = 8.1 Hz, 4H), 7.45 – 7.35 (overlapping, 12H), 6.86 (t, $J$ = 1.9 Hz, 2H), 6.15 – 6.04 (m, 8H), 5.92 (s, 2H), 3.50 (t, $J$ = 1.7 Hz, 2H), 3.43 (overlapping singlets, 12H), 3.16 (s, 6H), 1.96 (d, $J$ = 6.1 Hz, 1H), 1.93 (d, $J$ = 6.2 Hz, 1H), 1.33 (s, 24H).

*Dinorbornene [10]CPP macrocycles **II.24***
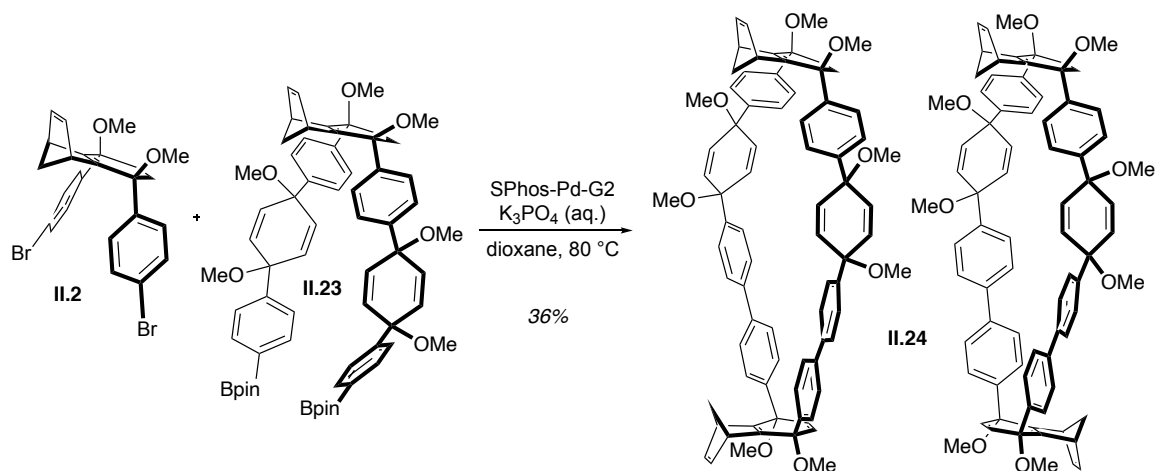


A flame-dried flask was charged with dibromide **II.2** (100.0 mg, 0.195 mmol, 1.00 equiv.), bisboronate **II.23** (221.8 mg, 0.214 mmol, 1.10 equiv.), and Pd SPhos Gen II (14.0 mg, 0.019 mmol, 0.10 equiv.). The flask was evacuated and backfilled with nitrogen for 5 cycles. The flask was then purged with nitrogen for 30 min. A 2.00 M. aqueous solution of K$_3$PO$_4$ was sparged with nitrogen for 1 hr. Dry dioxane (65 mL) was added to the reaction flask, sparged for 20 min., then heated to 80 °C for 30 min. 6.5 mL of K$_3$PO$_4$ solution was added. The reaction was stirred for 2.5 hr at 80 °C. After the reaction was cooled to room temperature, the dioxane was removed under reduced pressure, then the resulting material was filtered through a celite pad with DCM and water. The filtrate was extracted with DCM (3x). The combined organic layers were washed with water (2x) and brine (1x), then dried over sodium sulfate and concentrated under reduced pressure. The material was purified by automated silica gel column chromatography (0-15% ethyl acetate in DCM), yielding 87 mg as a yellow solid (36%). This material was a mixture of isomers, which could be partially separated by washing

the material with acetone. $^1$H NMR (500 MHz, CDCl$_3$): δ (ppm) first isomer 7.53 – 7.49 (overlapping, 8H), 7.44 – 7.32 (overlapping, 16H), 6.97 (t, $J$ = 1.7 Hz, 2H), 6.88 (t, $J$ = 1.9 Hz, 2H), 6.32 (dd, $J$ = 10.2, 2.5 Hz, 2H), 6.27 (dd, $J$ = 10.2, 2.5 Hz, 2H), 6.14 (dd, $J$ = 10.3, 2.4 Hz, 2H), 6.08 (dd, $J$ = 10.2, 2.5 Hz, 2H), 6.02 (s, 2H), 5.99 (s, 2H), 3.73 (d, $J$ = 2.9 Hz, 2H), 3.63 (d, $J$ = 2.5 Hz, 2H), 3.48 (s, 6H), 3.42 (s, 6H), 3.22 (s, 6H), 3.16 (s, 6H), 2.12 – 2.08 (m, 2H), 1.98 (s, 2H); second isomer 7.53 – 7.49 (overlapping, 8H), 7.47 – 7.34 (overlapping, 16H), 6.97 (t, $J$ = 1.9 Hz, 2H), 6.88 (t, $J$ = 1.9 Hz, 2H), 6.30 (dd, $J$ = 10.1, 2.5 Hz, 2H), 6.26 (dd, $J$ = 10.2, 2.5 Hz, 2H), 6.14 (dd, $J$ = 10.2, 2.4 Hz, 2H), 6.07 (dd, $J$ = 10.2, 2.5 Hz, 2H), 6.03 (s, 2H), 6.01 (s, 2H), 3.73 (d, $J$ = 2.7 Hz, 2H), 3.61 (t, $J$ = 1.7 Hz, 2H), 3.48 (s, 6H), 3.42 (s, 6H), 3.22 (s, 6H), 3.16 (s, 6H), 2.11 (m, 2H), 2.05 – 1.95 (m, 2H).

*Dinorbornene [10]CPP **II.10***
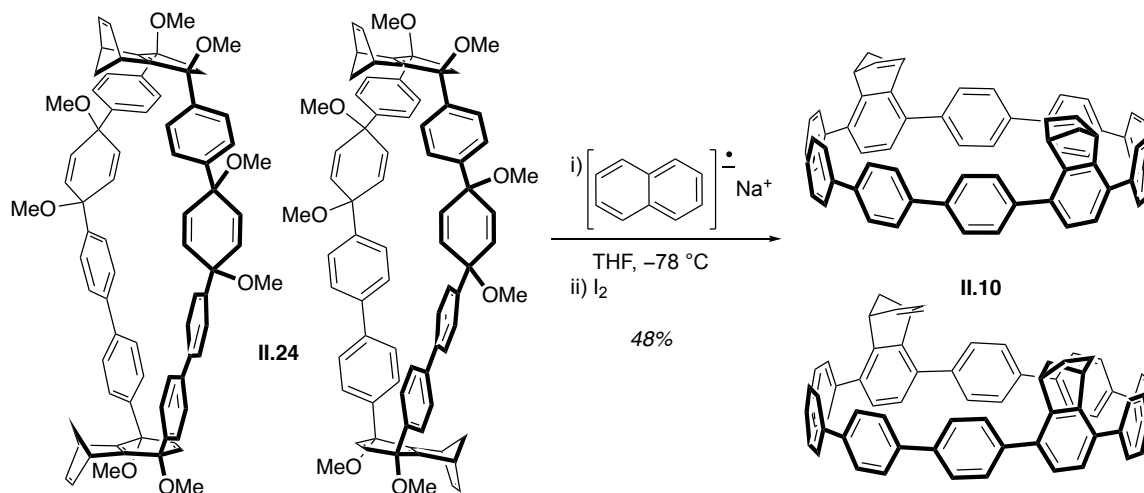


A 0.5 M. sodium naphthalenide solution was prepared by sonicating sodium and naphthalene in THF in a flame-dried flask, then stirring the solution overnight. Macrocycle **II.24** (87.0 mg, 0.077 mmol, 1.00 equiv.) was dispersed in THF in a flame-dried flask and stirred at -78 °C for 30 min. Sodium naphthalenide solution (2.3 mL, 1.147 mmol, 15.00 equiv.) was added dropwise to the reaction flask until the mixture was brown. The reaction was stirred for 30 minutes and then quenched with dropwise addition of 1 M. iodine solution in THF until orange. Sodium thiosulfate was added until the orange color dissipated, and the reaction was warmed to room temperature. THF was removed under reduced pressure, and the resulting solution was extracted with DCM

(3x). The combined organic layers were washed with water (2x) and brine (1x), then dried over sodium sulfate and concentrated under reduced pressure. The material was adsorbed on silica and purified by automated silica gel column chromatography (15-35% DCM in hexanes), yielding 33 mg (48%) as a mixture of isomers. $^1$H NMR (500 MHz, CDCl$_3$): δ (ppm) first isomer 7.62 – 7.56 (overlapping, 24H), 7.40 (d, $J$ = 8.6 Hz, 8H), 7.07 (t, $J$ = 1.8 Hz, 4H), 6.67 (s, 4H), 4.42 (t, $J$ = 1.7 Hz, 4H), 2.48 (d, $J$ = 7.0 Hz, 2H), 2.36 (d, $J$ = 7.4 Hz, 2H); second isomer 7.62 – 7.56 (overlapping, 24H), 7.39 (d, $J$ = 8.6 Hz, 8H), 7.09 (t, $J$ = 1.8 Hz, 4H), 6.68 (s, 4H), 4.39 (t, $J$ = 1.3 Hz, 4H), 2.44 (d, $J$ = 6.2 Hz, 2H), 2.32 (d, $J$ = 7.5 Hz, 2H).

*Nine-ring norbornene dipyridine dichloride **II.26***
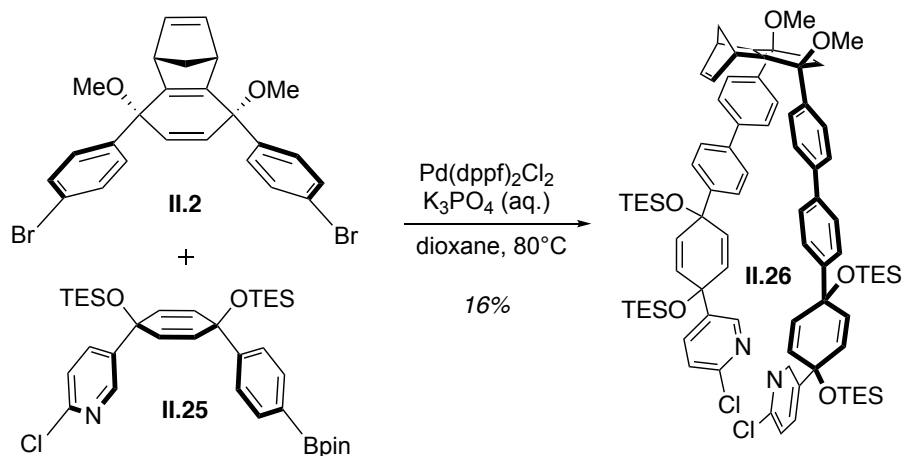


Dibromide **II.2** (1.00 g, 1.945 mmol, 1.00 equiv.), pyridine chloroboronate **II.25** (2.61 g, 3.986 mmol, 2.05 equiv.), and Pd(dppf)Cl$_2$·DCM (238.2 mg, 0.292 mmol, 0.15 equiv.) were added to a flame-dried flask. The flask was evacuated and backfilled with nitrogen for 5 cycles. Dry dioxane (40 mL) was added to the reaction flask, and the solution was sparged with nitrogen for 20 min. A 2.00 M. aqueous solution of K$_3$PO$_4$ was sparged with nitrogen for 20 min. The reaction mixture was heated to 80 °C, then 4.0 mL of K$_3$PO$_4$ solution was added. The reaction was stirred overnight at 80 °C. After the reaction was cooled to room temperature, the dioxane was removed under reduced pressure, then the resulting material was filtered through a celite pad with DCM and water. The filtrate was extracted with DCM (3x). The combined organic layers were washed with water (2x) and brine (1x), then dried over sodium sulfate and concentrated under reduced pressure. The

material was purified by silica gel column chromatography in 20-100% DCM in hexanes, yielding 0.44 g (16%). $^1$H NMR (500 MHz, CDCl$_3$) δ 8.36 (d, $J$ = 2.5 Hz, 2H), 7.62 – 7.55 (overlapping, 12H), 7.53 (dd, $J$ = 8.4, 2.6 Hz, 2H), 7.38 (d, $J$ = 8.4 Hz, 4H), 7.18 (d, $J$ = 8.3 Hz, 2H), 6.91 (t, $J$ = 1.9 Hz, 2H), 6.14 (d, $J$ = 10.1 Hz, 4H), 6.01 (s, 2H), 5.92 (d, $J$ = 9.9 Hz, 4H), 3.60 (p, $J$ = 1.7 Hz, 2H), 3.22 (s, 6H), 2.07 – 2.02 (m, 2H), 0.96 (t, $J$ = 7.9 Hz, 18H), 0.92 (t, $J$ = 7.9 Hz, 18H), 0.66 (q, $J$ = 7.9 Hz, 12H), 0.57 (q, $J$ = 7.9 Hz, 12H). $^{13}$C NMR (126 MHz, CDCl$_3$) δ 154.03, 150.26, 148.01, 144.55, 142.60, 140.80, 140.14, 139.64, 136.65, 134.68, 132.69, 132.66, 130.53, 130.50, 127.20, 127.11, 126.72, 126.26, 123.66, 76.39, 74.31, 71.11, 70.28, 52.91, 50.13, 7.15, 6.61, 6.52.

*nb[9]bipyCPP macrocycle II.27*
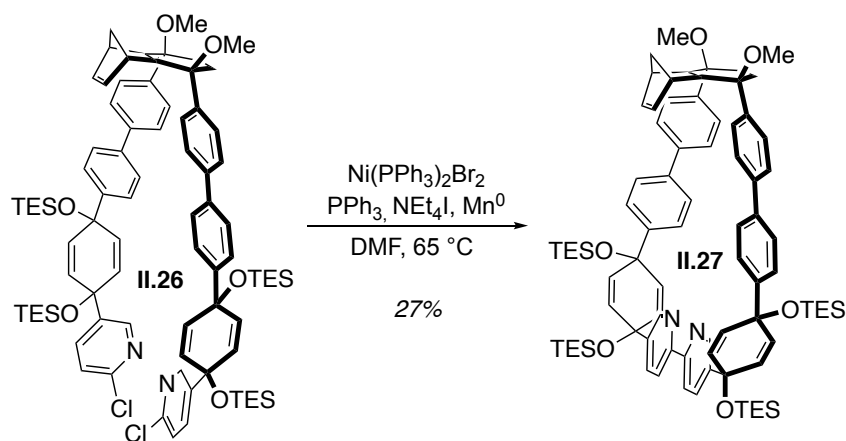


*This reaction is extremely air-sensitive, so extra care was taken to avoid introduction of oxygen, including increasing the flow of nitrogen and sealing syringe and nitrogen inlet joints with parafilm.* Dichloride **II.26** (170.0 mg, 0.121 mmol, 1.00 equiv.) was added to a flame-dried flask. Ni(PPh$_3$)$_2$Br$_2$ (135.0 mg, 0.181 mmol, 1.50 equiv.), PPh$_3$ (95.0 mg, 0.363 mmol, 3.00 equiv.), Mn powder (20.0 mg, 0.363 mmol, 3.00 equiv.), and NEt$_4$I (47.0 mg, 0.181 mmol, 1.50 equiv.) were added to a second flask, which was evacuated and backfilled with nitrogen for 5 cycles. 1.2 mL dry DMF was added to the flask with the catalyst mixture, and 4.0 mL was added to the flask with the dichloride. The catalyst was sonicated until activated (brick red) then placed in an oil bath at 65 °C. The dichloride solution was sparged for 30 minutes, then added to the reaction flask over three hours via syringe pump. Once addition was complete, the reaction was stirred for 30 min. The mixture was then stirred vigorously with ethyl acetate and NH$_3$-EDTA. Next, it

was filtered. The filtrate was extracted with EtOAc (3x), then washed with LiCl solution (3x), water (2x), and brine (1x), and dried over sodium sulfate. The material was purified by silica gel column chromatography (20-100% DCM in hexanes, then 0-5% ethyl acetate in DCM), yielding 43 mg (27%). $^1$H NMR (500 MHz, CDCl$_3$) δ 8.69 (d, $J$ = 2.3 Hz, 2H), 8.31 (d, $J$ = 8.3 Hz, 2H), 7.77 (dd, $J$ = 8.3, 2.3 Hz, 2H), 7.64 (d, $J$ = 8.2 Hz, 4H), 7.64 (d, $J$ = 8.6 Hz, 4H), 7.53 (d, $J$ = 8.6 Hz, 4H), 7.43 (d, $J$ = 8.2 Hz, 4H), 6.92 (t, $J$ = 1.9 Hz, 2H), 6.14 – 6.07 (m, 4H), 6.03 – 5.95 (overlapping, 6H), 3.60 (p, $J$ = 1.7 Hz, 2H), 3.21 (s, 6H), 2.00 (dt, $J$ = 6.3, 1.7 Hz, 1H), 1.96 (d, $J$ = 6.0 Hz, 1H), 0.96 (overlapping triplets, $J$ = 7.9 Hz, 36H), 0.65 (overlapping quartets, $J$ = 7.9 Hz, 24H). $^{13}$C NMR (126 MHz, CDCl$_3$) δ 154.92, 154.00, 147.52, 144.97, 142.67, 142.32, 141.90, 139.48, 139.41, 134.75, 134.63, 132.46, 132.42, 130.66, 130.56, 126.92, 126.82, 126.70, 126.24, 120.61, 76.72, 74.36, 71.40, 70.60, 52.87, 49.94, 7.20, 6.64, 6.61.

*nb[9]bipyCPP* **II.11**
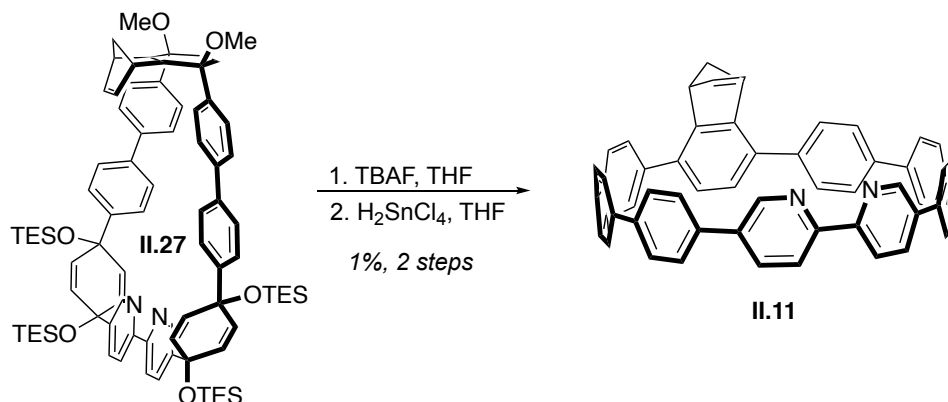


Macrocycle **II.27** (27.0 mg, 0.020 mmol, 1.00 equiv.) was added to a flame-dried flask and dissolved in THF (0.2 mL). TBAF (0.16 mL, 0.161 mmol, 8.00 equiv.) was added slowly to the solution, and the reaction was stirred for 1 hr. The reaction mixture was concentrated under reduced pressure, followed by the addition of water, resulting in a precipitate. This material was sonicated, filtered, and washed with water, before being added to a second flame-dried flask. THF (minimal) was used to rinse in the material, then a 0.05 M. (in THF) solution of H$_2$SnCl$_4$ (1.6 mL, 0.081 mmol, 4.00 equiv.) was added dropwise. The reaction was stirred at room temperature for 1.5 hrs, then quenched with saturated sodium bicarbonate solution. THF was removed under reduced pressure, and the resulting material was filtered through celite using water and DCM. The filtrate

was extracted with DCM (3x), and the combined organic layers were washed with water (2x) and brine (1x) before being dried over sodium sulfate. Solvent was removed under reduced pressure. The material was purified by column chromatography (alumina, 0-100% DCM in hexanes, then 0-5% ethyl acetate in DCM), yielding 2.0 mg probable product (1% over two steps). $^1$H NMR (500 MHz, CDCl$_3$): δ (ppm) 8.84 (m, 2H), 8.19 (m, 2H), 7.87 (d, $J = 8.5$ Hz, 2H), 7.54 – 7.46 (overlapping, 12H), 7.40 (overlapping, 10H), 7.33 (overlapping, 4H), 6.95 (t, $J = 1.6$ Hz, 2H), 3.75 (s, 2H), 2.25 (d, $J = 6.3$ Hz, 1H), 2.14 (m, 1H).

## 2.6 Bridge to Chapter III

The emphasis of the previous work was to use a controlled route to prepare polymeric carbon nanomaterials from CPPs. This controlled method allowed us to systematically change the size and composition of the polymers to alter their properties. The next chapter discusses the study of CPP-based conjugated polymers for which there currently is no controlled synthetic route. Despite this limitation, we uncovered unusual optical and electronic properties in these conjugated polymers due to the combination of linear and radial pi system components.

CHAPTER III

INTERPLAY BETWEEN LINEAR AND RADIAL CONJUGATION IN

CYCLOPARAPHENYLENE POLYMERS

Chapter III includes published and unpublished co-authored material. Section 3.2 is based on a manuscript published in *Journal of the American Chemical Society* under the title "Linear and Radial Conjugation in Extended Pi-Electron Systems."[2] Dr. Garvin Peters and Haley Bates carried out polymer synthesis and optoelectronic characterization of the resultant polymers. Dr. Girishma Grover performed computations. Dr. Curtis Colwell and W. Alex Edgell contributed to monomer synthesis and characterization. Prof. J. D. Tovar wrote the manuscript and Prof. Ramesh Jasti and Prof. Miklos Kertesz edited the manuscript. Section 3.3 is based on unpublished work co-authored with Eric Peterson, Prof. J. D. Tovar, Prof. Miklos Kertesz, and Prof. Ramesh Jasti.

## 3.1 Introduction

Conjugated polymers are critical components of the electronic devices that pervade modern society.[184,185] Although linear conjugated polymers have been studied for decades, very little is known about the role that radial pi-conjugated motifs[186] could play in polymers. Radial conjugation is rare; even among conjugated macrocycles, most do not have a radially-oriented pi system.[187] Cycloparaphenylenes (CPPs) are a family of synthetically accessible molecules possessing this property. Numerous studies have shown that bending benzene into a circle, such that the pi orbitals are radially oriented, leads to different electronic properties than in linear paraphenylenes.[188–190] The modularity of CPP synthesis and the ability to readily alter their HOMO and LUMO levels by changing nanohoop size,[191] substituting benzene for other aromatic units,[192–194] and breaking nanohoop symmetry[138] enable detailed study of the electronic effects of structural modifications. With this in mind, we set out to determine what electronic properties would emerge when radial and linear pi systems are combined in conjugated polymers.

**3.2 Results and Discussion for Contiguous Linear/Radial Polymers**

**3.2.1 Monomer and Polymer Synthesis**

We designed CPPs derivatized with two alkynes on one benzene unit that could be incorporated into polymers via Sonogashira cross-coupling polymerization. Nanohoop monomers of two sizes were prepared according to the modular synthetic approach shown in Scheme 3.1. The common coupling partner **III.2** was prepared on multigram scale from dibromodiiodobenzene via successive Sonogashira coupling and Miyaura borylation. Advanced intermediates **III.3** and **III.6** were prepared using known synthetic methods involving lithiation-addition steps with high control of diastereoselectivity, followed by protection of the resultant alcohols as methyl or triethylsilyl (TES) ethers. In this manner, curved intermediates with varying numbers of phenyl rings or cyclohexadienes as masked phenylenes could be assembled rapidly, allowing formation of macrocycles in the next step. Macrocyclizations of either **III.3** or **III.6** with bisboronate **III.2** were then carried out under dilute Suzuki cross-coupling conditions to yield **III.4** and **III.7** in 22 and 29% yield, respectively. Finally, global deprotection of the silyl groups and reductive aromatization using mild tin chloride conditions[195] yielded the final dialkyne CPP monomers **III.5** and **III.8**.

These CPPs were polymerized along with dihalogenated benzene and thiophene coupling partners via Sonogashira reactions, and a series of model polymers was prepared using terphenyl in place of the CPP units (Fig. 3.1a). Due to the step-growth polymerization method employed, molecular weights of these polymers could not be well-controlled. We were pleased to find, however, that at least the lower molecular weight portions of these materials were soluble considering the small number of alkyl solubilizing groups (R and R') relative to unsubstituted benzene rings in these structures.

**3.2.2 Optoelectronic Properties of Contiguous Polymers**

The electronic properties of the resulting polymers were characterized primarily by UV-Vis absorption spectroscopy. As expected, each polymer shows a red-shifted absorbance as compared to the respective monomers due to pi extension in the polymer backbones, but we also observed that in each case, polymers containing CPP units had further red-shifted absorbance peaks compared to the model terphenyl-based
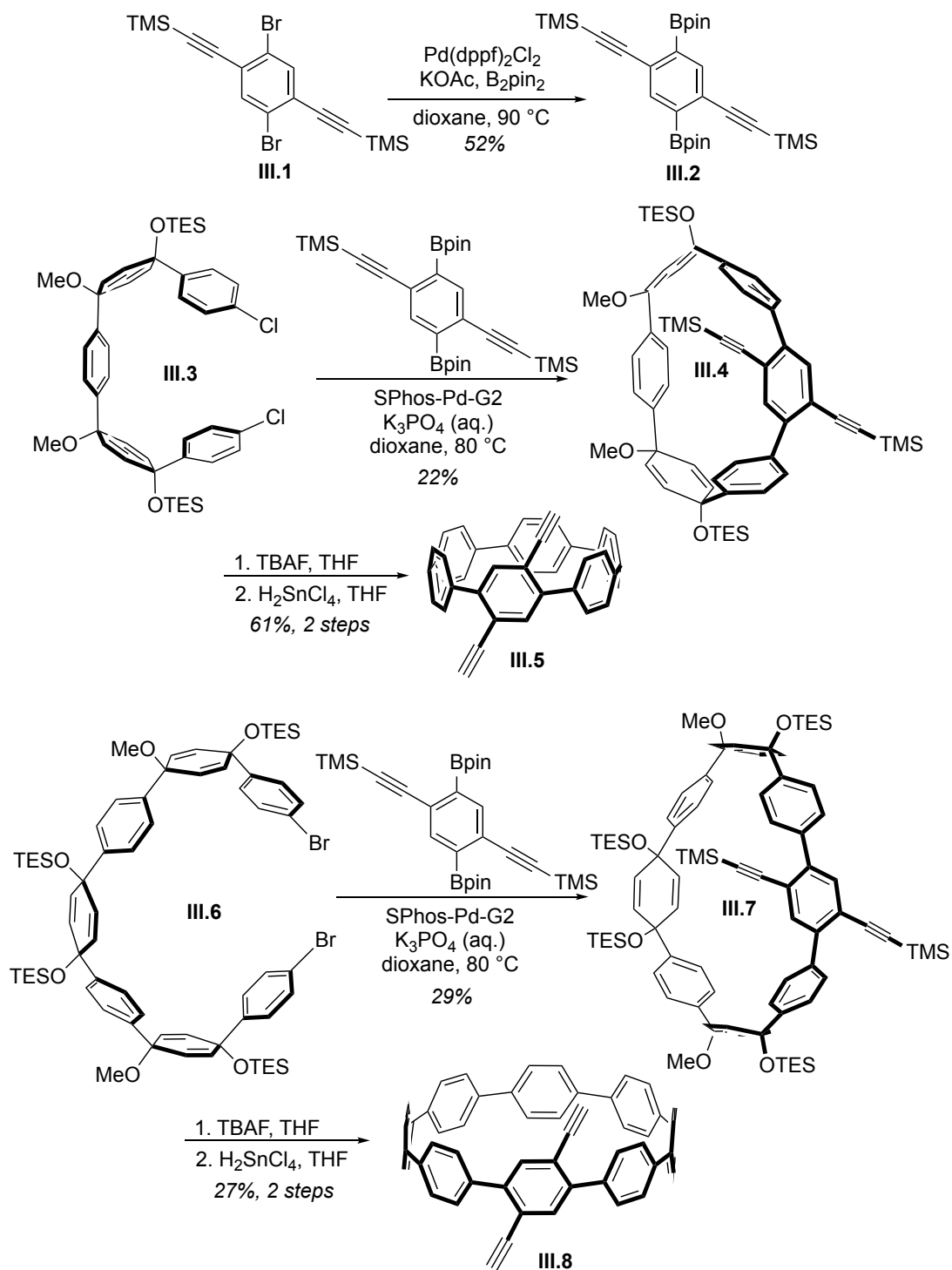
**Scheme 3.1.** Synthetic routes for dialkyne CPP monomers **III.5** and **III.8**.

polymers (Fig. 3.1b). This additional red-shifting can be attributed to increased delocalization in the CPP polymers due to a combination of the linear and radial components of the pi system. Computational results indicated that the red-shifted
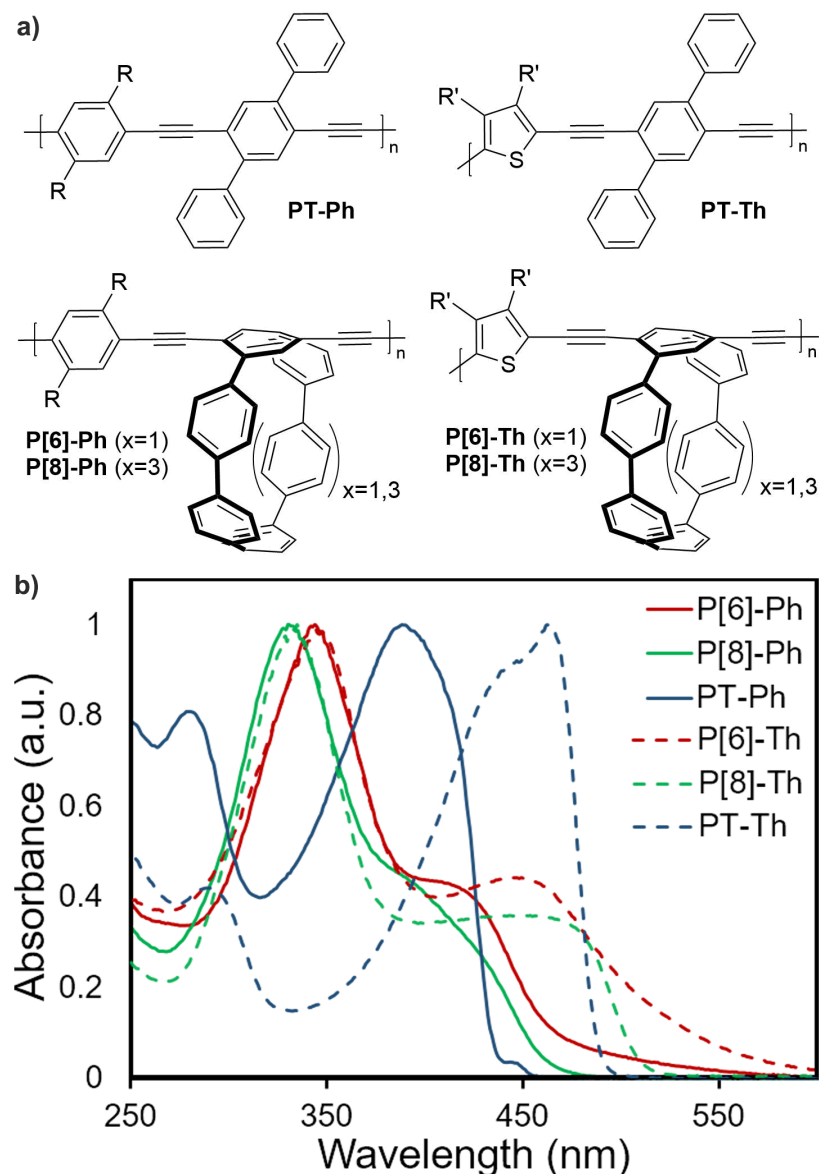
**Figure 3.1.** a) Structures of conjugated polymers with linear and cyclic side chains investigated in this study. R = 2-ethylhexyl; R' = octyl. b) UV-Vis absorption spectra showing the red-shifted absorption of P[6]-Ph and P[8]-Ph compared to PT-Ph as well as P[6]-Th and P[8]-Th compared to PT-Th.

absorbance in the CPP polymers was not due to differences in molecular weight of the polymers. In fact, the experimental absorption wavelengths correlate to a conjugation length of about two to three repeat units, with more extended conjugation being prevented by the many possible conformations possible for the polymer backbone. Computations did reveal that unique electronic transitions, such as radial-to-linear transitions, exist in these hybrid materials (Fig. 3.2). Our computational results help

explain why these radial/linear hybrid conjugated polymers differ from previously reported poly(paraphenylene)s with CPP side chains (Fig. 3.3),[75] which showed little change in electronics from the CPP monomers. First, the phenylene units in the poly(paraphenylene) backbone are unlikely to be in plane with each other, leading to little delocalization, and second, matching the energy levels of the polymer backbone and the CPP side chains is critical to achieve orbital mixing in the final material.
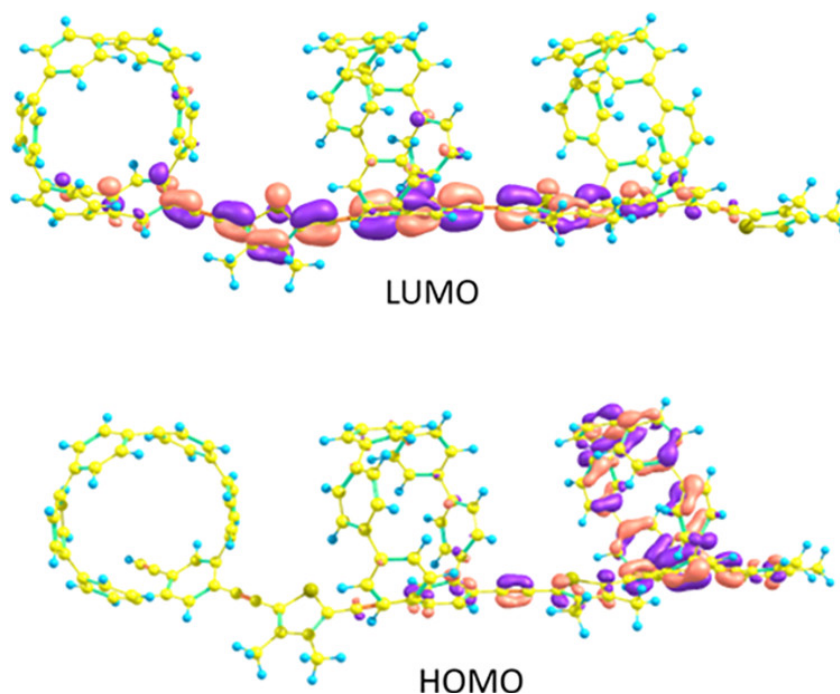


**Figure 3.2.** Radial-to-linear transitions, like the HOMO-LUMO transition shown here for a **P[6]-Th** fragment, are unique to these hybrid materials. Image reused with permission from Peters, G. M.; Grover, G.; Maust, R. L.; Colwell, C. E.; Bates, H.; Edgell, W. A.; Jasti, R.; Kertesz, M.; Tovar, J. D. *J. Am. Chem. Soc.* **2020**, *142*, 2293-2300. Copyright 2020 American Chemical Society.

## 3.3 Results and Discussion for Disjoint Linear/Radial Polymers

### 3.3.1 Monomer and Polymer Synthesis

We next began an investigation of delocalization pathways through conjugated CPP-containing polymers based on the placement of connection points on the CPP monomers. We envisioned that placement of two alkynes on opposite sides of a nanohoop could lead to delocalization pathways through the nanohoop units. The oligomeric nature of CPPs and the ability to embed functionality at precise positions on
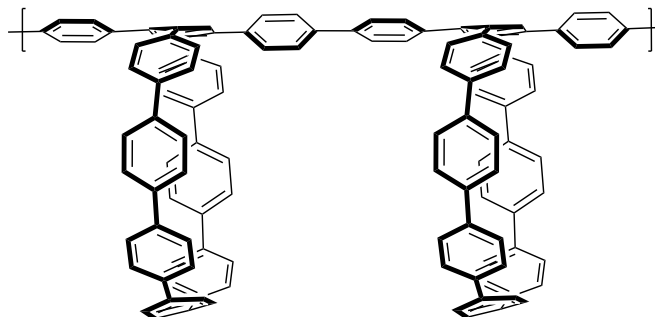
**Figure 3.3.** A CPP-based polymer with a poly(paraphenylene) backbone exhibited little orbital mixing between the linear and radial pi components.

the nanohoop enable comparison of a disjoint system like this with the previous contiguous polymers. Preliminary computations indicated that there could be slight differences in properties between regioisomers (Fig. 3.4), and for synthetic ease we targeted pseudo-eclipsed dialkyne [8]CPP compound **III.16**. The synthetic pathway to this molecule is shown in Scheme 3.2. To obtain the singly alkyne-functionalized segments, bromochloroiodobenzene was subjected to a Sonogashira reaction with triisopropylsilyl (TIPS) acetylene. Then, dichloride **III.12** with alkynes on distal benzene rings was prepared through a series of lithiation-addition steps and TES protection reactions. Bisboronate **III.13** was prepared in a similar manner through known chemistry. **III.12** and **III.13** were subjected to dilute Suzuki cross-coupling conditions to yield macrocycle **III.14**. **III.14** was reductively aromatized by treatment with tin chloride, yielding disjoint di(TIPS-ethynyl) [8]CPP **III.15**. Interestingly, the usual synthetic sequence—deprotection of the triisopropylsilyl (TIPS) groups followed by treatment of the compound with tin chloride—produced the diketone compound **III.17** (Fig. 3.5) via hydrolysis and tautomerization. This compound may in its own right be a useful precursor to new polymers, such as polyketanils or similar.[196] After aromatization, disjoint di(TIPS-ethynyl) [8]CPP **III.15** was deprotected using TBAF, yielding the final monomer **III.16**. This monomer was then subjected to Sonogashira cross-coupling polymerization as with the previous examples to obtain disjoint conjugated polymers **Dis-P[8]-Ph** and **Dis-P[8]-Th** (Fig. 3.6).
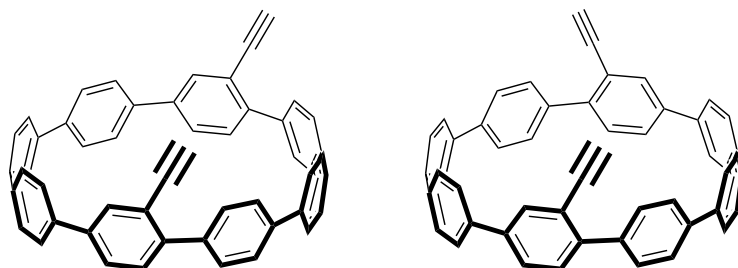
**Figure 3.4.** Two possible regioisomers of [8]CPP with alkynes on opposite sides of the nanohoop.

### 3.3.2 Optoelectronic Properties of Disjoint Polymers

Like with the contiguous polymers containing [8]CPP units, the disjoint polymers exhibited similar fluorescence spectra to [8]CPP itself, so differences in the UV-Vis absorbance spectra were the main source of insight. Both Dis-P[8]-Ph and Dis-P[8]-Th had slightly blue-shifted absorbance maxima when compared to [8]CPP ($\lambda_{max}$ = 340 nm),[119] at 329 and 331 nm, respectively. While a broad, lower-energy absorbance is present in spectra for both disjoint polymer types, it differs from the low-energy absorbance in the contiguous polymers. In the disjoint polymers, this absorbance ranges from 375 to 450 nm, the same region where the formally forbidden HOMO-LUMO transition appears in the absorbance spectrum of [8]CPP. The decrease in symmetry in these disjoint systems could contribute to an increase in the oscillator strength of this transition. For Dis-P[8]-Ph and Dis-P[8]-Th, two extracts were obtained for each, corresponding to lower and higher molecular weight fractions (Table 3.2), allowing a comparison of the optical properties of the polymers based on molecular weight. The absorbance spectra of the lower and higher molecular weight fractions did not differ drastically in either case, but a small degree of vibronic character was observed in the spectra of the lower molecular weight fractions. Computations will be critical in fully interpreting what the optical properties of disjoint CPP-based polymers mean in terms of radial and linear conjugation pathways and extent of delocalization in these materials.

**Scheme 3.2.** Synthetic route to disjoint dialkyne [8]CPP monomer **III.16**.
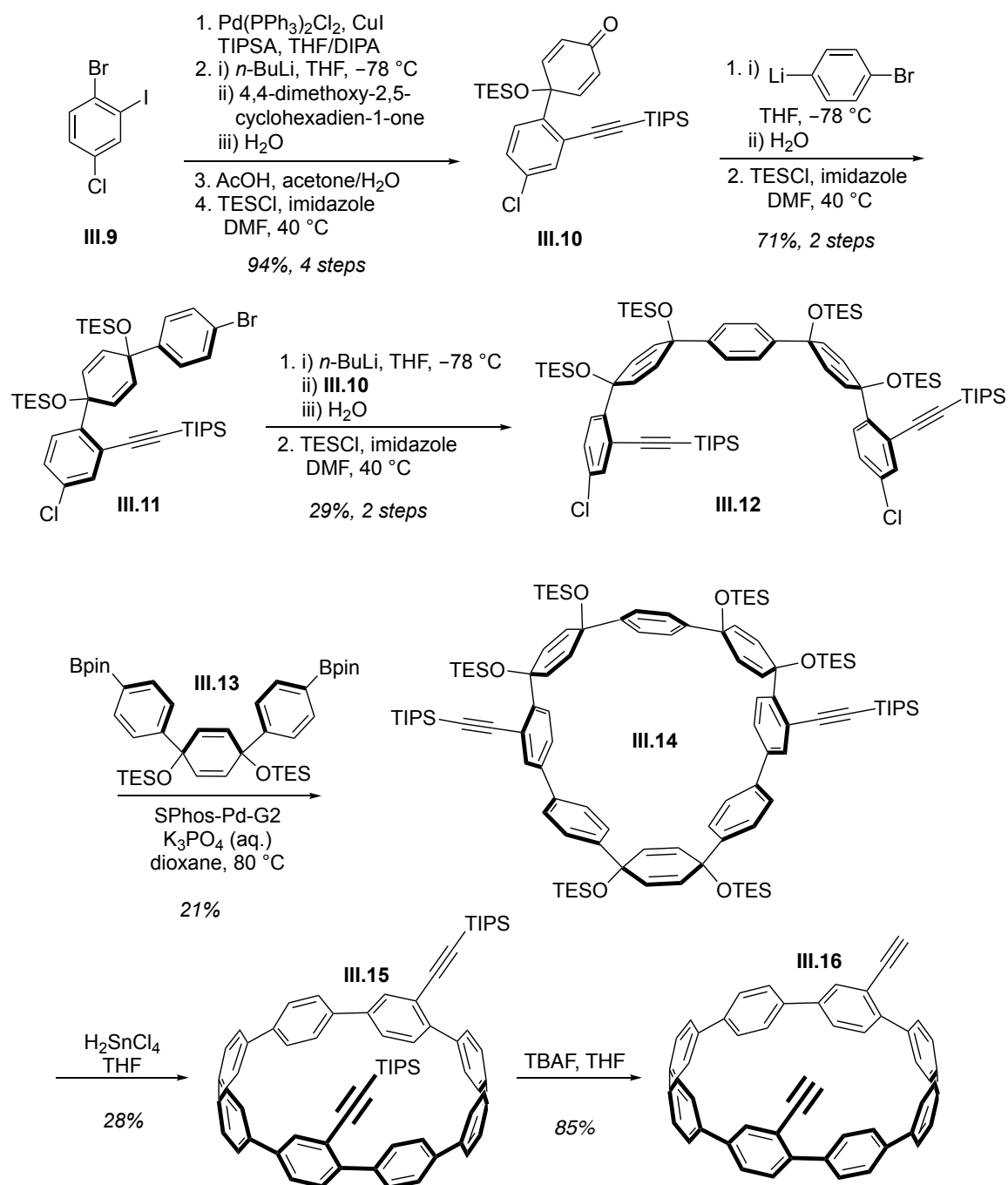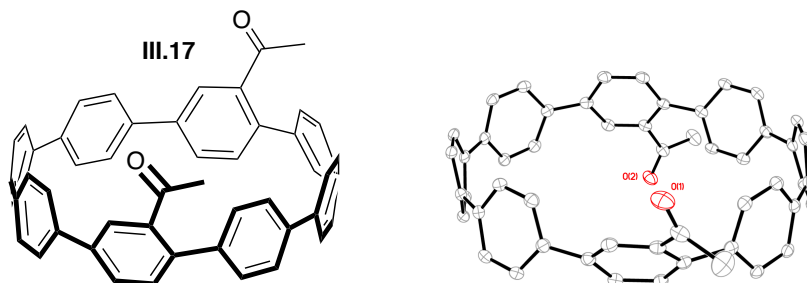
**Figure 3.5.** Diketone [8]CPP compound (left) produced by an initial deprotection and aromatization attempt of macrocycle **III.14** and its crystal structure (right).
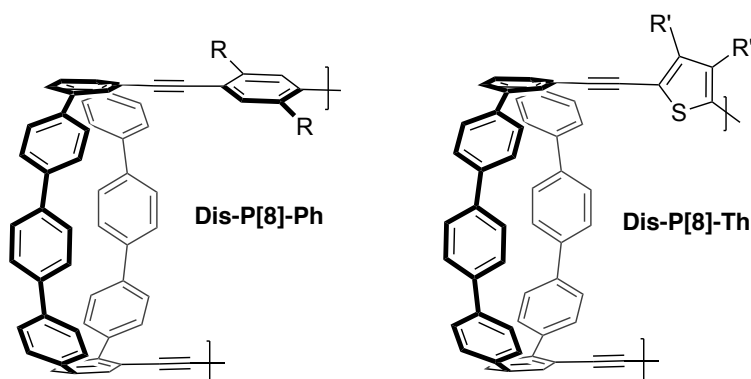


**Figure 3.6.** Structures of two disjoint conjugated polymers containing [8]CPP units.

### 3.4 Conclusions and Outlook

Conjugated polymers built from both radial and linear components are an exciting addition to the array of organic materials. Studying this type of novel polymers can contribute significantly to the fundamental understanding of conjugation in different types of pi systems. Importantly, these studies are enabled by synthetic access to precise radially conjugated structures, namely CPPs. Using this family of molecules, we can systematically compare the properties of materials made from different sizes of CPPs as well as CPPs with substituents in different positions. To date, research in this area has uncovered unique materials properties based on CPP size (**P[6]-Ph** vs. **P[8]-Ph**; **P[6]-Th** vs. **P[8]-Th**), polymer backbone structure (poly(phenylene ethynylene) vs. poly(thiophene ethynylene) vs. poly(paraphenylene), and polymer backbone connectivity (**P[8]-Ph** vs. **Dis-P[8]-Ph**; **P[8]-Th** vs. **Dis-P[8]-Th**). There are certainly many avenues left to be explored, including incorporation of other types of aromatic units in the CPP units or the polymer backbone and investigation of branched, interlocked, and other

polymer topologies. As understanding of this area grows, we are gaining more and more tools to design new organic electronic materials with desirable properties.

## 3.5 Experimental Section

### 3.5.1 General Experimental

Commercially available materials were used without purification. Moisture- and oxygen-sensitive reactions were carried out in flame-dried glassware and under an inert atmosphere of purified nitrogen using syringe/septa technique. Tetrahydrofuran (THF), 1,4-dioxane, and dimethylformamide (DMF) were dried by filtration through alumina according to the methods described by Grubbs.[169] Thin Layer Chromatography (TLC) was performed using Sorbent Technologies Silica Gel XHT TLC plates. Developed plates were visualized using UV light at wavelengths of 254 and 365 nm. Silica column chromatography was conducted with Zeochem Zeoprep 60 Eco 40-63 μm silica gel. Automated flash chromatography was performed using a Biotage Isolera One. Recycling gel permeation chromatography (GPC) was performed using a Japan Analytical Industry LC-9101 preparative HPLC with JAIGEL-1H/JAIGEL-2H columns in series using $CHCl_3$. Gel permeation chromatography for polymer molecular weight determination was performed on an Agilent 1260 Infinity Series (degasser, iso pump, TCC, DAD) using unstabilized THF at 40º C vs. Agilent EasiVial PS-M polystyrene standards. ^{1}H and ^{13}C NMR spectra of monomers and intermediates were recorded on a Bruker Avance III HD 500 MHz ([1]H: 500 MHz, [13]C: 126 MHz). ^{1}H NMR spectra were taken in $CDCl_3$ (referenced to TMS, δ 0.00 ppm) or acetone-$d_6$ (referenced to solvent peak, δ 2.05 ppm). ^{13}C NMR spectra were taken in $CDCl_3$ (referenced to solvent peak, δ 77.16 ppm) or acetone-$d_6$ (referenced to solvent peak, δ 29.84 ppm). ^{1}H NMR spectra of polymer samples were obtained on either a Bruker Avance II 400 MHz Spectrometer or Bruker Avance III 400 MHz Spectrometer, with residual protio-solvent resonances used as the internal standard ($CHCl_3$: 7.26 ppm, $CHDCl_2$: 5.32 ppm). UV-Vis absorption and fluorescence spectra were recorded on an Agilent Cary 100 spectrophotometer and a Horiba Jobin Yvon Fluoromax-4 Fluorometer, respectively. All absorption and fluorescence measurements were carried out under ambient conditions.

### 3.5.2 Detailed Synthetic Procedures for Contiguous Monomers

Compounds **III.1**,[197] **III.3**,[183] **III.6**,[138] SPhos-Pd-G2,[178] and SPhos-Pd-G3[198] were prepared according to the literature.

*1,4-diBpin-2,5-diTMSA benzene **III.2**.*
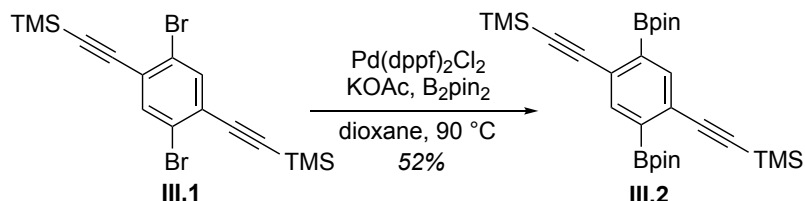


KOAc (6.05 g, 61.6 mmol, 6.6 eq) was added to a round bottom flask under vacuum and flame dried. Upon cooling, dibromide **II.X** (4.00 g, 9.34 mmol, 1 eq), Pd(dppf)$_2$Cl$_2$ (229 mg, 280 µmol, 0.03 eq) and bis(pinacolato)diboron (5.69 g, 22.4 mmol, 2.4 eq) were added. The vessel was fitted with a rubber septum and evacuated/backfilled with nitrogen. Dioxane was added, the reaction was warmed to 90 °C and stirred at this temperature overnight. In the morning, it was filtered through celite, washed with EtOAc, and concentrated under reduced pressure. The resulting residue was recrystallized in EtOH to yield brown crystals (2.54 g, 52%). $^1$H NMR (500 MHz, CDCl$_3$) δ 7.82 (s, 2H), 1.36 (s, 24H), 0.25 (s, 18H). $^{13}$C NMR (126 MHz, CDCl$_3$) δ 139.54, 126.81, 105.47, 97.81, 84.27, 25.08, 0.09, $^{13}$C-B signal not observed. IR (neat): 2981, 2154, 1372, 1324, 1249 cm$^{-1}$. HRMS (ASAP) (m/z): [M+H]$^+$ calculated for C$_{28}$H$_{45}$B$_2$O$_4$Si$_2$, 523.3042; found, 523.3091.

*DiTMSA [6]macrocycle diOTES diOMe **III.4**.*
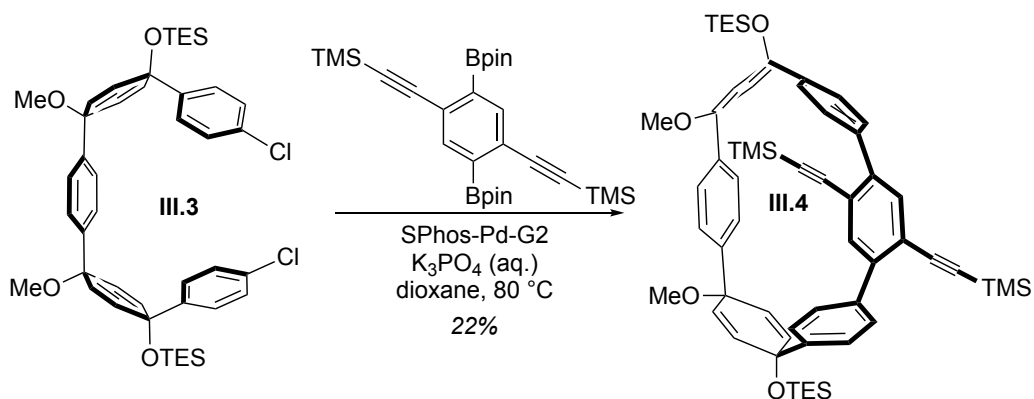
A flame-dried flask was charged with bisboronate **III.2** (318 mg, 0.609 mmol, 1.05 equiv.), dichloride **III.3** (450 mg, 0.580 mmol, 1.00 equiv.), and SPhos Pd Gen II (63 mg, 0.087 mmol, 0.15 equiv.). The flask was evacuated for 5 minutes and backfilled with nitrogen for 5 cycles. The flask was then purged with nitrogen for 1 hr. Dry dioxane (290 mL, 2 mM) was sparged for 1 hr, added to the reaction flask, and heated to 80 °C. A 2 M. aqueous solution of $K_3PO_4$ was sparged with nitrogen for 1 hr., then 29 mL of $K_3PO_4$ solution was added to the reaction. The reaction was stirred for 2 hr at 80 °C. After the reaction was cooled to room temperature, the dioxane was removed under reduced pressure, then the resulting material was filtered through a celite pad with ethyl acetate and water. The filtrate was extracted with ethyl acetate (2x). The combined organic layers were washed with water (2x) and brine (1x), then dried over sodium sulfate and concentrated under reduced pressure. The material was purified by automated column chromatography in 0% to 15% EtOAc in hexanes and by gel permeation chromatography to yield 245 mg (22%). $^1$H NMR (500 MHz, CDCl$_3$) δ 7.40 (d, $J$ = 8.3 Hz, 4H), 7.33 (s, 2H), 7.30 (d, $J$ = 8.4 Hz, 4H), 6.85 (s, 4H), 6.31 (dd, $J$ = 10.2, 2.5 Hz, 2H), 6.12 (dd, $J$ = 10.3, 2.5 Hz, 2H), 5.79 (dd, $J$ = 10.3, 2.5 Hz, 2H), 5.44 (dd, $J$ = 10.0, 2.5 Hz, 2H), 3.28 (s, 6H), 0.98 (t, $J$ = 7.9 Hz, 18H), 0.67 (q, $J$ = 7.9 Hz, 12H), 0.19 (s, 18H). $^{13}$C NMR (126 MHz, CDCl$_3$) δ 144.52, 142.84, 142.59, 140.25, 137.99, 137.30, 133.53, 131.64, 128.98, 126.62, 125.97, 125.95, 119.54, 104.63, 99.50, 74.26, 71.43, 51.59, 7.18, 6.68, 0.15. IR (neat): 2935, 2875, 2821, 2151, 1491, 1459, 1402, 1248, 1176, 1073, 1005, 948, 820, 721 cm$^{-1}$. HRMS (FTMS +c ESI) (m/z): [M]$^+$ calculated for C$_{60}$H$_{76}$O$_4$Si$_4$, 972.4815; found, 972.4827.

*Diethynyl [6]macrocycle diOMe diol **III.9***.
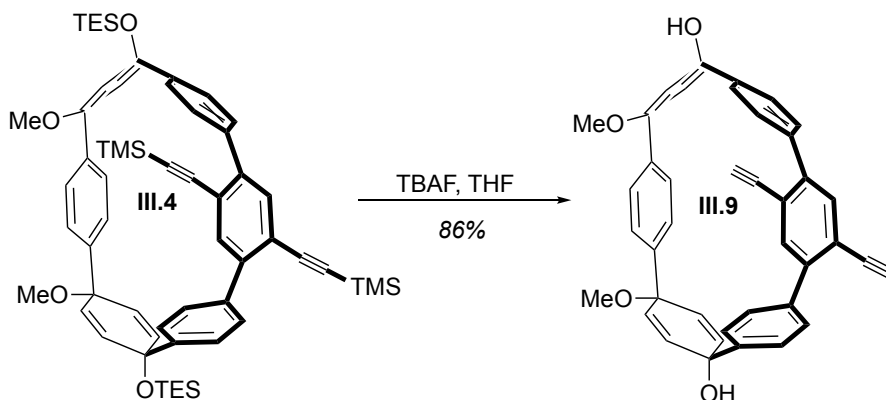
Macrocycle **III.4** (225 mg, 0.231 mmol, 1.00 equiv.) was added to a flame-dried flask and dissolved in THF (1.5 mL, 150 mM). A 1 M. solution of TBAF (1.0 mL, 0.971 mmol, 4.20 equiv.) was added slowly to the solution, and the reaction was stirred for 1 hr. The reaction was quenched with water and extracted with DCM (3x). The combined organic layers were washed with water (2x) and brine (1x) before being dried over sodium sulfate. Solvent was removed under reduced pressure. The product was purified by column chromatography in 0% to 100% ethyl acetate in dichloromethane (120 mg, 86%). $^1$H NMR (500 MHz, CDCl$_3$) δ 7.45 (d, $J$ = 8.6 Hz, 4H), 7.41 (s, 2H), 7.40 (d, $J$ = 8.7 Hz, 4H), 6.85 (s, 4H), 6.30 (dd, $J$ = 10.2, 2.5 Hz, 2H), 6.14 (dd, $J$ = 10.1, 2.6 Hz, 2H), 5.81 (dd, $J$ = 10.2, 2.5 Hz, 2H), 5.45 (dd, $J$ = 10.1, 2.4 Hz, 2H), 3.27 (s, 6H), 2.21 (s, 2H). $^{13}$C NMR (126 MHz, CDCl$_3$) δ 142.74, 142.69, 142.50, 140.54, 138.25, 136.78, 132.78, 132.50, 129.05, 128.09, 126.47, 125.83, 118.67, 82.97, 82.05, 74.46, 69.70, 51.30, 22.81, 14.27. IR (neat): 3275, 2931, 2870, 1483, 1461, 1403, 1352, 1173, 1052, 1021, 945, 831, 764 cm$^{-1}$. HRMS (TOF MS EI+) (m/z): [M]$^+$ calculated for C$_{42}$H$_{32}$O$_4$, 600.2301; found, 600.2302.

*Diethynyl [6]CPP* **III.5**.
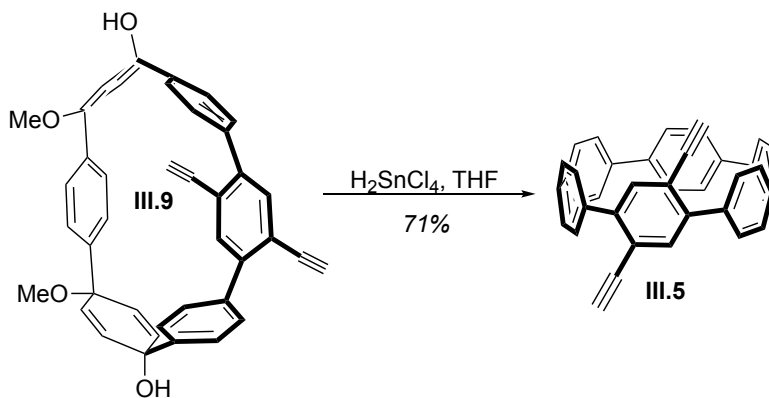


Deprotected macrocycle **III.9** (20 mg, 0.033 mmol, 1.00 equiv.) was added to a flame-dried flask and dissolved in THF (0.2 mL, 20 mM). Then a 0.05 M (in THF) solution of H$_2$SnCl$_4$ (1.5 mL, 0.073 mmol, 2.20 equiv.) was added dropwise. The reaction was stirred at room temperature for 30 min, then quenched with saturated sodium bicarbonate solution. The material was filtered through celite using water and DCM. The filtrate was extracted with DCM (3x), and the combined organic layers were washed with water (2x) and brine (1x) before being dried over sodium sulfate. Solvent was removed under

reduced pressure. The material was purified by pipet column chromatography in 20% DCM in hexanes, yielding a red solid (12 mg, 71%). IR (neat): 3283, 3023, 2932, 2825, 1584, 1482, 1462, 1352, 1252, 1173, 1056, 947, 832, 819, 766, 728, 705 cm$^{-1}$. $^1$H NMR (500 MHz, CDCl$_3$, -10 °C) δ 8.52 (s, 2H), 7.72 (s, 2H), 7.68 – 7.48 (overlapping, 18H), 3.64 (s, 2H). $^{13}$C NMR (126 MHz, CDCl$_3$, -10 °C) δ 137.49, 137.33, 135.58, 135.35, 135.13, 134.48, 133.35, 128.44, 128.03, 127.89, 127.53, 127.41, 127.39, 127.28, 127.21, 127.07, 118.59, 84.88, 83.40. See spectra section for $^1$H and $^{13}$C NMR spectra at -10 °C and 25 °C with assignments. HRMS (TOF MS EI+) (m/z): [M]$^+$ calculated for C$_{40}$H$_{24}$, 504.1878; found, 504.1878.

*DiTMSA [8]macrocycle tetraOTES diOMe III.7.*
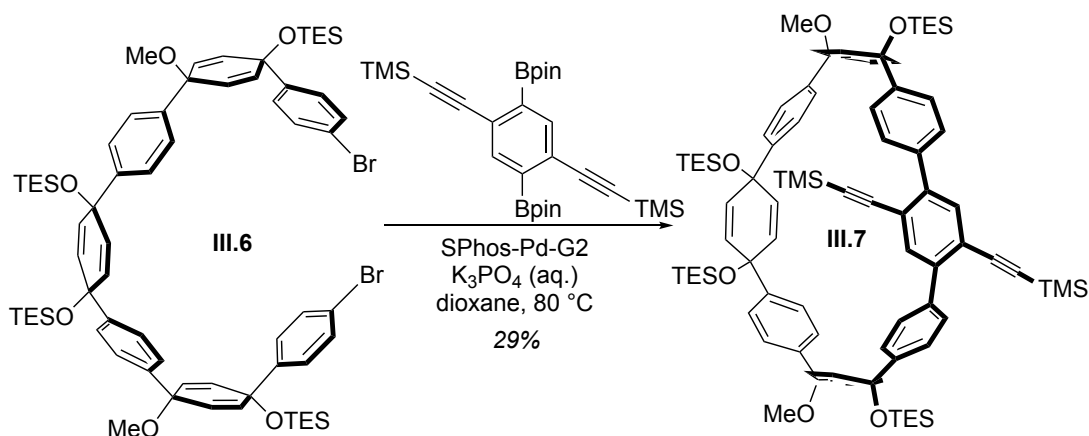


Dibromide **III.6** (1.8 g, 1.4 mmol, 1.00 eq), bisboronate **III.2** (882 mg, 1.7 mmol, 1.20 eq), and 3rd generation SPhos precatalyst (110 mg, 140 μmol, 0.1 eq) were dissolved in dioxane (280 mL, 5 mM) and purged with nitrogen while heating to 80 °C. An aqueous solution of K$_3$PO$_4$ (28 mL) was added and the mixture was stirred for 18 hrs. The mixture was then filtered through celite and dried over anhydrous sodium sulfate. Solvent was removed under reduced pressure to yield a brown solid. The solid was purified by column chromatography on silica (hexanes to DCM) to yield **III.7** as an orange solid (558 mg, 29%). $^1$H NMR (600 MHz, CDCl$_3$) δ 7.46 (s, 2H), 7.39 (d, *J* = 8.4 Hz, 4H), 7.32 (d, *J* = 8.4 Hz, 4H), 7.29 (d, *J* = 8.4 Hz, 4H), 7.18 (d, *J* = 8.6 Hz, 4H), 6.19 (dd, *J* = 10.1, 2.5 Hz, 2H), 6.16 (dd, *J* = 10.1, 2.4 Hz, 2H), 6.12 (m, 4H), 5.95 (dd, *J* = 10.2, 2.5 Hz, 2H), 5.90 (dd, *J* = 10.1, 2.5 Hz, 2H), 3.31 (s, 6H), 1.01 (t, *J* = 7.9 Hz, 18H), 0.86 (t, *J* = 8.0 Hz, 18H), 0.71 (q, *J* = 7.8 Hz, 12H), 0.49 (q, *J* = 7.7 Hz, 12H), 0.13 (s, 12H). $^{13}$C NMR (126

MHz, CDCl$_3$) δ 146.67, 144.63, 142.67, 142.07, 138.50, 136.23, 135.64, 134.82, 134.71, 133.31, 129.45, 126.43, 126.12, 125.09, 104.53, 99.40, 74.60, 72.48, 69.55, 51.85, 7.33, 7.22, 6.82, 6.69. IR (neat): 2953, 2875, 2155, 1477, 1409, 1249 cm$^{-1}$. HRMS (ASAP) (m/z): [M]$^+$ calculated for C$_{84}$H$_{114}$O$_6$Si$_6$, 1386.7231; found, 1386.7169.

*Diethynyl [8]macrocycle diOMe tetraol **III.10**.*
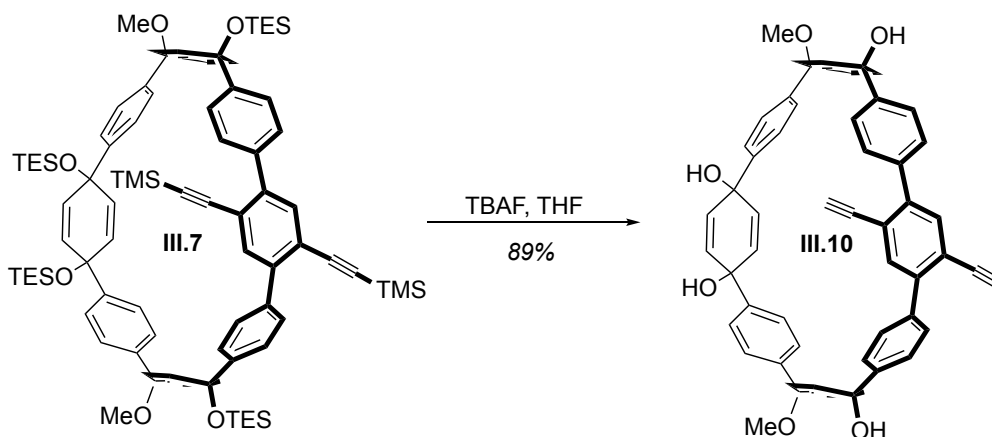


Macrocycle **III.7** (558 mg, 402 µmol, 1.00 eq) was dissolved in THF (2 mL, 200 mM) and a 1 M. solution of TBAF in THF (3.2 mL, 3.2 mmol, 8.00 eq) was added. The reaction was stirred for 1 h and quenched with water. THF was removed under reduced pressure to yield a suspension. The material was filtered and washed with water and DCM to yield an off-white solid (283 mg, 89%). $^1$H NMR (500 MHz, acetone-d$_6$) δ 7.57 (s, 2H), 7.56 (d, J = 8.8 Hz, 4H), 7.50 (d, J = 8.2 Hz, 4H), 7.36 (d, J = 8.8 Hz, 4H), 7.21 (d, J = 8.4 Hz, 4H), 6.27 (d, J = 10.1 Hz, 4H), 5.95 (s, 4H), 5.84 (d, J = 10.1 Hz, 4H), 3.79 (s, 2H), 3.29 (s, 6H). $^{13}$C NMR (126 MHz, acetone-d$_6$) δ 145.73, 143.45, 143.09, 138.93, 136.56, 136.26, 135.57, 130.11, 129.93, 126.83, 126.65, 126.36, 121.51, 84.24, 83.10, 75.61, 67.58, 51.59. IR (neat): 3293, 2958, 1477, 1409 cm$^{-1}$.

*Diethynyl [8]CPP **III.8**.*
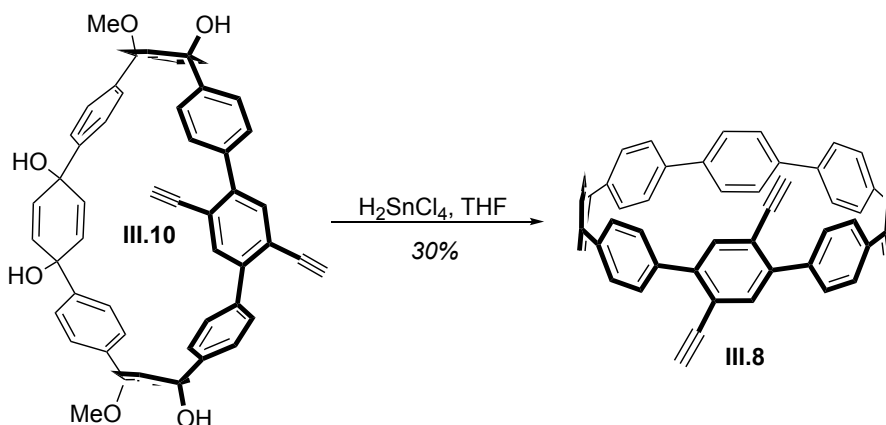


Deprotected macrocycle **III.10** (100 mg, 127 μmol, 1.00 eq) was dissolved in THF (3 mL, 40 mM). A solution of $SnCl_2 \cdot 2H_2O$ (95 mg, 420 μmol, 3.30 eq) and 12 M. HCl (67 μL, 800 μmol, 6.30 eq) in THF (3.2 mL) was added and the reaction was stirred for 1 hrs. The reaction was then quenched with a 1 M. aqueous solution of NaOH and extracted with DCM (3 x 5 mL). The combined extracts were dried over anhydrous sodium sulfate and solvent was removed under reduced pressure to yield a yellow solid. The material was purified by column chromatography in 40% to 100% DCM in hexanes to yield a yellow solid (25 mg, 30%). $^1$H NMR (500 MHz, CDCl$_3$) δ 7.62 (d, $J$ = 8.7 Hz, 4H), 7.54 – 7.49 (m, 8H), 7.48 – 7.44 (m, 14H), 7.42 (d, $J$ = 8.8 Hz, 4H), 3.26 (s, 2H). $^{13}$C NMR (126 MHz, CDCl$_3$) δ 140.78, 139.53, 138.15, 137.88, 137.87, 137.82, 137.54, 136.18, 135.56, 129.75, 127.91, 127.56, 127.54, 127.43, 127.27, 120.39, 83.02, 82.56. LRMS (MALDI) (m/z): [M]$^+$ calculated for $C_{52}H_{32}$, 656.250; found, 656.257.

### 3.5.3 Contiguous Polymer Synthesis and Characterization

Diethynyl terphenyl monomer **mT,**[199] 1,4-bis(2-ethylhexyl)-2,5-diiodobenzene,[200] and 2,5-diiodo-3,4-dioctylthiophene[201] were prepared according to the literature.

*PT-Ph*



Diethynyl terphenyl monomer **mT** (25 mg, 90 μmol), 1,4-bis(2-ethylhexyl)-2,5-diiodobenzene (50 mg, 90 μmol), Pd(PPh₃)₄ (5 mg, 4 μmol), and copper (I) iodide (2 mg, 9 μmol) were added to a Schlenk flask, which was then evacuated and backfilled with nitrogen three times. Dry and degassed diisopropylamine (4 mL) and toluene (4 mL) were added, and the reaction mixture was stirred at 80° C for 72 hrs. The solution was then cooled to room temperature and concentrated to approximately 0.5 mL before being rapidly added to MeOH (50 mL). The precipitate was collected by filtration and was purified by Soxhlet extraction: methanol (24 h), acetone (24 h), chloroform (2 h). The chloroform extract was concentrated and precipitated with 30 mL MeOH. Filtration yielded **PT-Ph** as a bright yellow solid (32 mg). ¹H NMR (400 MHz, CDCl₃): δ 7.81 – 7.68 (m), 7.55 – 7.35 (m), 7.09 (m), 2.62 – 0.45 (m).

*PT-Th*
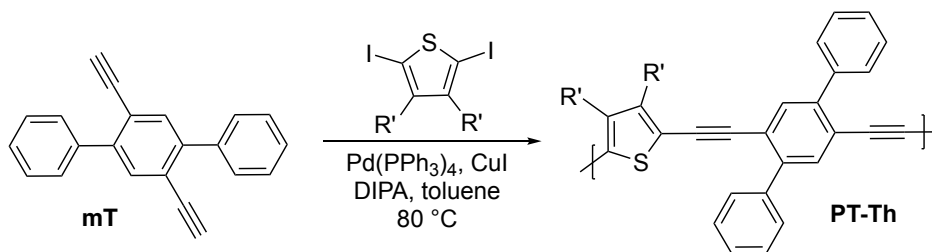


Diethynyl terphenyl monomer **mT** (25 mg, 90 μmol), 2,5-diiodo-3,4-dioctylthiophene (50 mg, 90 μmol), Pd(PPh₃)₄ (5 mg, 4 μmol), and copper (I) iodide (2 mg, 9 μmol) were added to a Schlenk flask, which was then evacuated and backfilled with nitrogen three times. Dry and degassed diisopropylamine (4 mL) and toluene (4 mL) were added, and the reaction mixture was stirred at 80° C for 72 hrs. The solution was then cooled to room temperature and concentrated to approximately 0.5 mL before being rapidly added to MeOH (50 mL). The precipitate was collected by filtration and was purified by Soxhlet

extraction: methanol (24 h), acetone (24 h), chloroform (2 h). The chloroform extract was concentrated and precipitated with 30 mL MeOH. Filtration yielded **PT-Th** as an orange solid (28 mg). ^{1}H NMR (400 MHz, CDCl$_3$): δ 7.71 – 7.60 (m), 7.52 – 7.39 (m), 1.31 – 1.09 (m).

## *P[6]-Ph*



**III.5** (12 mg, 20 µmol), 1,4-bis(2-ethylhexyl)-2,5-diiodobenzene (13 mg, 20 µmol), Pd(PPh$_3$)$_4$ (1 mg, 1 µmol), and copper (I) iodide (0.5 mg, 2 µmol) were added to a Schlenk tube, which was then evacuated and backfilled with nitrogen three times. Dry and degassed diisopropylamine (2 mL) and toluene (2 mL) were added, and the reaction mixture was stirred at 80° C for 72 hrs. The solution was then cooled to room temperature and concentrated to approximately 0.5 mL before being rapidly added to MeOH (50 mL). The precipitate was collected by filtration and was purified by Soxhlet extraction: methanol (24 h), acetone (24 h), chloroform (2 h). The chloroform extract was concentrated and precipitated with 30 mL MeOH. Filtration yielded **P[6]-Ph** as a red solid (6 mg). ^{1}H NMR (400 MHz, CDCl$_3$): δ 7.84 – 7.60 (m), 1.38 – 1.02 (m), 0.93 – 0.61 (m).

## *P[6]-Th*

**III.5** (12 mg, 20 μmol), 2,5-diiodo-3,4-dioctylthiophene (13 mg, 20 μmol), Pd(PPh$_3$)$_4$ (1 mg, 1 μmol), and copper (I) iodide (0.5 mg, 2 μmol) were added to a Schlenk tube, which was then evacuated and backfilled with nitrogen three times. Dry and degassed diisopropylamine (2 mL) and toluene (2 mL) were added, and the reaction mixture was stirred at 80° C for 72 hrs. The solution was then cooled to room temperature and concentrated to approximately 0.5 mL before being rapidly added to MeOH (50 mL). The precipitate was collected by filtration and was purified by Soxhlet extraction: methanol (24 h), acetone (24 h), chloroform (2 h). The chloroform extract was concentrated and precipitated with 30 mL MeOH. Filtration yielded **P[6]-Th** as a red solid (3 mg). $^1$H NMR (400 MHz, CDCl$_3$): δ 7.91 – 7.34 (m), 2.10 – 0.51 (m), 0.86 (t).

*P[8]-Ph*



**III.8** (13 mg, 20 μmol), 1,4-bis(2-ethylhexyl)-2,5-diiodobenzene (11 mg, 20 μmol), Pd(PPh$_3$)$_4$ (1 mg, 1 μmol), and copper (I) iodide (0.4 mg, 2 μmol) were added to a Schlenk tube, which was then evacuated and backfilled with nitrogen three times. Dry and degassed diisopropylamine (2 mL) and toluene (2 mL) were added, and the reaction mixture was stirred at 80° C for 72 hrs. The solution was then cooled to room temperature and concentrated to approximately 0.5 mL before being rapidly added to MeOH (50 mL). The precipitate was collected by filtration and was purified by Soxhlet extraction: methanol (24 h), acetone (24 h), chloroform (2 h). The chloroform extract was concentrated and precipitated with 30 mL MeOH. Filtration yielded **P[8]-Ph** as a bright yellow solid (6 mg). $^1$H NMR (400 MHz, CDCl$_3$): δ 7.89 – 7.28 (m), 1.89 – 1.07 (m), 1.01 – 0.56 (m).

*P[8]-Th*
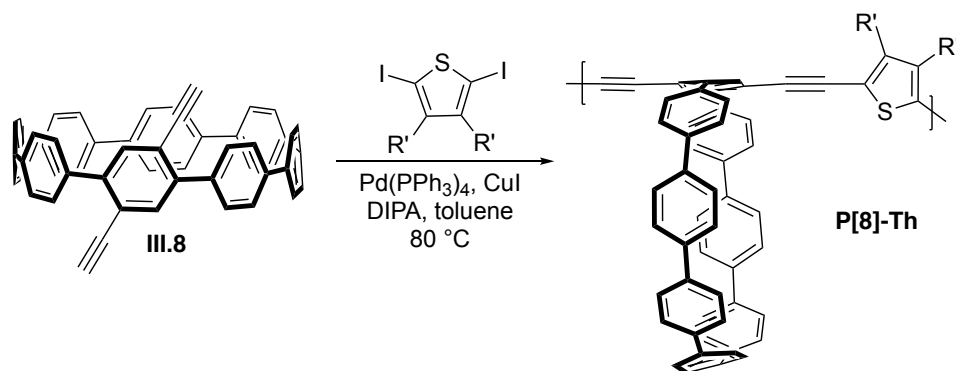


**III.8** (12 mg, 20 µmol), 2,5-diiodo-3,4-dioctylthiophene (12 mg, 20 µmol), Pd(PPh$_3$)$_4$ (1 mg, 1 µmol), and copper (I) iodide (0.4 mg, 2 µmol) were added to a Schlenk tube, which was then evacuated and backfilled with N$_2$ three times. Dry and degassed diisopropylamine (2 mL) and toluene (2 mL) were added, and the reaction mixture was stirred at 80° C for 72 hrs. The solution was then cooled to room temperature and concentrated to approximately 0.5 mL before being rapidly added to MeOH (50 mL). The precipitate was collected by filtration and was purified by Soxhlet extraction: methanol (24 h), acetone (24 h), chloroform (2 h). The chloroform extract was concentrated and precipitated with 30 mL MeOH. Filtration yielded **P[8]-Th** as an orange solid (5 mg). $^1$H NMR (400 MHz, CDCl$_3$): δ 7.80 – 7.33 (m), 2.42 – 0.78 (m).

| | PT-Ph | PT-Th | P[6]-Ph | P[6]-Th | P[8]-Ph | P[8]-Th |
|---|---|---|---|---|---|---|
| $M_w$ (g/mol) | 6,880 | 176,000 | 14,800 | 21,600 | 6,330 | 9,060 |
| DP | 12 | 292 | 18 | 27 | 7 | 9 |
| Đ | 1.44 | 3.48 | 2.44 | 6.29 | 1.41 | 1.36 |

**Table 3.1.** Weight average molecular weights ($M_w$), approximate degrees of polymerization (DP), and dispersity values (Đ) for contiguous conjugated polymer samples.

### 3.5.4 Detailed Synthetic Procedures for Disjoint Monomers

Bisboronate **III.13**[195] and SPhos-Pd-G2[178] were prepared according to the literature.

*TIPSA chloroketone **III.10**.*



1. Pd(PPh$_3$)$_2$Cl$_2$, CuI
   TIPSA, THF/DIPA
2. i) *n*-BuLi, THF, −78 °C
   ii) 4,4-dimethoxy-2,5-
       cyclohexadien-1-one
   iii) H$_2$O
3. AcOH, acetone/H$_2$O
4. TESCl, imidazole
   DMF, 40 °C

*94%, 4 steps*
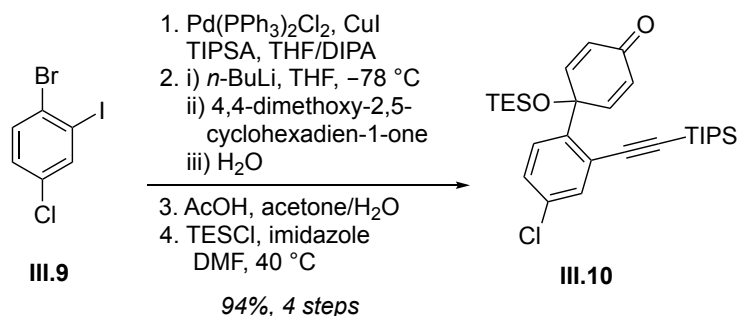
A flame-dried flask was charged with 1-bromo-4-chloro-2-iodobenzene (3.50 g, 11.0 mmol, 1.00 equiv.), Pd(PPh$_3$)$_2$Cl$_2$ (77 mg, 0.1 mmol, 0.01 equiv.), and CuI (42 mg, 0.2 mmol, 0.02 equiv.). The flask was evacuated and backfilled with nitrogen 5 times. THF (55 mL) was added and the mixture was sparged. DIPA was sparged separately. TIPSA (2.52 mL, 11.2 mmol, 1.02 equiv.) was added to the reaction mixture, followed quickly by 55 mL DIPA. The reaction was stirred at room temperature for ~1 week ($^1$H NMR showed approximately 95:5 product to starting material). The reaction mixture was concentrated under reduced pressure, then washed through a silica plug with hexanes. The filtrate was concentrated to yield a light brown oil, which was carried directly to the next reaction. This oil was added to a flame-dried flask, then dissolved in THF (17 mL) and cooled to -78 °C for 20 minutes. *n*-BuLi (5.00 mL, 12.0 mmol, 1.11 equiv.) was added dropwise, the reaction was stirred at -78 °C for another 20 minutes, then benzoquinone monoketal (1.85 g, 12.0 mmol, 1.11 equiv.) was added dropwise. The reaction was stirred at -78 °C for 1 hour, then quenched with water and warmed to room temperature. The THF was removed under reduced pressure, and the resulting material was extracted with ethyl acetate (3x). The combined organic layers were washed with water (2x) and brine (1x), then dried over sodium sulfate and concentrated. Acetone (17.50 mL), acetic acid (1.75 mL), and water (15.75 mL) were added to the material, and this mixture was stirred overnight. The reaction was quenched with a solution of sodium bicarbonate. The resulting mixture was extracted with ethyl acetate (3x). The combined organic layers were washed with water (2x) and brine (1x), then dried over sodium sulfate and concentrated. Finally, this material was added to a flame-dried flask with imidazole (1.63 g, 24.0 mmol, 2.22 equiv.) and dissolved in DMF (15.00 mL). TESCl

(3.02 mL, 18.0 mmol, 1.67 equiv.) was added slowly to the reaction and the reaction mixture was heated to 40 °C. After stirring overnight, the reaction was quenched with a solution of sodium bicarbonate. The resulting mixture was extracted with ethyl acetate (3x). The combined organic layers were washed with 5% LiCl solution (3x), water (2x), and brine (1x), then dried over sodium sulfate and concentrated. The material was purified by automated column chromatography on silica gel in 0% to 4% ethyl acetate in hexanes, yielding 5.23 g of a yellow oil (94% over 4 steps). $^1$H NMR (600 MHz, CDCl$_3$) δ 7.87 (d, $J$ = 8.7 Hz, 1H), 7.44 (d, $J$ = 2.3 Hz, 1H), 7.36 (dd, $J$ = 8.7, 2.3 Hz, 1H), 6.69 (d, $J$ = 10.3 Hz, 2H), 6.27 (d, $J$ = 10.2 Hz, 2H), 1.08 (s, 21H), 0.94 (t, $J$ = 7.9 Hz, 9H), 0.64 (q, $J$ = 7.9 Hz, 6H). $^{13}$C NMR (151 MHz, CDCl$_3$) δ 185.61, 147.72, 138.42, 136.07, 133.76, 129.27, 129.10, 127.82, 122.88, 103.80, 101.28, 71.65, 18.89, 11.39, 7.05, 6.42. IR (neat): 2954.5, 2864.8, 2147.4, 1672.3, 1631.7, 1459.0, 1382.0, 1236.7, 1075.3, 1001.4, 973.9, 921.3, 882.3, 826.1, 719.4 677.3 cm$^{-1}$. HRMS (TOF MS ASAP+) (m/z): [M+H]$^+$ calculated for C$_{29}$H$_{44}$ClO$_2$Si$_2$, 515.2568; found, 515.2575.

*Three-ring TIPSA chlorobromide **III.11**.*
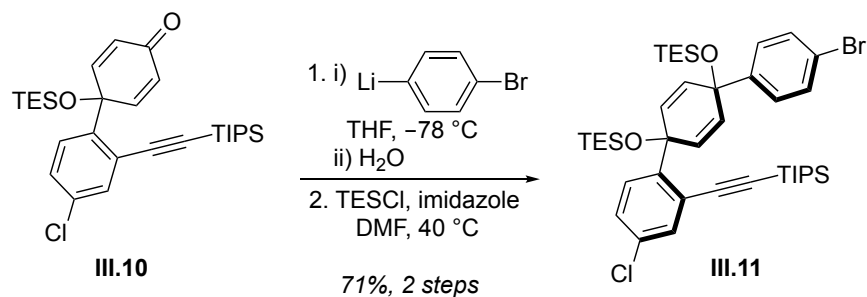


A flame-dried flask was charged with 1,4-dibromobenzene (0.32 g, 1.3 mmol, 1.30 equiv.), which was dissolved in THF (1.5 mL) and cooled to -78 °C for 20 minutes. *n*-BuLi (0.51 mL, 1.2 mmol, 1.20 equiv.) was added dropwise, the reaction was stirred at -78 °C for another 20 minutes, then chloroketone **III.10** (0.53 g, 1.0 mmol, 1.00 equiv.) was added dropwise and rinsed in with a small amount of THF. The reaction was stirred at -78 °C for 1 hour, then quenched with water and warmed to room temperature. The THF was removed under reduced pressure, and the resulting material was extracted with ethyl acetate (3x). The combined organic layers were washed with water (2x) and brine

(1x), then dried over sodium sulfate and concentrated. This material was added to a flame-dried flask with imidazole (0.14 g, 2.1 mmol, 2.00 equiv.) and dissolved in DMF (1.3 mL). TESCl (0.26 mL, 1.5 mmol, 1.50 equiv.) was added slowly to the reaction and the reaction mixture was heated to 40 °C. After stirring overnight, the reaction was quenched with a solution of sodium bicarbonate. The resulting mixture was extracted with ethyl acetate (3x). The combined organic layers were washed with 5% LiCl solution (3x), water (2x), and brine (1x), then dried over sodium sulfate and concentrated. The material was purified by automated column chromatography on silica gel in 0% to 3% ethyl acetate in hexanes, yielding 573 mg of a colorless oil (71% over 2 steps). $^1$H NMR (500 MHz, CDCl$_3$) δ 7.54 (dd, $J$ = 1.7, 0.9 Hz, 1H), 7.29 (d, $J$ = 8.7 Hz, 2H), 7.15 (overlapping, 2H), 7.05 (d, $J$ = 8.5 Hz, 2H), 6.69 (d, $J$ = 10.3 Hz, 2H), 5.85 (d, $J$ = 10.3 Hz, 2H), 1.16 (overlapping, 21H), 0.97 (t, $J$ = 7.9 Hz, 9H), 0.82 (t, $J$ = 7.9 Hz, 9H), 0.68 (q, $J$ = 7.9 Hz, 6H), 0.51 (q, $J$ = 8.0 Hz, 6H). $^{13}$C NMR (151 MHz, CDCl$_3$) δ 145.18, 144.90, 136.32, 133.15, 132.44, 131.19, 129.87, 128.07, 127.53, 127.39, 124.73, 120.98, 105.90, 99.07, 71.21, 71.01, 18.86, 11.62, 7.21, 7.13, 6.57, 6.43. IR (neat): 2953.4, 2864.8, 2153.2, 1463.3, 1267.8, 1235.7, 1072.7, 1006.4, 892.7, 883.1, 817.1, 803.6, 741.0, 726.8, 678.2 cm$^{-1}$. HRMS (TOF MS ASAP+) (m/z): [M]$^+$ calculated for C$_{41}$H$_{62}$BrClO$_2$Si$_3$, 784.2930; found, 784.2903.

*Five-ring diTIPSA dichloride **III.12***.
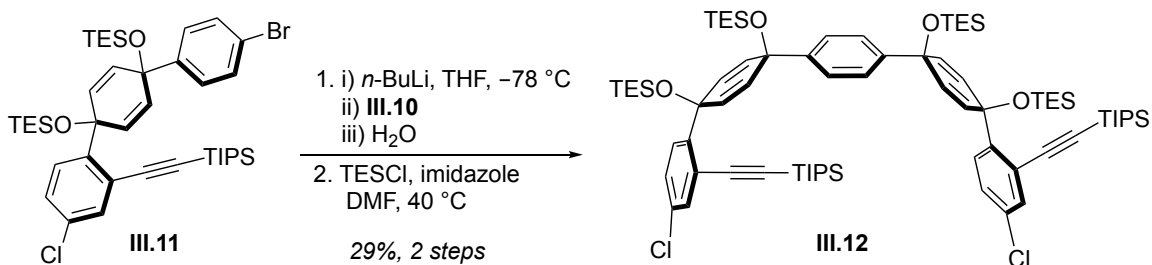


Bromochloride **III.11** (0.56 g, 0.7 mmol, 1.00 equiv.) was added to a flame-dried flask and dissolved in THF (1.0 mL), then cooled to -78 °C for 20 minutes. *n*-BuLi (0.31 mL, 0.8 mmol, 1.05 equiv.) was added dropwise, the reaction was stirred at -78 °C for another 20 minutes, then chloroketone **III.10** (0.37 g, 0.7 mmol, 1.00 equiv.) was added dropwise

and rinsed in with a small amount of THF. The reaction was stirred at -78 °C for 1 hour, then quenched with water and warmed to room temperature. The THF was removed under reduced pressure, and the resulting material was extracted with ethyl acetate (3x). The combined organic layers were washed with water (2x) and brine (1x), then dried over sodium sulfate and concentrated to a yellow oil. This material was added to a flame-dried flask with imidazole (0.10 g, 1.4 mmol, 2.00 equiv.) and dispersed in DMF (9 mL). TESCl (0.18 mL, 1.1 mmol, 1.50 equiv.) was added slowly to the reaction and the reaction mixture was heated to 40 °C. After stirring overnight, the reaction was quenched with a solution of sodium bicarbonate. The resulting mixture was extracted with ethyl acetate (3x). The combined organic layers were washed with 5% LiCl solution (3x), water (2x), and brine (1x), then dried over sodium sulfate and concentrated. The material was purified by sonication with 1:1 methanol/acetone and filtration. Additional product was obtained from the concentrated filtrate using automated column chromatography on silica gel in 0% to 2% ethyl acetate in hexanes. Total yield was 274 mg of a white solid (29% over 2 steps). $^1$H NMR (600 MHz, CDCl$_3$) δ 7.53 (d, $J$ = 2.1 Hz, 2H), 7.17 – 7.12 (overlapping, 4H), 7.00 (s, 4H), 6.63 (d, $J$ = 10.3 Hz, 4H), 5.82 (d, $J$ = 10.2 Hz, 4H), 1.15 (m, 42H), 0.95 (t, $J$ = 7.9 Hz, 18H), 0.81 (t, $J$ = 8.0 Hz, 18H), 0.66 (q, $J$ = 7.9 Hz, 12H), 0.49 (q, $J$ = 7.9 Hz, 12H). $^{13}$C NMR (151 MHz, CDCl$_3$) δ 145.48, 144.39, 136.25, 133.04, 133.00, 129.32, 127.91, 127.65, 125.17, 124.76, 106.06, 98.90, 71.28, 71.05, 18.86, 11.64, 7.22, 7.14, 7.06, 6.59, 6.46, 6.40. IR (neat): 2952.9, 2874.5, 2160.9, 1584.7, 1553.2, 1463.5, 1404.0, 1238.2, 1075.2, 1006.0, 958.5, 881.9, 853.5, 716.2, 662.4 cm$^{-1}$. HRMS (TOF MS ASAP+) (m/z): [M+H]$^+$ calculated for C$_{76}$H$_{121}$Cl$_2$O$_4$Si$_6$, 1335.7258; found, 1335.6367.

*Disjoint diTIPSA [8] macrocycle **III.14**.*
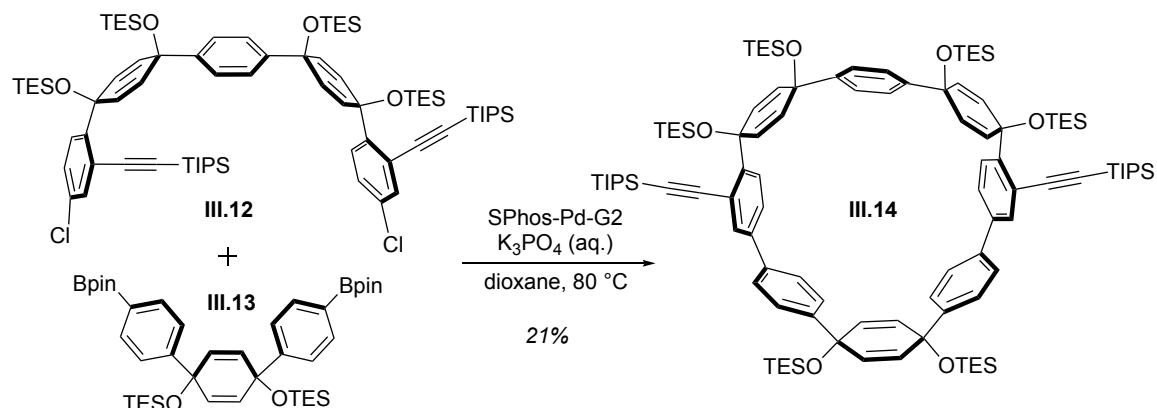


A flame-dried flask was charged with dichloride **III.12** (1.35 g, 1.0 mmol, 1.00 equiv.), bisboronate **III.13** (789 mg, 1.1 mmol, 1.05 equiv.), and SPhos Pd Gen II (73 mg, 0.1 mmol, 0.10 equiv.). The flask was evacuated for 5 minutes and backfilled with nitrogen for 5 cycles. The flask was then purged with nitrogen for 1 hr. Dry dioxane (337 mL, 3 mM) was sparged for 1 hr, added to the reaction flask, and heated to 80 °C. A 2 M. aqueous solution of $K_3PO_4$ was sparged with nitrogen for 1 hr., then 33.7 mL of $K_3PO_4$ solution was added to the reaction. The reaction was stirred for 1 hour at 80 °C. After the reaction was cooled to room temperature, the dioxane was removed under reduced pressure, then the resulting material was filtered through a celite pad with dichloromethane and water. The filtrate was extracted with dichloromethane (2x). The combined organic layers were washed with water (2x) and brine (1x), then dried over sodium sulfate and concentrated under reduced pressure. The material was purified by automated column chromatography in 0% to 15% dichloromethane in hexanes. A small amount of hexanes was added to the collected, concentrated product, which precipitated as a white solid on acetone addition. Filtration yielded 372 mg (21%). $^1$H NMR (600 MHz, CDCl$_3$) δ 7.81 (d, $J$ = 2.0 Hz, 2H), 7.37 – 7.35 (m, 4H), 7.34 (d, $J$ = 2.1 Hz, 2H), 7.28 (d, $J$ = 8.3 Hz, 2H), 7.17 (s, 4H), 7.13 – 7.09 (m, 4H), 6.73 (d, $J$ = 10.1 Hz, 4H), 6.11 (s, 4H), 5.81 (d, $J$ = 10.1 Hz, 4H), 1.17 (s, 42H), 0.99 (q, $J$ = 7.8 Hz, 36H), 0.79 (t, $J$ = 7.9 Hz, 18H), 0.73 (q, $J$ = 8.0 Hz, 12H), 0.66 (q, $J$ = 7.9 Hz, 12H), 0.49 (q, $J$ = 7.9 Hz, 12H). $^{13}$C NMR (151 MHz, CDCl$_3$) δ 145.82, 144.89, 144.01, 139.37, 138.17, 135.03, 132.43, 132.34, 129.81, 127.06, 126.63, 126.49, 126.27, 125.30, 123.38, 107.54, 97.29, 72.32, 70.82, 70.80, 18.93, 11.70, 7.30, 7.23, 7.20, 6.63, 6.42. IR (neat): 2949.8, 2874.3,

2147.1, 1458.0, 1407.7, 1238.3, 1186.3, 1064.0, 1006.4, 953.3, 882.2, 721.3, 676.4 cm$^{-1}$. HRMS (TOF MS ASAP+) (m/z): [M+H]$^+$ calculated for C$_{106}$H$_{163}$O$_6$Si$_8$, 1756.0604; found, 1756.0531.

*Disjoint diTIPSA [8]CPP **III.15***.
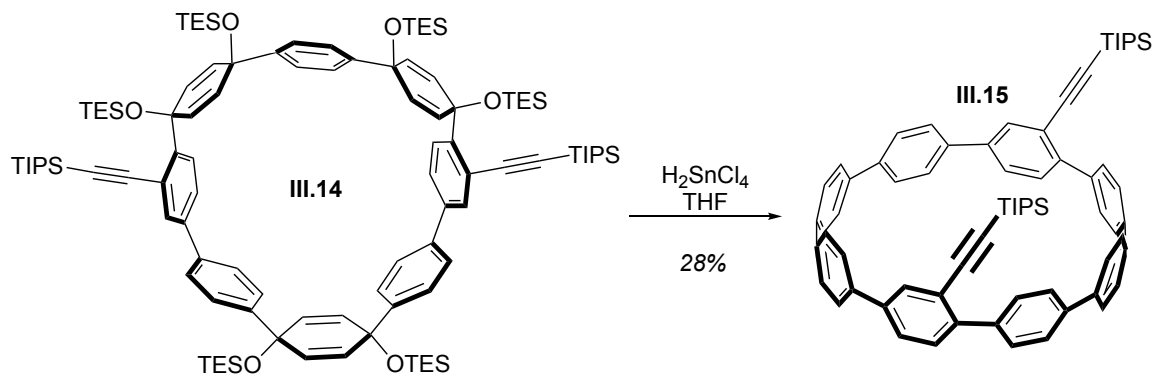


Macrocycle **III.14** (356 mg, 0.2 mmol, 1.00 equiv.) was added to a flame-dried flask and dissolved in minimal THF. Then a 0.05 M (in THF) solution of H$_2$SnCl$_4$ (20.3 mL, 1.0 mmol, 5.00 equiv.) was added dropwise. The reaction was stirred at room temperature for 1.5 hours, then quenched with saturated sodium bicarbonate solution. The material was filtered through celite using water and dichloromethane. The filtrate was extracted with dichloromethane (3x), and the combined organic layers were washed with water (2x) and brine (1x) before being dried over sodium sulfate. Solvent was removed under reduced pressure. The material was purified by adsorbing on alumina then running a pipet column 0% to in 20% ethyl acetate in hexanes, yielding a yellow solid (55 mg, 28%). $^1$H NMR (500 MHz, CDCl$_3$) δ 7.82 (d, $J$ = 2.1 Hz, 2H), 7.77 (d, $J$ = 8.6 Hz, 4H), 7.53 – 7.42 (m, 16H), 7.39 (d, $J$ = 8.6 Hz, 4H), 7.08 (dd, $J$ = 8.6, 2.1 Hz, 2H), 6.99 (d, $J$ = 8.5 Hz, 2H), 1.15 – 1.11 (m, 42H). $^{13}$C NMR (151 MHz, CDCl$_3$) δ 140.71, 138.31, 138.10, 137.69, 137.67, 137.49, 132.27, 130.78, 130.09, 128.88, 127.62, 127.32, 119.90, 106.93, 94.67, 18.89, 11.59. IR (neat): 2916.3, 2848.6, 2148.9, 1463.5, 1374.7, 1071.8, 1015.5, 997.0, 882.3, 815.9, 726.6 cm$^{-1}$. HRMS (TOF MS ASAP+) (m/z): [M+H]$^+$ calculated for C$_{70}$H$_{73}$Si$_2$, 969.5251; found, 969.5242.

*Disjoint diethynyl [8]CPP **III.16**.*
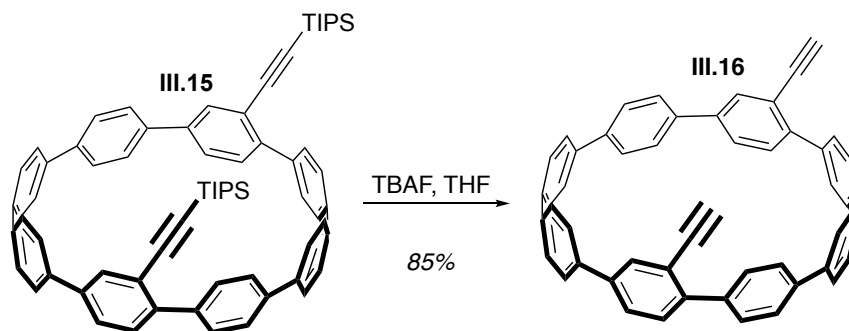


Macrocycle **III.14** (47 mg, 0.048 mmol, 1.00 equiv.) was added to a flame-dried flask and dissolved in THF (1.0 mL). TBAF (0.1 mL, 0.10 mmol, 2.10 equiv.) was added slowly to the solution, and the reaction was stirred for 1 hr. The reaction was quenched with water, then extracted with DCM (3x), and the combined organic layers were washed with water (2x) and brine (1x) before being dried over magnesium sulfate. Solvent was removed under reduced pressure. The material was purified using a silica plug in 25% DCM in hexanes, yielding a yellow solid (48 mg, 85%). $^1$H NMR (400 MHz, CDCl$_3$): δ 7.87 (d, $J$ = 2.0 Hz, 2H), 7.69 (d, $J$ = 8.9 Hz, 4H), 7.56 – 7.39 (m, 20H), 7.07 (dd, $J$ = 8.5, 2.0 Hz, 2H), 6.95 (d, $J$ = 8.5 Hz, 2H).

*Dimethylketone [8]CPP **III.17**.*
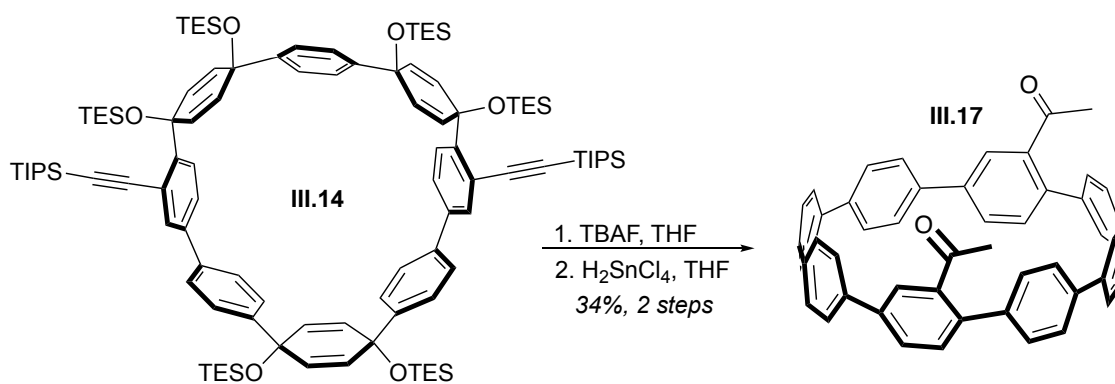


Macrocycle **III.14** (39 mg, 0.022 mmol, 1.00 equiv.) was added to a flame-dried flask and dissolved in THF (0.2 mL). TBAF (0.3 mL, 0.266 mmol, 12.00 equiv.) was added slowly to the solution, and the reaction was stirred for 1 hr. The reaction was quenched

with water, then concentrated under reduced pressure, resulting in a precipitate. This material was sonicated, filtered, and washed with water, before being added to a second flame-dried flask. THF (minimal) was used to rinse in the material, then a 0.05 M (in THF) solution of $H_2SnCl_4$ (2.2 mL, 0.111 mmol, 5.00 equiv.) was added dropwise. The reaction was stirred at room temperature for 40 min., then quenched with saturated sodium bicarbonate solution. THF was removed under reduced pressure, and the resulting material was filtered through celite using water and DCM. The filtrate was extracted with DCM (3x), and the combined organic layers were washed with water (2x) and brine (1x) before being dried over sodium sulfate. Solvent was removed under reduced pressure. The material was purified by adsorbing on alumina then running a pipet column 0% to in 100% DCM in hexanes, yielding a yellow solid (~5 mg, 34% over 2 steps). $^1$H NMR (500 MHz, CDCl$_3$) δ 8.20 (d, $J$ = 2.1 Hz, 2H), 7.52 – 7.45 (m, 12H), 7.42 (s, 4H), 7.40 (d, $J$ = 8.3 Hz, 4H), 7.20 (dd, $J$ = 8.3, 2.1 Hz, 2H), 7.19 (d, $J$ = 8.7 Hz, 4H), 6.99 (d, $J$ = 8.3 Hz, 2H), 2.63 (s, 6H). Crystals suitable for X-ray crystallography were obtained by slow evaporation of pentane into a solution of **III.17** in THF.

### 3.5.5 Disjoint Polymer Synthesis and Characterization
*Dis-P[8]-Ph*
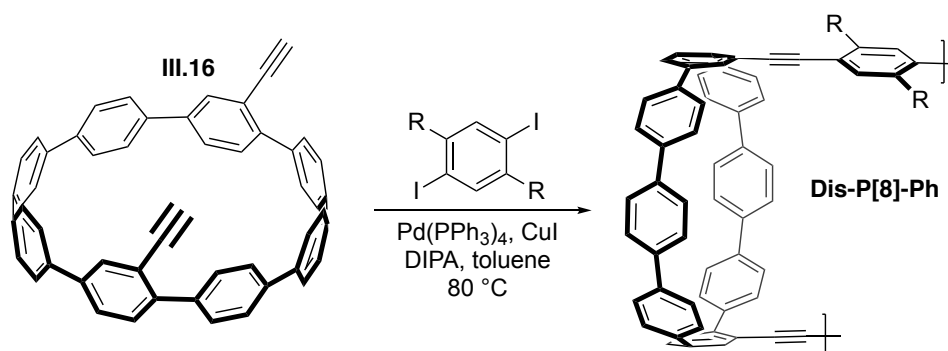


Pd(PPh$_3$)$_4$ (1.1 mg, 0.9 µmol, 4 mol%), and copper (I) iodide (0.5 mg, 3µmol, 13 mol%) were added to a Schlenk tube which was then evacuated and backfilled with nitrogen three times. **III.16** (1.0 mL of a 20 mM solution in toluene, 20 µmol, 1 eq), 1,4-bis(2-ethylhexyl)-2,5-diiodobenzene (0.5 mL of a 40 mM solution in toluene, 20 µmol, 1 eq), and additional toluene (0.5 mL) was added. Degassed diisopropylamine (2 mL) was added before heating to 80 °C in an oil bath. The solution was stirred at 80 °C for 72 hr

before cooling to room temperature. The crude was concentrated to ~0.5 mL in vacuo and then rapidly injected into methanol (50 mL). The yellow precipitate was purified by Soxhlet extraction in methanol (24 hr), acetone (24 hr), and chloroform (24 hr) to give the product (acetone: 6 mg yellow solid; chloroform: 6 mg yellow solid). $^1$H NMR (400 MHz, CDCl$_3$): δ 7.72 – 7.63 (m), 7.58 – 7.38 (m), 1.38 – 1.16 (m), 0.93 – 0.77 (m).

***Dis-P[8]-Th***
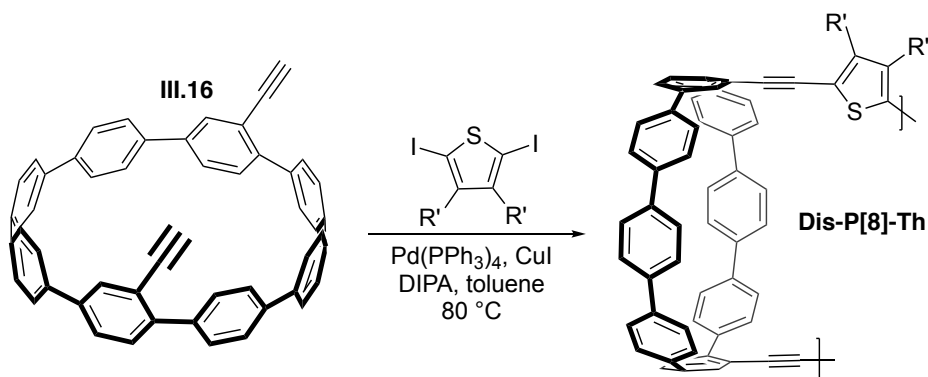


Pd(PPh$_3$)$_4$ (1.0 mg, 0.9 µmol, 4 mol%), and copper (I) iodide (0.5 mg, 3µmol, 13 mol%) were added to a Schlenk tube which was then evacuated and backfilled with nitrogen three times. **III.16** (1.0 mL of a 20 mM solution in toluene, 20 µmol, 1 eq), 2,5-diiodo-3,4-dioctylthiophene (0.5 mL of a 40 mM solution in toluene, 20 µmol, 1 eq), and additional toluene (0.5 mL) was added. Degassed diisopropylamine (2 mL) was added before heating to 80°C in an oil bath. The solution was stirred 80 °C for 72 hr before cooling to room temperature. The crude was concentrated to ~0.5 mL in vacuo and then rapidly injected into methanol (50 mL). The yellow precipitate was purified by Soxhlet extraction in methanol (24 hr), acetone (24 hr), and chloroform (24 hr) to give the product (acetone: 6 mg yellow solid; chloroform: 6 mg yellow solid). $^1$H NMR (400 MHz, CDCl$_3$): δ 7.87 (s), 7.78 – 7.62 (m), 7.58 – 7.36 (m), 7.14 – 6.95 (m) 1.38 – 1.02 (m), 0.95 – 0.65 (m).

|  | Dis-P[8]-Ph Acetone | Dis-P[8]-Ph Chloroform | Dis-P[8]-Th Acetone | Dis-P[8]-Th Chloroform |
|---|---|---|---|---|
| $M_w$ (g/mol) | 1,770 | 3,400 | 1,340 | 3,880 |
| DP | 8 | 15 | 7 | 19 |
| Đ | 1.19 | 1.42 | 1.17 | 1.86 |

**Table 3.2.** Weight average molecular weights ($M_w$), approximate degrees of polymerization (DP), and dispersity values (Đ) for disjoint conjugated polymer samples.


**3.6 Bridge to Chapter IV**

  Chapter III described the development of conjugated polymers containing CPP units to study the interplay between linear and radial pi systems in these hybrid materials. The chemistry used to make CPP monomers can also be applied to synthesize cyclic monomer structures that are not intended to remain cyclic in the final materials. Chapter IV relates two such strategies: one in which strained cyclic monomers ring-open during polymerization, and the second in which cyclic units in polymers can be ring-opened using mechanical force.

CHAPTER IV

NOVEL MATERIALS FROM RING-OPENING OF STRAINED MACROCYCLES

Chapter IV includes published and unpublished co-authored material. Section 4.2 is based on a manuscript published in *Materials Chemistry Frontiers* under the title "Ring-Opening Metathesis Polymerization of a Strained Stilbene-Based Macrocyclic Monomer."[3] Dr. Brock Lynde and Dr. Daniel Lee performed polymerization studies. Dr. Brock Lynde wrote the manuscript. Prof. Ramesh Jasti and Prof. A. J. Boydston edited the manuscript. Section 4.3 is based on unpublished work co-authored with Jinghui Yang, Prof. Yan Xia, and Prof. Ramesh Jasti.

## 4.1 Introduction

In the course of developing synthetic methodologies for preparing various CPP derivatives, we conceived that the same strain-building chemistry could be useful for preparing strained cyclic structures intended to ring-open.

For instance, these synthetic strategies could be used to add to the strained cyclic scaffolds available for ring-opening metathesis polymerization (ROMP). The large majority of monomers for ROMP are based on a small number of strained cyclic scaffolds such norbornenes, cyclobutenes, cyclopropenes, and cyclooctenes. Thus, while the functionalities on polymers prepared with ROMP vary widely, the backbone structures are limited. Polymers with more unusual backbones have been obtained via ROMP by using larger, unstrained macrocycles. These systems tend to suffer from lower efficiency, however, due to a lack of driving force from the release of ring strain.[202] Because of this trade-off, strained cyclic monomers with unique structures which can undergo ROMP are desirable targets.

Secondly, CPPs have drastically different properties than their linear counterparts due to strain. If CPPs could be embedded in a material and then opened in response to some stimulus, there should be a notable change in the material's properties. With this goal in mind, we conceptualized that placing a mechanochemically active unit in the backbone of a CPP as a "weak link" would allow the entire macrocyclic unit to open with

applied mechanical force. Using this type of structure in a polymer backbone could effect changes in bulk material properties.

## 4.2 Results and Discussion for ROMP of Stilbene Macrocycles

Despite the value of strained macrocycles for ROMP, there are few efficient synthetic routes to obtain macrocyclic monomers with enough ring strain to drive ring-opening polymerization. We therefore sought to take advantage of the scalable methods developed in our lab for the synthesis of CPPs to prepare strained macrocyclic monomers that could undergo ROMP and add diversity to the polymer structures that can be accessed through this method. We designed a synthetic route to *cis*-stilbene-based macrocycle **IV.3** employing oxidative bisboronate homocoupling—a simple, scalable, and efficient strain-building reaction.[183] (Scheme 4.1). This novel cyclic scaffold has a calculated ring strain of 28.9 kcal/mol (calculated by homodesmotic reactions[3]), on par with norbornene.[203]
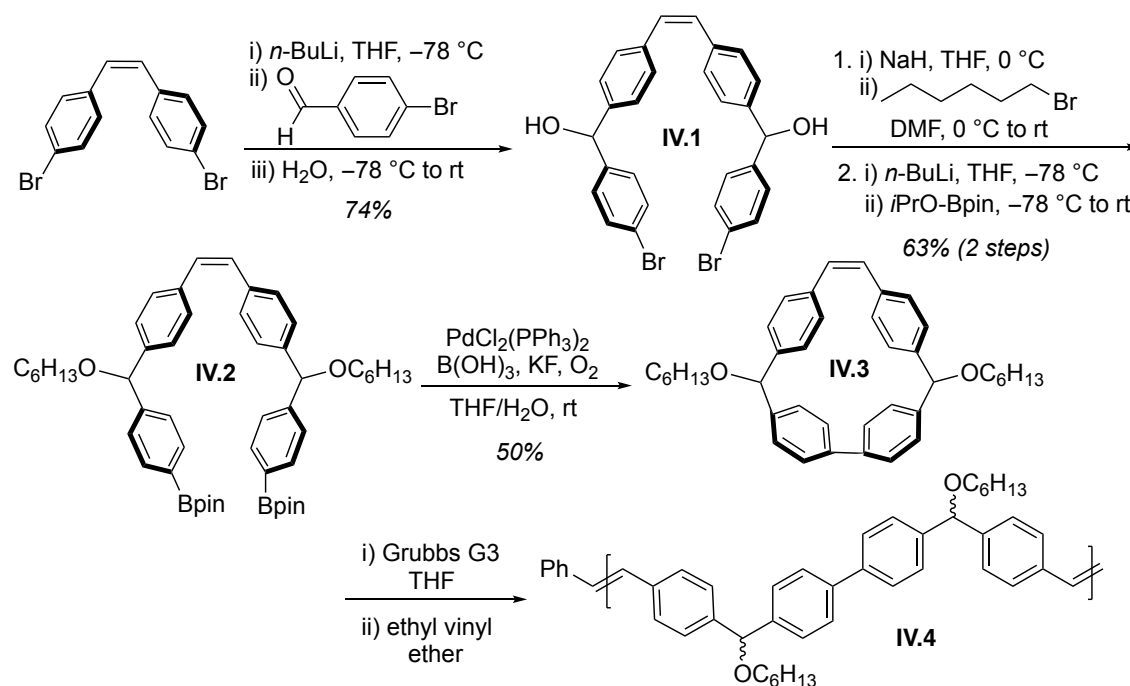


**Scheme 4.1.** Synthesis and ROMP of a *cis*-stilbene-based macrocyclic monomer.

To prepare this strained macrocycle, we first constructed curved diol intermediate **IV.1** by double lithiation of 4,4'-dibromostilbene and subsequent nucleophilic addition to 4-bromobenzaldehyde. Deprotonation of the free alcohols with sodium hydride and treatment with 1-bromohexane yielded the dihexyl derivative. Lithium-halogen exchange followed by treatment with 2-isopropoxy-4,4,5,5-tetramethyl-1,3,2-dioxaborolane yielded bisboronate **IV.2**. Finally, **IV.2** was subjected to mild Pd-catalyzed oxidative homocoupling conditions to yield final macrocyclic monomer **IV.3** on a multigram scale. This key cyclization step, which is run open to air, yielded 50%, with the remaining mass balance primarily attributed to oligomeric byproducts. In principle, other sized macrocycles could form as well, but we did not observe these products to any appreciable extent.

Upon subjection to ROMP conditions, macrocycle **IV.3** was successfully polymerized. Molecular weight scaled linearly with conversion to polymer, as expected for a controlled, chain growth polymerization (Fig. 4.1). We did observe chain transfer, evidenced by increasing dispersity values as the polymerization proceeded. When two samples of distinct molecular weight were combined and subjected to bromopyridyl Grubbs G3, the molecular weight equilibrated to an intermediate value, further confirming chain transfer. Despite the occurrence of chain transfer, this polymerization is quite well-controlled compared to step-growth methods which are still the only available method to prepare many types of polymers.

We hypothesized that increasing steric bulk around the alkene in this scaffold could decrease the prevalence of the secondary metathesis reactions involved in chain transfer. Toward this end, we designed monomers **IV.5** and **IV.6**, with one and two proximal methyl groups, respectively (Fig. 4.2). The synthetic sequence for these derivatives followed closely from the synthesis of **IV.3**, with mono- and di-methylated dibromostilbenes (**IV.10** and **IV.12**, Scheme 4.2) used as precursors. Phosphonium salt **IV.9** was prepared from 4-bromo-2-methyl benzoic acid (**IV.7**) according to the literature.[204,205] A Wittig reaction between **IV.9** and 4-bromobenzaldehyde yielded monomethylated dibromostilbene **IV.10**. 4-bromo-2-methyl-benzenemethanol (**IV.8**), an intermediate in the synthesis of **IV.9**, was subjected to Swern oxidation conditions to obtain 4-bromo-2-methyl benzaldehyde **IV.11**. A Wittig reaction between **IV.9** and
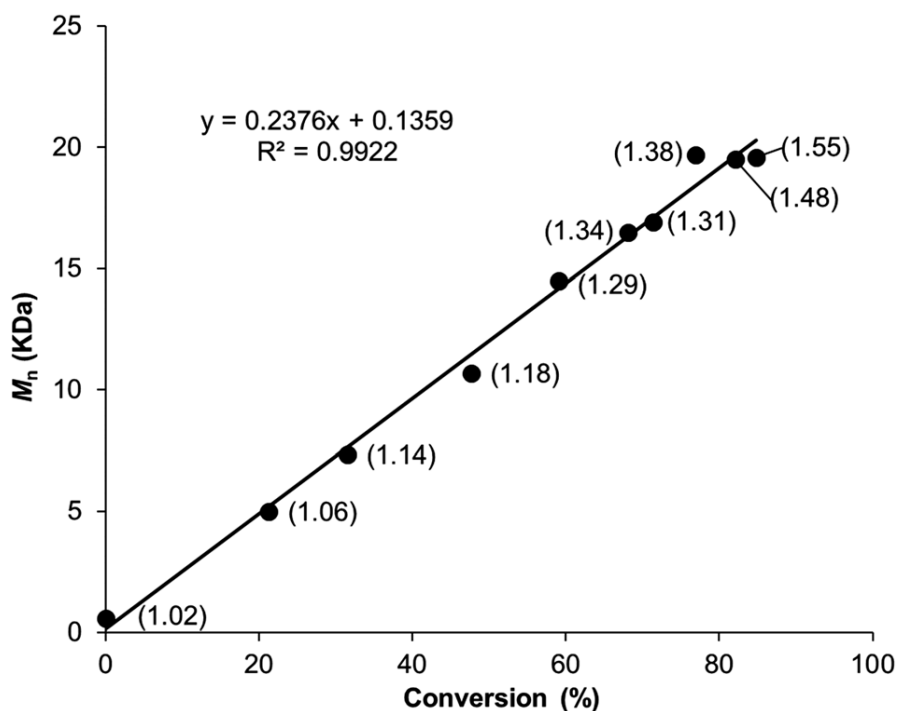
**Figure 4.1.** $M_n$ vs. conversion plot for the polymerization of **IV.4** follows a linear progression consistent with a chain growth mechanism. Dispersity (Đ) for each time point is shown in parenthesis. Reproduced from Lynde, B. E.; Maust, R. L.; Li, P.; Lee, D. C.; Jasti, R.; Boydston, A. J. *Mater. Chem. Front.* **2020**, *4*, 252-256 with permission from the Chinese Chemical Society (CCS), Institute of Chemistry of Chinese Academy of Sciences (IC), and the Royal Society of Chemistry.

**IV.11** produced dimethylated compound **IV.12**. Macrocycles **IV.5** and **IV.6** were obtained via lithiation-addition reactions with 4-bromobenzaldehyde, followed by silyl protection of the free alcohols, borylation, and finally macrocyclization via oxidative homocoupling. When these compounds were subjected to ROMP conditions, however, no polymerization was observed. Even at elevated temperatures (55-60 °C), only oligomer (DP ~5) was formed, indicating that even one methyl substituent close to the alkene prevents the desired primary metathesis reaction from occurring efficiently. (Notably, the TES substituents are not the reason for the unsuccessful polymerizations— unmethylated stilbene-based macrocycles with TES substituents were polymerized previously. However, the substituents do play a role. Macromonomers based on the same structure with poly(L-lactide) substituents were also unable to be polymerized via ROMP.)
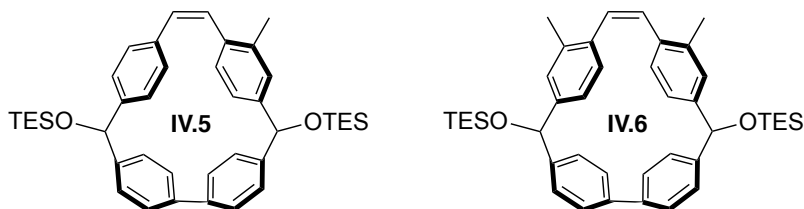
**Figure 4.2.** Mono- and di-methylated stilbene-based macrocycles.
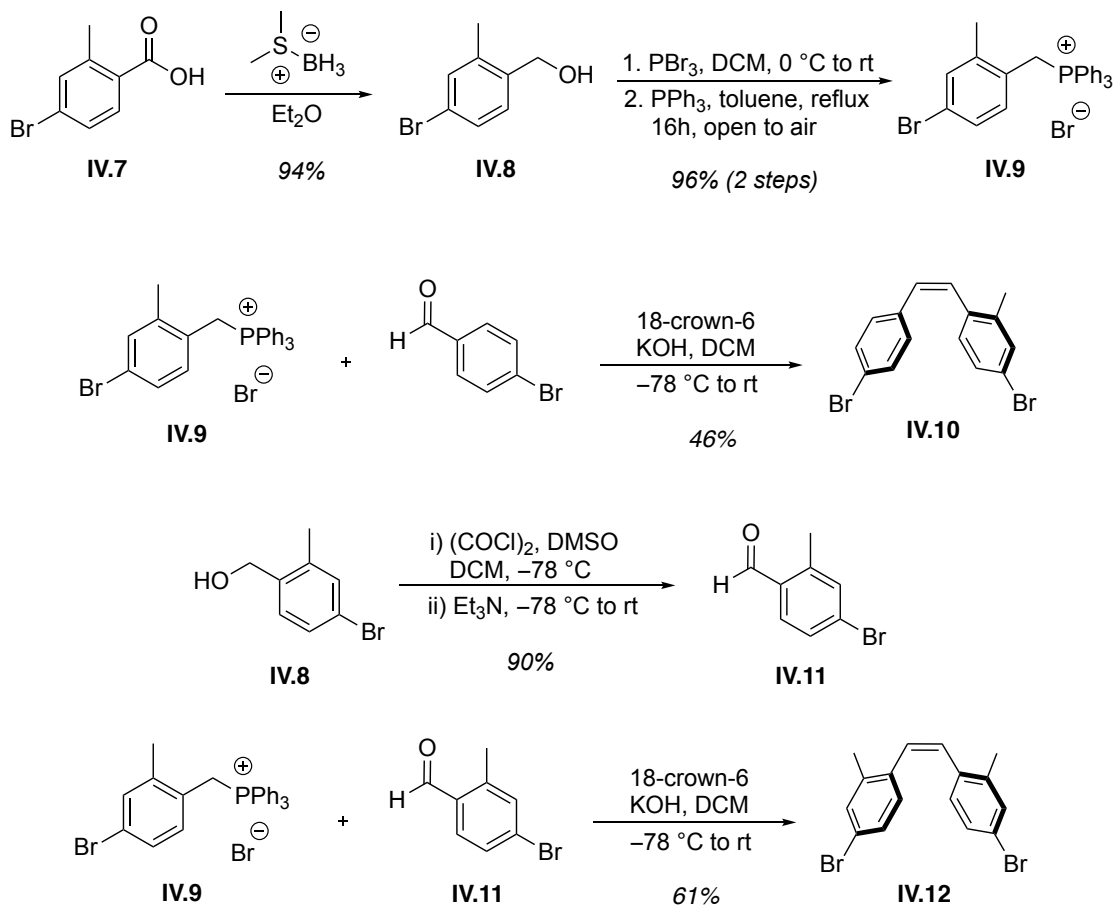


**Scheme 4.2.** Synthesis of dibromostilbenes **IV.10** and **IV.12** as precursors for mono- and di-methylated stilbene-based macrocycles.

Strain-building chemistry can be employed to access macrocyclic scaffolds useful for ROMP. This approach gives rise to unique polymer backbones through chain-growth polymerization. The polymers synthesized this way bear some resemblance to the high-performance polymer PEEK (polyether ether ketone), which can currently only be made by step-growth polymerization (Fig. 4.3). We have identified limitations in the substituents which can be placed on these cyclic monomers in order for them to undergo

polymerization, but other modifications to this scaffold could produce sequence-controlled polymers which were previously synthetically inaccessible.
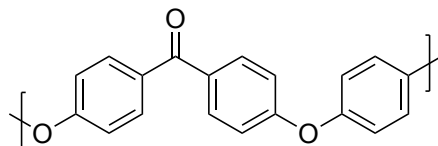


**Figure 4.3.** Structure of poly(ether ether ketone), also known as PEEK, a high-performance polymer.

## 4.3 Results and Discussion for Cyclobutane CPP Mechanophores

Responsive polymers are an attractive area of research. As discussed in previous chapters, the ability to design and precisely synthesize interesting monomers vastly expands the types of polymer structures which can be accessed. Recently numerous groups have employed cyclobutane-based mechanophores to prepare force-responsive polymers (Fig. 4.4a).[116,117,206–208] Cyclobutane is a useful motif which when ring-opened can enable conjugation extension, mechanochromism, and release of "stored" length in the polymer backbone, among other applications.[208] In conjunction with the Xia group we conceived of CPP-like monomers with a cyclobutane unit in the CPP backbone. We envisioned that these macrocyclic structures could be polymerized, then converted to linear paraphenylene segments under mechanical force such as grinding, sonication, or stretching. Such a transformation from cyclic to linear repeat units would be expected to produce changes in the optical and physical properties of the material. CPPs and linear paraphenylenes with the same number of phenylene rings fluoresce distinctly[119,209] and also have dissimilar intermolecular interactions leading to different solubility and packing patterns.

We targeted two macrocycle sizes with an embedded cyclobutane unit (Fig. 4.5). The synthesis of macrocycles **IV.14** and **IV.15** was achieved in a straightforward manner using cyclobutane-containing dibromide **IV.13** and bisboronate intermediates common to other CPP syntheses. Following the macrocyclization reactions between **IV.13** and bisboronate coupling partners of varying sizes, the resulting compounds were subjected

to ten-mediated reductive aromatization conditions to yield [7+1cb]CPP **IV.14** and [9+1cb]CPP **IV.15**.
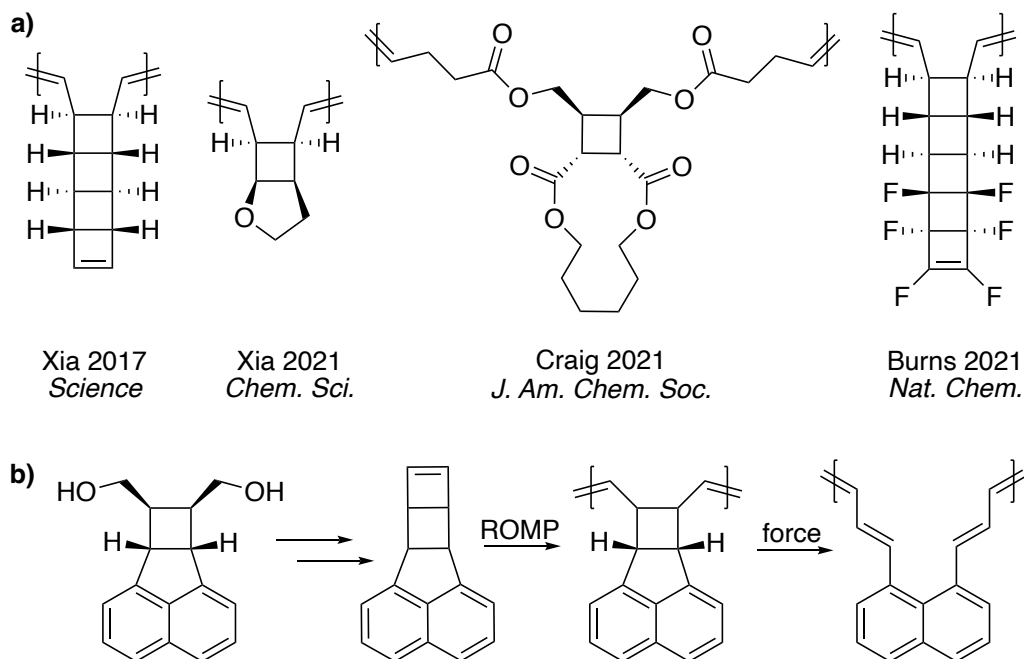


**Figure 4.4.** a) Representative examples of cyclobutane-based mechanophore units which have been incorporated in polymers. b) Steps to obtain a conjugated, ring-opened polymer from a cyclobutane diol precursor, as described in reference 211.
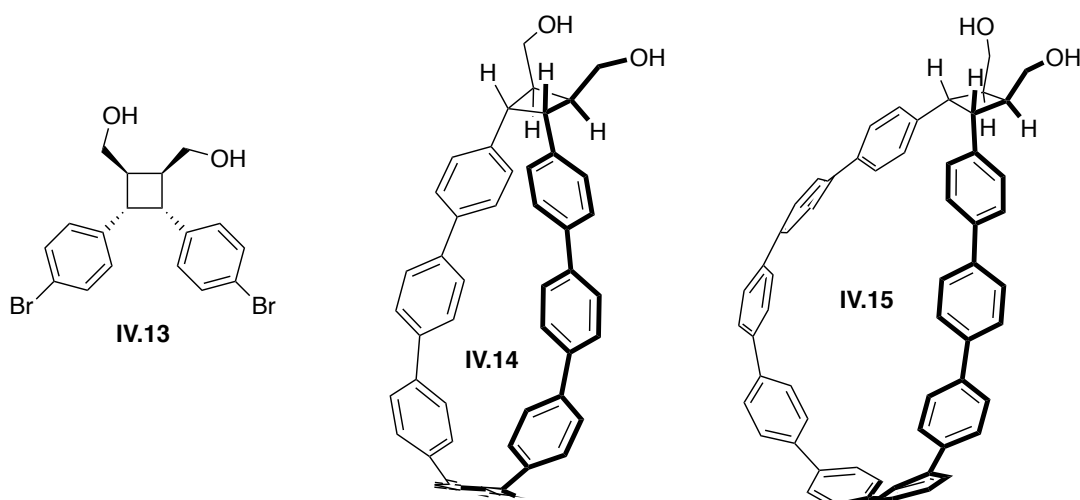


**Figure 4.5.** Two sizes of mechanophore macrocycles were prepared in a modular manner using coupling partner **IV.13** and common CPP intermediates.

112

Due to the small amount of material initially made, the first mechanochemical experiments focused on polymers with one [9+1cb]CPP unit at the middle of the polymer chain, the location where most mechanical force is concentrated.[210] These chain-centered polymers were prepared by first converting the free alcohols on **IV.15** to 2-bromoisobutyrate functionalities. These groups were then used to initiate the atom transfer radical polymerization (ATRP) of methyl acrylate, extending the structure out in two directions (Scheme 4.3). Polymer **IV.17** was sonicated for 1 hour, and the optical properties were compared before and after sonication to assess the effectiveness of mechanochemical activation. The fluorescence emission maximum of [9+1cb]CPP **IV.15** (and derivative polymer **IV.17**) falls between the emission maxima of [9]CPP (494 cm) and [10]CPP (466 nm),[119] at 481 nm. After sonication, new peaks appeared in the emission spectrum from 375-425 nm, consistent with some degree of linearization of the paraphenylene segments.[209] A slight change was also observed in the absorbance of the polymer after sonication.
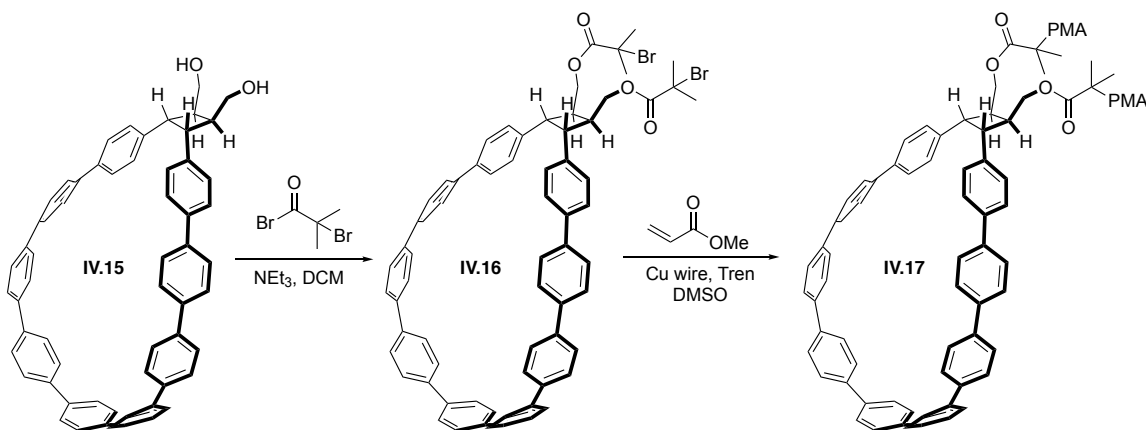


**Scheme 4.3.** Steps to convert [9+1cb]CPP **IV.15** to chain-centered polymer **IV.17**. PMA = poly(methyl acrylate).

Our initial results suggest that this strategy is a viable way to produce a measurable change in polymer properties due to mechanical force. We will continue to explore this promising area, including conducting the same type of preliminary experiment with macrocycle **IV.14** and eventually making polymers fully composed of

macrocyclic mechanophore units, following a similar strategy to that shown in Figure 4.4b, to enable more drastic changes in the material.

## 4.4 Conclusions and Outlook

Not only do strained macrocycles have fascinating properties in their own right, they can also serve as scaffolds for making otherwise inaccessible linear structures through ring-opening. Efficient, scalable, and modular synthetic pathways to strained macrocycles are of utmost importance for this purpose. Using chemistry developed for the synthesis of CPPs, we have established two new classes of strained macrocyclic monomers which open into linear structures either during the polymerization process or in response to mechanical force. Like with CPPs, these macrocyclic monomers lend themselves to precise functionalization, which may lead to as-yet unexplored materials with different properties. Similarly, the controlled polymerization methods used so far to make polymers from these monomers will enable the synthesis of more complex polymeric materials with properties dependent on their composition and sequence.

## 4.5 Experimental Section
### 4.5.1 General Experimental

Deuterated solvents were purchased from Cambridge Isotopes. Anhydrous tetrahydrofuran (THF), 1,4-dioxane, dimethylformamide (DMF), and pyridine were obtained from a solvent purification system. All other reagents were obtained from commercial sources and used as received. Moisture- and oxygen-sensitive reactions during monomer synthesis were carried out in flame-dried glassware and under an inert atmosphere of purified nitrogen using syringe/septa technique. Thin Layer Chromatography (TLC) was performed using Sorbent Technologies Silica Gel XHT TLC plates. Developed plates were visualized using UV light at wavelengths of 254 and 365 nm. Silica column chromatography was conducted with Zeochem Zeoprep 60 Eco 40-63 µm silica gel. Automated flash chromatography was performed using a Biotage Isolera One. $^1$H and $^{13}$C NMR spectroscopy was performed on a 300, 500, or 600 MHz Bruker NMR spectrometer. Spectra taken in CDCl$_3$ are reported in parts per million (ppm) referenced to TMS ($\delta$ 0.00 ppm) for $^1$H NMR and residual CHCl$_3$ ($\delta$ 77.16 ppm) for $^{13}$C

NMR. Spectra taken in THF-$d_8$ are reported in parts per million (ppm) referenced to residual protio-solvent ($^1$H: 3.58, 1.72).

MALDI-TOF/MS was performed using a Bruker Daltonics AutoFlex II MALDI-TOF Mass spectrometer. The polymer matrix used was 1,8,9-anthracenetriol in THF, and data was obtained in linear (positive) mode.

Gel permeation chromatography (GPC) was performed using an Agilent Technologies Infinity Series II pump, 3 in line columns (MZ Gel), Wyatt Technology light scattering and refractive index detectors with tetrahydrofuran (THF) as the mobile phase with an flow rate of 1 mL/min. Number average molecular weights ($M_n$) and weight-average molecular weights ($M_w$) were calculated from light scattering and refractive index data using Astra software from Wyatt Technology The absolute weight-average molecular weights were determined by a dn/dc value which was measured by assuming 100% mass recovery of the polymers after passing the columns.

### 4.5.2 Detailed Synthetic Procedures for Stilbene Macrocycles

*Cis*-4,4'-dibromostilbene,[211] **IV.9**[204,205] and pyridyl Grubbs G3 and bromopyridyl Grubbs G3 initiators[179] were synthesized using previously reported procedures.

*(Z)-(ethene-1,2-diylbis(4,1-phenylene))bis((4-bromophenyl)methanol)* **IV.1**.
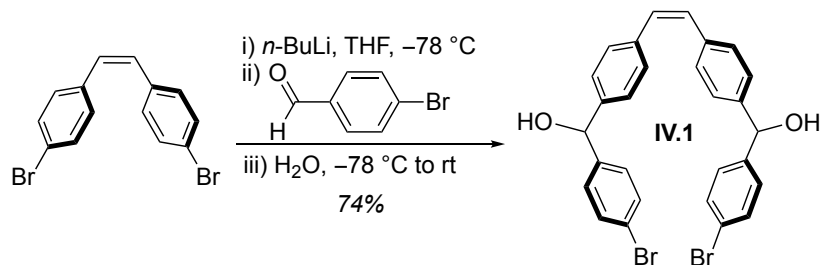


4,4'-dibromostilbene (12.0 g, 35.5 mmol, 1.00 equiv.) and THF (200 mL) were added to a 500 mL round bottom flask with a magnetic stir bar. The solution was cooled to -78 °C, then *n*-butyllithium (31.6 mL, 2.3 M in hexane, 2.05 equiv.) was added over the course of 20 min. After stirring at -78 °C for 3 min, 4-bromobenzaldehyde (13.1 g, 71.0 mmol, 2.00 equiv.) in THF (40 mL) was added in stream via cannula, during which the solution gradually became viscous with solid crashed out. The cold bath was removed, and the mixture was kept stirring at room temperature for 2 hours. The reaction mixture was

quenched with water (20 mL). The THF was removed under reduced pressure, then DCM (200 mL) was added to the mixture, which was washed with water (100 mL) and brine (100 mL) and dried over $Na_2SO_4$. Concentration under reduced pressure resulted in a yellow gel. The material was dissolved in DCM (80 mL) and stored in the freezer (-20 °C) overnight, resulting in powdered precipitate. The precipitate was collected by filtration and washed with DCM (10 mL) to give the product as a white powder (7.55 g). The filtrate was concentrated, and the residue was purified by column chromatography (silica, 0% to 3% ethyl acetate in DCM) to yield more product (6.58 g). Overall, the product was obtained in a yield of 74%. $^1H$ NMR (600 MHz, $CDCl_3$): δ 7.46 (d, $J = 8.4$ Hz, 4H, Ar-H), 7.25 (d, $J = 8.4$ Hz, 4H, Ar-H), 7.22 (d, $J = 8.4$ Hz, 4H, Ar-H), 7.19 (d, $J = 8.4$ Hz, 4H, Ar-H), 6.55 (s, 2H, C=C-H), 5.76 (d, $J = 3.4$ Hz, 2H, CH), 2.18 (d, $J = 3.4$ Hz, 2H, OH); $^{13}C$ NMR (150 MHz, $CDCl_3$): δ 142.74, 142.34, 136.90, 131.73, 130.11, 129.25, 128.34, 126.59, 121.63, 75.62. IR (neat): 3264.5, 1484.0, 1404.3, 1172.5, 1067.9, 1027.3, 1008.0, 819.5, 799.7 cm$^{-1}$. HRMS (TOF MS ASAP+) (m/z): [M+H]$^+$ calculated for $C_{28}H_{23}Br_2O_2$: 549.0065; found 549.0039.

*(Z)-1,2-bis(4-((4-bromophenyl)(n-hexyloxy)methyl)phenyl)ethene **IV.18**.*
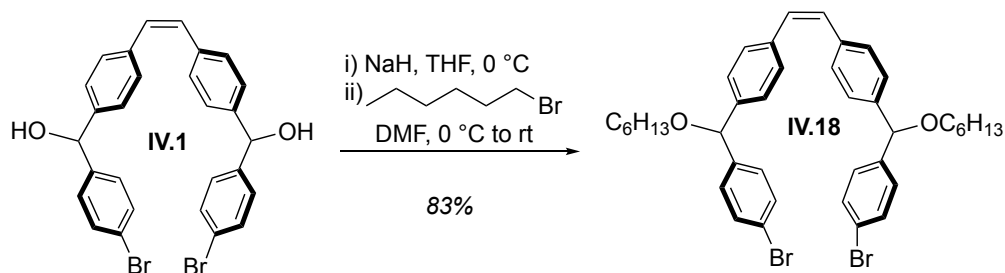


NaH (4.10 g, 60 wt% in mineral oil, 102.5 mmol, 4.00 equiv.) and THF (150 mL) were added to a 500 mL round bottom flask. The slurry was cooled to 0 °C at which point **IV.1** (14.1 g, 25.6 mmol, 1.00 equiv.) in THF (30 mL) was added in stream. The mixture was stirred at 0 °C for 1 hour. Then 1-bromohexane (28.8 mL, 205 mmol, 8.00 equiv.) and DMF (30 mL) were added and the reaction was stirred at room temperature overnight. The reaction was carefully quenched with water. After THF was removed under vacuum, DCM (150 mL) was added. The solution was washed with water (100 mL), 5 wt% aqueous LiCl solution (3×100 mL), and brine (100 mL) and dried over $Na_2SO_4$. After concentration under reduced pressure, the crude solid was purified via column

chromatography (silica, 0% to 8% ethyl acetate in hexanes) to yield a colorless oil (15.0 g, 83%). $^1$H NMR (600 MHz, CDCl$_3$): δ 7.44 (d, $J$ = 8.4 Hz, 4H, Ar-H), 7.22 (d, $J$ = 8.4 Hz, 4H, Ar-H), 7.20 (d, $J$ = 8.1 Hz, 4H, Ar-H), 7.15 (d, $J$ = 8.1 Hz, 4H, Ar-H), 6.52 (s, 2H, C=C-H), 5.24 (s, 2H, CH), 3.42 (td, $J$ = 6.6, 3.1 Hz, 4H, OCH$_2$), 1.62 (dt, $J$ = 15.0, 6.6 Hz, 4H, CH$_2$), 1.37 (p, $J$ = 7.0 Hz, 4H, CH$_2$), 1.33-1.22 (overlap, 8H, CH$_2$), 0.88 (t, $J$ = 7.0 Hz, 6H, CH$_3$); $^{13}$C NMR (150 MHz, CDCl$_3$): δ 141.75, 141.14, 136.61, 131.58, 130.01, 129.03, 128.82, 126.89, 121.36, 82.87, 69.46, 31.79, 29.94, 26.04, 22.75, 14.21. IR (neat): 2927.3, 2855.3, 1484.3, 1395.0, 1088.7, 1069.8, 1009.8, 816.0, 799.2 cm$^{-1}$. HRMS (TOF MS ASAP+) (m/z): [M+H]$^+$ calculated for C$_{40}$H$_{47}$Br$_2$O$_2$: 717.1943; found 717.1893.

*(Z)-1,2-bis(4-((n-hexyloxy)(4-(4,4,5,5-tetramethyl-1,3,2-dioxaborolan-2-yl)phenyl)-methyl)phenyl)ethene **IV.2**.*
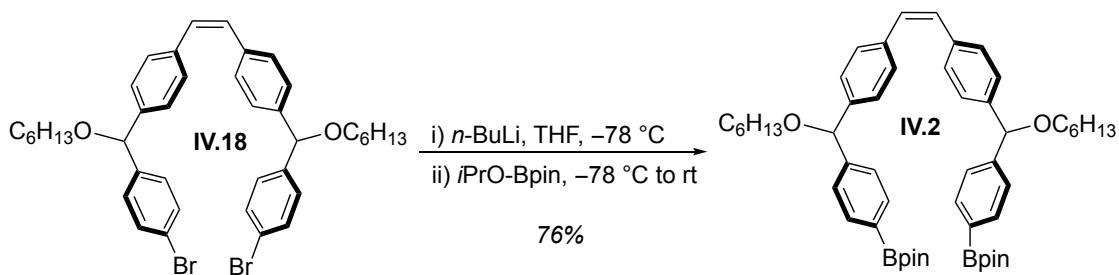


**IV.18** (14.7 g, 20.5 mmol, 1.00 equiv.) was dissolved in THF and cooled to -78 °C. Then *n*-butyllithium (21.5 mL, 2.3 M in hexane, 2.40 equiv.) was added slowly via syringe. Isopropyl pinacol borate (16.7 mL, 81.8 mmol, 4.00 equiv.) was quickly added in stream. The mixture was stirred at -78 °C for 5 min. and allowed to warm to room temperature. After 2 hours, the reaction was carefully quenched with water. The mixture was extracted with dichloromethane (3x), and the combined organic layers were washed with brine and dried over Na$_2$SO$_4$. The material was purified by column chromatography (silica, 0% to 8% ethyl acetate in hexanes), yielding a colorless oil (12.4 g, 76%). $^1$H NMR (600 MHz, CDCl$_3$): δ 7.77 (d, $J$ = 8.0 Hz, 4H, Ar-H), 7.36 (d, $J$ = 8.0 Hz, 4H, Ar-H), 7.22 – 7.13 (m, 8H, Ar-H), 6.48 (s, 2H, C=C-H), 5.29 (s, 2H, CH), 3.42 (t, $J$ = 6.7 Hz, 4H, OCH$_2$), 1.63 (dt, $J$ = 15.0, 6.7 Hz, 4H, CH$_2$), 1.42 – 1.20 (overlapping, 36H, CH$_2$ and CH$_3$), 0.88 (t, $J$ = 6.9 Hz, 6H, CH$_3$); $^{13}$C NMR (150 MHz, CDCl$_3$): δ 145.76, 141.52, 136.38, 135.01, 129.91, 128.92, 126.94, 126.48, 83.86, 83.53, 69.43, 31.82, 29.97, 26.05, 25.01, 22.76,

14.22, $^{13}$C-B signal not observed. IR (neat): 2929.0, 2856.5, 1610.9, 1511.2, 1397.2, 1357.4, 1319.2, 1270.6, 1142.6, 1085.9, 1019.6, 961.8, 858.2, 824.7, 798.9, 656.7 cm$^{-1}$. HRMS (TOF MS ASAP+) (m/z): [M+H]$^+$ calculated for $C_{52}H_{71}B_2O_6$: 813.5437; found 813.5327.

*(Z)-3,8-bis(n-hexyloxy)-1,2,4,7(1,4)-tetrabenzenacyclooctanophan-5-ene IV.3.*
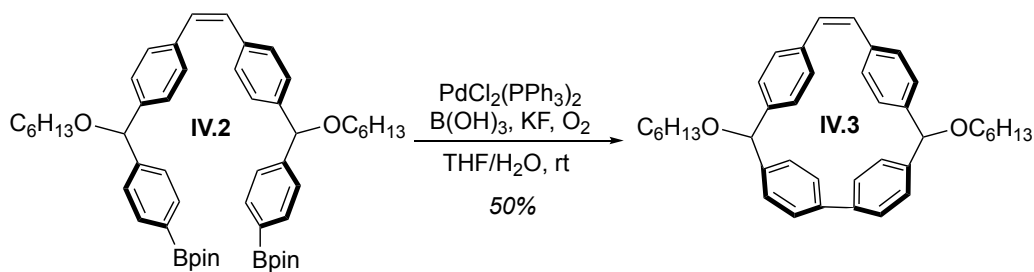


Bisboronate **IV.2** (3.00 g, 3.76 mmol, 1.00 equiv.), PdCl$_2$(PPh$_3$)$_2$ (0.26 g, 0.38 mmol, 0.10 equiv.), and B(OH)$_3$ (1.16 g, 18.8 mmol, 5.00 equiv.) were dissolved in THF (450 mL) in a 500 mL round bottom flask equipped with a stir bar. The mixture was stirred open to air at room temperature for 10 min. until a clear yellow solution was achieved. Then KF (0.44 g, 7.52 mmol, 2.00 equiv.) was dissolved in water (45 mL) and added. The mixture was sonicated until orange color appeared, after which it was stirred overnight at room temperature. After THF was removed under vacuum, DCM was added. The solution was washed with water and brine and dried over Na$_2$SO$_4$. The material was purified by column chromatography (silica, 0% to 50% DCM in hexanes), yielding a colorless oil which solidified upon standing (1.05 g, 50%). $^1$H NMR (600 MHz, CDCl$_3$): δ *trans* 7.45 (dd, $J$ = 8.5, 2.0 Hz, 2H, Ar-H), 7.39 (dd, $J$ = 8.5, 2.0 Hz, 2H, Ar-H), 7.35 (dd, $J$ = 8.3, 2.0 Hz, 2H, Ar-H), 7.02 (dd, $J$ = 8.3, 2.0 Hz, 2H, Ar-H), 6.65 (d, $J$ = 8.3 Hz, 4H, Ar-H), 6.53 (d, $J$ = 8.3 Hz, 4H, Ar-H), 6.46 (s, 2H, C=C-H), 5.28 (s, 2H, CH), 3.77 (dt, $J$ = 9.0, 6.7 Hz, 2H, OCH$_2$), 3.61 (dt, $J$ = 9.0, 6.7 Hz, 2H, OCH$_2$), 1.78-1.69 (m, 4H, CH$_2$), 1.50 – 1.41 (m, 4H, CH$_2$), 1.37 – 1.26 (overlapping, 8H, CH$_2$), 0.90 (t, $J$ = 6.9 Hz, 6H, CH$_3$); *cis* 7.46 (dd, $J$ = 8.5, 2.0 Hz, 2H, Ar-H), 7.39 (dd, $J$ = 8.5, 2.0 Hz, 2H, Ar-H), 7.34 (dd, $J$ = 8.3, 2.0 Hz, 2H, Ar-H), 7.03 (dd, $J$ = 8.3, 2.0 Hz, 2H, Ar-H), 6.65 (d, $J$ = 8.3 Hz, 4H, Ar-H), 6.53 (d, $J$ = 8.3 Hz, 4H, Ar-H), 6.46 (s, 2H, C=C-H), 5.27 (s, 2H, CH), 3.77 (dt, $J$ = 9.0, 6.7 Hz, 2H, OCH$_2$), 3.61(dt, $J$ = 9.0, 6.7 Hz, 2H, OCH$_2$), 1.78-1.69 (m, 4H, CH$_2$), 1.50 – 1.41 (m, 4H, CH$_2$), 1.37 – 1.26 (overlapping, 8H, CH$_2$), 0.90 (t, $J$ = 6.9

Hz, 6H, CH$_3$); $^{13}$C NMR (150 MHz, CDCl$_3$): δ *trans* 144.48, 142.46, 140.92, 135.90, 130.71, 128.30, 128.03, 127.94, 127.36, 126.43, 125.87, 82.65, 69.59, 31.88, 30.06, 26.15, 22.81, 14.23; *cis* 144.50, 142.51, 140.96, 135.87, 130.70, 128.28, 127.91, 127.14, 126.58, 125.78, 82.60, 69.56, 31.89, 30.06, 25.15, 22.81, 14.24. IR (neat): 2950.6, 2925.6, 2851.0, 1450.0, 1414.2, 1332.9, 1186.3, 1094.1, 1015.2, 836.8, 805.2, 751.0, 735.1, 705.9 cm$^{-1}$. HRMS (TOF MS ASAP+) (m/z): [M+H]$^+$ calculated for C$_{40}$H$_{47}$O$_2$: 559.3576; found 559.3565.

Cis-*4,4'-dibromo-2-methylstilbene* **IV.10**.
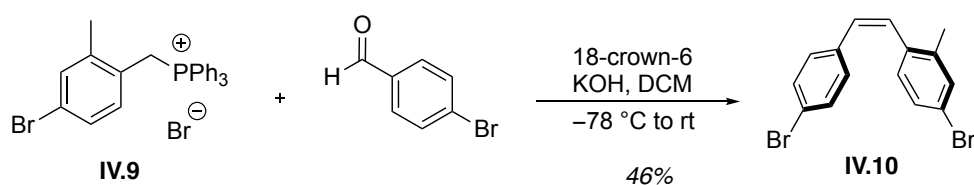


((4-Bromo-2-methylphenyl)methyl)triphenylphosphonium bromide (**IV.9**, 24.39 g, 46.3 mmol, 1.05 equiv.), 4-bromobenzaldehyde (8.17 g, 44.1 mmol, 1.00 equiv.), and 18-crown-6 (1.17 g, 4.4 mmol, 0.10 equiv.) were dissolved in DCM (165 mL) and cooled to -78 °C under nitrogen. Freshly ground potassium hydroxide (6.44 g, 114.8 mmol, 2.60 equiv.) was added, and the reaction was stirred for 1.5 hr at -78 °C, then overnight at room temperature. The solids were filtered from the reaction mixture and the filtrate was concentrated under reduced pressure. The material was loaded on a silica gel column and eluted with generous volumes of hexanes. The *cis*-stilbene eluted slightly before the *trans*. 7.1 g of pure *cis* product was obtained (46%) as well as an additional 6.5 g of a *cis*/*trans* mixture. $^1$H NMR (500 MHz, CDCl$_3$): δ 7.35 (s, 1H), 7.29 (dd, *J* = 8.5, 2.1 Hz, 2H), 7.17 (d, *J* = 8.0 Hz, 1H), 6.95 (overlapping dt, *J* = 8.4, 2.6 Hz, 3H), 6.56 (d, *J* = 2.1 Hz, 2H), 2.23 (d, *J* = 2.0 Hz, 3H).

*Methyl dibromide diol **IV.19**.*
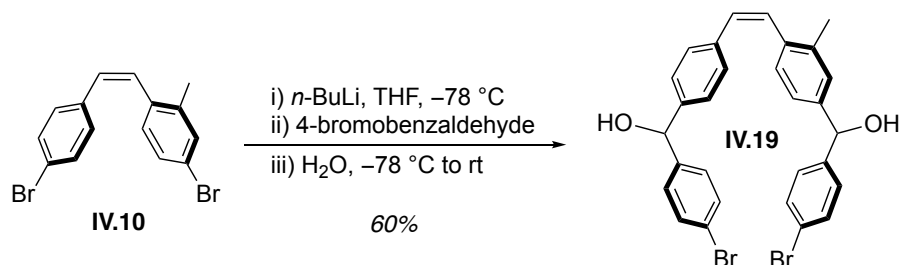


A flame-dried flask was charged with dibromide **IV.10** (7.10 g, 20.2 mmol, 1.00 equiv.), which was dissolved in THF (90 mL) and then cooled to -78 °C for 20 minutes. *n*-BuLi (16.5 mL, 41.3 mmol, 2.05 equiv.) was added dropwise. The reaction was stirred at -78 °C for 20 minutes, after which a solution of 4-bromobenzaldehyde (7.65 g, 41.3 mmol, 2.05 equiv.) in THF (10 mL) was added dropwise. *Reaction may need to be warmed during 4-bromobenzaldehye addition to allow continuous stirring.* The reaction was warmed to 0 °C and stirred for 1 hour. The reaction was then quenched with water and warmed to room temperature. The THF was removed under reduced pressure, and the resulting solution was extracted with ethyl acetate (3x). The combined organic layers were washed with water (3x) and brine (1x), then dried over sodium sulfate and concentrated under reduced pressure. The product was purified by automated silica gel column chromatography (0-7% ethyl acetate in hexanes) to yield 6.85 g (60%). ^{1}H NMR (500 MHz, CDCl$_3$): δ 7.45 (dd, *J* = 10.9, 8.0 Hz, 4H), 7.24 – 6.98 (overlapping, 11H), 6.58 (dd, *J* = 14.2, 1.8 Hz, 2H), 5.74 (dd, *J* = 16.2, 3.4 Hz, 2H), 2.23 (s, 3H), 2.15 (dd, *J* = 20.6, 3.5 Hz, 2H).

*Methyl dibromide **IV.20**.*
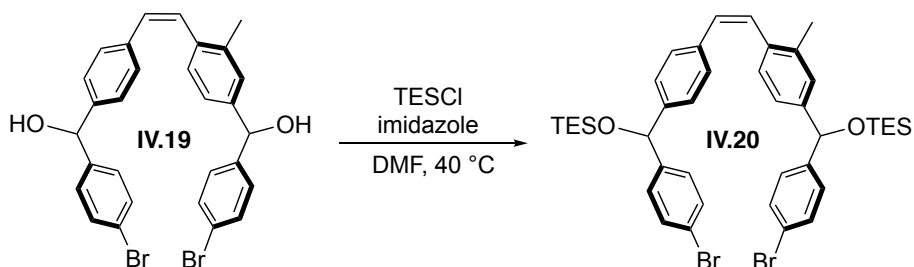


Diol **IV.19** (6.8 g, 12.0 mmol, 1.00 equiv.) and imidazole (3.3 g, 48.2 mmol, 4.00 equiv.) were added to a flame-dried flask under nitrogen. To this was added dry DMF (30 mL). This was stirred until all solids were in solution. TESCl (6.1 mL, 36.1 mmol, 3.00 equiv.)

was then added dropwise to the stirring solution. This solution was heated at 40 °C for 90 minutes then cooled to room temperature. Saturated aqueous sodium bicarbonate was added to the crude reaction, which was then extracted with ethyl acetate (3x). The combined organic layers were washed with 5% aqueous LiCl (3x), water (2x), and finally brine (1x), then dried over sodium sulfate and concentrated under reduced pressure. By ^{1}H NMR, the reaction proceeded cleanly, producing only silanol as a byproduct, so the crude product was carried on to the next reaction. ^{1}H NMR (500 MHz, CDCl$_3$): δ 7.40 (tt, $J$ = 10.2, 1.5 Hz, 4H), 7.24 (dd, $J$ = 8.7, 1.9 Hz, 2H), 7.19 (dd, $J$ = 8.3, 1.9 Hz, 2H), 7.10 (s, 1H), 7.07-7.01 (m, 3H), 7.01 – 6.96 (m, 3H), 6.55 (dd, $J$ = 17.2, 4.6 Hz, 2H), 5.62 (d, $J$ = 17.7 Hz, 2H), 2.19 (d, $J$ = 1.7 Hz, 3H), 0.91 – 0.82 (m, 18H), 0.58 – 0.49 (m, 12H).

*Methyl bisboronate **IV.21**.*
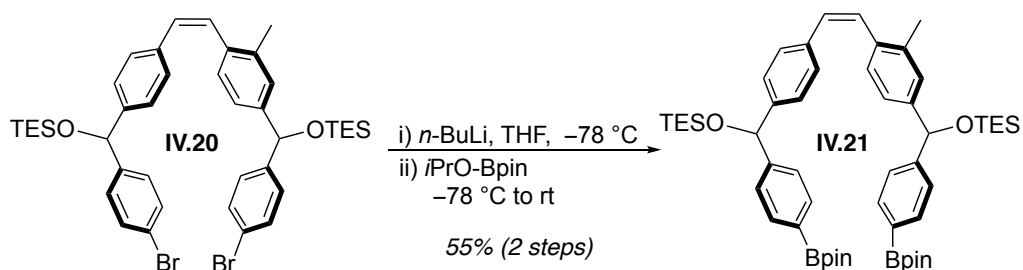


A flame-dried flask was charged with crude dibromide **IV.20** (theoretical 9.55 g, 12.0 mmol, 1.00 equiv.), which was dissolved in THF (120 mL) and then cooled to -78 °C for 20 minutes. *n*-butyllithium (12.5 mL, 31.2 mmol, 2.60 equiv.) was added dropwise. Upon complete *n*-BuLi addition, isopropoxy pinacolborane (9.8 mL, 48.0 mmol, 4.00 equiv.) was added quickly in stream. The reaction was stirred at -78 °C for 5 minutes then allowed to warm to room temperature and stirred 1 hour. The crude reaction was quenched with water. THF was removed under reduced pressure, then the resulting solution was extracted with DCM (3x). The combined organic layers were washed with water (2x) and brine (1x), then dried over sodium sulfate and concentrated under reduced pressure. The crude solid was washed with hexanes and the product was collected by vacuum filtration, yielding 5.88 g (55% over 2 steps). ^{1}H NMR (500 MHz, CDCl$_3$): δ 7.73 (dd, $J$ = 13.9, 7.5 Hz, 4H), 7.38 (d, $J$ = 7.6 Hz, 2H), 7.33 (d, $J$ = 7.6 Hz, 2H), 7.12 – 7.05 (m, 3H), 7.02 (s, 2H), 6.98 (d, $J$ = 7.8 Hz, 2H), 6.52 (dd, $J$ = 16.6, 4.1 Hz, 2H), 5.68

(d, $J$ = 18.6 Hz, 2H), 2.17 (s, 3H), 1.32 (d, $J$ = 4.0 Hz, 24H), 0.86 (dt, $J$ = 16.2, 7.9 Hz, 18H), 0.54 (dq, $J$ = 16.3, 8.0 Hz, 12H).

*Singly methylated stilbene macrocycle **IV.5***.
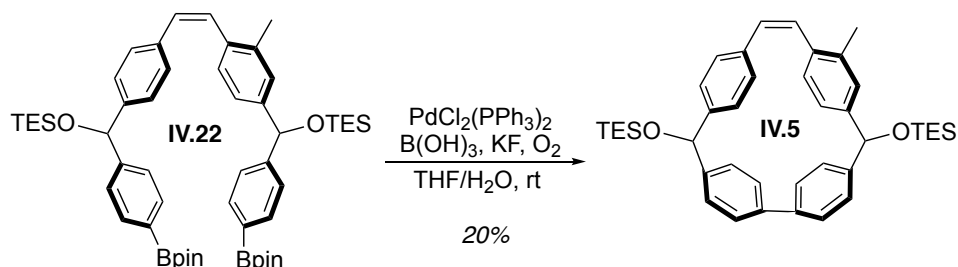


Diboronic ester **IV.22** (3.00 g, 3.4 mmol, 1.00 equiv.) was added to a flask with bis(triphenylphosphine)palladium(II) dichloride (237 mg, 0.3 mmol, 0.10 equiv.) and boric acid (1.05 g, 16.9 mmol, 5.00 equiv.). The solids were dissolved in THF (560 mL) and the mixture was stirred open to air for 10 minutes. Potassium fluoride (393 mg, 6.8 mmol, 2.00 equiv.) was dissolved in water (56 mL) and added to the reaction mixture. The reaction mixture was stirred at room temperature overnight. The THF was removed under reduced pressure and the resulting solution was extracted with DCM (3x). The combined organic layers were washed with water (3x) and brine (1x), then dried over sodium sulfate and concentrated under reduced pressure. The product was isolated by automated silica gel column chromatography (15% DCM in hexanes) as a mixture of *cis* and *trans* isomers. 0.42 g product was obtained (20%). [^1]H NMR (500 MHz, CDCl₃): δ 7.51 – 6.87 (overlapping, 9H), 6.56 – 6.21 (overlapping, 8H), 5.70 – 5.59 (d and m, 2H), 2.19, 2.03 (two s, 3H), 1.03 – 0.78 (m, 18H), 0.73 – 0.51 (m, 12H).

*4-bromo-2-methyl-benzaldehyde **IV.11***.
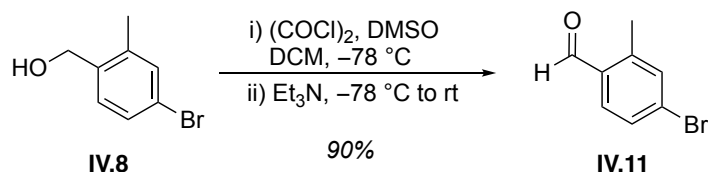


A solution of oxalyl chloride (26.7 mL, 0.31 mol, 5.00 equiv.) and 3 Å molecular sieves in DCM (60 mL) was cooled to -78 °C under nitrogen. A solution of DMSO (44.6 mL, 0.62 mol, 10.00 equiv.) in DCM (60 mL) was added slowly to the reaction flask. After 15

min. a solution of 4-bromo-2-methyl-benzenemethanol (**IV.8**, 12.5 g, 62.2 mmol, 1.00 equiv.) in DCM (190 mL) was added slowly. The reaction was stirred for 1 hr., then triethylamine (130 mL, 0.93 mol, 15.00 equiv.) was added. The reaction was stirred for 30 min. at -78 °C, then warmed to room temperature. The reaction was quenched with water, and the mixture was extracted with DCM (3x). The combined organic layers were washed with water (2x) and brine (1x), then dried over sodium sulfate and concentrated under reduced pressure. The material was purified by silica gel column chromatography (0-4% ethyl acetate in hexanes), yielding 11.13 g (90%). $^1$H NMR (500 MHz, CDCl$_3$): δ 10.22 (s, 1H), 7.66 (d, $J$ = 8.2 Hz, 1H), 7.51 (d, $J$ = 8.3 Hz, 1H), 7.45 (s, 1H), 2.65 (s, 3H).

Cis-*4,4'-dibromo-2,2'-dimethylstilbene* **IV.12**.
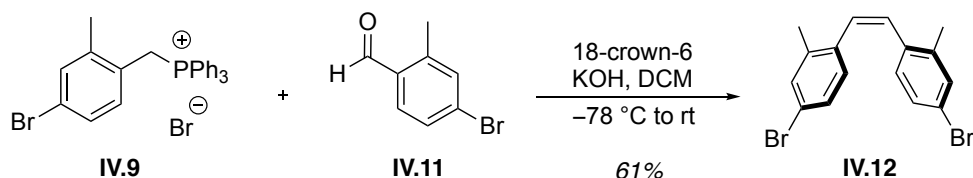


((4-Bromo-2-methylphenyl)methyl)triphenylphosphonium bromide (**IV.9**, 30.90 g, 58.7 mmol, 1.05 equiv.), aldehyde **IV.11** (11.13 g, 55.9 mmol, 1.00 equiv.), and 18-crown-6 (1.48 g, 5.6 mmol, 0.10 equiv.) were dissolved in DCM (200 mL) and cooled to -78 °C under nitrogen. Freshly ground potassium hydroxide (8.16 g, 145.4 mmol, 2.60 equiv.) was added, and the reaction was stirred for 1.5 hr at -78 °C, then overnight at room temperature. The solids were filtered from the reaction mixture and the filtrate was concentrated under reduced pressure. The material was washed through a silica plug with generous volumes of hexanes and concentrated. Washing with ethanol removed all impurities except some of the *trans*-stilbene. Pure *cis*-stilbene was obtained with some difficulty by recrystallization from ethanol. Total product obtained was 3.32 g *cis*-stilbene (16%) and 9.79 g with a 95:5 *cis/trans* ratio (45%). $^1$H NMR (500 MHz, CDCl$_3$): δ 7.30 (s, 2H), 7.06 (d, $J$ = 8.3 Hz, 2H), 6.75 (dd, $J$ = 8.2, 1.5 Hz, 2H), 6.64 (t, $J$ = 1.2 Hz, 2H), 2.24 (s, 6H).

*Dimethyl dibromide diol **IV.23**.*
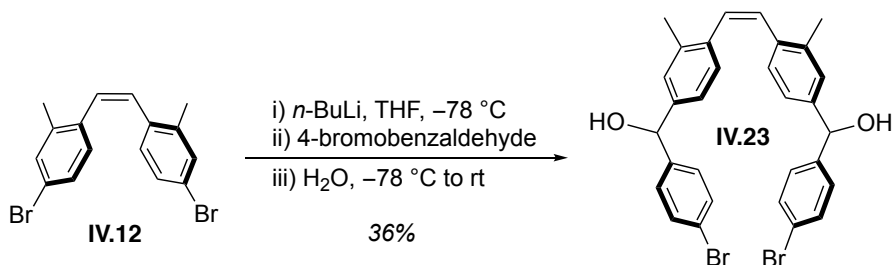


A flame-dried flask was charged with dibromide **IV.12** (9.75 g, 26.6 mmol, 1.00 equiv.), which was dissolved in THF (133 mL) and then cooled to -78 °C for 20 minutes. *n*-butyllithium (28.0 mL, 54.6 mmol, 2.05 equiv.) was added dropwise. The reaction was stirred at -78 °C for 20 minutes, after which a solution of 4-bromobenzaldehyde (9.85 g, 53.3 mmol, 2.00 equiv.) in THF was added dropwise. *Reaction may need to be warmed during 4-bromobenzaldehye addition to allow continuous stirring.* The reaction was moved to an ice bath and stirred for 1 hour. The reaction was quenched with water, warmed to room temperature, and the THF was removed under reduced pressure. The resulting material was extracted with ethyl acetate (3x), and the combined organic layers were washed with water (3x) and brine (1x), then dried over sodium sulfate and concentrated. The material was purified by silica gel column chromatography (0-5% ethyl acetate in DCM). 5.52 g (36%) product was isolated. $^1$H NMR (500 MHz, CDCl$_3$): δ 7.45 (d, $J$ = 8.4 Hz, 4H), 7.23 (d, $J$ = 8.4 Hz, 4H), 7.11 (s, 2H), 6.91 – 6.86 (m, 4H), 6.66 (s, 2H), 5.70 (d, $J$ = 3.4 Hz, 2H), 2.25 (s, 6H), 2.13 (d, $J$ = 3.4 Hz, 2H).

*Dimethyl dibromide **IV.24**.*
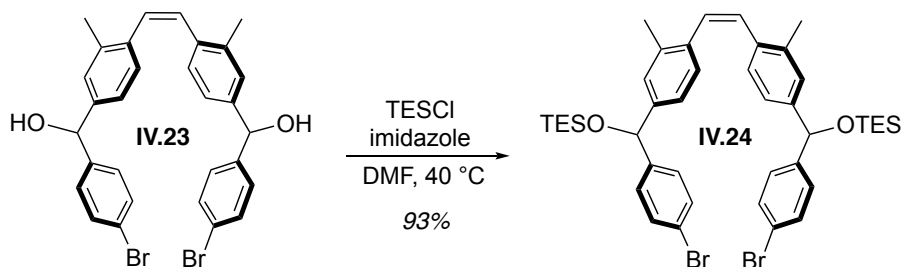


Diol **IV.23** (1.20 g, 2.1 mmol, 1.00 equiv.) and imidazole (0.57 g, 8.3 mmol, 4.00 equiv.) were added to a flame-dried flask under nitrogen. To this was added dry DMF (5.2 mL). This was stirred until all solids were in solution. TESCl (1.04 mL, 6.2 mmol, 3.00 equiv.) was then added dropwise to the stirring solution. This solution was heated at 40 °C for 90

minutes then cooled to room temperature. Saturated aqueous sodium bicarbonate was added to the crude reaction, which was then extracted with ethyl acetate (3x). The combined organic layers were washed with 5% aqueous LiCl (3x), water (2x), and finally brine (1x), then dried over sodium sulfate and concentrated under reduced pressure. The material was purified by automated silica gel column chromatography (1-3% ethyl acetate in hexanes), yielding 1.55 g (93%). $^1$H NMR (500 MHz, CDCl$_3$): δ 7.39 (d, $J$ = 8.6 Hz, 4H), 7.20 (d, $J$ = 8.1 Hz, 4H), 7.04 (s, 2H), 6.85 – 6.79 (m, 4H), 6.63 (s, 2H), 5.58 (s, 2H), 2.21 (s, 6H), 2.04 (s, 2H), 0.85 (t, $J$ = 8.0 Hz, 18H), 0.53 (q, $J$ = 7.9 Hz, 12H).

*Dimethyl bisboronate **IV.25**.*
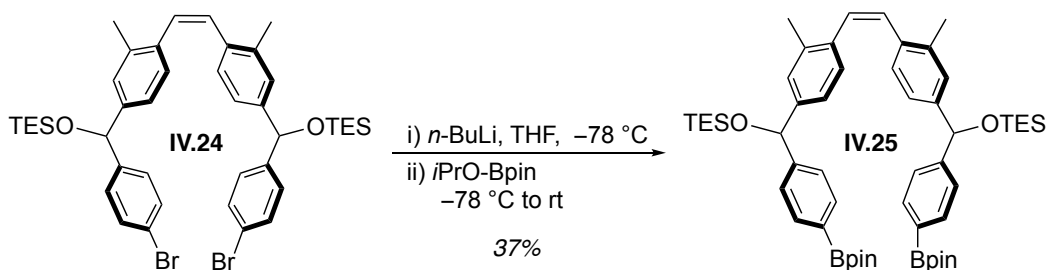


A flame-dried flask was charged with dibromide **IV.24** (1.55 g, 1.9 mmol, 1.00 equiv.), which was dissolved in THF (20 mL) and then cooled to -78 °C for 20 minutes. *n*-butyllithium (2.56 mL, 5.0 mmol, 2.60 equiv.) was added dropwise. Upon complete *n*-BuLi addition, isopropoxy pinacolborane (1.6 mL, 7.7 mmol, 4.00 equiv.) was added quickly in stream. The reaction was stirred at -78 °C for 5 minutes then allowed to warm to room temperature and stirred 2 hr. The reaction was quenched with water. THF was removed under reduced pressure, then the resulting solution was extracted with DCM (3x). The combined organic layers were washed with water (2x) and brine (1x), then dried over sodium sulfate and concentrated under reduced pressure. The crude solid was sonicated with hexanes and the product was collected by vacuum filtration. Additional product was obtained by concentrating the filtrate and repeating the filtration and washing process, yielding a total of 0.64 g (37%). $^1$H NMR (500 MHz, CDCl$_3$): δ 7.72 (dd, $J$ = 8.0, 1.6 Hz, 4H), 7.34 (dd, $J$ = 8.2, 1.8 Hz, 4H), 7.05 (s, 2H), 6.87 (d, $J$ = 7.8 Hz, 2H), 6.81 (d, $J$ = 8.1 Hz, 2H), 6.60 (s, 2H), 5.65 (s, 2H), 2.18 (s, 6H), 1.32 (s, 24H), 0.86 (td, $J$ = 7.9, 1.8 Hz, 18H), 0.53 (qd, $J$ = 7.9, 1.8 Hz, 12H).

*Dimethyl stilbene macrocycle **IV.6**.*
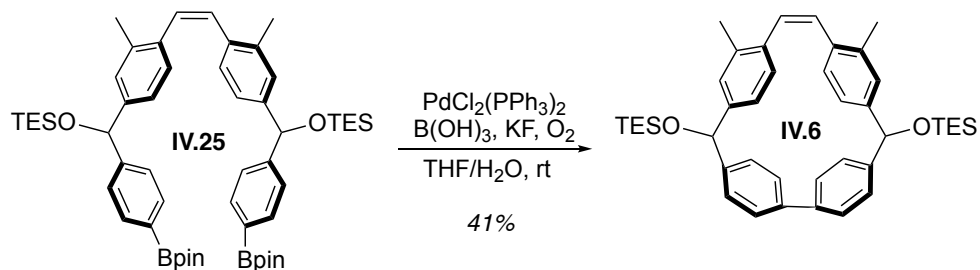


Diboronic ester **IV.25** (78.0 mg, 0.09 mmol, 1.00 equiv.) was added to a flask with

bis(triphenylphosphine)palladium(II) dichloride (6.1 mg, 0.01 mmol, 0.10 equiv.) and

boric acid (26.8 mg, 0.43 mmol, 5.00 equiv.). The solids were dissolved in THF (14.5

mL) and the mixture was stirred open to air for 10 minutes. Potassium fluoride (10.1 mg,

0.17 mmol, 2.00 equiv.) was dissolved in water (1.5 mL) and added to the reaction

mixture. The reaction mixture was stirred at room temperature overnight. The THF was

removed under reduced pressure and the resulting solution was extracted with DCM (3x).

The combined organic layers were washed with water (3x) and brine (1x), then dried over

sodium sulfate and concentrated under reduced pressure. The product was isolated by

automated silica gel column chromatography (0-30% DCM in hexanes), yielding 23 mg

(41%). $^1$H NMR (500 MHz, CDCl$_3$): δ (ppm) 7.49 – 7.21 (m, 6H), 6.97 (dd, $J$ = 30.1, 8.3

Hz, 2H), 6.86 (d, $J$ = 3.3 Hz, 2H), 6.45 (s, 2H), 6.36 (dd, $J$ = 8.1, 2.2 Hz, 2H), 6.01 (t, $J$ =

6.2 Hz, 2H), 5.59 (d, $J$ = 2.9 Hz, 2H), 2.01 (s, 6H), 0.99 (td, $J$ = 8.0, 2.6 Hz, 18H), 0.69

(qd, $J$ = 7.9, 3.9 Hz, 12H).

## 4.5.3 Synthesis and Characterization of Stilbene-Based Polymers

We investigated the polymerization of **IV.3** using the third generation Grubbs

catalysts in tetrahydrofuran-$d_8$ ([**IV.4**]$_0$ = 1 M) with an initial monomer to initiator ratio

of 100:1 (Table 4.1, entries 1 and 2). With each initiator, conversion reached 99% within

12 hrs. at 60 °C, as determined by $^1$H NMR spectroscopy. From these experiments, we

found that the molecular weight distribution of **IV.4** was monomodal with a $M_w$ = 107

kDa and Đ of 1.7, based upon SEC analysis using multi-angle laser light scattering and

refractive index detection. The dn/dc of **IV.4** was found to be 0.246 (mL/g). The structure

of **IV.4** was confirmed by $^1$H NMR spectroscopy and matrix-assisted laser desorption

ionization time of flight mass spectrometry (MALDI-TOF/MS). In the $^1$H NMR spectrum of **IV.4**, only a single vinylic signal at $\delta$ = 7.24 ppm was observed, while no other vinylic signals were present above the detection limit (Fig. 4.6). This observation is consistent with the backbone being primarily *trans*-stilbene isomers. MALDI-TOF/MS then was used to better understand the structural speciation within samples of **IV.4**. The repeat unit for **IV.4** has an experimental mass of 558.9 amu (Fig. 4.8), which is consistent with the predicted molecular weight of **IV.3**. Notably, we did not see evidence of cyclic polymer structures from any of the analyses.

| | [M]:[I] | Conc. (M.) | Temp. (°C) | Conv. (%) | $M_{n, theo}$ (kg/mol) | $M_n$ (kg/mol) | $M_w$ (kg/mol) | Đ |
|---|---|---|---|---|---|---|---|---|
| 1[a] | 100:1 | 1 | 60 | >99 | 55.9 | 62.1 | 107.0 | 1.7 |
| 2[b] | 100:1 | 1 | 60 | 99 | 55.9 | 55.4 | 102.2 | 1.7 |
| 3[a] | 75:1 | 0.1 | 40 | >99 | 42.4 | 53.4 | 79.7 | 1.5 |
| 4[a,c] | 35:1 | 1 | 20 | 45 | 8.6 | 8.0 | 8.7 | 1.1 |
| 5[a,c] | 35:1 | 1 | 30 | >99 | 20.1 | 18.3 | 27.8 | 1.5 |
| 6[a,c] | 35:1 | 1 | 40 | >99 | 18.4 | 23.9 | 36.0 | 1.5 |

**Table 4.1**. Summary of ROMP experiments with **IV.3**. [a]Initiator = pyridyl Grubbs G3. [b]Initiator = bromopyridyl Grubbs G3. [c]Average of 3 experiments.

*Molecular weight vs. conversion*

In a dry box, **IV.3** (0.4965 g, 0.89 mmol) was charged into a flame-dried and nitrogen-purged 25 mL 3-neck flask with 7.9 mL of anhydrous THF and sealed, before being removed from the glovebox and being placed in a 34 °C oil bath. An oven-dried 7 mL vial was charged with bromopyridyl Grubbs G3 (0.0228 g, 0.026 mmol) and 1 mL of anhydrous THF before being sealed and removed from the glovebox. The solution of bromopyridyl Grubbs G3 was added to the 3-neck flask, followed by the immediate removal of a 0.2 mL aliquot of the reaction mixture which was quenched with 1 mL ethyl vinyl ether. The sample was split into 2 equal portions. GPC data was gathered on one portion and conversion was determined with the remaining.

*Polymer-polymer molecular weight equilibrium*

In a dry box, 71.5 kDa **IV.4** (0.0788 g, 0.0011 mmol) and 15.2 kDa poly(1) (0.0167 g, 0.0011 mmol) were charged into a 2-dram vial followed by 0.512 mL of

anhydrous THF. Bromopyridyl Grubbs G3 (0.00973 g, 0.0011 mmol) was added, and the vial was removed from the dry box and placed into 40 °C oil bath. After 3.5 hours, the reaction was quenched with ethyl vinyl ether and diluted with THF before obtaining a crude GPC.

*Polymer-*trans*-stilbene molecular weight equilibrium*

In a dry box, 41.5 kDa **IV.4** (0.0748 g, 0.0018 mmol) was added to a 7 mL vial, followed by bromopyridyl Grubbs G3 (0.0012 g, 0.002 mmol), trans-stilbene (0.024 g, 0.133 mmol) and 0.3 mL of anhydrous THF. The vial was placed in a 40 °C oil bath. After 3.5 hours the reaction was quenched with ethyl vinyl ether and diluted with THF before obtaining a crude GPC.
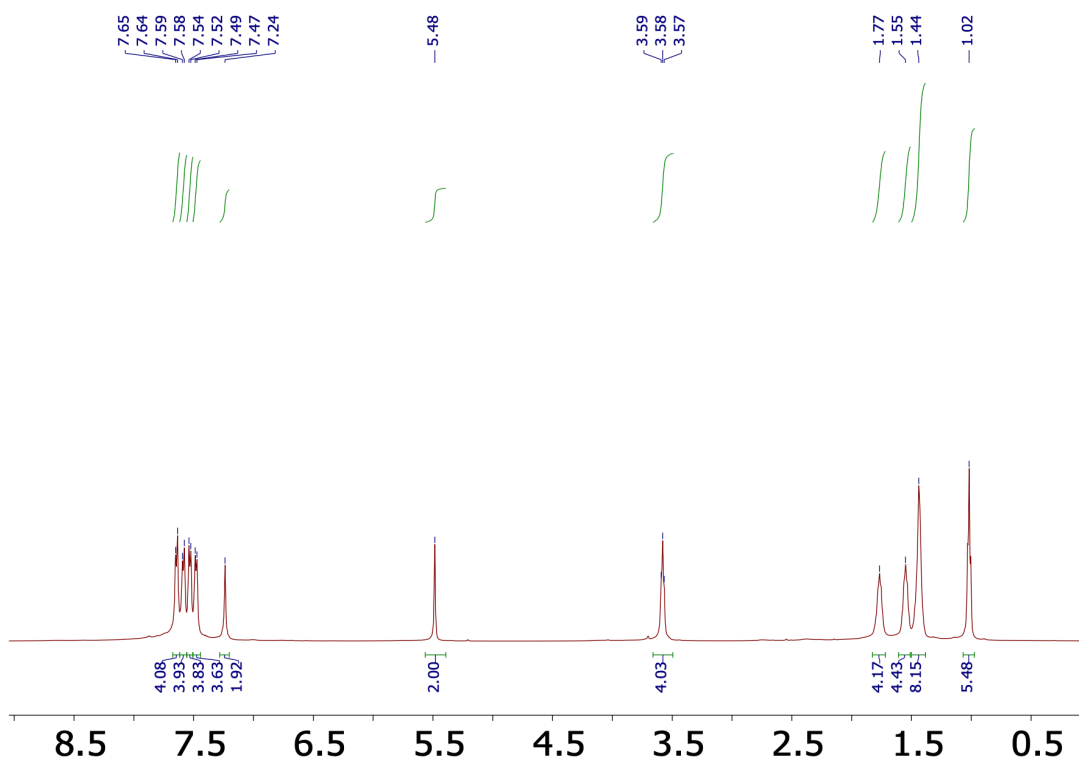


**Figure 4.6.** $^1$H NMR spectrum for **IV.4** in THF-$d_8$. Reproduced from Lynde, B. E.; Maust, R. L.; Li, P.; Lee, D. C.; Jasti, R.; Boydston, A. J. *Mater. Chem. Front.* **2020**, *4*, 252-256 with permission from the Chinese Chemical Society (CCS), Institute of Chemistry of Chinese Academy of Sciences (IC), and the Royal Society of Chemistry.
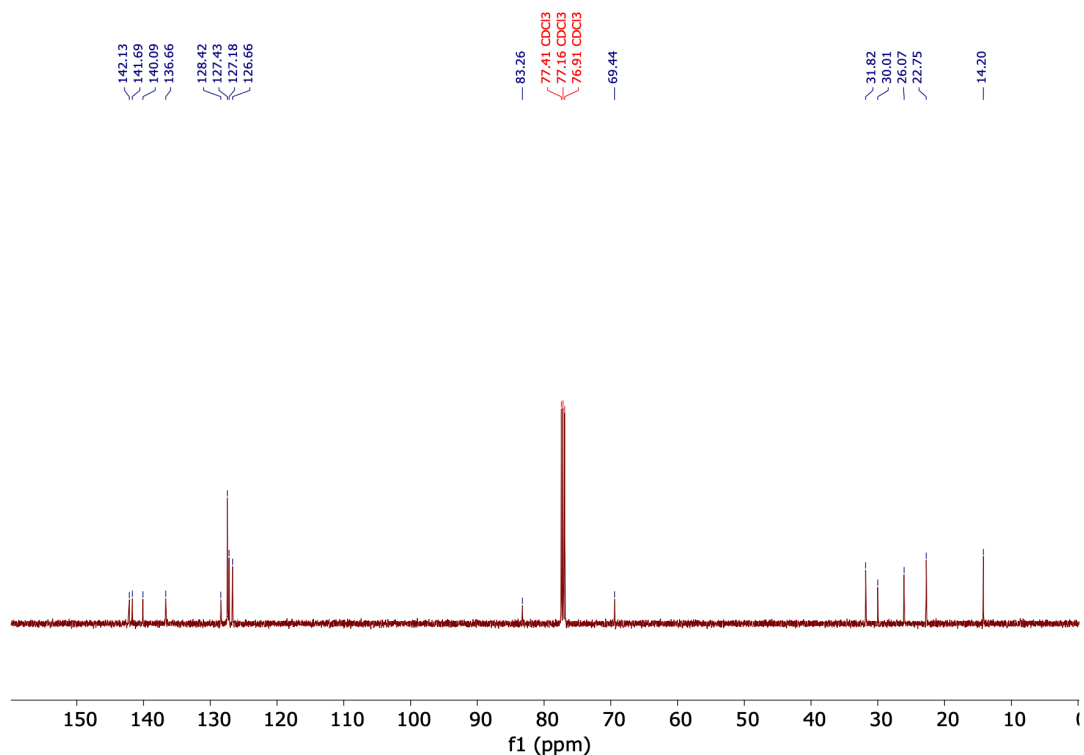
**Figure 4.7.** $^{13}$C NMR spectrum for **IV.4** in CDCl$_3$. Reproduced from Lynde, B. E.; Maust, R. L.; Li, P.; Lee, D. C.; Jasti, R.; Boydston, A. J. *Mater. Chem. Front.* **2020**, *4*, 252-256 with permission from the Chinese Chemical Society (CCS), Institute of Chemistry of Chinese Academy of Sciences (IC), and the Royal Society of Chemistry.
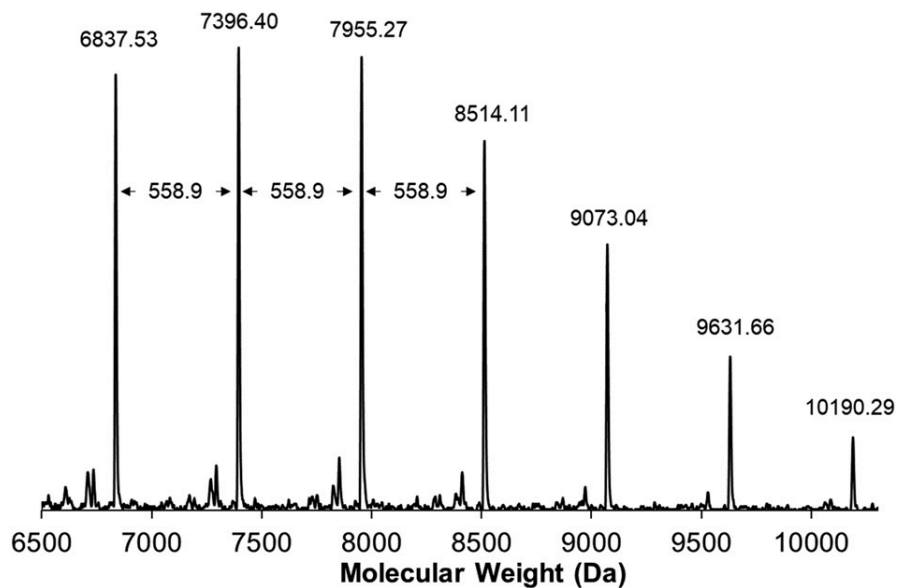


**Figure 4.8.** MALDI-TOF/MS spectrum for **IV.4**. Reproduced from Lynde, B. E.; Maust, R. L.; Li, P.; Lee, D. C.; Jasti, R.; Boydston, A. J. *Mater. Chem. Front.* **2020**, *4*, 252-256 with permission from the Chinese Chemical Society (CCS), Institute of Chemistry of Chinese Academy of Sciences (IC), and the Royal Society of Chemistry.

129

## 4.5.4 Detailed Synthetic Procedures for Cyclobutane CPPs

Bisboronate **IV.28**,[145] bromochloride **IV.30**,[138] and SPhos-Pd-G2[178] were synthesized according to the literature.

*3,4-bis(4-bromophenyl)-(1R,2S,3R,4S)-rel-1,2-cyclobutanedimethanol **IV.13**.*
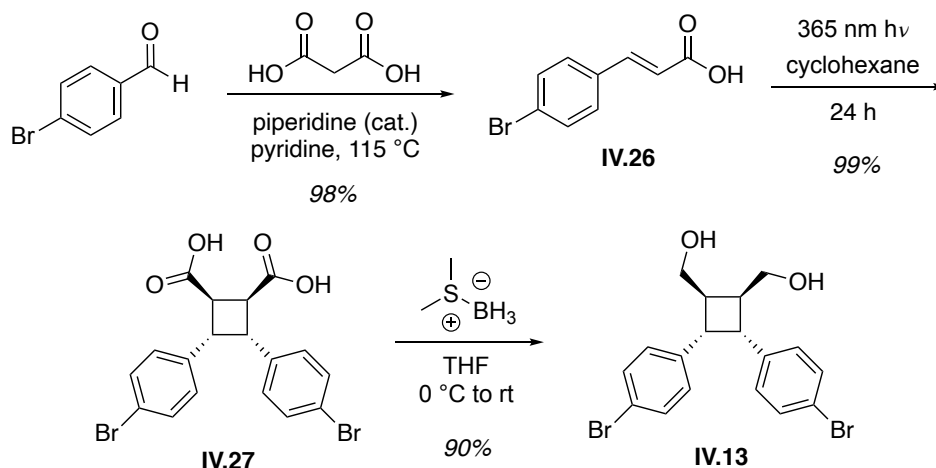


Dibromide **IV.13** was prepared from 4-bromobenzaldehyde and malonic acid over 3 steps. Procedures followed closely from literature reports.[212]

*[7+1cb] macrocycle **IV.29**.*
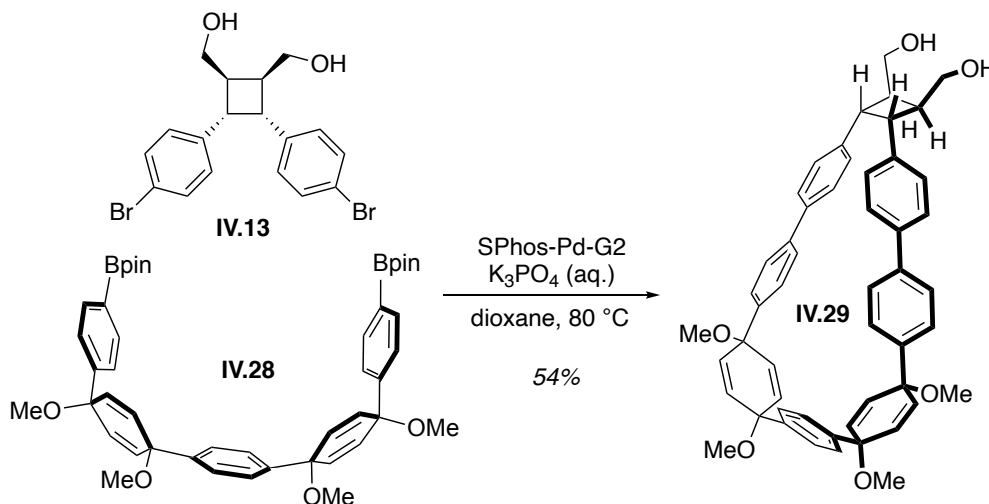


A flame-dried flask was charged with bisboronate **IV.28** (1.21 g, 1.48 mmol, 1.05 equiv.), dibromide **IV.13** (600.0 mg, 1.41 mmol, 1.00 equiv.), and Pd SPhos Gen II (101.0 mg, 0.14 mmol, 0.10 equiv.). The flask was evacuated and backfilled with nitrogen for 5 cycles. The flask was then purged with nitrogen. A 2.00 M. aqueous

solution of $K_3PO_4$ was sparged with nitrogen for 45 min. Dioxane (470 mL) was added to the reaction flask, and the solution was sparged for 15 min. before being heated to 80 °C for 20 min. 47 mL of $K_3PO_4$ solution was added, and the reaction was stirred for 30 min. at 80 °C. After the reaction was cooled to room temperature, the dioxane was removed under reduced pressure, then the resulting material was filtered through a celite pad with DCM and water. The filtrate was extracted with DCM (3x). The combined organic layers were washed with water (2x) and brine (1x), then dried over sodium sulfate and concentrated under reduced pressure. The material was purified by automated silica gel column chromatography (0-100% ethyl acetate in DCM), yielding 581 mg of a white solid (54%). *Material is poorly soluble in both DCM and ethyl acetate, and it sticks to silica, requiring copious solvent flushing to get it all off.* ^{1}H NMR (600 MHz, CDCl₃): δ 7.44 (s, 4H), 7.44 (d, $J$ = 8.4 Hz, 4H), 7.30 (d, $J$ = 8.2 Hz, 4H), 7.15 (d, $J$ = 8.2 Hz, 4H), 6.86 (d, $J$ = 8.1 Hz, 4H), 6.11 – 6.04 (m, 8H), 4.17 – 4.11 (m, 2H), 3.92 (dd, $J$ = 11.2, 3.4 Hz, 2H), 3.66 (d, $J$ = 5.6 Hz, 2H), 3.45 (s, 6H), 3.42 (s, 6H), 3.29 (m, 2H), 2.87 (s, 2H). ^{13}C NMR (151 MHz, CDCl₃) δ 143.17, 142.66, 140.83, 138.92, 138.49, 133.52, 133.47, 133.33, 133.25, 128.39, 127.22, 126.66, 126.28, 126.17, 74.59, 74.47, 62.82, 52.20, 52.04, 44.57, 38.90. IR (neat): 3376.5 (br), 3029.3, 2931.2, 2896.8, 2823.0, 1495.6, 1472.2, 1398.9, 1246.8, 1174.3, 1080.6, 1016.3, 950.7, 820.6, 767.9, 662.3 cm⁻¹.

*[7+1cb]CPP* **IV.14**.
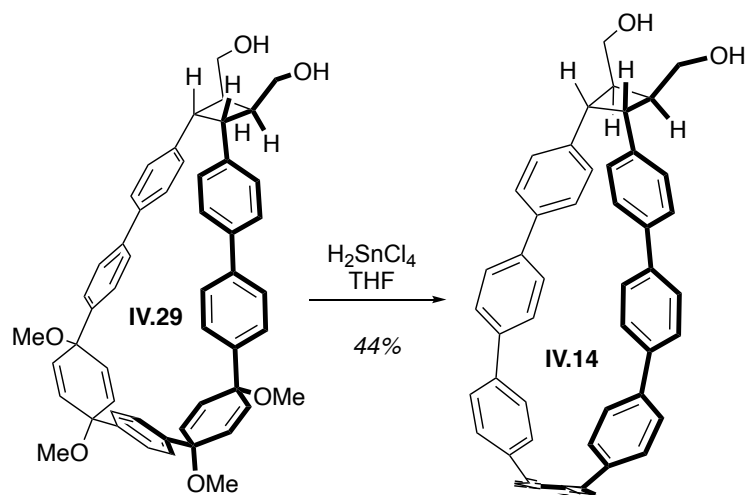


Macrocycle **IV.29** (27.0 mg, 0.04 mmol, 1.00 equiv.) was added to a flame-dried flask and rinsed down from sides with minimal THF. A 0.05 M (in THF) solution of $H_2SnCl_4$

(2.8 mL, 0.14 mmol, 4.00 equiv.) was added. The reaction was stirred at room temperature for 1.5 hrs, then quenched with saturated sodium bicarbonate solution. THF was removed under reduced pressure, and the resulting material was filtered through celite using water and DCM. The filtrate was extracted with DCM (3x), and the combined organic layers were washed with water (2x) and brine (1x) before being dried over sodium sulfate. Solvent was removed under reduced pressure. The material was purified by silica gel column chromatography (0-5% MeOH in DCM), yielding 10 mg (44%). $^{1}$H NMR (500 MHz, CDCl$_3$): δ 7.51 – 7.39 (m, 16H), 7.36 (d, $J$ = 8.4 Hz, 4H), 7.16 (d, $J$ = 8.0 Hz, 4H), 6.87 (d, $J$ = 8.1 Hz, 4H), 4.12 – 4.03 (m, 2H), 3.93 – 3.84 (m, 2H), 3.64 (d, $J$ = 5.4 Hz, 2H), 3.43 (d, $J$ = 14.2 Hz, 2H), 3.20 – 3.14 (m, 2H). $^{13}$C NMR (151 MHz, CDCl$_3$) δ 138.83, 138.73, 138.28, 138.15, 137.59, 137.45, 136.30, 128.48, 128.39, 128.30, 128.16, 128.07, 127.35, 127.26, 127.14, 127.02, 126.25, 62.70, 43.95, 40.91. IR (neat): 3299.6 (br), 2919.0, 2849.6, 1713.8, 1667.8, 1600.3, 1488.8, 1461.8, 1393.4, 1377.0, 1248.1, 1173.5, 1109.5, 1066.3, 1028.3, 1003.0, 955.1, 810.3, 727.1 cm$^{-1}$.

*1,4-benzenediboronic acid pinacol ester.*
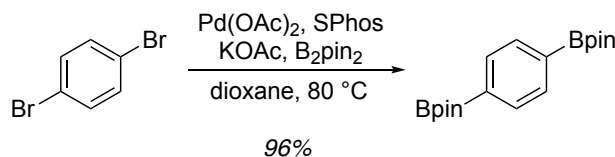


B$_2$pin$_2$ (7.11 g, 28.0 mmol, 3.00 equiv.), dibromobenzene (2.20 g, 9.30 mmol, 1.00 equiv.), Pd(OAc)$_2$ (209 mg, 0.90 mmol, 0.10 equiv.), SPhos (995 mg, 2.40 mmol, 0.26 equiv.), and oven-dried potassium acetate (5.49 g, 56.0 mmol, 6.00 equiv.) were added to a flame-dried flask, which was then evacuated and backfilled with nitrogen for 5 cycles. The flask was sealed with a septum and purged with nitrogen. Dry dioxane (50 mL) was sparged with nitrogen for 1 hr. then added to reaction flask. The reaction was heated to 80 °C, then stirred overnight. After the reaction was cooled to room temperature, the mixture was washed through a plug of celite with DCM, and the filtrate was concentrated under reduced pressure. The material was then sonicated with methanol and filtered, yielding 2.97 g (96%). Spectral data match what was previously reported in the literature.[213]

*7-ring dichloride **IV.31**.*
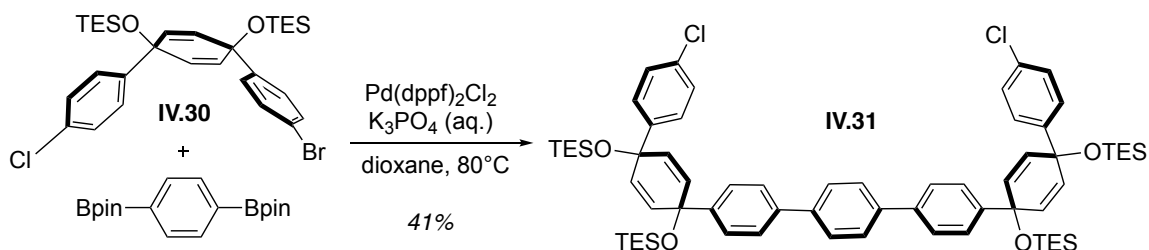


Bromochloride **IV.30** (1.88 g, 3.11 mmol, 2.05 equiv.), 1,4-benzenediboronic acid pinacol ester (0.50 g, 1.51 mmol, 1.00 equiv.) and Pd(dppf)Cl$_2$ (123.7 mg, 0.15 mmol, 0.10 equiv.) were added to a flame-dried flask equipped with a stir bar. The flask was evacuated for 5 minutes and backfilled with nitrogen for 5 cycles. Dry dioxane (50 mL) was sparged with nitrogen for 1 hour, then added to reaction flask and sparged 30 additional min. A 2.00 M. aqueous solution of K$_3$PO$_4$ was sparged with nitrogen for 1 hr. The reaction mixture was heated to 80 °C, then 5.1 mL of K$_3$PO$_4$ solution was added. The reaction was stirred overnight at 80 °C. After the reaction was cooled to room temperature, the dioxane was removed under reduced pressure, then the resulting material was filtered through a celite pad with DCM and water. The filtrate was extracted with DCM (3x). The combined organic layers were washed with water (2x) and brine (1x), then dried over sodium sulfate and concentrated under reduced pressure. The solid was dissolved in dichloromethane and rinsed through a silica plug to remove the palladium, then concentrated, yielding 1.45 g (41%). $^1$H NMR (500 MHz, CDCl$_3$): δ 7.66 (s, 4H), 7.55 (d, $J$ = 8.6 Hz, 4H), 7.39 (d, $J$ = 8.5 Hz, 4H), 7.29 (d, $J$ = 8.6 Hz, 4H), 7.24 (d, $J$ = 8.6 Hz, 4H), 6.05 (d, $J$ = 10.4 Hz, 4H), 5.97 (d, $J$ = 10.1 Hz, 4H), 0.98 – 0.93 (overlapping, 36H), 0.65 – 0.60 (overlapping, 24H). $^{13}$C NMR (151 MHz, CDCl$_3$) δ 145.29, 145.02, 140.00, 133.38, 132.17, 131.56, 128.47, 127.64, 127.59, 126.96, 126.61, 71.71, 71.60, 7.11, 6.90, 6.86. IR (neat): 3029.5, 2977.8, 2936.2, 2820.3, 1488.4, 1449.2, 1401.1, 1230.9, 1184.9, 1172.3, 1082.2, 1066.9, 1013.1, 942.4, 815.7, 763.3, 666.0, 640.7.

*7-ring bisboronate **IV.32**.*
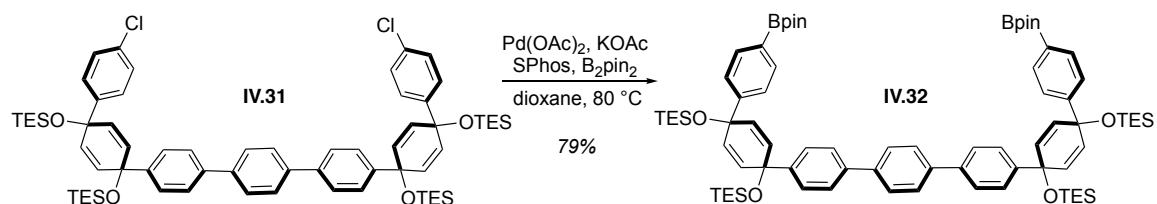


Oven-dried potassium acetate (574.2 mg, 5.85 mmol, 6.60 equiv.) was added to a flame-dried flask equipped with a stir bar. The KOAc was flame-dried again under vacuum until all apparent moisture was removed. Pd(OAc)$_2$ (10.0 mg, 0.044 mmol, 0.05 equiv.), SPhos (45.5 mg, 0.11 mmol, 0.13 equiv.), B$_2$pin$_2$ (899.8 mg, 3.5 mmol, 4.00 equiv.) and dichloride **IV.31** (1.00 g, 0.89 mmol, 1.00 equiv.) were added to the flask. The flask was evacuated for 30 minutes. Dioxane (3.0 mL) was added, and the reaction mixture was sparged for 10 minutes. It was then placed in a preheated oil bath at 80 °C and allowed to stir overnight. After the reaction was cooled to room temperature, the mixture was filtered through a plug of celite, and the filtrate was concentrated under reduced pressure. The material was then sonicated with ethanol and filtered to yield 918 mg (79%). $^1$H NMR (500 MHz, CDCl$_3$): δ 7.73 (d, $J$ = 8.3 Hz, 4H), 7.65 (s, 4H), 7.54 (d, $J$ = 8.6 Hz, 4H), 7.41 (d, $J$ = 8.4 Hz, 6H), 7.39 (d, $J$ = 8.4 Hz, 2H), 6.01 (s, 8H), 1.34 (s, 24H), 0.96 (t, $J$ = 7.9 Hz, 18H), 0.92 (d, $J$ = 7.9 Hz, 18H), 0.65 (q, $J$ = 8.0 Hz, 12H), 0.59 (q, $J$ = 7.9 Hz, 12H). $^{13}$C NMR (126 MHz, CDCl$_3$) δ 149.34, 145.28, 139.79, 139.62, 134.87, 131.77, 131.49, 127.52, 126.87, 126.44, 125.41, 83.89, 71.70, 71.54, 67.25, 25.02, 7.22, 7.20, 6.61.

*[9+1cb] macrocycle **IV.33**.*
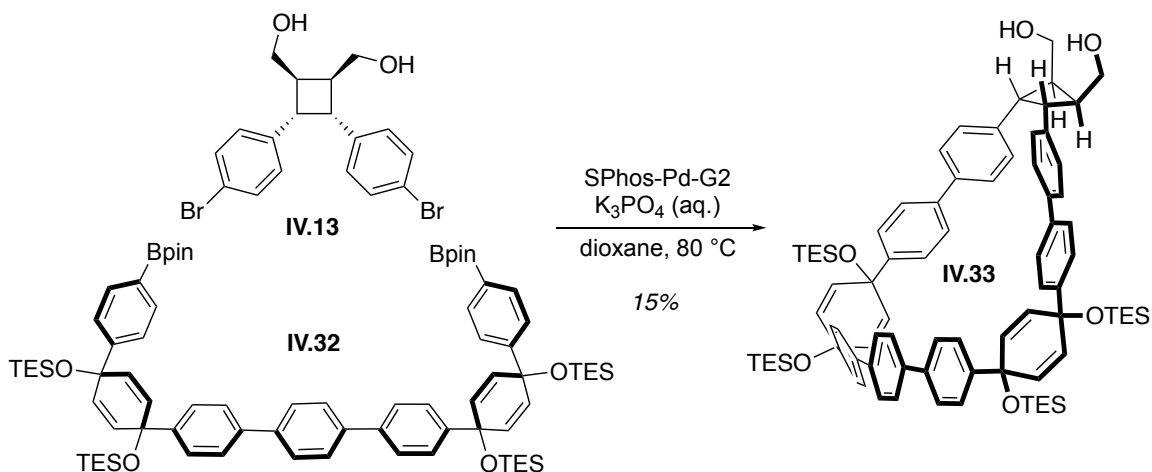


A flame-dried flask was charged with bisboronate **IV.32** (485.0 mg, 0.37 mmol, 1.05 equiv.), dibromide **IV.13** (150.0 mg, 0.35 mmol, 1.00 equiv.), and Pd SPhos Gen II (25.0 mg, 0.04 mmol, 0.10 equiv.). The flask was evacuated and backfilled with nitrogen for 5 cycles. The flask was then purged with nitrogen. A 2.00 M. aqueous solution of $K_3PO_4$ was sparged with nitrogen for 45 min. Dioxane (120 mL) was added to the reaction flask, and the solution was sparged for 15 min. before being heated to 80 °C for 20 min. 12 mL of $K_3PO_4$ solution was added, and the reaction was stirred for 2 hours at 80 °C. After the reaction was cooled to room temperature, the dioxane was removed under reduced pressure, then the resulting material was filtered through a celite pad with DCM and water. The filtrate was extracted with DCM (3x). The combined organic layers were washed with water (2x) and brine (1x), then dried over sodium sulfate and concentrated under reduced pressure. The material was purified by automated silica gel column chromatography (0-25% ethyl acetate in DCM), followed by a final wash of the concentrated material with hexanes, yielding 70 mg of a white solid (15%). ^{1}H NMR (500 MHz, CDCl$_3$): δ 7.53 (s, 4H), 7.41 – 7.37 (m, 8H), 7.34 (d, *J* = 8.5 Hz, 4H), 7.32 (d, *J* = 8.5 Hz, 4H), 7.24 (d, *J* = 8.6 Hz, 4H), 7.22 (d, *J* = 8.3 Hz, 4H), 6.13 – 6.03 (m, 9H), 4.04 (m, 2H), 3.97 (m, 2H), 3.72 (m, 2H), 3.08 (m, 2H), 2.75 (dd, *J* = 6.4, 4.6 Hz, 2H), 0.98 (t, *J* = 7.9 Hz, 18H), 0.93 (t, *J* = 7.9 Hz, 18H), 0.67 (q, *J* = 7.9 Hz, 12H), 0.61 (q, *J* = 7.9 Hz, 12H). ^{13}C NMR (151 MHz, CDCl$_3$) δ 144.42, 144.38, 140.34, 140.11, 139.96, 139.08, 132.53, 132.02, 131.75, 131.24, 128.41, 127.64, 127.45, 126.98, 126.88, 126.69,

126.46, 72.06, 71.73, 62.73, 43.77, 43.30, 7.23, 7.18, 6.64, 6.59. IR (neat): 3336.0 (br), 3033.9, 2954.4, 2874.7, 1489.7, 1456.8, 1071.9, 1004.4, 960.7, 813.0, 719.5.

*[9+1cb]CPP **IV.15***.
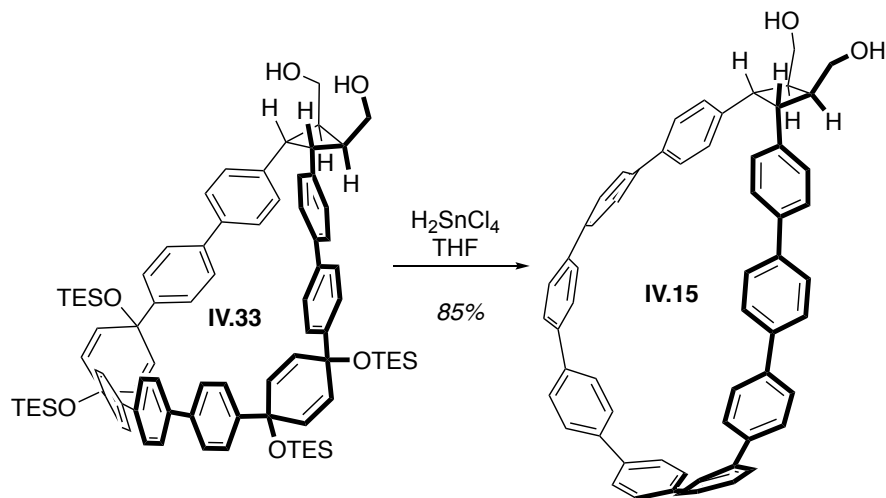


Macrocycle **IV.33** (65.0 mg, 0.049 mmol, 1.00 equiv.) was added to a flame-dried flask. A 0.05 M (in THF) solution of $H_2SnCl_4$ (4.0 mL, 0.20 mmol, 4.00 equiv.) was added. The reaction was stirred at room temperature for 1.5 hrs, then quenched with saturated sodium bicarbonate solution. THF was removed under reduced pressure, and the resulting material was filtered through celite using water and DCM. The filtrate was extracted with DCM (3x), and the combined organic layers were washed with water (2x) and brine (1x) before being dried over sodium sulfate. Solvent was removed under reduced pressure. The material was purified by automated silica gel column chromatography (0-5% MeOH in DCM), followed by a silica gel prep plate in 5% MeOH in DCM, yielding 33.5 mg of a yellow solid (85%). ^{1}H NMR (500 MHz, CDCl$_3$): δ 7.58 (s, 4H), 7.56 – 7.51 (m, 8H), 7.49 – 7.41 (overlapping, 16H), 7.33 (d, $J$ = 8.0 Hz, 4H), 7.01 (d, $J$ = 7.9 Hz, 4H), 4.10 (t, $J$ = 9.8 Hz, 2H), 3.94 (d, $J$ = 11.2 Hz, 2H), 3.69 (d, $J$ = 5.1 Hz, 2H), 3.29 – 3.19 (m, 2H), 3.00 (s, 2H). ^{13}C NMR (126 MHz, CDCl$_3$) δ 139.26, 139.08, 138.89, 138.75, 138.39, 138.30, 137.73, 137.71, 128.57, 127.83, 127.66, 127.45, 127.26, 127.22, 127.03, 126.30, 62.79, 44.12, 41.02.

# Chapter V
## CONCLUDING REMARKS

The combination of bottom-up organic synthesis and polymer chemistry methods offers unprecedented access to exciting new carbon materials. This dissertation describes the design and synthesis of cycloparaphenylenes (CPPs) and related strained macrocycles that have been appropriately functionalized to serve as monomers. The ability to synthesize these macrocyclic building blocks with atomic precision allows the careful study of how structural changes in the monomers affected the resultant polymers. Additionally, in the realm of polymers, molecular weight, composition, and sequence become critical design parameters on top of the factors at play for small molecules such as polarity and functionality. In this work, we examined several CPP sizes in homopolymers as well as size combinations in copolymers and observed differences in fluorescence and supramolecular characteristics of the polymers. We investigated multiple modes of connectivity, including polymerizations which kept the CPP units electronically isolated and those which allowed delocalization across CPP units. We also prepared macrocyclic monomers containing a functional group which would enable ring-opening. We anticipate that using macrocycles as building blocks for complex polymeric materials will continue to be a fruitful area of research.

REFERENCES CITED

1.  Maust, R. L.; Li, P.; Shao, B.; Zeitler, S. M.; Sun, P. B.; Reid, H. W.; Zakharov, L. N.; Golder, M. R.; Jasti, R. Controlled Polymerization of Norbornene Cycloparaphenylenes Expands Carbon Nanomaterials Design Space. *ACS Cent. Sci.* **2021**, Article ASAP.

2.  Peters, G. M. G. M.; Grover, G.; Maust, R. L. R. L.; Colwell, C. E. C. E.; Bates, H.; Edgell, W. A. W. A.; Jasti, R.; Kertesz, M.; Tovar, J. D. J. D. Linear and Radial Conjugation in Extended π-Electron Systems. *J. Am. Chem. Soc.* **2020**, *142*, 2293–2300.

3.  Lynde, B. E.; Maust, R. L.; Li, P.; Lee, D. C.; Jasti, R.; Boydston, A. J. Ring-Opening Metathesis Polymerization of a Strained Stilbene-Based Macrocyclic Monomer. *Mater. Chem. Front.* **2020**, *4*, 252–256.

4.  Namazi, H. Polymers in Our Daily Life. *BioImpacts* **2017**, *7*, 73–74.

5.  Staudinger, H. Über Polymerisation. *Berichte der Dtsch. Chem. Gesellschaft (A B Ser.* **1920**, *53*, 1073–1085.

6.  *Nobel Laureates in Chemistry 1901-1992*; James, L. K., Ed.; American Chemical Society and Chemical Heritage Foundation, 1993.

7.  Geyer, R.; Jambeck, J. R.; Law, K. L. Production, Use, and Fate of All Plastics Ever Made. *Sci. Adv.* **2017**, *3*, e1700782.

8.  Programme, U. N. E. *Single-Use Plastic Bags and Their Alternatives - Recommendations from Life Cycle Assessments*; 2020.

9.  Lodge, T. P. Celebrating 50 Years of Macromolecules. *Macromolecules* **2017**, *50*, 9525–9527.

10. Pyun, J.; Zhou, X.-Z.; Drockenmuller, E.; Hawker, C. J. Macromolecules of Controlled Architecture. *J. Mater. Chem.* **2003**, *13*, 2653–2660.

11. Lutz, J. F.; Lehn, J. M.; Meijer, E. W.; Matyjaszewski, K. From Precision Polymers to Complex Materials and Systems. *Nat. Rev. Mater.* **2016**, *1*, 1–14.

12. Szwarc, M. 'Living' Polymers. *Nature* **1956**, *178*, 1168–1169.

13. Wang, J.-S.; Matyjaszewski, K. Controlled/"living" Radical Polymerization. Atom Transfer Radical Polymerization in the Presence of Transition-Metal Complexes. *J. Am. Chem. Soc.* **1995**, *117*, 5614–5615.

14. Kato, M.; Kamigaito, M.; Sawamoto, M.; Higashimura, T. Polymerization of Methyl Methacrylate with the Carbon Tetrachloride/Dichlorotris-(Triphenylphosphine)Ruthenium(II)/Methylaluminum Bis(2,6-Di-Tert-Butylphenoxide) Initiating System: Possibility of Living Radical Polymerization. *Macromolecules* **1995**, *28*, 1721–1723.

15. Chiefari, J.; Chong, Y. K.; Ercole, F.; Krstina, J.; Jeffery, J.; Le, T. P. T.; Mayadunne, R. T. A.; Meijs, G. F.; Moad, C. L.; Moad, G.; et al. Living Free-Radical Polymerization by Reversible Addition−Fragmentation Chain Transfer: The RAFT Process. *Macromolecules* **1998**, *31*, 5559–5562.

16. Higashimura, T.; Kishiro, O. Possible Formation of Living Polymers of P-Methoxystyrene by Iodine. *Polym. J.* **1977**, *9*, 87–93.

17. Webster, O. W. Living Polymerization Methods. *Science* **1991**, *251*, 887–893.

18. Alvarez, A.; Costa-Fernández, J. M.; Pereiro, R.; Sanz-Medel, A.; Salinas-Castillo, A. Fluorescent Conjugated Polymers for Chemical and Biochemical Sensing. *Trends Anal. Chem.* **2011**, *30*, 1513–1525.

19. Fouquey, C.; Lehn, J.-M.; Levelut, A.-M. Molecular Recognition Directed Self-Assembly of Supramolecular Liquid Crystalline Polymers from Complementary Chiral Components. *Adv. Mater.* **1990**, *2*, 254–257.

20. Dong, S.; Zheng, B.; Wang, F.; Huang, F. Supramolecular Polymers Constructed from Macrocycle-Based Host − Guest Molecular Recognition Motifs. *Acc. Chem. Res.* **2014**, *47*, 1982–1994.

21. Wang, F.; Zhang, J.; Ding, X.; Dong, S.; Liu, M.; Zheng, B.; Li, S.; Wu, L.; Yu, Y.; Gibson, H. W.; et al. Metal Coordination Mediated Reversible Conversion between Linear and Cross-Linked Supramolecular Polymers. *Angew. Chem. Int. Ed.* **2010**, *49*, 1090–1094.

22. Dong, S.; Luo, Y.; Yan, X.; Zheng, B.; Ding, X.; Yu, Y.; Ma, Z.; Zhao, Q.; Huang, F. A Dual-Responsive Supramolecular Polymer Gel Formed by Crown Ether Based Molecular Recognition. *Angew. Chem. Int. Ed.* **2011**, *50*, 1905–1909.

23. Kissel, P.; Erni, R.; Schweizer, W. B.; Rossell, M. D.; King, B. T.; Bauer, T.; Götzinger, S.; Schlüter, A. D.; Sakamoto, J. A Two-Dimensional Polymer Prepared by Organic Synthesis. *Nat. Chem.* **2012**, *4*, 287–291.

24. Servalli, M.; Schlüter, A. D. Synthetic Two-Dimensional Polymers. *Annu. Rev. Mater. Res.* **2017**, *47*, 361–389.

25. Alsbaiee, A.; Smith, B. J.; Xiao, L.; Ling, Y.; Helbling, D. E.; Dichtel, W. R. Rapid Removal of Organic Micropollutants from Water by a Porous β-Cyclodextrin Polymer. *Nature* **2015**, *529*, 190–194.

26. Xiao, L.; Ling, Y.; Alsbaiee, A.; Li, C.; Helbling, D. E.; Dichtel, W. R. β-Cyclodextrin Polymer Network Sequesters Perfluorooctanoic Acid at Environmentally Relevant Concentrations. *J. Am. Chem. Soc.* **2017**, *139*, 7689–7692.

27. Gu, Y.; Alt, E. A.; Wang, H.; Li, X.; Willard, A. P.; Johnson, J. A. Photoswitching Topology in Polymer Networks with Metal–Organic Cages as Crosslinks. *Nature* **2018**, *560*, 65–69.

28. Lei, T.; Guan, M.; Liu, J.; Lin, H.-C.; Pfattner, R.; Shaw, L.; McGuire, A. F.; Huang, T.-C.; Shao, L.; Cheng, K.-T.; et al. Biocompatible and Totally Disintegrable Semiconducting Polymer for Ultrathin and Ultralightweight Transient Electronics. *Proc. Natl. Acad. Sci.* **2017**, *114*, 5107–5112.

29. Palermo, E. F.; McNeil, A. J. Gradient Sequence π-Conjugated Copolymers. In *Sequence-Controlled Polymers: Synthesis, Self-Assembly, and Properties*; Lutz, J.-F., Meyer, T. Y., Ouchi, M., Sawamoto, M., Eds.; 2014; p 287.

30. Bucknall, D. G.; Anderson, H. L. Polymers Get Organized. *Science* **2003**, *302*, 1904–1905.

31. Mai, Y.; Eisenberg, A. Self-Assembly of Block Copolymers. *Chem. Soc. Rev.* **2012**, *41*, 5969–5985.

32. Matyjaszewski, K.; Tsarevsky, N. V. Nanostructured Functional Materials Prepared by Atom Transfer Radical Polymerization. *Nat. Chem.* **2009**, *1*, 276–288.

33. Palermo, E. F.; van der Laan, H. L.; McNeil, A. J. Impact of π-Conjugated Gradient Sequence Copolymers on Polymer Blend Morphology. *Polym. Chem.* **2013**, *4*, 4606–4611.

34. Gutekunst, W. R.; Hawker, C. J. A General Approach to Sequence-Controlled Polymers Using Macrocyclic Ring Opening Metathesis Polymerization. *J. Am. Chem. Soc.* **2015**, *137*, 8038–8041.

35. Swisher, J. H.; Nowalk, J. A.; Meyer, T. Y. Property Impact of Common Linker Segments in Sequence-Controlled Polyesters. *Polym. Chem.* **2019**, *10*, 244–252.

36. Staudinger, H. Macromolecular Chemistry. In *Nobel Lecture*; 1953.

37. Matyjaszewski, K. Architecturally Complex Polymers with Controlled Heterogeneity. *Science* **2011**, *333*, 1104–1105.

38. Rzayev, J. Molecular Bottlebrushes: New Opportunities in Nanomaterials Fabrication. *ACS Macro Lett.* **2012**, *1*, 1146–1149.

39. Haque, F. M.; Grayson, S. M. The Synthesis, Properties, and Potential Applications of Cyclic Polymers. *Nat. Chem.* **2020**, *12*, 433–444.

40. Oike, H.; Imaizumi, H.; Mouri, T.; Yoshioka, Y.; Uchibori, A.; Tezuka, Y. Designing Unusual Polymer Topologies by Electrostatic Self-Assembly and Covalent Fixation. *J. Am. Chem. Soc.* **2000**, *122*, 9592–9599.

41. Laurent, B. A.; Grayson, S. M. An Efficient Route to Well-Defined Macrocyclic Polymers via "Click" Cyclization. *J. Am. Chem. Soc.* **2006**, *128*, 4238–4239.

42. Boydston, A. J.; Xia, Y.; Kornfield, J. A.; Gorodetskaya, I. A.; Grubbs, R. H. Cyclic Ruthenium-Alkylidene Catalysts for Ring-Expansion Metathesis Polymerization. *J. Am. Chem. Soc.* **2008**, *130*, 12775–12782.

43.  Culkin, D. A.; Jeong, W.; Csihony, S.; Gomez, E. D.; Balsara, N. P.; Hedrick, J. L.; Waymouth, R. M. Zwitterionic Polymerization of Lactide to Cyclic Poly(Lactide) by Using N-Heterocyclic Carbene Organocatalysts. *Angew. Chem. Int. Ed.* **2007**, *46*, 2627–2630.

44.  Wang, T.-W.; Golder, M. R. Advancing Macromolecular Hoop Construction: Recent Developments in Synthetic Cyclic Polymer Chemistry. *Polym. Chem.* **2021**, *12*, 958–969.

45.  Honda, S.; Yamamoto, T.; Tezuka, Y. Tuneable Enhancement of the Salt and Thermal Stability of Polymeric Micelles by Cyclized Amphiphiles. *Nat. Commun.* **2013**, *4*, 1574.

46.  Gonsales, S. A.; Kubo, T.; Flint, M. K.; Abboud, K. A.; Sumerlin, B. S.; Veige, A. S. Highly Tactic Cyclic Polynorbornene: Stereoselective Ring Expansion Metathesis Polymerization of Norbornene Catalyzed by a New Tethered Tungsten-Alkylidene Catalyst. *J. Am. Chem. Soc.* **2016**, *138*, 4996–4999.

47.  Niu, W.; Gonsales, S. A.; Kubo, T.; Bentz, K. C.; Pal, D.; Savin, D. A.; Sumerlin, B. S.; Veige, A. S. Polypropylene: Now Available without Chain Ends. *Chem* **2019**, *5*, 237–244.

48.  Roovers, J. Viscoelastic Properties of Polybutadiene Rings. *Macromolecules* **1988**, *21*, 1517–1521.

49.  Gu, Y.; Zhao, J.; Johnson, J. A. A (Macro)Molecular-Level Understanding of Polymer Network Topology. *Trends Chem.* **2019**, *1*, 318–334.

50.  Whitfield, R.; Truong, N. P.; Messmer, D.; Parkatzidis, K.; Rolland, M.; Anastasaki, A. Tailoring Polymer Dispersity and Shape of Molecular Weight Distributions: Methods and Applications. *Chem. Sci.* **2019**, *10*, 8724–8734.

51.  Gentekos, D. T.; Sifri, R. J.; Fors, B. P. Controlling Polymer Properties through the Shape of the Molecular-Weight Distribution. *Nat. Rev. Mater.* **2019**, *4*, 761–774.

52.  Yadav, V.; Harkin, A. V; Robertson, M. L.; Conrad, J. C. Hysteretic Memory in PH-Response of Water Contact Angle on Poly(Acrylic Acid) Brushes. *Soft Matter* **2016**, *12*, 3589–3599.

53.  Martin, T. B.; Dodd, P. M.; Jayaraman, A. Polydispersity for Tuning the Potential of Mean Force between Polymer Grafted Nanoparticles in a Polymer Matrix. *Phys. Rev. Lett.* **2013**, *110*, 018301.

54.  Liu, X.; Wang, C.-G.; Goto, A. Polymer Dispersity Control by Organocatalyzed Living Radical Polymerization. *Angew. Chem. Int. Ed.* **2019**, *58*, 5598–5603.

55.  Yadav, V.; Jaimes-Lizcano, Y. A.; Dewangan, N. K.; Park, N.; Li, T.-H.; Robertson, M. L.; Conrad, J. C. Tuning Bacterial Attachment and Detachment via the Thickness and Dispersity of a PH-Responsive Polymer Brush. *ACS Appl. Mater. Interfaces* **2017**, *9*, 44900–44910.

56. Sifri, R. J.; Padilla-Vélez, O.; Coates, G. W.; Fors, B. P. Controlling the Shape of Molecular Weight Distributions in Coordination Polymerization and Its Impact on Physical Properties. *J. Am. Chem. Soc.* **2020**, *142*, 1443–1448.

57. Kottisch, V.; Gentekos, D. T.; Fors, B. P. "Shaping" the Future of Molecular Weight Distributions in Anionic Polymerization. *ACS Macro Lett.* **2016**, *5*, 796–800.

58. Yan, J.; Kristufek, T.; Schmitt, M.; Wang, Z.; Xie, G.; Dang, A.; Hui, C. M.; Pietrasik, J.; Bockstaller, M. R.; Matyjaszewski, K. Matrix-Free Particle Brush System with Bimodal Molecular Weight Distribution Prepared by SI-ATRP. *Macromolecules* **2015**, *48*, 8208–8218.

59. Doncom, K. E. B.; Blackman, L. D.; Wright, D. B.; Gibson, M. I.; O'Reilly, R. K. Dispersity Effects in Polymer Self-Assemblies: A Matter of Hierarchical Control. *Chem. Soc. Rev.* **2017**, *46*, 4119–4134.

60. Widin, J. M.; Schmitt, A. K.; Schmitt, A. L.; Im, K.; Mahanthappa, M. K. Unexpected Consequences of Block Polydispersity on the Self-Assembly of ABA Triblock Copolymers. *J. Am. Chem. Soc.* **2012**, *134*, 3834–3844.

61. Schmitt, A. L.; Repollet-Pedrosa, M. H.; Mahanthappa, M. K. Polydispersity-Driven Block Copolymer Amphiphile Self-Assembly into Prolate-Spheroid Micelles. *ACS Macro Lett.* **2012**, *1*, 300–304.

62. Nunes, S. P. Block Copolymer Membranes for Aqueous Solution Applications. *Macromolecules* **2016**, *49*, 2905–2916.

63. Terreau, O.; Bartels, C.; Eisenberg, A. Effect of Poly(Acrylic Acid) Block Length Distribution on Polystyrene-b-Poly(Acrylic Acid) Block Copolymer Aggregates in Solution. 2. A Partial Phase Diagram. *Langmuir* **2004**, *20*, 637–645.

64. Gentekos, D. T.; Fors, B. P. Molecular Weight Distribution Shape as a Versatile Approach to Tailoring Block Copolymer Phase Behavior. *ACS Macro Lett.* **2018**, *7*, 677–682.

65. Miyake, G. M.; Piunova, V. A.; Weitekamp, R. A.; Grubbs, R. H. Precisely Tunable Photonic Crystals From Rapidly Self-Assembling Brush Block Copolymer Blends. *Angew. Chem. Int. Ed.* **2012**, *51*, 11246–11248.

66. McKeown, G. R.; Ye, S.; Cheng, S.; Seferos, D. S. Homogenous Synthesis of Monodisperse High Oligomers of 3-Hexylthiophene by Temperature Cycling. *J. Am. Chem. Soc.* **2019**, *141*, 17053–17056.

67. Gangloff, N.; Höferth, M.; Stepanenko, V.; Sochor, B.; Schummer, B.; Nickel, J.; Walles, H.; Hanke, R.; Würthner, F.; Zuckermann, R. N.; et al. Linking Two Worlds in Polymer Chemistry: The Influence of Block Uniformity and Dispersity in Amphiphilic Block Copolypeptoids on Their Self-Assembly. *Biopolymers* **2019**, *110*, e23259.

68.  Van Genabeek, B.; De Waal, B. F. M.; Ligt, B.; Palmans, A. R. A.; Meijer, E. W. Dispersity under Scrutiny: Phase Behavior Differences between Disperse and Discrete Low Molecular Weight Block Co-Oligomers. *ACS Macro Lett.* **2017**, *6*, 674–678.

69.  Lawrence, J.; Goto, E.; Ren, J. M.; McDearmon, B.; Kim, D. S.; Ochiai, Y.; Clark, P. G.; Laitar, D.; Higashihara, T.; Hawker, C. J. A Versatile and Efficient Strategy to Discrete Conjugated Oligomers. *J. Am. Chem. Soc.* **2017**, *139*, 13735–13739.

70.  Hawker, C. J.; Wooley, K. L. The Convergence of Synthetic Organic and Polymer Chemistries. *Science* **2005**, *309*, 1200–1205.

71.  Povie, G.; Segawa, Y.; Nishihara, T.; Miyauchi, Y.; Itami, K. Synthesis of a Carbon Nanobelt. *Science* **2017**, *356*, 172–175.

72.  Povie, G.; Segawa, Y.; Nishihara, T.; Miyauchi, Y.; Itami, K. Synthesis and Size-Dependent Properties of [12], [16], and [24]Carbon Nanobelts. *J. Am. Chem. Soc.* **2018**, *140*, 10054–10059.

73.  Cheung, K. Y.; Gui, S.; Deng, C.; Liang, H.; Xia, Z.; Liu, Z.; Chi, L.; Miao, Q. Synthesis of Armchair and Chiral Carbon Nanobelts. *Chem* **2019**, *5*, 838–847.

74.  Sun, Z.; Ikemoto, K.; Fukunaga, T. M.; Koretsune, T.; Arita, R.; Sato, S.; Isobe, H. Finite Phenine Nanotubes with Periodic Vacancy Defects. *Science* **2019**, *363*, 151–155.

75.  Huang, Q.; Zhuang, G.; Zhang, M.; Wang, J.; Wang, S.; Wu, Y.; Yang, S.; Du, P. A Long π-Conjugated Poly(Para-Phenylene)-Based Polymeric Segment of Single-Walled Carbon Nanotubes. *J. Am. Chem. Soc.* **2019**, *141*, 18938–18943.

76.  Yang, X.; Dou, X.; Rouhanipour, A.; Zhi, L.; Räder, H. J.; Müllen, K. Two-Dimensional Graphene Nanoribbons. *J. Am. Chem. Soc.* **2008**, *130*, 4216–4217.

77.  Nguyen, G. D.; Tsai, H. Z.; Omrani, A. A.; Marangoni, T.; Wu, M.; Rizzo, D. J.; Rodgers, G. F.; Cloke, R. R.; Durr, R. A.; Sakai, Y.; et al. Atomically Precise Graphene Nanoribbon Heterojunctions from a Single Molecular Precursor. *Nat. Nanotechnol.* **2017**, *12*, 1077–1082.

78.  Senese, A. D.; Chalifoux, W. A. Nanographene and Graphene Nanoribbon Synthesis via Alkyne Benzannulations. *Molecules* **2019**, *24*, 118.

79.  Yano, Y.; Mitoma, N.; Ito, H.; Itami, K. A Quest for Structurally Uniform Graphene Nanoribbons: Synthesis, Properties, and Applications. *J. Org. Chem.* **2020**, *85*, 4–33.

80.  Fitzgibbons, T. C.; Guthrie, M.; Xu, E.; Crespi, V. H.; Davidowski, S. K.; Cody, G. D.; Alem, N.; Badding, J. V. Benzene-Derived Carbon Nanothreads. *Nat. Mater.* **2014**, *14*, 43–47.

81.  Ward, M. D.; Tang, W. S.; Zhu, L.; Popov, D.; Cody, G. D.; Strobel, T. A. Controlled Single-Crystalline Polymerization of C10H8·C10F8 under Pressure. *Macromolecules* **2019**, *52*, 7557–7563.

82. Gerthoffer, M. C.; Wu, S.; Chen, B.; Wang, T.; Huss, S.; Oburn, S. M.; Crespi, V. H.; Badding, J. V; Elacqua, E. 'Sacrificial' Supramolecular Assembly and Pressure-Induced Polymerization: Toward Sequence-Defined Functionalized Nanothreads. *Chem. Sci.* **2020**, *11*, 11419–11424.

83. Huss, S.; Wu, S.; Chen, B.; Wang, T.; Gerthoffer, M. C.; Ryan, D. J.; Smith, S. E.; Crespi, V. H.; Badding, J. V; Elacqua, E. Scalable Synthesis of Crystalline One-Dimensional Carbon Nanothreads through Modest-Pressure Polymerization of Furan. *ACS Nano* **2021**, *15*, 4134–4143.

84. Stuparu, M. C. Rationally Designed Polymer Hosts of Fullerene. *Angew. Chem. Int. Ed.* **2013**, *52*, 7786–7790.

85. Mishra, A.; Ulaganathan, M.; Edison, E.; Borah, P.; Mishra, A.; Sreejith, S.; Madhavi, S.; Stuparu, M. C. Polymeric Nanomaterials Based on the Buckybowl Motif: Synthesis through Ring-Opening Metathesis Polymerization and Energy Storage Applications. *ACS Macro Lett.* **2017**, *6*, 1212–1216.

86. Karunathilake, A. A. K.; Thompson, C. M.; Perananthan, S.; Ferraris, J. P.; Smaldone, R. A. Electrochemically Active Porous Organic Polymers Based on Corannulene. *Chem. Commun.* **2016**, *52*, 12881–12884.

87. Chaudhuri, S.; Mohanan, M.; Willems, A. V; Bertke, J. A.; Gavvalapalli, N. β-Strand Inspired Bifacial π-Conjugated Polymers. *Chem. Sci.* **2019**, *10*, 5976–5982.

88. Barbon, S. M.; Rolland, M.; Anastasaki, A.; Truong, N. P.; Schulze, M. W.; Bates, C. M.; Hawker, C. J. Macrocyclic Side-Chain Monomers for Photoinduced ATRP: Synthesis and Properties versus Long-Chain Linear Isomers. *Macromolecules* **2018**, *51*, 6901–6910.

89. Lo Meo, P.; Lazzara, G.; Liotta, L.; Riela, S.; Noto, R. Cyclodextrin–Calixarene Co-Polymers as a New Class of Nanosponges. *Polym. Chem.* **2014**, *5*, 4499–4510.

90. Ji, X.; Wu, R.-T.; Long, L.; Guo, C.; Khashab, N. M.; Huang, F.; Sessler, J. L. Physical Removal of Anions from Aqueous Media by Means of a Macrocycle-Containing Polymeric Network. *J. Am. Chem. Soc.* **2018**, *140*, 2777–2780.

91. Skala, L. P.; Yang, A.; Klemes, M. J.; Xiao, L.; Dichtel, W. R. Resorcinarene Cavitand Polymers for the Remediation of Halomethanes and 1,4-Dioxane. *J. Am. Chem. Soc.* **2019**, *141*, 13315–13319.

92. Marsella, M. J.; Swager, T. M. Designing Conducting Polymer-Based Sensors: Selective Ionochromic Response in Crown Ether Containing Polythiophenes. *J. Am. Chem. Soc.* **1993**, *115*, 12214–12215.

93. Ball, M.; Zhong, Y.; Fowler, B.; Zhang, B.; Li, P.; Etkin, G.; Paley, D. W.; Decatur, J.; Dalsania, A. K.; Li, H.; et al. Macrocyclization in the Design of Organic N-Type Electronic Materials. *J. Am. Chem. Soc.* **2016**, *138*, 12861–12867.

94. Mun, J.; Kang, J.; Zheng, Y.; Luo, S.; Wu, H.-C.; Matsuhisa, N.; Xu, J.; Wang, G.-J. N.; Yun, Y.; Xue, G.; et al. Conjugated Carbon Cyclic Nanorings as Additives for Intrinsically Stretchable Semiconducting Polymers. *Adv. Mater.* **2019**, *0*, 1903912.

95. Appel, E. A.; del Barrio, J.; Loh, X. J.; Scherman, O. A. Supramolecular Polymeric Hydrogels. *Chem. Soc. Rev.* **2012**, *41*, 6195–6214.

96. Schmidt, B. V. K. J.; Barner-Kowollik, C. Dynamic Macromolecular Material Design—The Versatility of Cyclodextrin-Based Host–Guest Chemistry. *Angew. Chem. Int. Ed.* **2017**, *56*, 8350–8369.

97. Wu, Q.; Rauscher, P. M.; Lang, X.; Wojtecki, R. J.; de Pablo, J. J.; Hore, M. J. A.; Rowan, S. J. Poly[n]Catenanes: Synthesis of Molecular Interlocked Chains. *Science* **2017**, *358*, 1434–1439.

98. Niu, Z.; Gibson, H. W. Polycatenanes. *Chem. Rev.* **2009**, *109*, 6024–6046.

99. Zhu, Z.; Bruns, C. J.; Li, H.; Lei, J.; Ke, C.; Liu, Z.; Shafaie, S.; Colquhoun, H. M.; Stoddart, J. F. Synthesis and Solution-State Dynamics of Donor–Acceptor Oligorotaxane Foldamers. *Chem. Sci.* **2013**, *4*, 1470–1483.

100. Ito, K. Novel Cross-Linking Concept of Polymer Network: Synthesis, Structure, and Properties of Slide-Ring Gels with Freely Movable Junctions. *Polym. J.* **2007**, *39*, 489–499.

101. Iwaso, K.; Takashima, Y.; Harada, A. Fast Response Dry-Type Artificial Molecular Muscles with [C2]Daisy Chains. *Nat. Chem.* **2016**, *8*, 625–632.

102. Murakami, T.; Schmidt, B. V. K. J.; Brown, H. R.; Hawker, C. J. One-Pot "Click" Fabrication of Slide-Ring Gels. *Macromolecules* **2015**, *48*, 7774–7781.

103. Takashima, Y.; Hayashi, Y.; Osaki, M.; Kaneko, F.; Yamaguchi, H.; Harada, A. A Photoresponsive Polymeric Actuator Topologically Cross-Linked by Movable Units Based on a [2]Rotaxane. *Macromolecules* **2018**, *51*, 4688–4693.

104. Miao, Y.-J.; Bazan, G. C. Paracyclophene Route to Poly(p-Phenylenevinylene). *J. Am. Chem. Soc.* **1994**, *116*, 9379–9380.

105. Yu, C.; Turner, M. L. Soluble Poly(P-phenylenevinylene)s through Ring-Opening Metathesis Polymerization. *Angew. Chem. Int. Ed.* **2006**, *45*, 7797–7800.

106. Gilch, H. G.; Wheelwright, W. L. Polymerization of α-Halogenated p-Xylenes with Base. *J. Polym. Sci. Part A-1 Polym. Chem.* **1966**, *4*, 1337–1349.

107. Kretzschmann, H.; Meier, H. A New Synthesis of Soluble Poly(1,4-Phenylenevinylene)s and Poly(2,5-Pyrimidinylenevinylene)S. *Tetrahedron Lett.* **1991**, *32*, 5059–5062.

108. Menk, F.; Mondeshki, M.; Dudenko, D.; Shin, S.; Schollmeyer, D.; Ceyhun, O.; Choi, T.-L.; Zentel, R. Reactivity Studies of Alkoxy-Substituted [2.2]Paracyclophane-1,9-Dienes and Specific Coordination of the Monomer Repeating Unit during ROMP. *Macromolecules* **2015**, *48*, 7435–7445.

109. Elacqua, E.; Gregor, M. Poly(Arylenevinylene)s through Ring-Opening Metathesis Polymerization of an Unsymmetrical Donor-Acceptor Cyclophane. *Angew. Chem. Int. Ed.* **2019**, *58*, 9527–9532.

110. Davis, D. A.; Hamilton, A.; Yang, J.; Cremar, L. D.; Van Gough, D.; Potisek, S. L.; Ong, M. T.; Braun, P. V; Martínez, T. J.; White, S. R.; et al. Force-Induced Activation of Covalent Bonds in Mechanoresponsive Polymeric Materials. *Nature* **2009**, *459*, 68–72.

111. Wang, Z.; Ma, Z.; Wang, Y.; Xu, Z.; Luo, Y.; Wei, Y.; Jia, X. A Novel Mechanochromic and Photochromic Polymer Film: When Rhodamine Joins Polyurethane. *Adv. Mater.* **2015**, *27*, 6469–6474.

112. Wang, T.; Zhang, N.; Dai, J.; Li, Z.; Bai, W.; Bai, R. Novel Reversible Mechanochromic Elastomer with High Sensitivity: Bond Scission and Bending-Induced Multicolor Switching. *ACS Appl. Mater. Interfaces* **2017**, *9*, 11874–11881.

113. Chan, Y.-H.; Gallina, M. E.; Zhang, X.; Wu, I.-C.; Jin, Y.; Sun, W.; Chiu, D. T. Reversible Photoswitching of Spiropyran-Conjugated Semiconducting Polymer Dots. *Anal. Chem.* **2012**, *84*, 9431–9438.

114. Peterson, G. I.; Larsen, M. B.; Ganter, M. A.; Storti, D. W.; Boydston, A. J. 3D-Printed Mechanochromic Materials. *ACS Appl. Mater. Interfaces* **2015**, *7*, 577–583.

115. Versaw, B. A.; McFadden, M. E.; Husic, C. C.; Robb, M. J. Designing Naphthopyran Mechanophores with Tunable Mechanochromic Behavior. *Chem. Sci.* **2020**, *11*, 4525–4530.

116. Chen, Z.; Mercer, J. A. M.; Zhu, X.; Romaniuk, J. A. H.; Pfattner, R.; Cegelski, L.; Martinez, T. J.; Burns, N. Z.; Xia, Y. Mechanochemical Unzipping of Insulating Polyladderene to Semiconducting Polyacetylene. *Science* **2017**, *357*, 475–479.

117. Yang, J.; Horst, M.; Romaniuk, J. A. H.; Jin, Z.; Cegelski, L.; Xia, Y. Benzoladderene Mechanophores: Synthesis, Polymerization, and Mechanochemical Transformation. *J. Am. Chem. Soc.* **2019**, *141*, 6479–6483.

118. Ghanem, M. A.; Basu, A.; Behrou, R.; Boechler, N.; Boydston, A. J.; Craig, S. L.; Lin, Y.; Lynde, B. E.; Nelson, A.; Shen, H.; et al. The Role of Polymer Mechanochemistry in Responsive Materials and Additive Manufacturing. *Nat. Rev. Mater.* **2021**, *6*, 84–98.

119. Darzi, E. R.; Jasti, R. The Dynamic, Size-Dependent Properties of [5]–[12]Cycloparaphenylenes. *Chem. Soc. Rev.* **2015**, *44*, 6401–6410.

120. Colwell, C. E.; Price, T. W.; Stauch, T.; Jasti, R. Strain Visualization for Strained Macrocycles. *Chem. Sci.* **2020**, *11*, 3923–3930.

121. Schaub, T. A.; Margraf, J. T.; Zakharov, L.; Reuter, K.; Jasti, R. Strain-Promoted Reactivity of Alkyne-Containing Cycloparaphenylenes. *Angew. Chem. Int. Ed.* **2018**, *57*, 16348–16353.

122. Omachi, H.; Nakayama, T.; Takahashi, E.; Segawa, Y.; Itami, K. Initiation of Carbon Nanotube Growth by Well-Defined Carbon Nanorings. *Nat. Chem.* **2013**, *5*, 572–576.

123. Steinberg, B. D.; Scott, L. T. New Strategies for Synthesizing Short Sections of Carbon Nanotubes. *Angew. Chem. Int. Ed.* **2009**, *48*, 5400–5402.

124. Jasti, R.; Bertozzi, C. R. Progress and Challenges for the Bottom-up Synthesis of Carbon Nanotubes with Discrete Chirality. *Chem. Phys. Lett.* **2010**, *494*, 1–7.

125. Van Raden, J. M.; White, B. M.; Zakharov, L. N.; Jasti, R. Nanohoop Rotaxanes from Active Metal Template Syntheses and Their Potential in Sensing Applications. *Angew. Chem. Int. Ed.* **2019**, *58*, 7341–7345.

126. White, B. M.; Zhao, Y.; Kawashima, T. E.; Branchaud, B. P.; Pluth, M. D.; Jasti, R. Expanding the Chemical Space of Biocompatible Fluorophores: Nanohoops in Cells. *ACS Cent. Sci.* **2018**, *4*, 1173–1178.

127. Van Raden, J. M.; Leonhardt, E.; Zakharov, L. N.; Pérez-Guardiola, A.; Pérez-Jiménez, A. J.; Marshall, C. R.; Brozek, C. K.; Sancho-García, J. C.; Jasti, R. Precision Nanotube Mimics via Self-Assembly of Programmed Carbon Nanohoops. *J. Org. Chem.* **2020**, *85*, 129–141.

128. Schaub, T. A.; Prantl, E. A.; Kohn, J.; Bursch, M.; Marshall, C. R.; Leonhardt, E. J.; Lovell, T. C.; Zakharov, L. N.; Brozek, C. K.; Waldvogel, S. R.; et al. Exploration of the Solid-State Sorption Properties of Shape-Persistent Macrocyclic Nanocarbons as Bulk Materials and Small Aggregates. *J. Am. Chem. Soc.* **2020**, *142*, 8763–8775.

129. Dinadayalane, T. C.; Leszczynski, J. Remarkable Diversity of Carbon-Carbon Bonds: Structures and Properties of Fullerenes, Carbon Nanotubes, and Graphene. *Struct. Chem.* **2010**, *21*, 1155–1169.

130. Pinzón, J. R.; Villalta-Cerdas, A.; Echegoyen, L. Fullerenes, Carbon Nanotubes, and Graphene for Molecular Electronics. In *Unimolecular and Supramolecular Electronics I*; Metzger, R. M., Ed.; Springer Berlin Heidelberg: Berlin, Heidelberg, 2012; pp 127–174.

131. Lim, S. Y.; Shen, W.; Gao, Z. Carbon Quantum Dots and Their Applications. *Chem. Soc. Rev.* **2015**, *44*, 362–381.

132. Segawa, Y.; Levine, D. R.; Itami, K. Topologically Unique Molecular Nanocarbons. *Acc. Chem. Res.* **2019**, *52*, 2760–2767.

133. Li, L.; Yan, X. Colloidal Graphene Quantum Dots. *J. Phys. Chem. Lett.* **2010**, *1*, 2572–2576.

134. Thomas, S. W.; Joly, G. D.; Swager, T. M. Chemical Sensors Based on Amplifying Fluorescent Conjugated Polymers. *Chem. Rev.* **2007**, *107*, 1339–1386.

135. Giacalone, F.; Martín, N. Fullerene Polymers: Synthesis and Properties. *Chem. Rev.* **2006**, *106*, 5136–5190.

136. Dawson, R.; Cooper, A. I.; Adams, D. J. Nanoporous Organic Polymer Networks. *Prog. Polym. Sci.* **2012**, *37*, 530–563.

137. Von Kugelgen, S.; Piskun, I.; Griffin, J. H.; Eckdahl, C. T.; Jarenwattananon, N. N.; Fischer, F. R. Templated Synthesis of End-Functionalized Graphene Nanoribbons through Living Ring-Opening Alkyne Metathesis Polymerization. *J. Am. Chem. Soc.* **2019**, *141*, 11050–11058.

138. Lovell, T. C.; Colwell, C. E.; Zakharov, L. N.; Jasti, R. Symmetry Breaking and the Turn-on Fluorescence of Small, Highly Strained Carbon Nanohoops. *Chem. Sci.* **2019**, *10*, 3786–3790.

139. Darzi, E. R.; Hirst, E. S.; Weber, C. D.; Zakharov, L. N.; Lonergan, M. C.; Jasti, R. Synthesis, Properties, and Design Principles of Donor-Acceptor Nanohoops. *ACS Cent. Sci.* **2015**, *1*, 335–342.

140. McDearmon, B.; Lim, E.; Lee, I.-H.; Kozycz, L. M.; O'Hara, K.; Robledo, P. I.; Venkatesan, N. R.; Chabinyc, M. L.; Hawker, C. J. Effects of Side-Chain Topology on Aggregation of Conjugated Polymers. *Macromolecules* **2018**, *51*, 2580–2590.

141. Gyanwali, G.; Hikkaduwa Koralege, R. S.; Hodge, M.; Ausman, K. D.; White, J. L. C60–Polymer Nanocomposite Networks Enabled by Guest–Host Properties. *Macromolecules* **2013**, *46*, 6118–6123.

142. Jasti, R.; Bhattacharjee, J.; Neaton, J. B.; Bertozzi, C. R. Synthesis, Characterization, and Theory of [9]-, [12]-, and [18]Cycloparaphenylene: Carbon Nanohoop Structures. *J. Am. Chem. Soc.* **2008**, *130*, 17646–17647.

143. Iwamoto, T.; Watanabe, Y.; Sadahiro, T.; Haino, T.; Yamago, S. Size-Selective Encapsulation of C60 by [10]Cycloparaphenylene: Formation of the Shortest Fullerene-Peapod. *Angew. Chem. Int. Ed.* **2011**, *50*, 8342–8344.

144. Xu, Y.; von Delius, M. The Supramolecular Chemistry of Strained Carbon Nanohoops. *Angew. Chem. Int. Ed.* **2020**, *59*, 559–573.

145. Xia, J.; Bacon, J. W.; Jasti, R. Gram-Scale Synthesis and Crystal Structures of [8]- and [10]CPP, and the Solid-State Structure of C60@[10]CPP. *Chem. Sci.* **2012**, *3*, 3018–3021.

146. Sisto, T. J.; Zakharov, L. N.; White, B. M.; Jasti, R. Towards Pi-Extended Cycloparaphenylenes as Seeds for CNT Growth: Investigating Strain Relieving Ring-Openings and Rearrangements. *Chem. Sci.* **2016**, *7*, 3681–3688.

147. Kayahara, E.; Qu, R.; Yamago, S. Bromination of Cycloparaphenylenes: Strain-Induced Site-Selective Bis-Addition and Its Application for Late-Stage Functionalization. *Angew. Chem. Int. Ed.* **2017**, *56*, 10428–10432.

148. Slugovc, C. The Ring Opening Metathesis Polymerisation Toolbox. *Macromol. Rapid Commun.* **2004**, *25*, 1283–1297.

149. Leitgeb, A.; Wappel, J.; Slugovc, C. The ROMP Toolbox Upgraded. *Polymer* **2010**, *51*, 2927–2946.

150. Choi, T.-L.; Grubbs, R. H. Controlled Living Ring-Opening-Metathesis Polymerization by a Fast-Initiating Ruthenium Catalyst. *Angew. Chem. Int. Ed.* **2003**, *42*, 1743–1746.

151. Grubbs, R. B.; Grubbs, R. H. 50th Anniversary Perspective: Living Polymerization—Emphasizing the Molecule in Macromolecules. *Macromolecules* **2017**, *50*, 6979–6997.

152. Bielawski, C. W.; Grubbs, R. H. Living Ring-Opening Metathesis Polymerization. *Prog. Polym. Sci.* **2007**, *32*, 1–29.

153. Lodge, T. P.; Hiemenz, P. C. *Polymer Chemistry*, Third Ed.; CRC: Boca Raton, 2020.

154. Darzi, E. R.; Sisto, T. J.; Jasti, R. Selective Syntheses of [7] − [12]Cycloparaphenylenes Using Orthogonal Suzuki − Miyaura Cross-Coupling Reactions. *J. Org. Chem.* **2012**, *77*, 6624–6628.

155. Fujitsuka, M.; Cho, D. W.; Iwamoto, T.; Yamago, S.; Majima, T. Size-Dependent Fluorescence Properties of [n]Cycloparaphenylenes (n = 8-13), Hoop-Shaped π-Conjugated Molecules. *Phys. Chem. Chem. Phys.* **2012**, *14*, 14585–14588.

156. Segawa, Y.; Fukazawa, A.; Matsuura, S.; Omachi, H.; Yamaguchi, S.; Irle, S.; Itami, K. Combined Experimental and Theoretical Studies on the Photophysical Properties of Cycloparaphenylenes. *Org. Biomol. Chem.* **2012**, *10*, 5979–5984.

157. Qiu, Z.-L.; Tang, C.; Wang, X.-R.; Ju, Y.-Y.; Chu, K.-S.; Deng, Z.-Y.; Hou, H.; Liu, Y.-M.; Tan, Y.-Z. Tetra-benzothiadiazole-based [12]Cycloparaphenylene with Bright Emission and Its Supramolecular Assembly. *Angew. Chem. Int. Ed.* **2020**, *59*, 20868–20872.

158. Della Sala, P.; Buccheri, N.; Sanzone, A.; Sassi, M.; Neri, P.; Talotta, C.; Rocco, A.; Pinchetti, V.; Beverina, L.; Brovelli, S.; et al. First Demonstration of the Use of Very Large Stokes Shift Cycloparaphenylenes as Promising Organic Luminophores for Transparent Luminescent Solar Concentrators. *Chem. Commun.* **2019**, *55*, 3160–3163.

159. Lavis, L. D.; Raines, R. T. Bright Ideas for Chemical Biology. *ACS Chem. Biol.* **2008**, *3*, 142–155.

160. Segawa, Y.; Kuwayama, M.; Hijikata, Y.; Fushimi, M.; Nishihara, T.; Pirillo, J.; Shirasaki, J.; Kubota, N.; Itami, K. Topological Molecular Nanocarbons: All-Benzene Catenane and Trefoil Knot. *Science* **2019**, *365*, 272–276.

161. Jiang, J.-X.; Su, F.; Trewin, A.; Wood, C. D.; Niu, H.; Jones, J. T. A.; Khimyak, Y. Z.; Cooper, A. I. Synthetic Control of the Pore Dimension and Surface Area in Conjugated Microporous Polymer and Copolymer Networks. *J. Am. Chem. Soc.* **2008**, *130*, 7710–7720.

162. Cooper, A. I. Conjugated Microporous Polymers. *Adv. Mater.* **2009**, *21*, 1291–1295.

163. Kumar, K. V.; Preuss, K.; Lu, L.; Guo, Z. X.; Titirici, M. M. Effect of Nitrogen Doping on the CO2 Adsorption Behavior in Nanoporous Carbon Structures: A Molecular Simulation Study. *J. Phys. Chem. C* **2015**, *119*, 22310–22321.

164. Hao, G. P.; Li, W. C.; Qian, D.; Lu, A. H. Rapid Synthesis of Nitrogen-Doped Porous Carbon Monolith for CO2 Capture. *Adv. Mater.* **2010**, *22*, 853–857.

165. Dawson, R.; Stöckel, E.; Holst, J. R.; Adams, D. J.; Cooper, A. I. Microporous Organic Polymers for Carbon Dioxide Capture. *Energy Environ. Sci.* **2011**, *4*, 4239–4245.

166. Van Raden, J. M.; Louie, S.; Zakharov, L. N.; Jasti, R. 2,2′-Bipyridyl-Embedded Cycloparaphenylenes as a General Strategy To Investigate Nanohoop-Based Coordination Complexes. *J. Am. Chem. Soc.* **2017**, *139*, 2936–2939.

167. Chen, B.; Metera, K.; Sleiman, H. F. Biotin-Terminated Ruthenium Bipyridine Ring-Opening Metathesis Polymerization Copolymers: Synthesis and Self-Assembly with Streptavidin. *Macromolecules* **2005**, *38*, 1084–1090.

168. Ter Huurne, G. M.; Gillissen, M. A. J.; Palmans, A. R. A.; Voets, I. K.; Meijer, E. W. The Coil-to-Globule Transition of Single-Chain Polymeric Nanoparticles with a Chiral Internal Secondary Structure. *Macromolecules* **2015**, *48*, 3949–3956.

169. Pangborn, A. B.; Giardello, M. A.; Grubbs, R. H.; Rosen, R. K.; Timmers, F. J. Safe and Convenient Procedure for Solvent Purification. *Organometallics* **1996**, *15*, 1518–1520.

170. Lakowicz, J. R. *Principles of Fluorescence Spectroscopy*, 3rd ed.; Springer, 2006.

171. Preus, S. A|e - UV-Vis-IR Spectral Software 2.2. FluorTools.

172. Thordarson, P. Determining Association Constants from Titration Experiments in Supramolecular Chemistry. *Chem. Soc. Rev.* **2011**, *40*, 1305–1323.

173. Stoermer, M. J.; Butler, D. N.; Warrener, R. N.; Weerasuria, K. D. V; Fairlie, D. P. Cycloadditions of Isobenzofuran to a Constrained Template Bearing Neighboring Dienophiles. *Chem. Eur. J.* **2003**, *9*, 2068–2071.

174. Essiz, S.; Dalkilic, E.; Sari, O.; Dastan, A.; Balci, M. Unexpected Regioselectivity Observed in the Bromination and Epoxidation Reactions of P-Benzoquinone-Fused Norbornadiene: An Experimental and Computational Study. *Tetrahedron* **2017**, *73*, 1640–1649.

175. Li, P.; Sisto, T. J.; Darzi, E. R.; Jasti, R. The Effects of Cyclic Conjugation and Bending on the Optoelectronic Properties of Paraphenylenes. *Org. Lett.* **2014**, *16*, 182–185.

176. Sisto, T. J.; Golder, M. R.; Hirst, E. S.; Jasti, R. Selective Synthesis of Strained [7]Cycloparaphenylene: An Orange-Emitting Fluorophore. *J. Am. Chem. Soc.* **2011**, *133*, 15800–15802.

177. Oda, M.; Kawase, T.; Okada, T.; Enomoto, T. 2-Cyclohexene-1,4-Dione. *Org. Synth.* **1996**, *73*, 253.

178. Brodnik, H.; Požgan, F.; Štefane, B. Synthesis of 8-Heteroaryl Nitroxoline Analogues via One-Pot Sequential Pd-Catalyzed Coupling Reactions. *Org. Biomol. Chem.* **2016**, *14*, 1969–1981.

179. Love, J. A.; Morgan, J. P.; Trnka, T. M.; Grubbs, R. H. A Practical and Highly Active Ruthenium-Based Catalyst That Effects the Cross Metathesis of Acrylonitrile. *Angew. Chem. Int. Ed.* **2002**, *41*, 4035–4037.

180. Sheldrick, G. M. Bruker/Siemens Area Detector Absorption Correction Program. Bruker AXS: Madison, WI 1998.

181. Van Der Sluis, P.; Spek, A. L. BYPASS: An Effective Method for the Refinement of Crystal Structures Containing Disordered Solvent Regions. *Acta Crystallogr. Sect. A* **1990**, *A46*, 194–201.

182. Sheldrick, G. M. Crystal Structure Refinement with SHELXL. *Acta Crystallogr. Sect. C* **2015**, *C71*, 3–8.

183. Darzi, E. R.; White, B. M.; Loventhal, L. K.; Zakharov, L. N.; Jasti, R. An Operationally Simple and Mild Oxidative Homocoupling of Aryl Boronic Esters To Access Conformationally Constrained Macrocycles. *J. Am. Chem. Soc.* **2017**, *139*, 3106–3114.

184. Swager, T. M. 50th Anniversary Perspective: Conducting/Semiconducting Conjugated Polymers. A Personal Perspective on the Past and the Future. *Macromolecules* **2017**, *50*, 4867–4886.

185. Root, S. E.; Savagatrup, S.; Printz, A. D.; Rodriquez, D.; Lipomi, D. J. Mechanical Properties of Organic Semiconductors for Stretchable, Highly Flexible, and Mechanically Robust Electronics. *Chem. Rev.* **2017**, *117*, 6467–6499.

186. Scott, L. T. Conjugated Belts and Nanorings with Radially Oriented p Orbitals. *Angew. Chem. Int. Ed.* **2003**, *42*, 4133–4135.

187. Iyoda, M.; Yamakawa, J.; Rahman, M. J. Conjugated Macrocycles: Concepts and Applications. *Angew. Chem. Int. Ed.* **2011**, *50*, 10522–10553.

188. Hirst, E. S.; Jasti, R. Bending Benzene: Syntheses of [n]Cycloparaphenylenes. *J. Org. Chem.* **2012**, *77*, 10473–10478.

189. Peña-Alvarez, M.; Qiu, L.; Taravillo, M.; Baonza, V. G.; Delgado, M. C. R.; Yamago, S.; Jasti, R.; Navarrete, J. T. L.; Casado, J.; Kertesz, M. From Linear to Cyclic Oligoparaphenylenes: Electronic and Molecular Changes Traced in the Vibrational Raman Spectra and Reformulation of the Bond Length Alternation Pattern. *Phys. Chem. Chem. Phys.* **2016**, *18*, 11683–11692.

190. Talipov, M. R.; Jasti, R.; Rathore, R. A Circle Has No End: Role of Cyclic Topology and Accompanying Structural Reorganization on the Hole Distribution in Cyclic and Linear Poly-p-Phenylene Molecular Wires. *J. Am. Chem. Soc.* **2015**, *137*, 14999–15006.

191. Iwamoto, T.; Watanabe, Y.; Sakamoto, Y.; Suzuki, T.; Yamago, S. Selective and Random Syntheses of [n]Cycloparaphenylenes (n = 8-13) and Size Dependence of Their Electronic Properties. *J. Am. Chem. Soc.* **2011**, *133*, 8354–8361.

192. Wassy, D.; Pfeifer, M.; Esser, B. Synthesis and Properties of Conjugated Nanohoops Incorporating Dibenzo[ a, e]Pentalenes: [2]DBP[12]CPPs. *J. Org. Chem.* **2020**, *85*, 34–43.

193. Yagi, A.; Venkataramana, G.; Segawa, Y.; Itami, K. Synthesis and Properties of Cycloparaphenylene-2,7-Pyrenylene: A Pyrene-Containing Carbon Nanoring. *Chem. Commun.* **2014**, *50*, 957–959.

194. Lu, D.; Wu, H.; Dai, Y.; Shi, H.; Shao, X.; Yang, S.; Yang, J.; Du, P. A Cycloparaphenylene Nanoring with Graphenic Hexabenzocoronene Sidewalls. *Chem. Commun.* **2016**, *52*, 7164–7167.

195. Patel, V. K.; Kayahara, E.; Yamago, S. Practical Synthesis of [n]Cycloparaphenylenes (N=5, 7–12) by H2SnCl4-Mediated Aromatization of 1,4-Dihydroxycyclo-2,5-Diene Precursors. *Chem. Eur. J.* **2015**, *21*, 5742–5749.

196. Iwan, A.; Sek, D. Processible Polyazomethines and Polyketanils: From Aerospace to Light-Emitting Diodes and Other Advanced Applications. *Prog. Polym. Sci.* **2008**, *33*, 289–345.

197. Takimiya, K.; Konda, Y.; Ebata, H.; Niihara, N.; Otsubo, T. Facile Synthesis, Structure, and Properties of Benzo[1,2-b:4,5-b']Dichalcogenophenes. *J. Org. Chem.* **2005**, *70*, 10569–10571.

198. Bruno, N. C.; Tudge, M. T.; Buchwald, S. L. Design and Preparation of New Palladium Precatalysts for C–C and C–N Cross-Coupling Reactions. *Chem. Sci.* **2013**, *4*, 916–920.

199. Shen, H.-C.; Tang, J.-M.; Chang, H.-K.; Yang, C.-W.; Liu, R.-S. Short and Efficient Synthesis of Coronene Derivatives via Ruthenium-Catalyzed Benzannulation Protocol. *J. Org. Chem.* **2005**, *70*, 10113–10116.

200. Kloppenburg, L.; Jones, D.; Bunz, U. H. F. High Molecular Weight Poly(p-Phenyleneethynylene)s by Alkyne Metathesis Utilizing "Instant" Catalysts: A Synthetic Study. *Macromolecules* **1999**, *32*, 4194–4203.

201. Grolleau, J.; Frère, P.; Gohier, F. Clean and Efficient Iodination of Thiophene Derivatives. *Synthesis* **2015**, *47*, 3901–3906.

202. Hodge, P. Entropically Driven Ring-Opening Polymerization of Strainless Organic Macrocycles. *Chem. Rev.* **2014**, *114*, 2278–2312.

203. Schleyer, P. V. R. R.; Wiliiams, J. E.; Blanchard, K. R.; Williams, J. E.; Blanchard, K. R. The Evaluation of Strain in Hydrocarbons. The Strain in Adamantane and Its Origin. *J. Am. Chem. Soc.* **1970**, *92*, 2377–2386.

204. Smith, J. A.; Moeller, K. D. Oxidative Cyclizations, the Synthesis of Aryl-Substituted c-Glycosides, and the Role of the Second Electron Transfer Step. *Org. Lett.* **2013**, *15*, 5818–5821.

205. Naganawa, A.; Matsui, T.; Ima, M.; Yoshida, K.; Tsuruta, H.; Yamamoto, S.; Yamamoto, H.; Okada, H.; Maruyama, T.; Nakai, H.; et al. Optimization of Sulfonamide Derivatives as Highly Selective EP1 Receptor Antagonists. *Bioorg. Med. Chem.* **2006**, *14*, 7774–7789.

206. Yang, J.; Xia, Y. Mechanochemical Generation of Acid-Degradable Poly(Enol Ether)S. *Chem. Sci.* **2021**, *12*, 4389–4394.

207. Boswell, B. R.; Mansson, C. M. F.; Cox, J. M.; Jin, Z.; Romaniuk, J. A. H.; Lindquist, K. P.; Cegelski, L.; Xia, Y.; Lopez, S. A.; Burns, N. Z. Mechanochemical Synthesis of an Elusive Fluorinated Polyacetylene. *Nat. Chem.* **2021**, *13*, 41–46.

208. Bowser, B. H.; Wang, S.; Kouznetsova, T. B.; Beech, H. K.; Olsen, B. D.; Rubinstein, M.; Craig, S. L. Single-Event Spectroscopy and Unravelling Kinetics of Covalent Domains Based on Cyclobutane Mechanophores. *J. Am. Chem. Soc.* **2021**, *143*, 5269–5276.

209. Banerjee, M.; Shukla, R.; Rathore, R. Synthesis, Optical, and Electronic Properties of Soluble Poly-p-Phenylene Oligomers as Models for Molecular Wires. *J. Am. Chem. Soc.* **2009**, *131*, 1780–1786.

210. Potisek, S. L.; Davis, D. A.; Sottos, N. R.; White, S. R.; Moore, J. S. Mechanophore-Linked Addition Polymers. *J. Am. Chem. Soc.* **2007**, *129*, 13808–13809.

211. Linseis, M.; Záliš, S.; Zabel, M.; Winter, R. F. Ruthenium Stilbenyl and Diruthenium Distyrylethene Complexes: Aspects of Electron Delocalization and Electrocatalyzed Isomerization of the Z-Isomer. *J. Am. Chem. Soc.* **2012**, *134*, 16671–16692.

212. Nguyen, T. B.; Al-Mourabit, A. Remarkably High Homoselectivity in [2 + 2] Photodimerization of: Trans -Cinnamic Acids in Multicomponent Systems. *Photochem. Photobiol. Sci.* **2016**, *15*, 1115–1119.

213. Grosjean, S.; Hassan, Z.; Wöll, C.; Bräse, S. Diverse Multi-Functionalized Oligoarenes and Heteroarenes for Porous Crystalline Materials. *European J. Org. Chem.* **2019**, *2019*, 1446–1460.